VOLUME 26 (1961) No. 2

# NUCLEAR PHYSICS

JOURNAL DEVOTED TO THE EXPERIMENTAL AND THEORETICAL STUDY OF THE FUNDAMENTAL CONSTITUENTS OF MATTER AND THEIR INTERACTIONS

EDITOR: L. ROSENFELD · COPENHAGEN

E. LEADER, The optical model in $\pi$-nuclear scattering . . . . . 177
K. G. NAIR, K. N. IYENGAR and R. RAMANNA, Energy and angular distributions of protons emitted from $Al^{27}$ due to 14.2 MeV neutron interactions . . . . 193
W. M. JONES, D. G. WATERS and V. M. ROUT, The angular distributions of charged particle groups from the deuteron bombardment of nitrogen . . . 203
A. SĂNDULESCU and M. IOSIFESCU, On favoured alpha transitions . . . . . 209
F. A. BRISBOUT, C. GAULD, C. B. A. McCUSKER, J. MALOS, K. NISHIKAWA, L. S. PEAK and L. G. VAN LOON, A comparison of pion and nucleon interactions in nuclear emulsions between $10^{11}$ and $10^{13}$ eV . . . . . 217
Y. NE'EMAN, Derivation of strong interactions from a gauge invariance . . 222
Y. NE'EMAN, Yukawa terms in the unitary gauge theory . . . . . 230
V. J. VANHUYSE and W. C. BARBER, Photoprotons from carbon . . . . . 233
G. GOLDRING and Z. VAGER, Energy loss of protons in rare earth oxides and reduced transition probabilities for $2^+ \rightarrow 0^+$ transitions in even rotational nuclei . . . . . 250
R. A. BERG and C. N. LINDNER, Electron-proton bremsstrahlung . . . . . 259
R. SOSNOWSKI, Z. WILHELMI and J. WOJTKOWSKA, Relative measurements on the longitudinal polarization of beta rays from $Na^{24}$, $Mn^{56}$, $Sb^{122}$, $Ho^{166}$ and $Au^{198}$ . . . . . 280
D. E. McCUMBER, Generalized self-consistent-field and random-phase approximations for multi-phase systems . . . . . 286
Yu. F. SMIRNOV and D. CHLEBOWSKA, Reduced widths for nucleon clusters in shell model . . . . . 306
G. MOSCATI, The $(\gamma, 3n)$ reaction in $Pr^{141}$ . . . . . 321
H. FRÖHLICH, The structure of momentum space, the neutrino and the Pauli principle . . . . . 324
D. TADIĆ, Induced pseudoscalar interaction in $0^- \rightarrow 0^+$ beta transitions . . 338
Erratum and Addendum . . . . . 351

August 1961

NORTH-HOLLAND PUBLISHING COMPANY-AMSTERDAM

## EDITORIAL BOARD

| | |
|---|---|
| AUSTRALIA & NEW ZEALAND: | H. Messel (Sydney), M. L. Oliphant (Canberra) |
| AUSTRIA: | B. Karlik (Vienna), H. Thirring (Vienna) |
| BELGIUM: | M. de Hemptinne (Louvain), J. Verhaeghe (Ghent) |
| CANADA: | G. Volkoff (Vancouver) |
| DENMARK: | C. Møller (Copenhagen), S. Rozental (Copenhagen), G. E. Brown (Copenhagen) |
| FINLAND: | L. Simons (Helsinki) |
| FRANCE: | A. Berthelot (Saclay), S. Gorodetzky (Strasbourg) |
| GERMANY (DEM. REP.): | G. Hertz (Leipzig) |
| GERMANY (FED. REP.): | W. Gentner (Freiburg i. B.), J. H. D. Jensen (Heidelberg) |
| GREAT BRITAIN: | W. E. Burcham (Birmingham), T. H. R. Skyrme (Harwell) |
| HUNGARY: | L. Janossy (Budapest) |
| INDIA: | H. Bhabha (Bombay), R. Ramanna (Trombay) |
| IRISH REPUBLIC: | J. McConnell (Maynooth) |
| ISRAEL: | G. Racah (Jerusalem) |
| ITALY: | E. Amaldi (Rome) |
| JAPAN: | S. Kikuchi (Tokay), S. Tomonaga (Tokyo) |
| MEXICO: | M. Moshinsky (Mexico) |
| NETHERLANDS: | H. Brinkman (Groningen), S. R. de Groot (Leiden) |
| NORWAY: | E. Hylleraas (Oslo), A. Lundby (Oslo), H. Wergeland (Trondheim) |
| POLAND: | L. Infeld (Warsaw), J. Werle (Warsaw) |
| PORTUGAL: | J. M. Araújo (Porto), J. R. de Almeida Santos (Coimbra) |
| SOUTH AMERICA: | G. Beck (Saõ Paulo), J. Leite Lopes (Rio de Janeiro) |
| SPAIN: | J. M. Otero (Madrid), C. Sanchez del Rio (Madrid) |
| SWEDEN: | O. Klein (Stockholm), K. Siegbahn (Uppsala), I. Waller (Uppsala) |
| SWITZERLAND: | P. Huber (Basel), P. Scherrer (Zürich) |
| U.A.R. & ARAB COUNTRIES: | F. El Bedewi (Cairo), M. G. Nooh (Cairo) |
| U.S.A.: | H. H. Barschall (Madison, Wisconsin), S. Devons (New York), V. F. Weisskopf (Cambridge, Mass.) |
| U.S.S.R.: | M. A. Markov (Moscow), I. S. Shapiro (Moscow), D. V. Skobeltzyn (Moscow) |
| YUGOSLAVIA: | I. Supek (Zagreb) |



CONTRIBUTIONS may be sent to the Editor, Professor L. Rosenfeld, NORDITA, Blegdamsvej 17, Copenhagen Ø, either directly, or preferably through the intermediary of one of the members of the Editorial Board of the country or region in which the author is working. They may be written in English, French or German.

NUCLEAR PHYSICS is published in fortnightly issues. The subscription price per volume of 700 pages is fl 57.00; 114s; $ 15.00. Post-free.

SUBSCRIPTIONS should be sent to the publishers, NORTH-HOLLAND PUBLISHING COMPANY P.O. Box 103, Amsterdam or to any subscription-agent.

BOOKS FOR REVIEW should be sent to Professor Rosenfeld.



*No part of this issue may be reproduced in any form, by print, photoprint, microfilm or any other means without permission from the publisher.*



**Printed in the Netherlands**

7.C

*Nuclear Physics* **26** (1961) 177—192; © *North-Holland Publishing Co., Amsterdam*

Not to be reproduced by photoprint or microfilm without written permission from the publisher

# THE OPTICAL MODEL IN $\pi$-NUCLEAR SCATTERING

E. LEADER

*University College, London* †

Received 17 February 1961

**Abstract:** The optical potential for the pion-$C^{12}$ interaction (in the 60—150 MeV region) is calculated in impulse approximation using the full energy dependence of the $\pi$-nucleon phase shifts. A critical discussion of the comparison with experimental well depths and differential cross sections is given. It is concluded that the model is perfectly adequate for predicting gross effects but that nothing conclusive can be said regarding its ability to account for the finer details, such as the differential cross-sections.

## 1. Introduction

In considering the experimental results for the elastic scattering of pions on nuclei it is customary to analyse the data in terms of some equivalent static optical potential which replaces the extremely complex interaction between projectile and struck nucleus and is chosen so as best to reproduce the actual experimental data. The effect of the existence of other channels for the interaction necessitates the use of a complex potential, whose imaginary part takes into account the attenuating effect of all the other possible channels.

In a series of papers Watson *et al.* [1]) †† have demonstrated how one can reduce the many-body scattering problem to the single particle scattering on a complex optical potential, which is determined from a knowledge of the meson-nucleon and the nucleon-nucleon interactions. Our lack of knowledge of the latter is circumvented by making use of the impulse [2]) approximation and the experimental knowledge of the pion-nucleon phase shifts, or equivalently, the energy shell matrix elements of the pion-nucleon transition operator.

Previously [3]), additional approximations have been made in the assumed form of the transition operator. In the following, we shall calculate the optical potential and cross-section for pions scattering on $C^{12}$, taking into account the exact experimental energy variation of the pion-nucleon phase shifts, thus limiting our approximations to the use of the impulse approximation and the arbitrariness in our knowledge of the off-energy-shell pion-nucleon matrix elements. The latter, however, does not contribute to the forward momentum space matrix elements of the potential, so that comparison of the theory with

† This work was carried out when the author held an Elsie Ballot Fellowship at St. John's College, and forms a section of Part I of a Ph. D. thesis submitted to the University of Cambridge.

†† In ref. [1]) a full bibliography is given.

the experimentally measured quantities is a fairly direct test of the usefulness of the impulse approximation. The significance of this sort of comparison is critically examined.

In sect. 2 we give briefly the formal expressions for the optical potential and develop the machinery necessary in order to evaluate the potential. Sect. 3 considers the application to the $C^{12}$ nucleus and discusses the approximations used in order to yield a manageable calculation. In sect. 4 we discuss the comparison between our results and the experimental data.

## 2. Basic Formalism

Let $E$ and $H_0$ be the energy and Hamiltonian of the *non-interacting* system consisting of a pion projectile and a nucleus of mass number $A$ in its ground state. We denote this unperturbed state as $|\mathrm{i}\rangle$. If $|\psi\rangle$ represents the interacting state of pion and nucleus, we have

$$|\psi\rangle = \bar{\Omega}|\mathrm{i}\rangle, \tag{2.1}$$

where the Möller wave operator [4]) $\bar{\Omega}$ is given by [5])

$$\bar{\Omega} = 1 + \frac{1}{\varepsilon}\sum_{\alpha=1}^{A}(v_\alpha + \Delta)\bar{\Omega}. \tag{2.2}$$

Here $v_\alpha$ is the interaction energy between the pion and the $\alpha^{\text{th}}$ nucleon and $\varepsilon$ is given by

$$\varepsilon = E - H_0 + i\xi, \tag{2.3}$$

where $\xi$ is the usual infinitesimal quantity which ensures outgoing waves.

As has been discussed in ref. [6]), $\Delta$ represents the effect of meson absorption and immediate re-creation from a two-nucleon cluster in the nucleus and may be considered as a diagonal operator in the nucleon co-ordinates.

Let $V$ denote the optical potential operator and let us further denote by $\langle\theta\rangle$ the ground state expectation value of any operator $\theta$. Then it is possible to show that $V$ is given by

$$V = \varepsilon_\pi \frac{1}{\langle\bar{\Omega}\rangle}\langle\bar{\Omega} - 1\rangle. \tag{2.4}$$

Here

$$\varepsilon_\pi = E_\pi - H_\pi + i\xi, \tag{2.5}$$

where $E_\pi$ and $H_\pi$ are respectively the energy and Hamiltonian of the pion projectile.

Using eq. (2.2) we may write

$$V = (\varepsilon_\pi - \langle\Delta\rangle)\frac{1}{\langle\Omega'\rangle}\langle\Omega' - 1\rangle + \langle\Delta\rangle, \tag{2.6}$$

where now $\Omega'$ is a modified Möller operator satisfying

$$\Omega' = 1 + \frac{1}{\varepsilon - \Delta} \sum_{\alpha=1}^{A} v_\alpha \Omega' \tag{2.7}$$

and the modified propagator reflects the average effect of the meson absorption between each $v_\alpha$ interaction of the meson.

In order to evaluate (2.6) one defines elementary scattering operators $t'_\alpha$ satisfying

$$t'_\alpha = v'_\alpha + v'_\alpha \frac{1}{\varepsilon - \Delta} t'_\alpha, \tag{2.8}$$

in terms of which we have

$$\Omega' = 1 + \sum_{\alpha}^{A} \frac{1}{\varepsilon - \Delta} t'_\alpha + \sum_{\alpha \neq \beta} \frac{1}{\varepsilon - \Delta} t'_\alpha \frac{1}{\varepsilon - \Delta} t'_\beta + \ldots . \tag{2.9}$$

No two adjacent indices in the sum are equal.

Substituting (2.9) into (2.7) would yield a series expansion for V in terms of the $t'_\alpha$. However, these are still many-body operators and in order to proceed further they must be related to the free pion-nucleon scattering operators. Let us define a scattering operator $t_\alpha$ which does not contain the two-nucleon absorption effect, i.e., let

$$t_\alpha = v_\alpha + v_\alpha \frac{1}{\varepsilon} t_\alpha. \tag{2.10}$$

Then it has been shown [6]) that

$$t'_\alpha \approx t_\alpha \tag{2.11}$$

to within a few percent at pion energies of about 60 → 120 MeV.

The impulse approximation now consists of replacing the $t_\alpha$ by the two-body pion-nucleon transition operator $t_\alpha^0$ given by

$$t_\alpha^0 = v_\alpha + v_\alpha \frac{1}{\varepsilon^0} t_\alpha^0, \tag{2.12}$$

where

$$\varepsilon^0 = E_\pi - H_\pi - T_\alpha + i\xi, \tag{2.13}$$

the term $T_\alpha$ being the kinetic energy of the $\alpha^{\text{th}}$ nucleon. The operator $t_\alpha^0$ is exactly the scattering operator which describes the free pion-nucleon interaction and its energy and momentum conserving matrix elements are therefore obtainable from the experimental phase shifts.

There has been much discussion [3]) of the validity of the assumption

$$t_\alpha \approx t_\alpha^0, \tag{2.14}$$

but from our point of view we shall consider the final comparison with experiment as a test of its validity.

In terms of the impulse approximation, the expression for the potential (eq. (2.6)) becomes

$$V = \sum_{\alpha}^{A} \langle t_\alpha^0 \rangle + \sum_{\alpha \neq \beta} \langle t_\alpha^0 \frac{1}{\varepsilon - \Delta} t_\beta^0 \rangle + \langle \Delta \rangle - \sum_{\alpha, \beta} \frac{\langle t_\alpha^0 \rangle \langle t_\beta^0 \rangle}{\varepsilon_\pi - \langle \Delta \rangle} + \ldots . \quad (2.15)$$

It is sometimes simpler to work with the total scattering operator T of the meson nuclear system, defined by

$$T = V + V \frac{1}{\varepsilon_\pi} T, \quad (2.16)$$

so that we have also, for the scattering of the meson from state $\mathbf{p}$ to $\mathbf{p}'$,

$$\langle \mathbf{p}' | T | \mathbf{p} \rangle = \sum_{\alpha}^{A} \langle \mathbf{p}' | t_\alpha^0 | \mathbf{p} \rangle + \langle \mathbf{p}' | \Delta | \mathbf{p} \rangle + \sum_{\alpha \neq \beta} \langle \mathbf{p}' | t_\alpha^0 \frac{1}{\varepsilon - \Delta} t_\beta^0 | \mathbf{p} \rangle . \quad (2.17)$$

## 3. Application to Pion Scattering on $C^{12}$

We now assume that $C^{12}$ is represented by an antisymmetrised sum of single-particle simple harmonic oscillator wave functions in $j-j$ coupling, so as to give zero total angular momentum. For want of a better method we shall simply assume that the isobaric spins are coupled in pairs.

Let $\Psi(1 \ldots \alpha \ldots A)$ be the $C^{12}$ ground state wave function, where $\alpha$ describes the position (or momentum) and the spin and isobaric spin-co-ordinates of the $\alpha^{\text{th}}$ nucleon.

We define the generalised one and two particle density matrices by

$$P(\alpha'/\alpha) = \int \Psi^*(1, 2 \ldots \alpha' \ldots A) \Psi(1, 2 \ldots \alpha \ldots A) \times \mathrm{d}1 \mathrm{d}2 \ldots \mathrm{d}(\alpha-1) \mathrm{d}(\alpha+1) \ldots \mathrm{d}A \quad (3.1)$$

and

$$P(\alpha'\beta'/\alpha\beta) = \int \Psi^*(1 \ldots \alpha' \ldots \beta' \ldots A) \Psi(1 \ldots \alpha \ldots \beta \ldots A) \times \mathrm{d}1 \ldots \mathrm{d}(\alpha-1) \mathrm{d}(\alpha+1) \ldots \mathrm{d}(\beta-1) \mathrm{d}(\beta+1) \ldots \mathrm{d}A. \quad (3.2)$$

(Here the integration symbol includes summations over spin and isospin coordinates.) Using the fact that the $t_\alpha^0$ are two-body operators and that they conserve momentum, the expression (2.15) for $V$ becomes

$$\begin{aligned}\langle \mathbf{p}'|V|\mathbf{p}\rangle &= \sum_\alpha \int P(\mathbf{k}_\alpha+\Delta\mathbf{p}, \zeta'_\alpha|\mathbf{k}_\alpha, \zeta_\alpha)\langle \mathbf{p}', \mathbf{k}_\alpha+\Delta\mathbf{p}, \zeta'_\alpha|t_\alpha{}^0|\mathbf{p}; \mathbf{k}_\alpha\zeta_\alpha\rangle \mathrm{d}^3\mathbf{k}_\alpha \\ &+ \sum_{\alpha\neq\beta}\int \{P(\mathbf{k}'_\alpha\zeta'_\alpha, \mathbf{k}'_\beta\zeta'_\beta|\mathbf{k}_\alpha\zeta_\alpha; \mathbf{k}_\beta\zeta_\beta) - P(\mathbf{k}'_\alpha\zeta'_\alpha|\mathbf{k}_\alpha\zeta_\alpha)P(\mathbf{k}'_\beta\zeta'_\beta|\mathbf{k}_\beta\zeta_\beta)\} \\ &\times \frac{\langle \mathbf{p}'\mathbf{k}'_\alpha\zeta'_\alpha|t_\alpha{}^0|\mathbf{p}''\mathbf{k}_\alpha\zeta_\alpha\rangle\langle \mathbf{p}''\mathbf{k}'_\beta\zeta'_\beta|t_\beta{}^0|\mathbf{p}\mathbf{k}_\beta\zeta_\beta\rangle}{E_\pi - E_\pi(p'')+i\xi} \mathrm{d}^3\mathbf{k}_\alpha \mathrm{d}^3\mathbf{k}_\beta \mathrm{d}^3\mathbf{p}'' \\ &+ \langle \mathbf{p}'|\Delta|\mathbf{p}\rangle + \ldots,\end{aligned} \tag{3.3}$$

with

$$\Delta\mathbf{p} = \mathbf{p}-\mathbf{p}', \qquad \mathbf{k}'_\alpha = \mathbf{k}_\alpha+\mathbf{p}''-\mathbf{p}', \qquad \mathbf{k}'_\beta = \mathbf{k}_\beta+\mathbf{p}-\mathbf{p}'',$$

and where $\zeta'_\alpha$ stands for the spin and isospin co-ordinates of nucleon $\alpha$.

The last term has been given by Breuckner, Serber and Watson [8]) as

$$\langle \mathbf{p}'|\Delta|\mathbf{p}\rangle = \frac{-iv}{2\lambda_a}\frac{1}{(2\pi)^3}\int \bar{\rho}(\mathbf{x})\,\mathrm{e}^{-i\mathbf{x}\cdot(\mathbf{p}'-\mathbf{p})}\mathrm{d}^3\mathbf{x}, \tag{3.5}$$

where $v$ is the pion velocity and $\lambda_a$ the mean free path for pion absorption, is given [9]) semi-empirically by

$$\frac{1}{\lambda_a} = \left(\frac{\mu c}{\hbar}\right) \times 0.107 \left[\frac{\mu c}{p}\left(0.14+\frac{p^2}{\mu^2 c^2}\right)\right]. \tag{3.6}$$

The quantity $\bar{\rho}(\mathbf{x})$ is the probability density of the centre of mass of a nucleon pair, so that

$$\int \bar{\rho}(\mathbf{x})\,\mathrm{d}^3\mathbf{x} = \tfrac{4}{3}\pi r_0{}^3 A = U, \tag{3.7}$$

where $U$ is the nuclear volume. For simplicity we write (3.4) as

$$\langle \mathbf{p}'|V|\mathbf{p}\rangle = \langle \mathbf{p}'|V^{(1)}|\mathbf{p}\rangle + \langle \mathbf{p}'|V^{(2)}|\mathbf{p}\rangle + \langle \mathbf{p}'|V^{(\mathrm{abs})}|\mathbf{p}\rangle. \tag{3.8}$$

It is clear that the $V^{(2)}$ term depends on nuclear correlations and would vanish if the nucleons were in independent single particle states. We therefore assume that it is small compared with $V^{(1)}+V^{(\mathrm{abs})}$ and shall return to consider it later.

Using the wave functions given in the appendix and the functions $G_{\mathrm{D}}$ and $G_{\mathrm{SF}}$, also given in the appendix, the term $V^{(1)}$ reduces to

$$\begin{aligned}\langle \mathbf{p}'|V^{(1)}|\mathbf{p}\rangle &= \tfrac{1}{2}A\int G_{\mathrm{D}}(\mathbf{k}+\Delta\mathbf{p}, \mathbf{k})\langle \mathbf{p}', \mathbf{k}+\Delta\mathbf{p}|t_{\mathrm{D}}|\mathbf{p}, \mathbf{k}\rangle \mathrm{d}^3\mathbf{k} \\ &+ \tfrac{1}{2}A\int G_{\mathrm{SF}}(\mathbf{k}+\Delta\mathbf{p}, \mathbf{k})\langle \mathbf{p}', \mathbf{k}+\Delta\mathbf{p})t_{\mathrm{SF}}|\mathbf{p}, \mathbf{k}\rangle \mathrm{d}^3\mathbf{k},\end{aligned} \tag{3.9}$$

where the subscripts D and SF refer to direct and spin-flip elements of $t$ and where we use such abbreviations as, e.g.,

$$t_{\mathrm{D}} = t_{\mathrm{D}}{}^0(\pi^+, \mathrm{p}) + t_{\mathrm{D}}{}^0(\pi^-, \mathrm{p}). \tag{3.10}$$

Looking at (3.9) one sees that one requires to know the $t$ matrix both on and off the energy shell. As to the off energy shell behaviour, we have no real indication of its nature. However, this arbitrariness is somewhat compensated by the fact that the $G$ functions tend to damp out the importance of these matrix elements. On the other hand it should be noted that for the forward matrix elements of $V^{(1)}$, i.e., for $\mathbf{p} = \mathbf{p}'$, only the energy shell matrix elements of $t$ contribute, so that $\langle \mathbf{p}|V^{(1)}|\mathbf{p}\rangle$ can be evaluated *exactly*.

In so far as the on-energy-shell behaviour of $t$ is concerned, various approximations have been made. Frank, Gammel and Watson [3]) estimate (3.9) by removing the matrix from the integral, yielding

$$\langle \mathbf{p}'|V^{(1)}|\mathbf{p}\rangle = \tfrac{1}{2}A\langle \mathbf{p}', \mathbf{k}+\Delta\mathbf{p}|t_{\mathrm{D}}|\mathbf{p}, \mathbf{k}\rangle_{\mathrm{AV}} \int G_{\mathrm{D}}(\mathbf{k}+\Delta\mathbf{p}, \mathbf{k})\mathrm{d}^3\mathbf{k}. \tag{3.11}$$

Further putting $\mathbf{p}' \approx \mathbf{p}$ in the matrix element, they get for the co-ordinate space representation of $V^{(1)}$

$$\langle \mathbf{x}'|V^{(1)}|\mathbf{x}\rangle \approx (2\pi)^3 \tfrac{1}{2}A\langle \mathbf{p}, \mathbf{k}|t_{\mathrm{D}}|\mathbf{p}, \mathbf{k}\rangle_{\mathrm{AV}} \rho(\mathbf{x})\delta(\mathbf{x}-\mathbf{x}'), \tag{3.12}$$

where $\rho(\mathbf{x})$ is the single particle nucleon density normalised to unity. We shall refer to this as the "quasi-local" approximation to the optical potential since it is local at each energy.

Kisslinger [3]), on the other hand, approximates $t$ by

$$\langle \mathbf{p}'|t^0|\mathbf{p}\rangle \approx a + b\,\mathbf{p}' \cdot \mathbf{p}, \tag{3.13}$$

corresponding to a $p^3$ and $p$ dependence for $\delta_{33}$ and the $s$ wave phase shifts respectively, and uses

$$\mathrm{e}^{i\delta} \sin\delta \approx \delta.$$

Eq. (3.13) is assumed to hold also for the off-energy-shell matrix elements and leads eventually to a co-ordinate space potential containing terms dependent on the gradient of the nuclear density.

We have attempted to get a more accurate estimate of (3.9) as follows. On the energy shell we have used Edsac II to evaluate the $t$ matrices exactly using the Anderson energy-dependent phase-shifts † and the necessary relativistic transformation theory [4]) and have carried out the integration in (3.9) numerically. For the off-energy-shell matrix elements we have used

$$\langle \mathbf{k}'|t^0|\mathbf{k}\rangle = t^0(k, k', \cos\theta) \approx t^0(\tfrac{1}{2}(k+k'), \cos\theta)_{\mathrm{E.S.}}, \tag{3.14}$$

where $\mathbf{k}\cdot\mathbf{k}' = kk'\cos\theta$ and $t^0_{\mathrm{E.S.}}$ is the $t$ matrix on the energy shell, corresponding to a mean energy between $k$ and $k'$. For $|\mathbf{p}| = |\mathbf{p}'|$ the function $\langle \mathbf{p}'|v^{(1)}|\mathbf{p}\rangle$ turned out to be reasonably insensitive to the type of off-energy-shell behaviour assumed.

† These are incorrectly given in ref. [12]).

However, if one attempts to estimate either the term $V^{(2)}$ or, equivalently, the last term in $T$ in eq. (2.17), the results turn out to be very much dependent on the assumed off-energy-shell behaviour. For this reason we have not considered it sensible to include these terms, so that for the rest of this paper we consider $V$ as given by

$$V = V^{(1)} + V^{(\mathrm{abs})}, \tag{3.15}$$

$$T = T^{(1)} + T^{(\mathrm{abs})}. \tag{3.16}$$

As we have mentioned before, $V^{(2)}$ is certainly expected to be negligible. The omission of $T^{(2)}$, however, is much more dubious, and means in fact that we are calculating the scattering from the Born approximation. This difficulty and a possible improvement on it are discussed in the next section.

## 4. Comparison with Experimental Data

The fact that we have a reliable estimate of only the energy conserving momentum space matrix elements of $V$ makes it extremely difficult to compare the theory with experiment. We shall therefore carry out this comparison on two levels, (i) via the potential and then (ii) via the differential cross sections.

(i) The experimental data are usually analysed in terms of a potential $V(\mathbf{x})$, local at each energy, chosen so as best to reproduce the experimental results. The potential $V(\mathbf{x})$ is usually written

$$V(\mathbf{x}) = V_{\mathrm{d}}\,\rho(\mathbf{x}), \tag{4.1}$$

where $V_{\mathrm{d}}$ is the complex well depth parameter depending on the energy of the incident meson and $\rho(\mathbf{x})$ describes the shape of the potential well and is normalised so that

$$\int \rho(\mathbf{x})\mathrm{d}^3\mathbf{x} = W = \tfrac{4}{3}\pi r_0^{\,3} A, \tag{4.2}$$

where $W$ is the volume of the equivalent potential well and is expected to be somewhat larger than the nuclear volume $U$.

Let us suppose for a moment that the optical potential at a given energy is in fact local in co-ordinate space and is faithfully represented by $V(\mathbf{x})$. Then we would have

$$\langle \mathbf{p}|V|\mathbf{p}\rangle = \frac{1}{(2\pi)^3}\int V(\mathbf{x})\,\mathrm{d}^3\mathbf{x}, \tag{4.3}$$

so that

$$\langle \mathbf{p}|V|\mathbf{p}\rangle = \frac{W}{(2\pi)^3}\,V_{\mathrm{d}}. \tag{4.4}$$

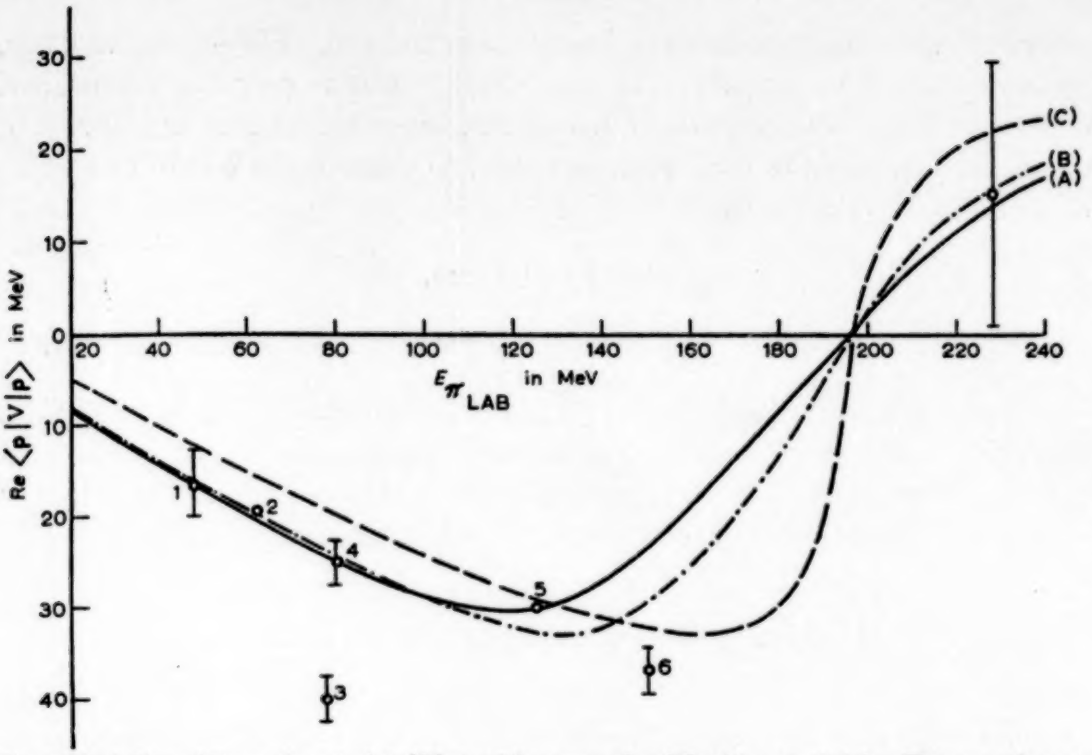


Fig. 1. Variation of the real part of $\langle \mathbf{p}|V|\mathbf{p}\rangle$ with energy for $C^{12}$ with $r_0 = 1.4$ fm. The experimenta points are taken from measurements by Shapir on $C^{12}$ (point 1), Byfield *et al.* on $C^{12}$ (point 2), Williams on $Cu^{64}$ (point 3), Pevsner on Al (point 4), Kessler on $C^{12}$ (point 5), Fuijii on $C^{12}$ (point 6) and Dzelepov on $C^{12}$ (point 7); see ref. [7]). The theoretical curves represent: (A) Re $\langle \mathbf{p}|V|\mathbf{p}\rangle$, (B) the Frank-Gammel-Watson approximation, (C) the F.-G.-W. approximation corrected for well depth.

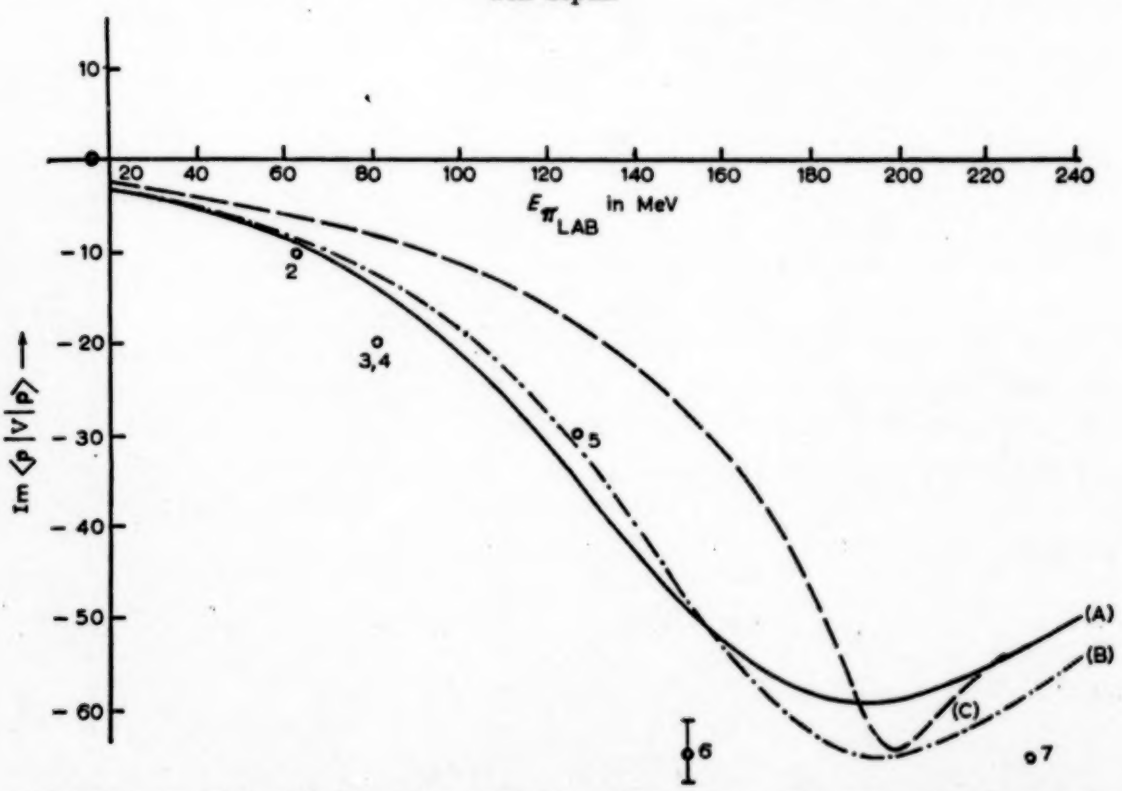


Fig. 2. Variation of the imaginary part of $\langle \mathbf{p}|V|\mathbf{p}\rangle$ with energy for $C^{12}$ with $r_0 = 1.4$ fm. For the experimental points see the caption fo fig. 1. The theoretical curves represent: (A) Im $\langle \mathbf{p}|V|\mathbf{p}\rangle$, (B) F.-G.-W. approximation, (C) F.-G.-W. approximation corrected for well depth.

In figs. 1 and 2 the experimental points correspond to the right hand side of (4.4) with $\hbar_0 \approx 1.7$ fm and $r_0 \approx 1.4$ fm. This corresponds to a potential well whose radius is roughly the nuclear radius plus half the pion Compton wave length. The solid curves represent the function $\langle \mathbf{p}|V|\mathbf{p}\rangle$ as we have calculated it. Also shown are the curves corresponding to the Frank-Gammel-Watson approximation to $V$ and a well depth correction suggested by these authors.

It is seen that there is good agreement between the theoretical curves and experiment. However, in evaluating the importance of this agreement one

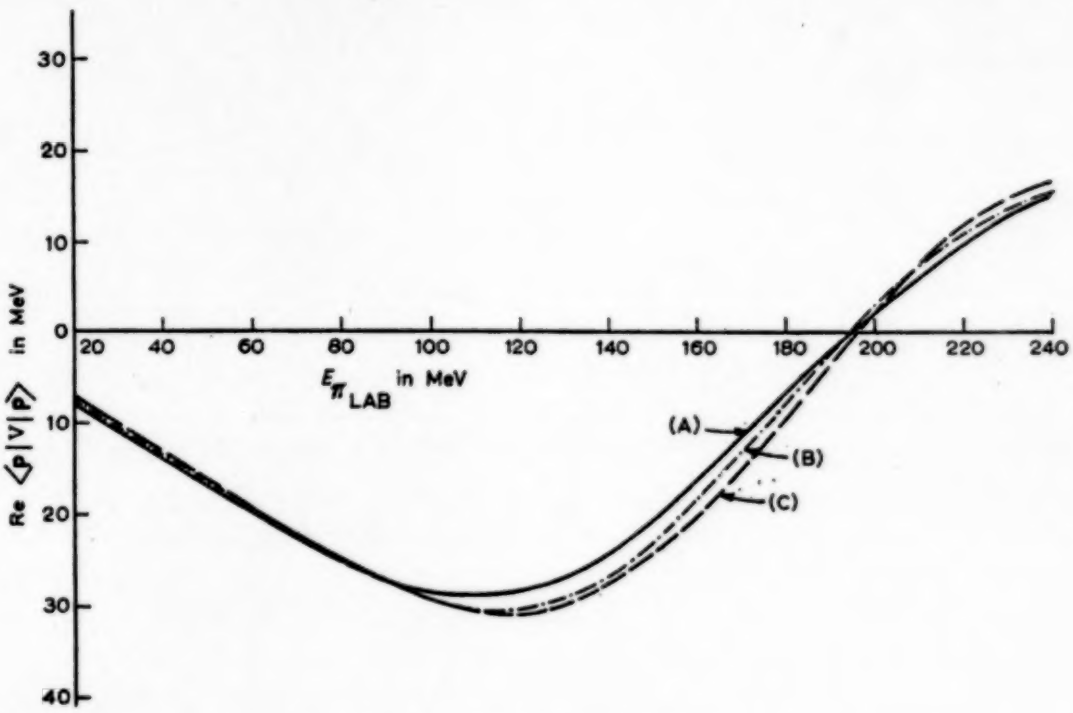


Fig. 3. Variation of the real part of $\langle \mathbf{p}|V|\mathbf{p}\rangle$ with energy for $C^{12}$ for different values of $r_0$. (A) $r_0 = 1.1$ fm, (B) $r_0 = 1.3$ fm, (C) $r_0 = 1.5$ fm.

should bear in mind that firstly the theoretical curves are fairly insensitive to variations in $r_0$ (see fig. 3) and that secondly the potentials $V(\mathbf{x})$ fail to reproduce well the experimental angular distributions.

Let us now suppose as in more reasonable, that the co-ordinate space representation of the optical potential is non-local and for simplicity separable, so that

$$\langle \mathbf{x}'|V|\mathbf{x}\rangle = G(\mathbf{R})g(\mathbf{r}), \tag{4.5}$$

where

$$\mathbf{R} = \tfrac{1}{2}(\mathbf{x}+\mathbf{x}'), \qquad \mathbf{r} = \mathbf{x}'-\mathbf{x}, \tag{4.6}$$

and let us associate

$$G(\mathbf{R}) \approx V(\mathbf{R}) = V_d \rho(\mathbf{R}). \tag{4.7}$$

We normalise $g(\mathbf{r})$ so that for a local potential

$$g(\mathbf{r}) \to \delta(\mathbf{r}). \tag{4.8}$$

The forward momentum space matrix elements of $V$ would be given by

$$\langle \mathbf{p}|V|\mathbf{p}\rangle = \frac{W}{(2\pi)^3} V_d \tilde{g}(\mathbf{p}), \tag{4.9}$$

where

$$\tilde{g}(\mathbf{p}) = \int e^{-i\mathbf{r}\cdot\mathbf{p}} g(\mathbf{r})\, d^3\mathbf{r}. \tag{4.10}$$

As an example consider

$$g(\mathbf{r}) = \left(\frac{\beta}{\pi}\right)^{\frac{3}{2}} e^{-\beta r^2}. \tag{4.11}$$

In this case (4.9) leads to

$$\frac{W}{(2\pi)^3} V_d = e^{p^2/4\beta} \langle \mathbf{p}|V|\mathbf{p}\rangle. \tag{4.12}$$

For $\beta$ very large one sees that $\tilde{g}(\mathbf{p})$ has no effect on the energy variation of $v_d$ and $g(\mathbf{r})$ approximates the behaviour of a $\delta$ function.

It would appear, therefore, that if the assumption of separability were reasonable, any large non-locality would show up strongly in the energy dependence of $V_d$, and in this case the results of figs. 1 and 2 would imply that the degree of non-locality is small.

However, there is no a priori reason for assuming a separable potential, and if one relaxes this restriction one has in general

$$\langle \mathbf{x}'|V|\mathbf{x}\rangle = \sum_i G_i(\mathbf{R}) g_i(\mathbf{r}), \tag{4.13}$$

and then

$$\langle \mathbf{p}|V|\mathbf{p}\rangle = \frac{W}{(2\pi)^3} \sum_i V_{di} \int e^{-i\mathbf{r}\cdot\mathbf{p}} g_i(\mathbf{r})\, d^3\mathbf{r}, \tag{4.14}$$

so that the relation between the experimental $V(\mathbf{x})$ and $\langle \mathbf{p}|V|\mathbf{p}\rangle$ is not very well defined.

It seems, thus, that unless one assumes that the optical potential is well represented by (4.1) (or better by (4.5) with $g(\mathbf{r})$ almost a $\delta$ function), the fit between experiment and the theoretical curves is fortuitous. The question then why, if eqs. (4.1) or (4.5) are faithful representations of the optical potential, they fail to predict reasonable angular cross sections, is discussed in the next section.

(ii) It is not simple to get from the optical potential to the differential cross section, since one requires a knowledge of the whole matrix $\langle \mathbf{p}'|V|\mathbf{p}\rangle$,

the off-energy-shell elements of which are rather sensitive to the assumed off-energy-shell behaviour of the $t_\alpha^0$ matrices.

As a first approximation we have calculated the scattering amplitude from eq. (3.16). This just correspond to the Born approximation in the potential $V$. The results are compared with experiment in figs. 4 and 5 for $\pi^-$ on $C^{12}$ at

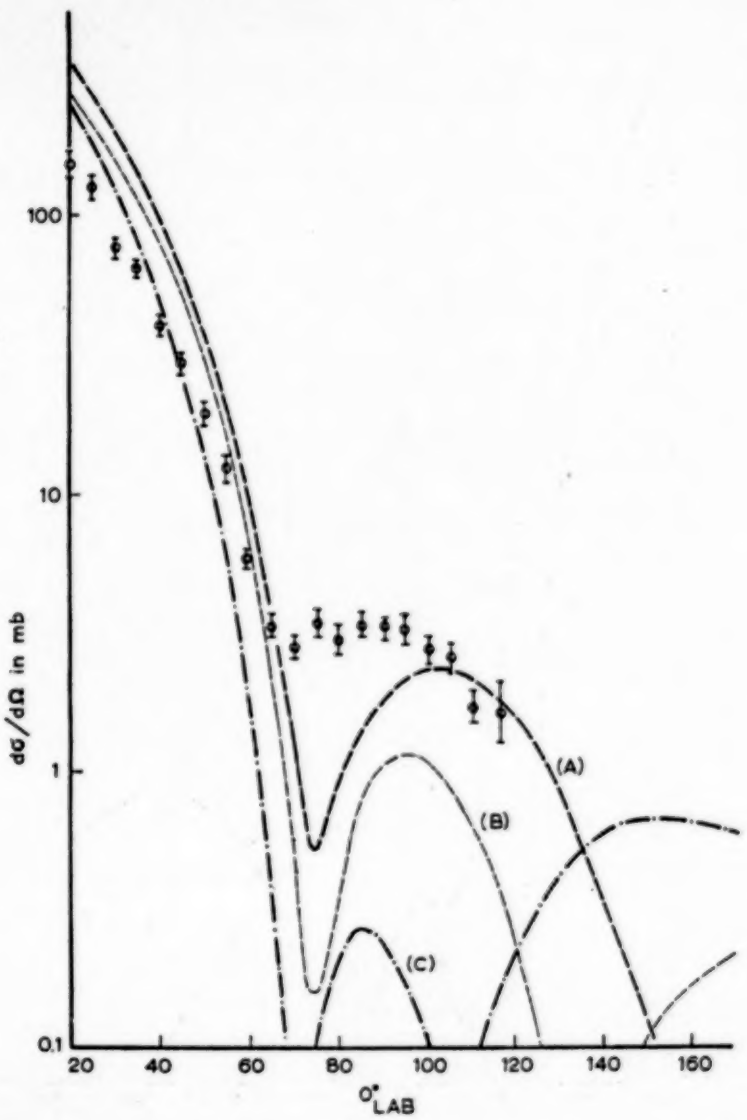


Fig. 4. Variation of the Born approximation cross section for $C^{12}$ at 80 MeV for different radii. (A) $r_0 = 1.1$ fm, (B) $r_0 = 1.2$ fm, (C) $r_0 = 1.4$ fm.

80 MeV and 150 MeV respectively. It is seen that although the over-all agreement is poor, the curves at 80 MeV reproduce well the characteristic maxima and minima of the experimental points, as well as the rather large backward scattering. The fit at 150 MeV, where the impulse approximation is more dubious, is much worse.

Guided by the discussion of the preceding section we have attempted to improve the estimate of the differential cross section as follows. Let us suppose that the potential $V$ is almost local in co-ordinate space at each energy, so that $G(\mathbf{R})$ of (4.5) would represent a good "local" approximation to $\langle \mathbf{x}'|V|\mathbf{x}\rangle$. It is then very reasonable to associate $G(\mathbf{R})$ with the quasi-local approximation of

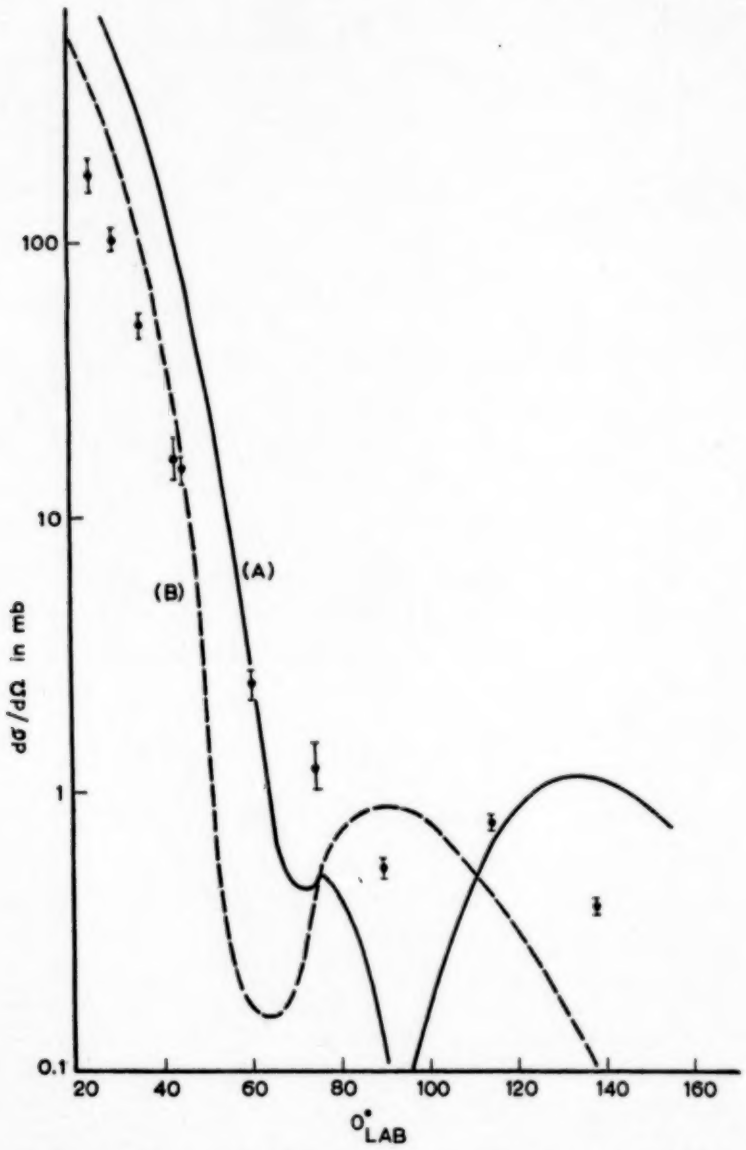


Fig. 5. Variation of the Born approximation cross section for $C^{12}$ at 150 MeV for different radii. (A) $r_0 = 1.1$ fm, (B) $r_0 = 1.4$ fm.

Frank, Gammel and Watson (eq. (3.12)) since theirs seems to be the most direct way of extracting a quasi-local approximation from the general expression for the optical potential.

Let $f(\theta)$ be the exact scattering amplitude in the true optical potential and

suppose that it can be expressed as a Born series in the form

$$f(\theta) = f_1(\theta) + \sum_{i=2}^{\infty} f_i(\theta), \tag{4.15}$$

so that $f_1(\theta)$ is just proportional to $\langle \mathbf{p}'|V|\mathbf{p}\rangle$.

Now let $\bar{f}(\theta)$ be the exact scattering amplitude corresponding to the quasi-local potential $G(\mathbf{R})$ and let its Born decomposition be

$$\bar{f}(\theta) = \bar{f}_1(\theta) + \sum_{i=2}^{\infty} \bar{f}_i(\theta). \tag{4.16}$$

We now assume that it is reasonable to approximate $f(\theta)$ by

$$f(\theta) = f_1(\theta) + \sum_{i=2}^{\infty} \bar{f}_i(\theta) \equiv \bar{f}(\theta) - \bar{f}_1(\theta) + f_1(\theta). \tag{4.17}$$

In this way we hope to be able to take into account approximately the full absorptive effect of the potential (which would be badly represented in Born approximation), and at the same time retain the angular dependence of the Born approximation to the true potential.

It is clear that the approximation will only be reasonable if the Born term of the local potential is not too different from the actual scattering amplitude of the local potential, so that $\bar{f}(\theta) - \bar{f}_1(\theta)$ represents a small overall correction to $f_1(\theta)$. (Of course, if the true optical potential was really well represented by the local potential, the latter requirement would be superfluous, but we know, from attempts to fit the cross sections with local potentials [10] †, that this is not so.)

We have evaluated $\bar{f}(\theta)$ for a number of local potentials by solving the Schroedinger equation numerically on the CERN Mercury computer and we have compared these with their Born approximations. It soon became evident that unless one considered potentials with a very detailed structure in co-ordinate space, it was impossible to ensure that $\bar{f}(\theta) - \bar{f}_1(\theta)$ was reasonably small, especially for values of $\theta > 50°$.

The results of the approximation (4.17) are compared with experiment in fig. 6, for the case of Gaussian and square wells. It is seen that the fit at smaller angles is much better than that obtained from just $f_1(\theta)$ (see fig. 4), but that at larger angles the agreement is still poor.

Thus although (4.17) is able to yield an improved estimate of the scattering, it cannot be considered as reliable, since it is too sensitive to the choice of local potential.

It seems, therefore, that the restriction of our knowledge of the optical potential being limited to only the energy-shell momentum space matrix

† For later experimental work see ref. [13]).

elements, precludes the possibility of making a reliable estimate of the differential cross section, so that the comparison with the experimental angular cross sections cannot be used as conclusive evidence for or against the model of the optical potential which we have used.

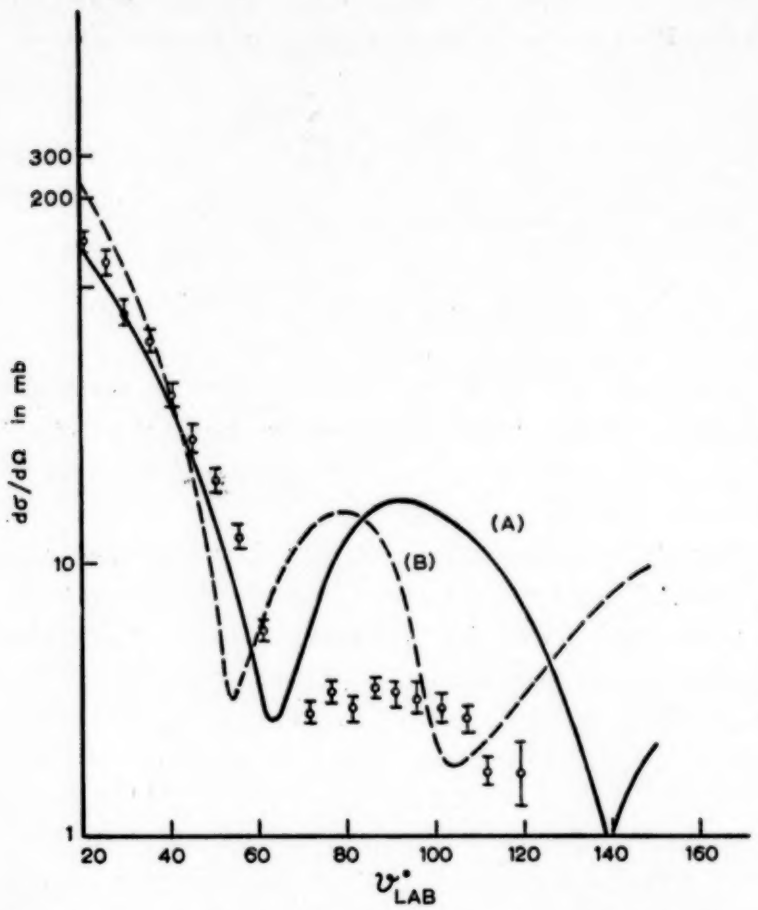


Fig. 6. Differential cross section of the scattering of $\pi^-$ on $C^{12}$ at 80 MeV according to the "quasi optical" model. The value $r_0 = 1.4$ fm is used. (A) Square well, (B) Gaussian well.

On the other hand, the comparison in sect. 4 of the forward matrix elements of the potential with experiment indicate, at least, that the impulsive model is perfectly adequate for predicting the gross or integrated effects of the pion-nucleus interaction.

I am very grateful to Dr. R. J. Eden for his constant encouragement and to the staff of the Mathematical Laboratories at both Cambridge and CERN for help with the numerical computations. Also I wish to thank the Board of the Elsie Ballot Scholarship Fund for their wonderful support during the past three years.

## Appendix

The normalised single particle momentum space wave functions are [11])

$$\phi_{nlm}(\mathbf{k}) = K_{nl}(\mathbf{k})Y_l^m(\theta), \phi) \tag{A.1}$$

with

$$K_{00}(\mathbf{k}) = \left(\frac{4}{\sqrt{\pi}\gamma^{\frac{3}{2}}}\right)^{\frac{1}{2}} \mathrm{e}^{-k^2/2\gamma}, \qquad K_{01}(\mathbf{k}) = \left(\frac{8}{3\sqrt{\pi}\gamma^{\frac{5}{2}}}\right)^{\frac{1}{2}} k\,\mathrm{e}^{-k^2/2\gamma}. \tag{A.2}$$

Neglecting the $n$ subscript and writing $\chi_u$, $\chi_d$ for the single nucleon spin functions the single particle wave functions can be coupled into eigenfunctions of total angular momentum $\psi_{ljm_j}$ as follows:

$$\begin{aligned}
\psi_{0\frac{1}{2}\frac{1}{2}} &= \phi_{00}\chi_u, \qquad \psi_{0\frac{1}{2}-\frac{1}{2}} = \phi_{00}\chi_d,\\
\psi_{1\frac{3}{2}\frac{3}{2}} &= \phi_{11}\chi_u, \qquad \psi_{1\frac{3}{2}-\frac{3}{2}} = \phi_{1-1}\chi_d,\\
\psi_{1\frac{3}{2}-\frac{1}{2}} &= \tfrac{1}{3}\sqrt{3}\{\phi_{11}\chi_d + \sqrt{2}\,\phi_{10}\chi_u\}\\
\psi_{1\frac{3}{2}-\frac{1}{2}} &= \tfrac{1}{3}\sqrt{3}\{\sqrt{2}\,\phi_{10}\chi_d + \phi_{1-1}\chi_u\}
\end{aligned} \tag{A.3}$$

For convenience we label these $\psi_1 \ldots \psi_6$.

The complete $C^{12}$ wave function with total angular momentum zero is then

$$\begin{aligned}
\Psi(1, 2, \ldots, 12) = \frac{1}{6!}\{ &\sum_{\substack{1,\ldots,6\\ \lambda_1,\ldots,\lambda_6}} \delta_{\lambda_1\ldots\lambda_6}\psi_{\lambda_1}(1)\ldots\psi_{\lambda_6}(6)\}\\
&\times\{\sum_{\substack{7,\ldots 12\\ \lambda_7,\ldots,\lambda_{12}}} \delta_{\lambda_7\ldots\lambda_{12}}\psi_{\lambda_7}(1)\ldots\psi_{\lambda_{12}}(12)\},
\end{aligned} \tag{A.4}$$

where $\lambda_i$ takes on the values $1 \ldots 6$ or $7 \ldots 12$ respectively and the first six nucleons may be considered as protons.

Using this wave function we get

$$\begin{aligned}
G_D(\mathbf{k}+\Delta\mathbf{p}, \mathbf{k}) &= \frac{1}{3(\pi\gamma)^{\frac{3}{2}}}\,\mathrm{e}^{-\Delta p^2/2\gamma}\,\mathrm{e}^{-(k^2+\mathbf{k}\cdot\Delta\mathbf{p})/\gamma}\left\{1+\frac{4}{3\gamma}(k^2+\mathbf{k}\cdot\Delta\mathbf{p})\right\},\\
G_{SF}(\mathbf{k}+\Delta\mathbf{p}, \mathbf{k}) &= \frac{1}{18(\pi\gamma)^{\frac{3}{2}}}\frac{1}{\gamma}\,\mathrm{e}^{-\Delta p^2/2\gamma}\,\mathrm{e}^{-(k^2+\mathbf{k}\cdot\Delta\mathbf{p})/\gamma}\{2k_xk_z + k_z\Delta p_x + k_x\Delta p_z\}.
\end{aligned} \tag{A.5}$$

The value of $\gamma$ is determined by relating the r.m.s. value of the radius to $R$ defined by

$$R = \mathrm{r}_0 A^{\frac{1}{3}} \tag{A.6}$$

and yields

$$\gamma = \frac{0.4138}{r_0^2}\,\mathrm{fm}^{-2}. \tag{A.7}$$

The normalised two-nucleon density matrices defined in (3.2), become

$$P_{\text{pp or nn}}(1'2'|12) = \tfrac{1}{15} \sum_{(\lambda_1,\lambda_2)}^{1,2} \{\psi^*_{\lambda_1}(1')\psi^*_{\lambda_2}(2') - \psi^*_{\lambda_1}(2)\psi^*_{\lambda_2}(1)\} \times \{\psi_{\lambda_1}(1)\psi_{\lambda_2}(2) - \psi_{\lambda_1}(2)\psi_{\lambda_2}(1)\}, \quad \text{(A.8)}$$

where the sum is over all pp or nn pairs, and

$$P_{\text{pn}}(1'2'|12) = \tfrac{1}{36} \sum_{\lambda,\mu}^{4} \psi_\lambda{}^*(1')\psi_\mu{}^*(2')\psi_\lambda(1)\psi_\mu(2).$$

Each of the products $\psi_i(1)\psi_j(2)$ can be expressed in terms of $\mathbf{R} = \frac{1}{2}(\mathbf{x}_1 + \mathbf{x}_2)$ and $\mathbf{r} = (\mathbf{x}_1 - \mathbf{x}_2)$, and the integration over $\mathbf{r}$ is then carried out yielding the two-nucleon C. M. distributions. We average over the pp, nn and np densities and get (see eq. (3.7)):

$$\bar{\rho}(R) = U\left(\frac{\nu}{\pi}\right)^{\frac{3}{2}} \{0.548 + 0.201\,\nu R^2 + 0.039\,\nu^2 R^4\}\, \mathrm{e}^{-\nu R^2}, \quad \text{(A.9)}$$

with

$$\nu = \gamma/\hbar^2.$$

## References


1) K. M. Watson and C. Zemach, Nuovo Cim. **10** (1958) 452
2) C. F. Chew and M. L. Goldberger, Phys. Rev. **87** (1952) 778
3) L. M. Frank, J. L. Gammel and K. M. Watson, Phys. Rev. **101** (1956) 891; L. Kisslinger, Phys. Rev. **98** (1955) 761
4) C. Møller, Mat. Fys. Medd. Dan. Vid. Selsk. **22**, No. 23 (1945)
5) B. Lippman and J. Schwinger, Phys. Rev. **79** (1950) 469
6) K. M. Watson, Phys. Rev. **89** (1953) 575
7) E. Leader, Thesis (Part I), Cambridge University 1960
8) K. A. Bruckner, R. Serber and K. M. Watson, Phys. Rev. **84** (1951) 258
9) M. Gell-Mann and K. M. Watson, An. Rev. Nuc. Sc. (1954)
10) J. G. Kessler and L. M. Lederman, Phys. Rev. **94** (1954) 689
11) I. Talmi, Helv. Phys. Acta **25** (1952) 185
12) Anderson, in Proc. of the Rochester Conf. (1956) p. 20
13) W. F. Baker, J. Rainwater and R. N Williams, Phys. Rev. **112** (1958) 1763

2·D: 2.F *Nuclear Physics* **26** (1961) 193—202; © *North-Holland Publishing Co., Amsterdam*
Not to be reproduced by photoprint or microfilm without written permission from the publisher

# ENERGY AND ANGULAR DISTRIBUTIONS OF PROTONS EMITTED FROM $Al^{27}$ DUE TO 14.2 MeV NEUTRON INTERACTIONS

K. G. NAIR, K. N. IYENGAR and R. RAMANNA
*Tata Institute of Fundamental Research, Bombay*

Received 30 January 1961

**Abstract:** The $Al^{27}(n, p)Mg^{27}$ reaction has been studied for an incident neutron energy of 14.2 MeV with emulsion technique. This was a preliminary experiment in a series to be conducted to test the validity of the statistical model and the various direct interaction models. In the present experiment the energy and angular distributions of the emitted protons indicate features of a non-compound-nucleus mechanism for the high energy part.

## 1. Introduction

The results from a large number of experiments reported during recent years concerning the cross sections [1]), energy spectra [2, 3]) and angular distributions [4–6]) of the protons emitted from various elements due to 14 MeV incident neutrons, show that the compound nucleus mechanism and the statistical theory cannot completely explain the experimental data. The main results of these experiments can be summarised as follows:

1. More protons are observed in the low as well as high energy part of the emitted proton spectrum in (n, p) reactions than are predicted by the statistical theory. Consequently, the level density obtained from experimental data does not fit very well with the conventional level density formula derived from the statistical theory.

2. The angular distribution of the protons shows a peaking in the forward direction whereas the statistical theory predicts an angular distribution which is symmetric about 90° in the c.m. system.

The increase in the high energy part of the spectrum has been explained by the volume direct interaction theory of Brown and Muirhead [7]) and the surface direct interaction theory of Austern, Butler and MacManus [8]). In order to explain the increase in the low energy part of the spectrum, many theories have been put forward such as the diffuseness of the nuclear potential (Kikuchi [9]) and the increase in penetrability due to the state of excitation of the residual nucleus. The latter effect has been treated in detail by Lane and Parker [10]).

All the direct interaction theories predict a peaking of the angular distribution in the forward direction. If one assumes isotropy in angular distribution in

compound nucleus decay, the anisotropic part experimentally found should give a measure of the total direct interaction contribution. In an earlier paper by Mani and Nair [11]), the volume direct interaction cross sections for processes of the type (n, p) and (n, n') were calculated assuming the theory of Brown and Muirhead [7]).

A detailed treatment of level density has been given by Ericson and Strutinsky [12]), Newton [13]) and Ericson [14]).

In the present paper, the results of a study of the energy and angular distributions of protons emitted from $Al^{27}$ due to the interactions with 14.2 MeV neutrons are reported. The asymmetries in the angular distributions of the protons have been attributed to a non-compound-nucleus mechanism. The level density and nuclear temperature parameters obtained from experiment are compared with the predictions of the statistical theory.

## 2. Experimental Procedure

Nuclear emulsion was used as the detector. The camera was similar to the one used by Allan [4]) in his studies of (n, p) reactions in Cu and $Fe^{54}$. A single 2.54 cm × 7.62 cm Ilford C2 nuclear emulsion plate of thickness 200 $\mu$m was surrounded symmetrically by a cylindrical aluminium foil of thickness 5 mg/cm$^2$, all parts of which were exposed to the incident neutron beam (fig. 1). The advantages of this set up are the high density of tracks in the plate and the fact that measurements on a single plate will give all the data required for the energy as well as angular distribution studies as compared to the conventional case where a number of such studies on different plates are required.

The nuclear emulsion was screened from the direct neutrons by a brass shadow cone 1.27 cm thick and 48.26 cm long. The surface of the emulsion was such that it was below that of the brass plate by 0.030 cm so that the entire length of the shadow cone was effective in shielding the emulsion from the direct neutrons. The camera was lined inside with 1 mm thick lead sheet to stop the recoil protons from brass.

The incident beam of neutrons was produced by the bombardment of a gold-backed tritium target with 350 keV deuterons in a Cockroft-Walton accelerator. The energy of the neutrons at 90° to the deuteron direction was 14.2 MeV with a possible spread of 7 %.

The plates were developed and subjected to the shrinkage inhibition treatment of Krishnamoorthy [15]). The tracks were measured with a Leitz Ortholux microscope using oil immersion and 800× magnification. The track selection criteria were as follows:

1. The track must originate from the emulsion surface and be oriented within the angle defined by the aluminium target. This was determined by finding the average dip angle as obtained from the peak of a dip distribution curve (fig. 2).

The width at half maximum of this curve gives the probable deviation from this value and hence the lower and upper limits to the dips of acceptable tracks.

2. The grain density must increase as one scans along the track away from the point of entry till it ends in the emulsion. This shows that the particle has

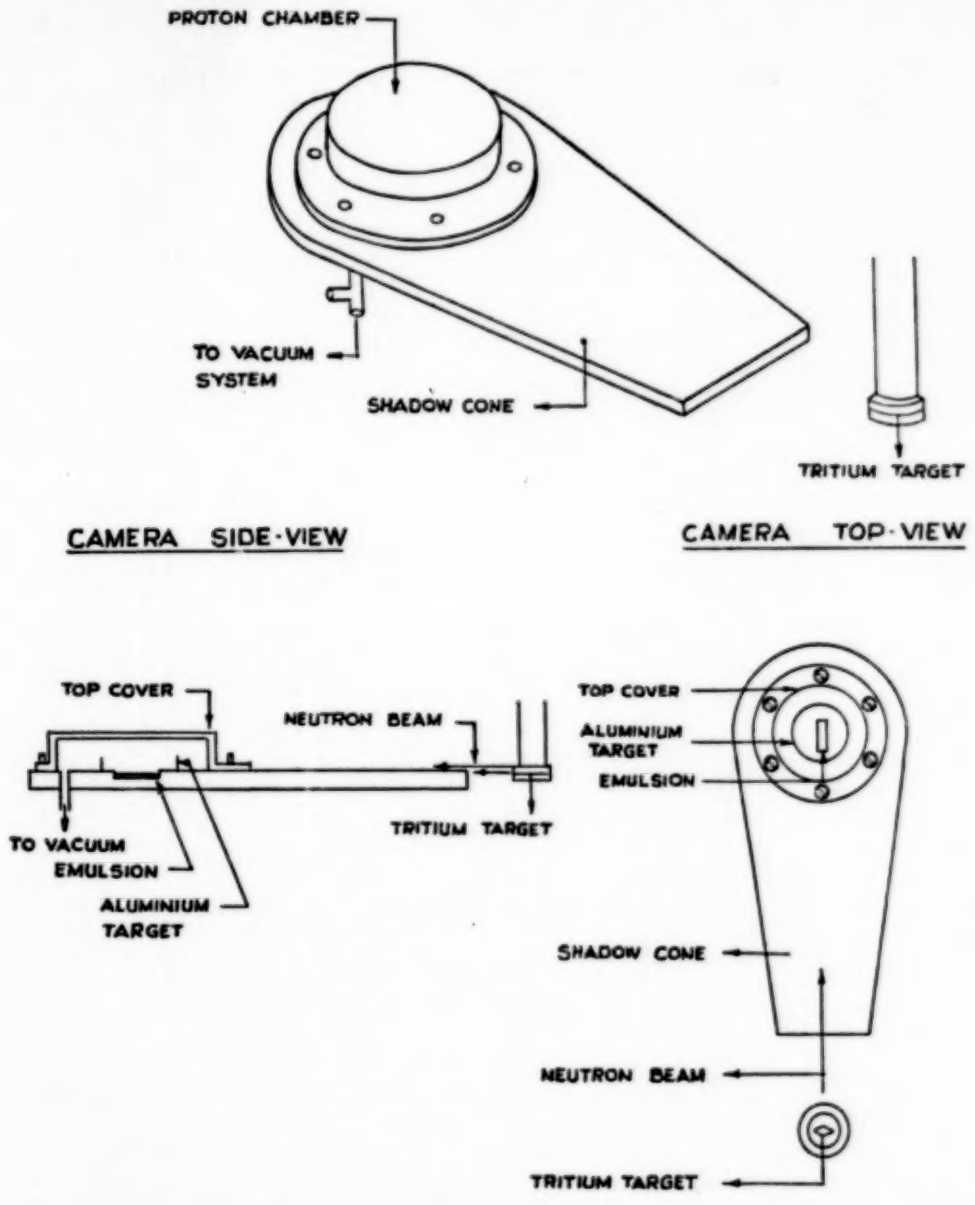


Fig. 1. A three-dimensional view of the camera.

entered from the surface and ended in emulsion. A track which ends either in the air or in the glass is rejected because its range measurement is not complete.

3. Because of the non-uniformity of the emulsion surface and possible distortions, all tracks starting from within $0-5$ $\mu$m of the emulsion surface are accepted as originating from the surface.

4. The tracks must not be alpha particle tracks and this is a very difficult criterion to satisfy specially for the shorter tracks with ranges less than about 10 $\mu$m.

A total emulsion area of about 3 cm$^2$ was scanned yielding over 1500 tracks out of which 800 were accepted finally as surviving all the screening. For each track the measurements made were its azimuth angle with respect to the

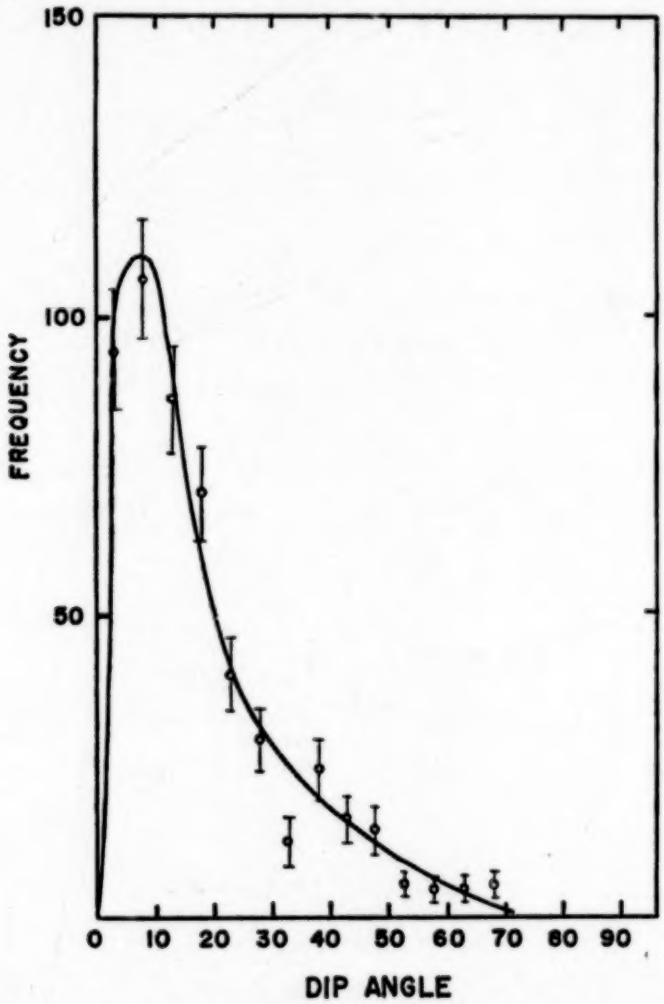


Fig. 2. A typical dip distribution curve for protons observed in the emulsion. The half-width is 17°.

incident neutron direction in the plane of the emulsion, its dip angle and the total range in the emulsion. From the dip and azimuth angles, the space angle $\theta_{c.m.}$ in the c.m. system was calculated. The energy of the proton corresponding to any range was calculated using the range-energy tables for dry emulsion experimentally determined by Rotblat [16]). Allowance was made for the loss of proton energy in passing through the target by adding to the observed energy of each proton the energy that it would have lost in traversing half the thickness of the foil taking into account the angle with which it dips towards the emulsion.

## 3. Results and Discussion

The total energy spectrum of protons in the c.m. system is given in fig. 3. The emitted protons are the results of the processes (n, p), (n, pn) and (n, np). The arrows show the proton energies corresponding to the known excited states in $Mg^{27}$ which are 1, 1.66, 3.5, 3.56, 3.75, 4.13 and 4.75 MeV above the ground

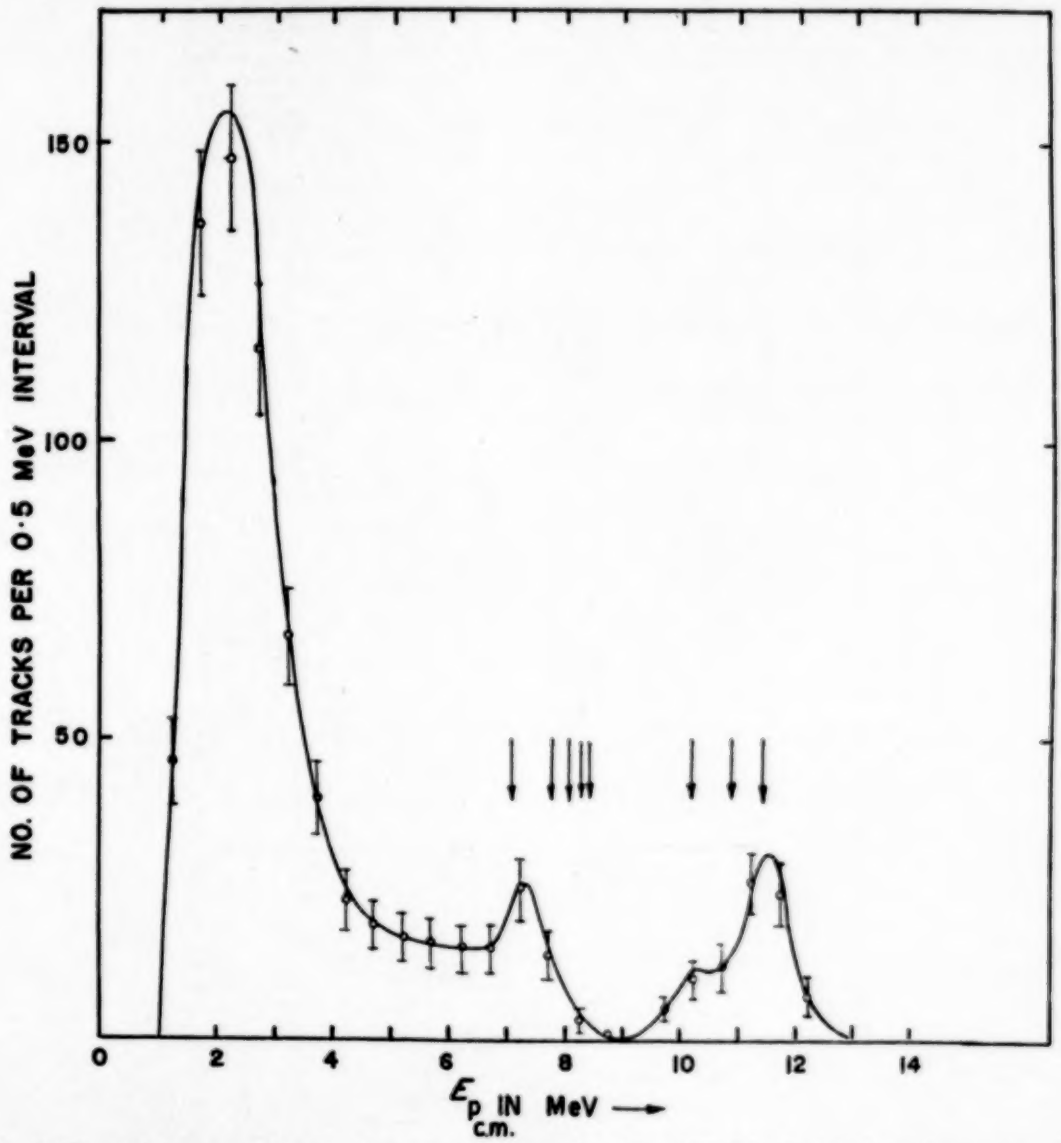


Fig. 3. The total energy distribution of protons emitted by $Al^{27}$. The incident neutron energy is 14.2 MeV.

level. These values were reported by Hinds, Middleton and Parry [17]) in a study of (d, p) reactions in $Mg^{26}$. The peak at 11.5 MeV, corresponding to the ground state of $Mg^{27}$, seems to be very much pronounced. The peaks reported by Colli *et al.* [18]) at 3.7 MeV and 5 MeV and by Allan [3]) at about 4 MeV are not observed by us. The levels are very dense in the range 0—5 MeV proton energy so that any peak which might be observed there cannot be due to the (n, p) process.

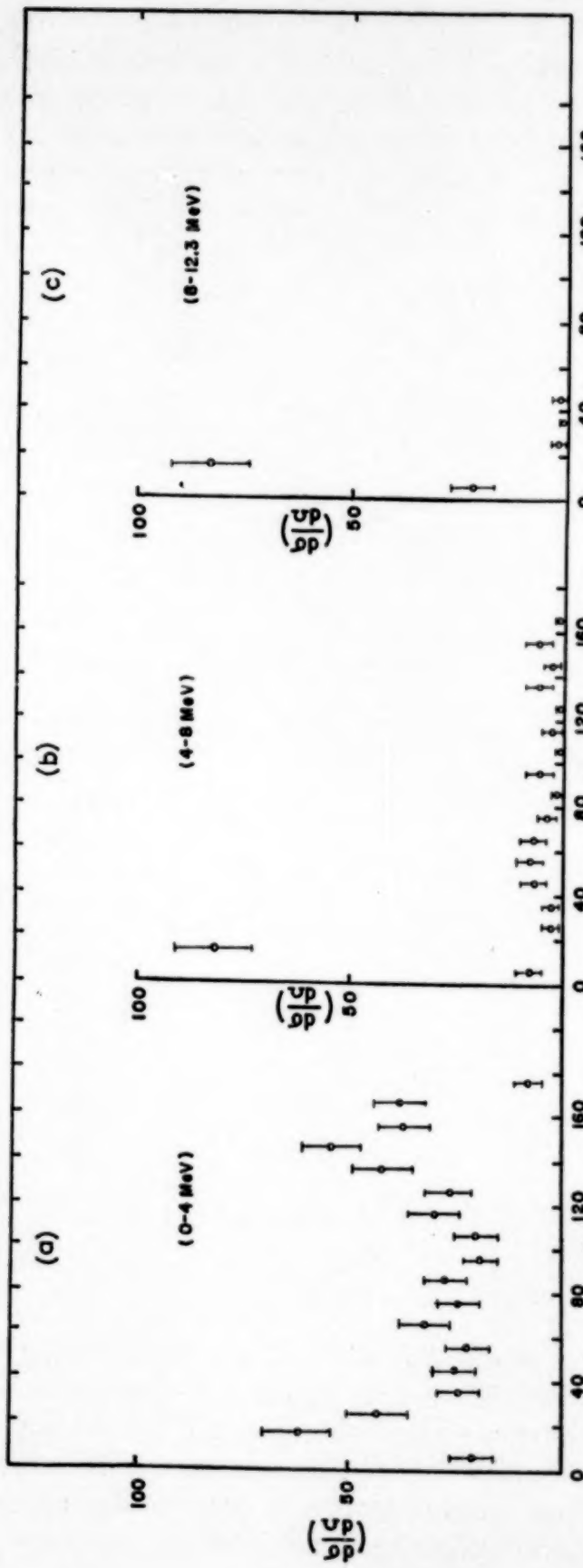


Fig. 4. Angular distributions for protons emitted by $Al^{27}$ for three proton energy intervals (shown between parentheses).

Angular distribution studies were made in three energy regions, 0—4 MeV, 4—8 MeV and 8—12.3 MeV (figs. 4(a), 4(b) and 4(c)). Fig. 4(a) shows an approximate symmetry about 90° indicating that in the low energies the decay follows the compound nucleus formation. In the higher energies the angular distribu-

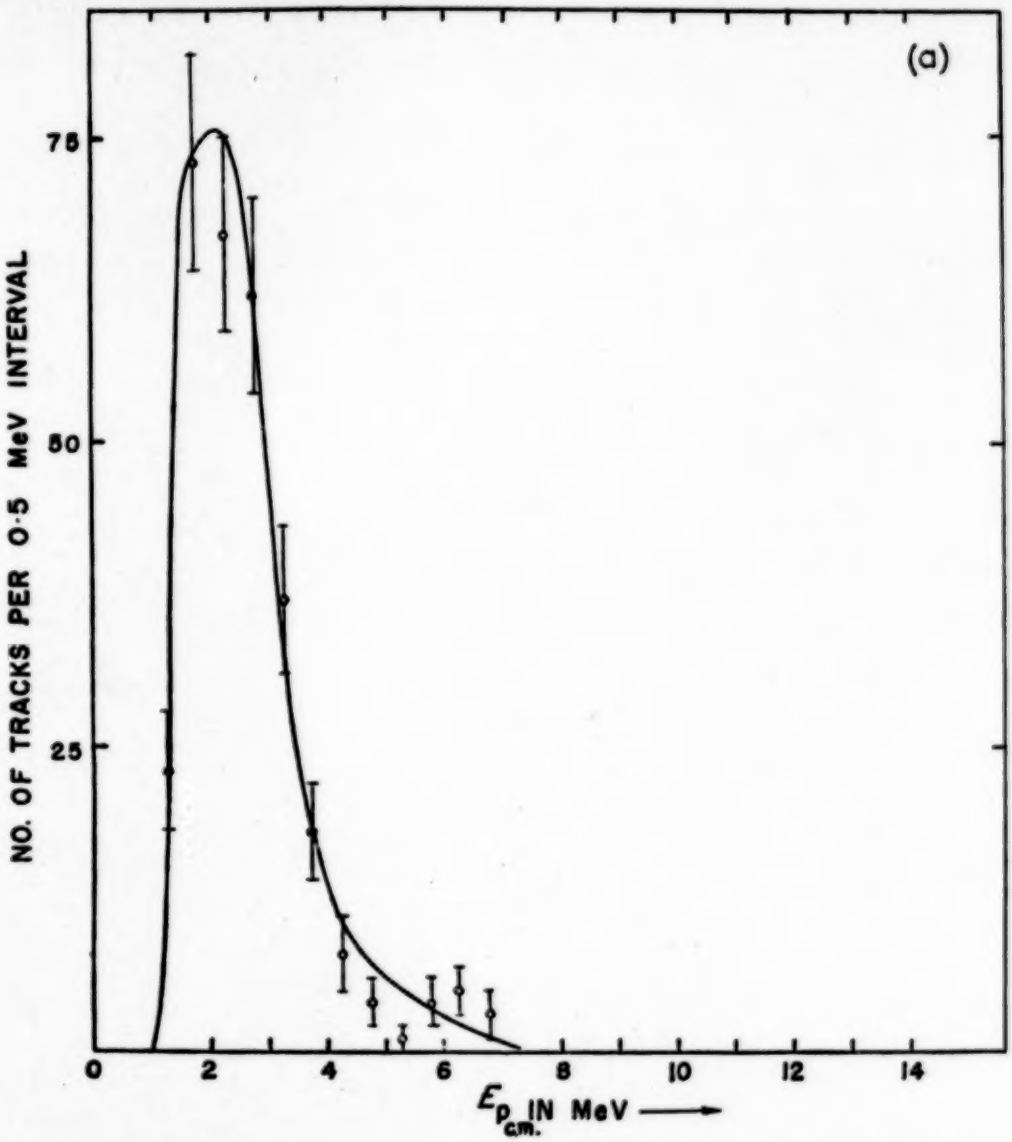


Fig. 5(a). Energy distribution of protons emitted in the backward directions by $Al^{27}$. The incident neutron energy is 14.2 MeV.

tion reported by Overseth and Peck [5]) does not show any forward peak whereas Brown *et al.* [19]) have a rising differential cross section at extreme forward angles, i.e. at 10° and 20°. Due to lack of statistics in the high energy range we cannot say anything conclusive. But in the angular distribution for the interval 8—12.3 MeV there are points at 10° and 20° far above the other points.

In figs. 5(a) and 5(b) the energy spectra in the forward and backward angles are given. In the spectrum for backward angles (fig. 5(a)) no protons are observ-

ed in the energy range 7—12.3 MeV. Since emission at backward angles essentially results from compound nucleus decay, it is safe to assume that most of the protons in the 7—12.3 MeV range, which are observed at forward angles, are emitted due to a non-compound process. In addition the energy distribution in

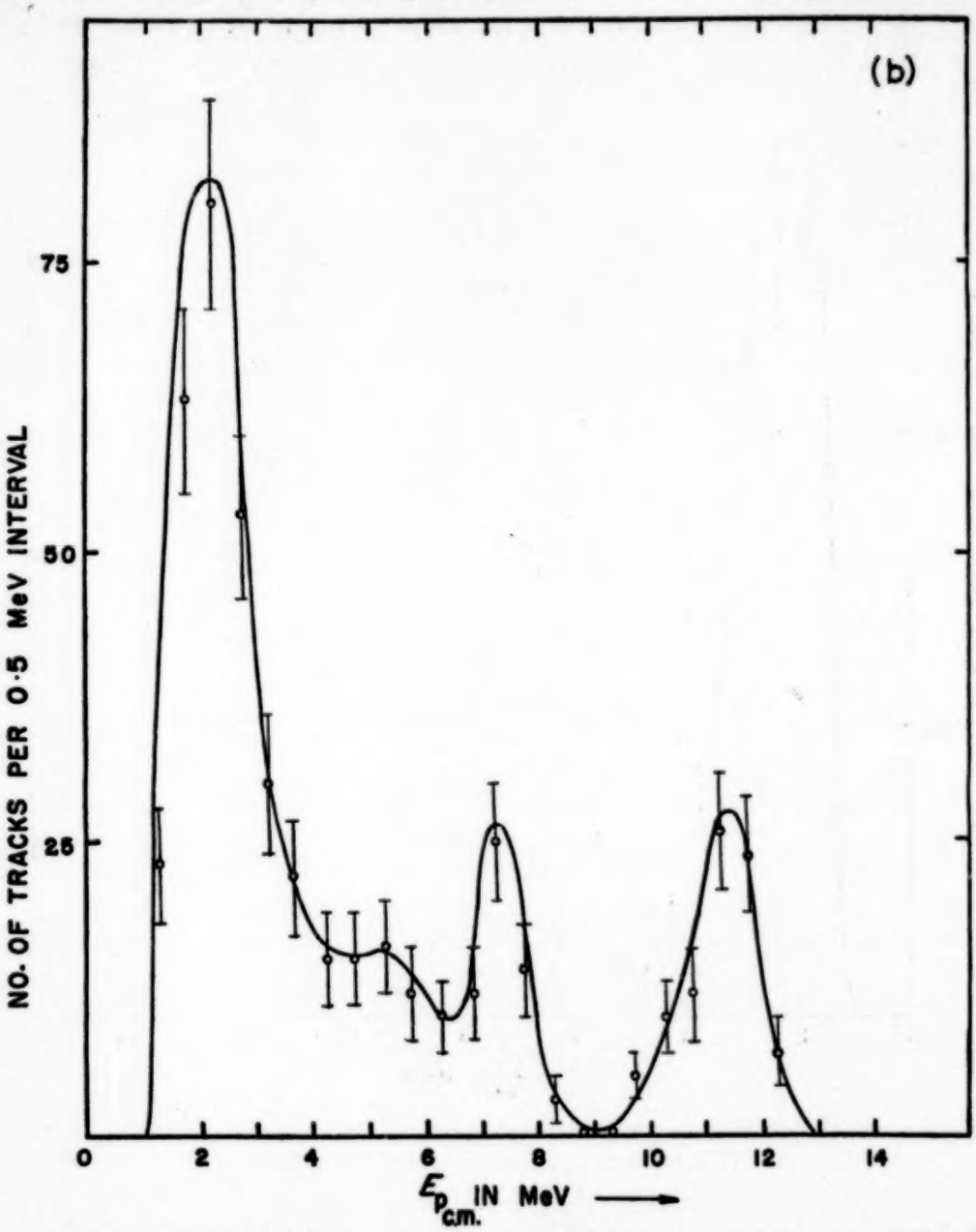


Fig. 5(b). Energy distribution of protons emitted in the forward directions by $Al^{27}$. The incident neutron energy is 14.2 MeV.

the forward angles (fig. 5(b)) shows peaks in the high energy part confirming the non-compound nature of the emission of high energy protons.

The quantity $n(E)/E\sigma$ is the level density of the residual nucleus at the excitation energy $E_0-E$, according to the statistical theory; here, $E_0$ is the

maximum energy of the emitted proton, $n(E)$ is the proton yield in the energy range between $E$ and $E+dE$ and $\sigma$ is the calculated cross section for compound nucleus formation by protons (Blatt and Weisskopf [20])) with $R = 1.35\ A^{\frac{1}{3}}$ fm. From the energy spectrum at backward angles the quantity $\ln [n(E)/E\sigma]$ was calculated and plotted as a function of the energy of the protons. Fig. 6

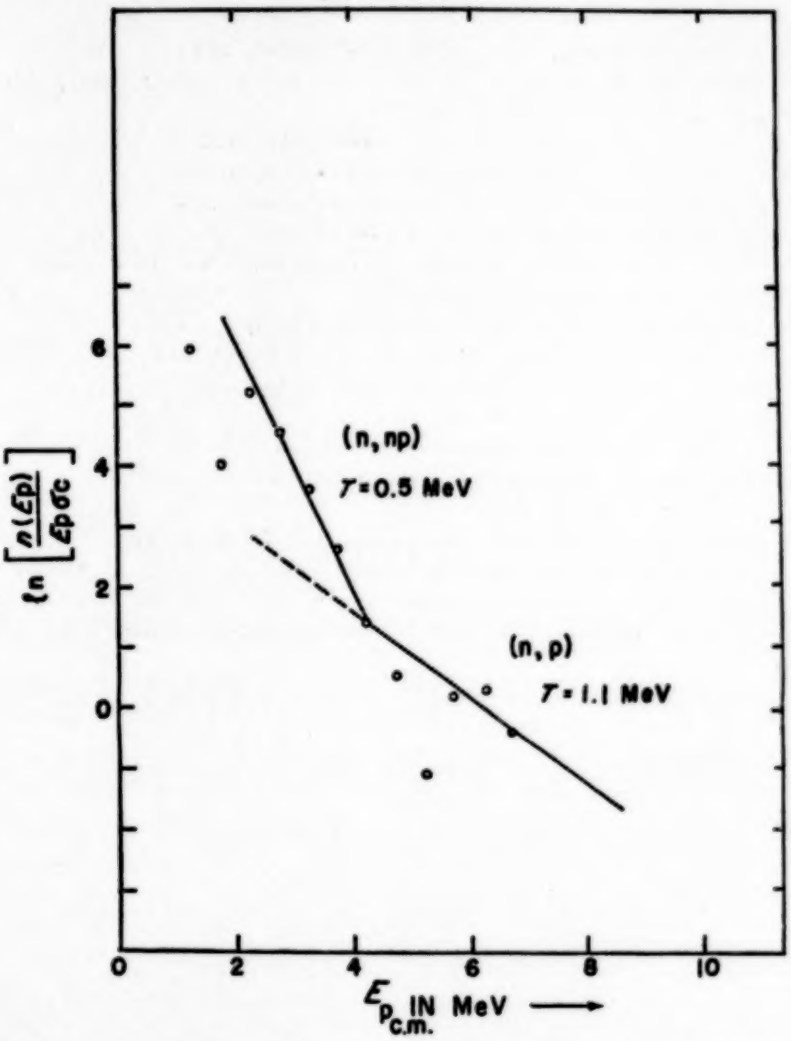


Fig. 6. A statistical theory plot of the level density of the residual nucleus.

shows this statistical theory plot of the level density, which consists of two straight lines corresponding to the reactions $Al^{27}$(n, p)$Mg^{27}$ and $Al^{27}$(n, np)$Mg^{26}$. The reciprocals of the slopes of the lines give the temperature parameters $T$ and it is found that for the (n, p) reaction $T = 1.1$ MeV and for the (n, np) reaction $T = 0.5$ MeV. At the low proton energies (0—2 MeV) this assignment of temperature may not be strictly valid because of the contributions from (n, d) and (n, $\alpha$) reactions, since deuterons, alphas and protons are indistinguishable in the emulsion in this range.

The authors are thankful to Dr. D. L. Allan for a private communication about the details of the track selection criteria and to Mr. M. R. Hiranandani for help in the processing of the nuclear emulsion plates. Thanks are due to Mr. P. N. Krishnamoorthy for some helpful discussions.

## References

1) E. B. Paul and R. L. Clarke, Can. J. Phys. **31** (1953) 267
2) L. Colli, M. Pignanelli, A. Rytz and R. Zurmuhle, Nuov. Cim. **9** (1958) 280
3) D. L. Allan, Proc. Phys. Soc. **70** (1957) 195
4) D. L. Allan, Nuclear Physics **6** (1958) 464; **10** (1959) 348
5) O. E. Overseth and R. A. Peck, Phys. Rev. **115** (1959) 993
6) I. Kumabe and R. W. Fink, Nuclear Physics **15** (1960) 316
7) G. Brown and H. Muirhead, Phil. Mag. **2** (1957) 473
8) N. Austern, S. T. Butler and H. MacManus, Phys. Rev. **92** (1953) 350
9) K. Kikuchi, Prog. Theo. Phys. **17** (1957) 643
10) A. M. Lane and K. Parker, Nuclear Physics **16** (1960) 690
11) G. S. Mani and K. G. Nair, Proc. Ind. Acad. Sci. **5** (1960) 243
12) T. Ericson and V. Strutinski, Nuclear Physics **8** (1958) 284
13) T. D. Newton, Can. J. Phys. **34** (1956) 804
14) T. Ericson, Nuclear Physics **8** (1958) 265; **11** (1959) 481
15) P. N. Krishnamoorthy, Proc. Ind. Acad. Sci. **5** (1957) 327
16) J. Rotblat, Nature **167** (1951) 550
17) S. Hinds, R. Middleton and G. Parry, Proc. Phys. Soc. **71** (1958) 49
18) L. Colli, F. Cvelbar, S. Micheletti and M. Pignanelli, Nuov. Cim. **14** (1959) 81
19) G. Brown, G. C. Morrison, H. Muirhead and W. T. Morton, Phil. Mag. **2** (1957) 785
20) J. M. Blatt and V. F. Weisskopf, Theoretical nuclear physics (John Wiley and Sons, New York, 1952)

2.D

*Nuclear Physics* **26** (1961) 203—208; © *North-Holland Publishing Co., Amsterdam*

Not to be reproduced by photoprint or microfilm without written permission from the publisher

# THE ANGULAR DISTRIBUTIONS OF CHARGED PARTICLE GROUPS FROM THE DEUTERON BOMBARDMENT OF NITROGEN

W. M. JONES, D. G. WATERS and V. M. ROUT

*Research Laboratory, Associated Electrical Industries, Aldermaston Court, Aldermaston, Berkshire, England*

Received 23 January 1961

**Abstract:** The reaction mechanism for the $p_0$, $p_1$, $p_2$, $p_3$ and $\alpha_0$ groups from the $N^{14}$(d, p)$N^{15}$ and $N^{14}$(d, $\alpha$)$C^{12}$ reactions in the region of 2 MeV bombarding energy appears to be predominantly that of compound nucleus formation with a comparatively small number of compound levels of opposite parity participating. These levels are not sufficiently numerous to be treated in a strictly statistical manner despite the high excitation energy of the $O^{16}$ compound nucleus which is in the region of 22 MeV.

## 1. Introduction

The angular distributions of the products of nuclear reactions induced by 1 to 3 MeV deuterons are of interest for the study of reaction mechanisms. In this energy range both direct interaction and compound nucleus processes may be expected to contribute to the reaction mechanism. If the compound nucleus mechanism predominates, the angular distributions from the $N^{14}$+D reactions might be expected to exhibit the features predicted from the statistical theory of compound nucleus processes, in view of the high excitation ($\approx$ 22 MeV) of the $O^{16}$ compound nucleus.

Reactions induced by deuterons incident on $N^{14}$ have been investigated in the energy range below 1 MeV (refs. [1–5])), and in the energy range around 8 MeV (refs. [6–8])). In the intermediate energy region results have been reported for the $p_0$ and ($p_1$+$p_2$) groups from the $N^{14}$(d, p)$N^{15}$ reaction [9]), and for the $\alpha_0$ group from the $N^{14}$(d, $\alpha$)$C^{12}$ reaction [10]).

The present paper reports the angular distribution results obtained for the $p_0$, ($p_1$+$p_2$) and $p_3$ groups from $N^{14}$(d, p)$N^{15}$ and the $\alpha_0$ group from $N^{14}$(d, $\alpha$)$C^{12}$ at a bombarding energy of 1.4 MeV and also for the $p_0$ and ($p_1$+$p_2$) groups from the same reaction at 2.4 MeV bombarding energy.

## 2. Experimental Method

The measurements were carried out using an angular distribution camera [11]) with the deuteron beam accelerated by the A.E.I. electrostatic generator. Two exposures were made, using Ilford C2 nuclear emulsions 200 $\mu$m thick. In the

first, the 1.4 MeV deuteron beam entered the camera which contained the nitrogen target gas at a pressure of 8 mm Hg. In the 2.4 MeV exposure, an air target at approximately the same pressure was used. For both exposures the gas scattering gap was enclosed by aluminium foils 0.1 mg/cm² thick in order to prevent emulsion fogging. For the most forward angles in the lower energy exposure, this foil thickness was increased to 3.5 mg/cm² to stop the high intensity, elastically scattered deuterons. The total beam charge was estimated from the charge collected by the vacuum Faraday cup mounted at the end of the scattering gap and connected to a beam current integrator.

## 3. Results

### 3.1. THE 1.4 MeV BOMBARDING ENERGY

A histogram of track lengths observed at 130° to the beam direction is shown in fig. 1. The $p_0$, $(p_1+p_2)$ and $p_3$ groups correspond to the ground, (5.28+5.31)

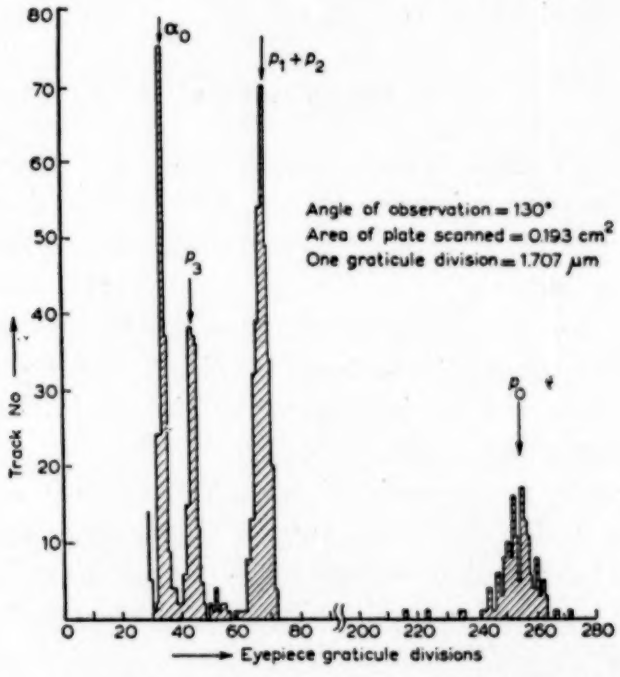


**Fig. 1. Histogram of proton and alpha particle tracks from the 1.4 MeV deuteron bombardment of nitrogen.**

MeV and 6.33 MeV states of $^{15}N$ whilst $\alpha_0$ is the ground state transition group for the $^{14}N(d, \alpha)^{12}C$ reaction. The angular distributions for these groups are shown in figs. 2, 3, 4 and 5. The statistical errors are shown for each point. The relative values of the total cross-sections are 1 : 2.31 : 0.92 : 1.24, respectively, to within a few per cent, assuming that the Legendre polynomial fits shown in the figures can be extrapolated to 0° and 180° at the extremes of the angular range.

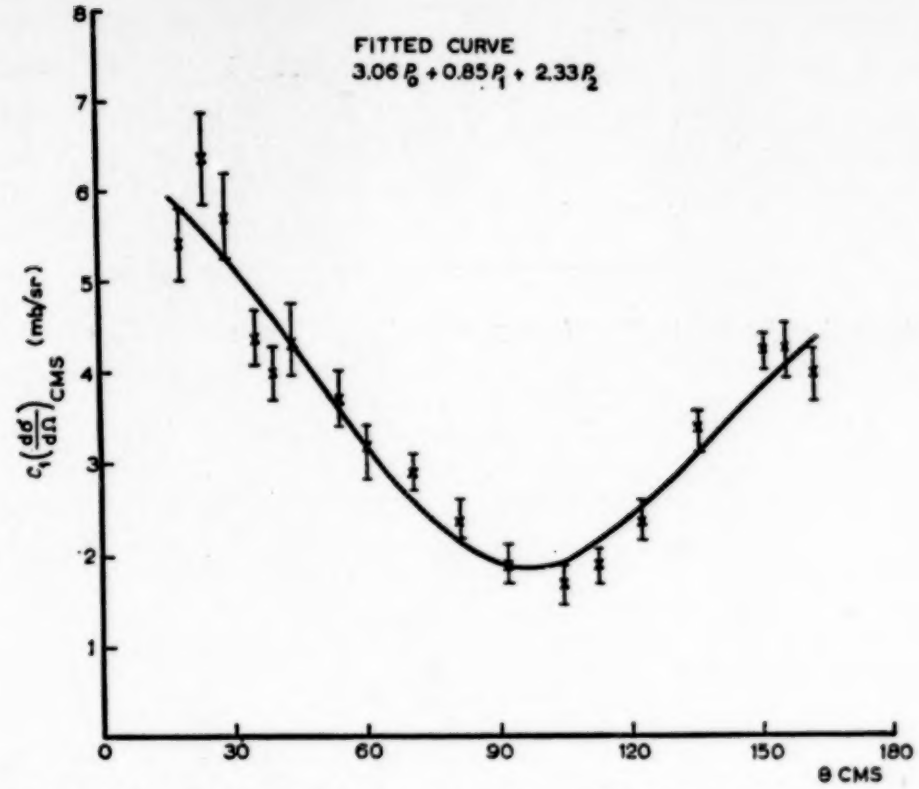


Fig. 2. Angular distribution of the $p_0$ group from $N^{14}(d, p)N^{15}$ at $E_d = 1.4$ MeV.

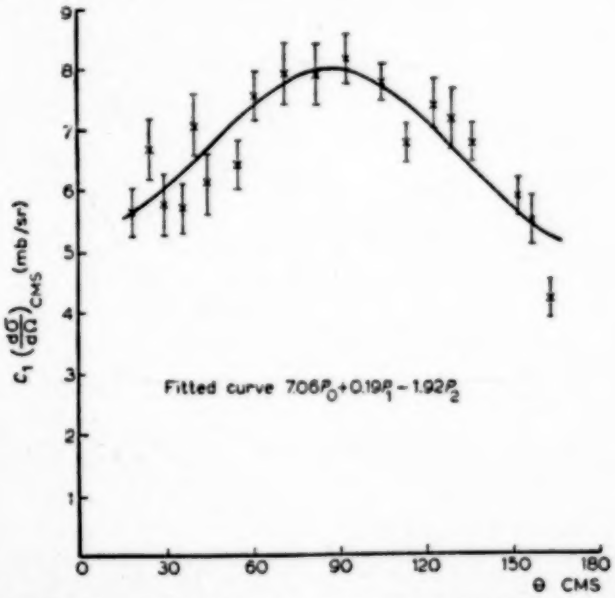


Fig. 3. Angular distribution of the $(p_1+p_2)$ group from $N^{14}(d, p)N^{15}$ at $E_d = 1.4$ MeV.

### 3.2. THE 2.4 MeV BOMBARDING ENERGY

The results of the $p_0$ and $(p_1+p_2)$ groups are shown in figs. 6 and 7. The relative values of the total cross-sections of these groups (calculated as for the previous section) are 1 : 2.08, respectively, to an accuracy of a few per cent.

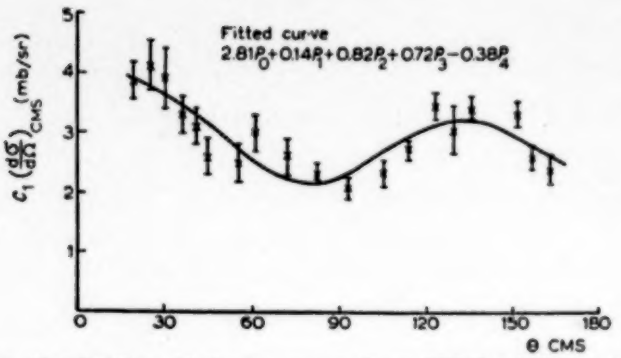


Fig. 4. Angular distribution of the $p_3$ group from $N^{14}(d, p)N^{15}$ at $E_d = 1.4$ MeV.

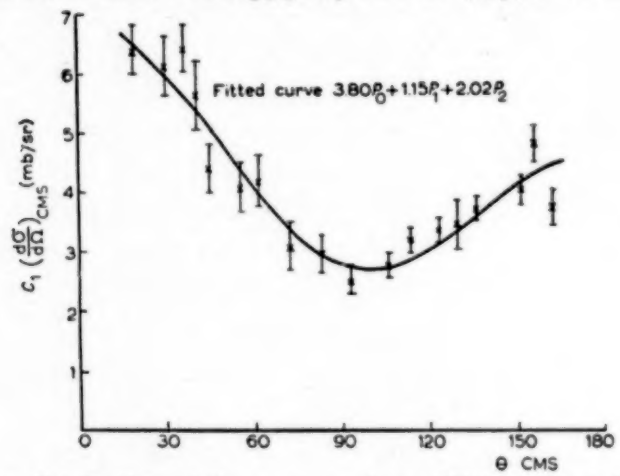


Fig. 5. Angular distribution of the $\alpha_0$ group from $N^{14}(d, \alpha)C^{12}$ at $E_d = 1.4$ MeV.

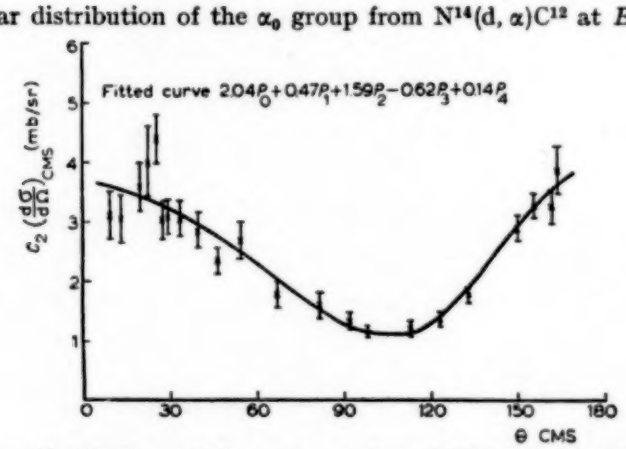


Fig. 6. Angular distribution of the $p_0$ group from $N^{14}(d, p)N^{15}$ at $E_d = 2.4$ MeV.

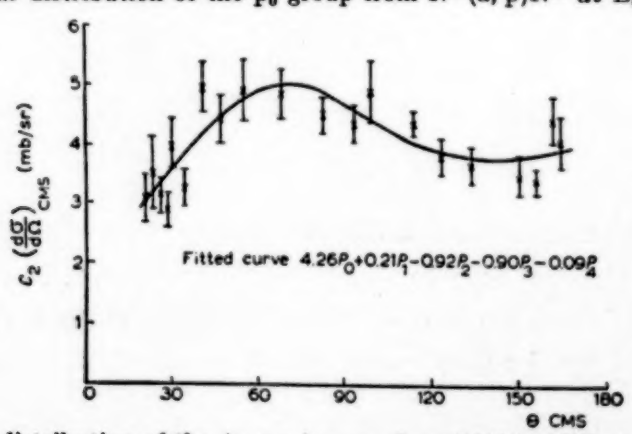


Fig. 7. Angular distribution of the $(p_1+p_2)$ group from $N^{14}(d, p)N^{15}$ at $E_d = 2.4$ MeV.

### 3.3. ABSOLUTE CROSS-SECTIONS

The absolute cross-sections for the various charged particle groups observed in this work cannot be measured directly because of uncertainties in the measurement of the total beam charge. These arise from the fact that only a fraction of the beam passing along the axis of the scattering gap is collected in the vacuum Faraday cup due mainly to scattering in the target gas and window. For the higher energies in which an air target was used, the intensity of the nitrogen groups may be referred to that of the $O^{16}$(d, p)$O^{17}$ ground state group whose absolute differential cross-section has been measured [12]) at 53° (CMS) to the beam direction for the deuteron energy range 2.3 to 3.9 MeV. The value given by these authors for the present deuteron energy of 2.41 MeV is $18\pm2$ mb/sr.

The deuteron energy spread in their target was approximately [13]) 185 keV compared to the beam energy spread of about 15 keV width at half-maximum in the present work due to straggling. The use of their value for the absolute differential cross-section in order to calculate the total beam in the present work is only justified if no narrow resonances occur in this region.

On this basis the constant of proportionality $C_2$ on figs. 6 and 7 is 1.3 with an error of $\pm0.2$.

No accurate estimate has been possible for the value of $C_1$ on the lower energy angular distributions but it is expected to lie between 1.4 $C_2$ and 2.8 $C_2$.

## 4. Discussion of Results

The results in figs. 2—7 are shown together with Legendre polynomial expansions fitted by the least squares method using a Pegasus digital computer.

The results for all the proton groups and the ground state $\alpha$ group require terms no higher than the fourth order to give a reasonable fit and in many cases terms up to the second order suffice. These results may be understood on the basis of a predominantly compound nucleus reaction mechanism. The existence of appreciable odd order terms in all these cases, except for the $(p_1+p_2)$ group at the lower energy, is contrary to what would occur if the participating compound nucleus levels could be treated statistically since this would dictate symmetry about 90°. The anisotropies expected in the statistical case cannot be calculated using the theory of Wolfenstein [14]) because the number of residual levels following the decay of the $O^{16}$ compound nucleus is few. This makes the choice of the $F(J)$ factor, which is related to the total width of a compound level of spin $J$ for all decay products, rather arbitrary. Nevertheless the observed anisotropies seem too large in general to be consistent with the assumption that the levels in the compound nucleus can be treated statistically.

The forms of the angular distributions of the $p_0$ and $(p_1+p_2)$ groups appear to change little with bombarding energy except that for the higher energy, the

inclusion of polynomials up to the fourth order shows the participation of d-wave deuterons in the reactions. The relative insensitivity of these distributions to changes in bombarding energy in this energy range is in agreement with the work of Wyly [9]), although the details of the distributions at similar energies are somewhat different.

## 5. Conclusions

It is concluded for the $p_0$, $(p_1+p_2)$, $p_3$ and $\alpha_0$ groups that

(a) the reactions giving rise to these groups occur predominantly via compound nucleus formation in which a limited number of levels of opposite parity participate;

(b) these participating levels, which occupy an excitation energy range of about 20 keV, are not sufficiently numerous to be treated in a strictly statistical manner;

(c) the variations in form of the $p_0$, $(p_1+p_2)$ and $\alpha_0$ angular distributions with beam energy seen in the present and earlier work are due to variations in the fairly small sample of compound nucleus levels involved.

The authors wish to thank Drs. D. R. Chick and S. E. Hunt for advice and encouragement, Dr. H. C. Newns and Professor B. H. Flowers for their comments on the direct interaction process and Dr. L. Goldfarb for advice on the statistical theory of nuclear reactions. The help of Mr. F. Cheetham in maintenance of the electrostatic generator and Misses S. J. May, R. A. P. Jemmett and O. V. Lake in scanning the plates is much appreciated. Messrs. J. E. Spinks and N. J. Freedman helped with the calculations.

Thanks are also due to Dr. T. E. Allibone, C.B.E., F.R.S., Director of the Laboratory, for permission to publish this paper.

## References

1) D. Cartwright, L. L. Green and J. C. Wilmott, Phil. Mag. **45** (1954) 742
2) H. M. Jongerius, F. P. G. Valckx and P. M. Endt, Physica **20** (1954) 29
3) A. G. Stanley, Phil. Mag. **45** (1954) 807
4) B. Sjogren and K. Ahnlund, Ark. för Fys. **12** (1957) 547
5) D. L. Booth, F. V. Price, D. Roaf and G. L. Salmon, Proc. Phys. Soc. **71** (1958) 325
6) W. M. Gibson and E. E. Thomas, Proc. Roy. Soc. **210** (1952) 543
7) R. D. Sharp and A. Sperduto, M.I.T. Laboratory for Nuclear Science, Annual Report, May (1955) p. 125
8) T. S. Green and R. Middleton, Proc. Phys. Soc. **69** (1956) 28
9) L. D. Wyly, Phys. Rev. **76** (1949) 104
10) N. Kawai, J. Phys. Soc. Japan **15** (1960) 930
11) W. M. Jones and D. G. Waters, J. Sci. Instr. **35** (1958) 286
12) T. F. Stratton, J. M. Blair, K. F. Famularo and R. V. Stuart, Phys. Rev. **98** (1955) 629
13) J. M. Blair, private communication
14) L. Wolfenstein, Phys. Rev. **82** (1951) 690

1.D.2:5 *Nuclear Physics* **26** (1961) 209—216; © *North-Holland Publishing Co., Amsterdam*
Not to be reproduced by photoprint or microfilm without written permission from the publisher

# ON FAVOURED ALPHA TRANSITIONS

A. SĂNDULESCU and M. IOSIFESCU
*Institute for Atomic Physics, Bucharest*

Received 24 February 1961

**Abstract:** Using the collective model in the strong coupling scheme, one establishes that the reduced width of a favoured α transition with single angular momentum for an odd-mass nucleus of mass number $A$ is proportional to the reduced width of the favoured α transition with the same angular momentum for the even-even nucleus $A-1$, if both nuclei have the same deformation. This makes it possible to express the α intensities of odd-mass nuclei in terms of the reduced widths of the α transitions in even-even nuclei. Values of the latter widths extracted by Rasmussen from experimental data have been used to calculate intensities of favoured α transitions of odd-mass nuclei and relative intensities of their components of given angular momentum. The theoretical results are in good agreement with experimental data.

## 1. Introduction

Bohr, Fröman and Mottelson [1]) have pointed out a class of transitions characterized by the selection rules $\Delta K = 0$ and $\Delta\pi = 0$ where $K$ represents the projection of the total angular momentum on the nuclear symmetry axis and $\pi$ the parity of the nuclear state. For even-even nuclei, this class is represented by the transitions to the rotational band associated with the fundamental level of the final nucleus and for odd-mass nuclei, by the transitions to the rotational band of the final nucleus for which the orbit of the last odd nucleon remains unchanged.

These two kinds of transitions, named favoured transitions present a great similarity. This similarity has been explained [1]) by supposing that for both even-even and odd-mass nuclei the α particle is formed from pairs of neutrons (protons) situated on orbits differing only in the sign of the projection $\Omega$ of the angular momentum along the nuclear symmetry axis.

In the same work [1]), using an analogy with the rules that appear in $\beta$ and $\gamma$ transitions of a given multipole order and populate different members of a rotational band, an approximate formula has been obtained for the intensities in the favoured α decays of odd-mass nuclei on the basis of those observed in the even-even nuclei.

In fact, denoting by $I_1, K_1$ ($I_f, K_f$) the spin and its projection on the symmetry axis of the initial (final) nucleus, the probability of a favoured α transition for an odd-mass nucleus is given by the formula

$$P = P_0(Z, E) \sum_l c_l [C^{I_1\ l\ I_f}_{K_1\ 0\ K_f}]^2, \qquad (1)$$

in which the centrifugal barrier is neglected and $P_0\ (Z,\ E)$ is given by the Geiger-Nuttall law

$$\log_{10} P_0 = C - DE^{-\frac{1}{2}}. \tag{2}$$

The constants $C$, $D$ and $c_l$ are determined from the $\alpha$ transition probabilities of the neighbouring even-even nuclei. Taking $c_0 = 1$, the constants $C$ and $D$ can be determined from the probabilities of the $\alpha$ transition to the fundamental state of the final nucleus. The other constants $c_l$ are determined from the $\alpha$ transition probabilities of the rotational band associated to the fundamental level of the final nucleus.

## 2. Development

In the present paper, we shall try to specify formula (1). To this purpose we shall use the formulation given by Thomas [2]) for the theory of alpha decay based upon the formal theory of the nuclear reactions. In this formulation, the $\alpha$ transition probability for heavy nuclei is given by the ratio between the level width $\Gamma$ and Planck's constant $\hbar$. The level width $\Gamma_l$ for a particle of angular momentum $l$ may be separated in two factors, the one representing the transition probability $T_l$ though an exterior barrier, and the other the reduced width $\gamma_l^2$. If many angular momenta are present, we have

$$P = \hbar^{-1}\Gamma = \hbar^{-1}\sum_l T_l \gamma_l^2 \tag{3}$$

We shall suppose, in the following, that the wave functions for the initial and final nuclei are given by the collective model in the strong-coupling scheme [3])†

$$\Psi^I_{MK} = \sqrt{\frac{2I+1}{16\pi^2(1+\delta_{K0})}}\,\{\chi_K D^I_{MK}(\theta_i) + \bar{\chi}_{-K} D^I_{M-K}(\theta_i)\}, \tag{4}$$

where $\chi_K$ describes the intrinsic motion of the nucleons in the deformed field of the nucleus, $D^I_{MK}$ the rotation of the nucleus and $\bar{\chi}_{-K} = (-)^{I-\Sigma\hat{j}_p}\chi_{-K}$.

The reduced width amplitude $\gamma_l$ for the emission of an alpha particle of orbital angular momentum $l$ is thus given by the expression [4, 5])

$$\gamma_l = \left(\frac{\hbar^2}{2\mathscr{M}}\right)^{\frac{1}{2}} \frac{1}{R_0}\int \Psi^{I_1 *}_{M_1 K_1}\, \Phi^{I_1 l}_{M_1}\, \mathrm{d}S, \tag{5}$$

where $\mathscr{M}$ is the reduced mass, $R_0$ the interaction radius and $\Phi^{I_1 l}_{M_1}$ the channel wave function

$$\Phi^{I_1 l}_{M_1} = \sum_{m_l, M_I} C^{I_I\ l\ I_1}_{M_I\ m_l\ M_1} \Psi^{I_I}_{M_I K_I}\, Y_m{}^l(\theta, \varphi)\, \psi_\alpha. \tag{6}$$

† Writing $\chi_K$ as an antisymmetric product of Nilsson wave functions (see formula (11)) it may be shown that if $K = 0$, i.e. if all nucleons are grouped in pairs on Nilsson's orbits, we have $\bar{\chi}_0 = \chi_0$, so that we can write the wave functions $\Psi^I_{MK}$ in the form (4).

In formula (6) $Y_m{}^l(\theta, \varphi)$ are the spherical harmonics of order $l$ in the fixed frame, $\theta, \varphi$ the angles that determine the direction of the position vector $\mathbf{r}_{f\alpha}$ between the $\alpha$ particle and the final nucleus and $\psi_\alpha$ the intrinsic wave function of the $\alpha$ particle.

In expression (4) the integral is taken on the channel surface, that is with respect to $\theta, \varphi$ and to the internal coordinates of the final nucleus and of the $\alpha$ particle.

Writing the wave function of the angular momentum in the nuclear frame

$$Y_m{}^l = \sum_r D^l_{mr} \chi_r{}^l, \tag{7}$$

and using (4) and (6), the expression (5) becomes [6])

$$\begin{aligned}\gamma_l = &\left(\frac{\hbar^2}{2\mathscr{M}}\right)^{\frac{1}{2}} \sqrt{\frac{2I_f+1}{(2I_1+1)(1+\delta_{K_1 0})(1+\delta_{K_f 0})}}\, \frac{1}{2R_0} \\ &\times \left\{\left[\int \chi^*_{K_1} \chi_{K_f} \chi_0{}^l \psi_\alpha + (-)^{I_f+l-I_1} \int \bar{\chi}^*_{-K_1} \chi_{-K_f} \chi_0{}^l \psi_\alpha\right] C^{I_f\ l\ I_1}_{K_f\ 0\ K_1} + \right. \\ &\left. + \left[\int \bar{\chi}^*_{-K_1} \chi_{K_f} \chi^l_{-K_1-K_f} \psi_\alpha + (-)^{I_f+l-I_1} \int \chi^*_{K_1} \bar{\chi}_{-K_f} \chi^l_{K_1+K_f} \psi_\alpha\right] C^{I_f\ \ l\ \ I_1}_{K_f\ -K_1-K_f\ -K_1}\right\}.\end{aligned} \tag{8}$$

The formula thus obtained may be simplified by observing that the two integrals contained in each square bracket differ only in the sign of the projections $K_1$, $K_f$. These signs may be changed by a rotation of angle $\pi$ around the $y$ axis,

$$\chi_m{}^j \to (-)^{j+m} \chi^j_{-m}. \tag{9}$$

Hence we obtain the following expression of the reduced width amplitude in favoured $\alpha$ transitions:

$$\begin{aligned}\gamma_l = &\left(\frac{\hbar^2}{2\mathscr{M}}\right)^{\frac{1}{2}} \sqrt{\frac{2I_f+1}{(2I_1+1)(1+\delta_{K_1 0})(1+\delta_{K_f 0})}}\, \frac{1}{R_0} \\ &\times \left\{C^{I_f\ l\ I_1}_{K_f\ 0\ K_1} \int \chi^*_{K_1} \chi_{K_f} \chi_0{}^l \psi_\alpha + C^{I_f\ \ l\ \ I_1}_{K_f\ -K_1-K_f\ -K_1} \int \bar{\chi}^*_{-K_1} \chi_{K_f} \chi^l_{-K_1-K_f} \psi_\alpha\right\}.\end{aligned} \tag{10}$$

Taking into account the Pauli principle and the hypotheses of the collective model in Nilsson's scheme [7]), the intrinsic wave function of the initial nucleus may be written in the form

$$\begin{aligned}\chi_{K_1} = &\frac{1}{\sqrt{N!}} \sum_{P_n} (-)^{P_n} \chi_{\Omega_1}(\mathrm{n}_1) \chi_{\Omega_2}(\mathrm{n}_2) \cdots \chi_{\Omega_{N-1}}(\mathrm{n}_{N-2}) \chi_{\Omega_N}(\mathrm{n}_N) \\ &\times \frac{1}{\sqrt{Z!}} \sum_{P_p} (-)^{P_p} \chi_{\Omega_1}(\mathrm{p}_1) \chi_{\Omega_2}(\mathrm{p}_2) \cdots \chi_{\Omega_{Z-1}}(\mathrm{p}_{Z-1}) \chi_{\Omega_Z}(\mathrm{p}_Z).\end{aligned} \tag{11}$$

The "intrinsic" channel wave function is

$$\chi_{K_f}\chi_{0}{}^{l}\psi_{\alpha} = \sqrt{\frac{2}{N!}}\sum_{P_n}(-)^{P_n}\chi_{\Omega_1}(n_1)\chi_{\Omega_2}(n_2)\ldots\chi_{\Omega_{N-2}}(n_{N-2})$$

$$\times\sqrt{\frac{2}{Z!}}\sum_{P_p}(-)^{P_p}\chi_{\Omega_1}(p_1)\chi_{\Omega_2}(p_2)\ldots\chi_{\Omega_{Z-2}}(p_{Z-2})\chi_{0}{}^{l}\psi_{\alpha}(n_{N-1}, n_N; p_{Z-1}, p_Z), \quad (12)$$

where $n_1, n_2, \ldots n_N$ ($p_1, p_2, \ldots p_Z$) represent the spatial and spin coordinates of the $N$ neutrons ($Z$ protons) and $P_n$ ($P_p$) the permutations of the two kinds of nucleons.

We suppose that in a favoured $\alpha$ transition the $\alpha$ particle is composed only of pairs of neutrons (protons) situated on the same neutronic (protonic) level, this level being the highest possible one.

Supposing, in addition, that the initial and final nuclei have the same deformation and integrating over the internal coordinates of the final nucleus, we have

$$\int\chi^{*}_{K_1}\chi_{K_f}\chi_{0}{}^{l}\psi_{\alpha}$$

$$=\int\frac{1}{\sqrt{2}}\begin{vmatrix}\chi^{*}_{-\Omega_N}(n) & \chi^{*}_{-\Omega_N}(n')\\ \chi^{*}_{\Omega_N}(n) & \chi^{*}_{\Omega_N}(n')\end{vmatrix}\frac{1}{\sqrt{2}}\begin{vmatrix}\chi^{*}_{-\Omega_Z}(p) & \chi^{*}_{-\Omega_Z}(p')\\ \chi^{*}_{\Omega_Z}(p) & \chi^{*}_{\Omega_Z}(p')\end{vmatrix}\chi_{0}{}^{l}\psi_{\alpha}(n,n',p,p')dn\,dn'\,dp\,dp' \quad (13)$$

and

$$\int\bar{\chi}^{*}_{-K_1}\chi_{K_f}\chi^{l}_{-K_1-K_f}\psi_{\alpha} = \begin{cases}\int\chi^{*}_{K_1}\chi_{-K_f}\chi^{l}_{K_1+K_f}\psi_{\alpha} & \text{for even-even nuclei } (K_1 = K_f = 0),\\ 0 & \text{for odd-mass nuclei.}\end{cases} \quad (14)$$

The reduced width amplitude of a favoured $\alpha$ transition for an even-even as well as for odd-mass nucleus is hence

$$\gamma_l = \left(\frac{\hbar^2}{2\mathcal{M}}\right)^{\frac{1}{2}}[(1+\delta_{K_1 0})(1+\delta_{K_f 0})]^{-\frac{1}{2}}\frac{2}{R_0}(-)^{I_1-I_f}C^{I_1\ l\ I_f}_{K_1\ 0\ K_f}$$

$$\times\int\frac{1}{\sqrt{2}}\begin{vmatrix}\chi^{*}_{-\Omega_N}(n)\chi^{*}_{-\Omega_N}(n') & \chi^{*}_{-\Omega_N}(n)\chi^{*}_{\Omega_N}(n')\\ \chi^{*}_{\Omega_N}(n)\chi^{*}_{-\Omega_N}(n') & \chi^{*}_{\Omega_N}(n)\chi^{*}_{\Omega_N}(n')\end{vmatrix}\frac{1}{\sqrt{2}}\begin{vmatrix}\chi^{*}_{-\Omega_Z}(p)\chi^{*}_{-\Omega_Z}(p') & \chi^{*}_{-\Omega_Z}(p)\chi^{*}_{\Omega_Z}(p')\\ \chi^{*}_{\Omega_Z}(p)\chi^{*}_{-\Omega_Z}(p') & \chi^{*}_{\Omega_Z}(p)\chi^{*}_{\Omega_Z}(p')\end{vmatrix}\chi_{0}{}^{l}\psi_{\alpha}(n,n';p,p')dn\,dn'\,dp\,dp'. \quad (15)$$

Taking into account the fact that in a favoured $\alpha$ transition of an odd-mass nuclues of mass number $A$ the same Nilsson wave functions participate as in a favoured $\alpha$ transition of the even-even nucleus of mass number $A-1$, having the same deformation as the first, we obtain

$$\gamma_l(A) = (-)^{I_1-I_f}C^{I_1\ l\ I_f}_{K_1\ 0\ K_f}\gamma_l(A-1), \quad (16)$$

where we have supposed that $R_0$ and $\mathcal{M}$ are approximately the same for both nuclei.

Using the hypothesis that the final nucleus is fixed in space while the $\alpha$ particle traverses the deformed barrier, the formula (16) allows us to calculate, using (3), the probabilities of the favoured $\alpha$ transitions for odd-mass nuclei.

In fact, in a favoured $\alpha$ transition of an even-even nucleus the $\alpha$ particles emerge with a well determined value of the angular momentum $l$. This allows us to extract the reduced width of these transitions from experimental data if we know the penetrabilities $T_l(A-1)$ by using

$$\gamma_l^2(A-1) = \hbar \frac{P(A-1)}{T_l(A-1)}. \tag{17}$$

We now make use of relations (3) and (16) and obtain the following expression for the probability of a favoured $\alpha$ transition of an odd-mass nucleus:

$$P(A) = \frac{1}{\hbar} \sum_l T_l(A)\gamma_l^2(A) = \frac{1}{\hbar} \sum_l [C^{I_1}_{K_1\ 0\ K_I}]^2 T_l(A)\gamma_l^2(A-1), \tag{18}$$

where we have taken into account the fact that to such a transition several angular momenta participate.

## 3. Comparison with Experimental Data

The penetrability factors $T_l$ $(A-1)$ for even-even nuclei have been calculated by Rasmussen [8]) in the WKB approximation, neglecting non-central interactions and supposing the existence of a Coulomb, a centrifugal and a nuclear potential. The nuclear potential used was an exponential one, deduced by G. Igo [9]) by an optical-model analysis of alpha particle scattering data.

In another paper [10]), Rasmussen has calculated with the same hypotheses, but neglecting the centrifugal potential, the penetrability factors $T_0$ for odd-mass nuclei. In this paper he has also offered the following approximate formula for the calculation of $T_l(A)$ with $l \neq 0$:

$$\frac{T_l(Z, A)}{T_0(Z, A)} = \exp[-2.027l(l+1)(Z-2)^{-\frac{1}{3}}(A-4)^{-\frac{1}{3}}], \tag{19}$$

where $Z$ and $A$ represent the charge and mass number of the parent nucleus.

Taking into account the hypotheses that the final nucleus is fixed during the traversal of the barrier by the $\alpha$ particle and that the odd-mass and the even-even nuclei have equal deformations, the neglect of non-central effects will produce equal modifications in the penetrabilities $T_l(A-1)$ and $T_l(A)$. We can therefore suppose that the reduced widths extracted from experimental data with the help of relation (17) neglecting non-central effects, may be used in formula (18) in which non-central effects have been neglected too.

TABLE 1

Comparison of calculated and experimental values

| Decay | $E$(MeV) [b] | $I_i$ | $I_f$ | $l$ | $\gamma_l^2(A-1)$ | $T_l(Z,A)$ | $\lambda_{I_f}^l$ % | $\lambda_{I_f}$ % | $\lambda_{I_f}$ % experimental | $\lambda_{I_f}$ % (Bohr-Fröman-Mottelson) |
|---|---|---|---|---|---|---|---|---|---|---|
| $_{92}U^{233} \rightarrow {}_{90}Th^{229}$ | 4.852 | $\frac{5}{2}$ | $\frac{5}{2}$ | 0 | 0.112 | $4.645 \times 10^{-33}$ | 73.10 | 82.51 | 83.44 [a]) | 86.95 |
| | | | | 2 | 0.193 | $2.766 \times 10^{-33}$ | 26.78 | | | |
| | | | | 4 | 0.0397 | $0.8254 \times 10^{-33}$ | 0.11 | | | |
| | 4.809 | $\frac{5}{2}$ | $\frac{7}{2}$ | 2 | 0.193 | $1.390 \times 10^{-33}$ | 97.81 | 15.14 | 14.88 [a]) | 11.30 |
| | | | | 4 | 0.0397 | $0.4149 \times 10^{-33}$ | 2.18 | | | |
| | | | | 6 | | | | | | |
| | 4.752 | $\frac{5}{2}$ | $\frac{9}{2}$ | 2 | 0.193 | $0.5507 \times 10^{-33}$ | 87.75 | 2.33 | 1.6 [a]) | 1.56 |
| | | | | 4 | 0.0397 | $0.1643 \times 10^{-33}$ | 12.25 | | | |
| | | | | 6 | | | | | | |
| | 4.525 | $\frac{5}{2}$ | $\frac{11}{2}$ | 4 | 0.0397 | $0.344 \times 10^{-35}$ | | 0.005 | 0.07 [a]) | 0.173 |
| | | | | 6 | | | | | | |
| | | | | 8 | | | | | | |
| $_{94}Pu^{239} \rightarrow {}_{92}U^{235}$ | 5.184 | $\frac{1}{2}$ | $\frac{1}{2}$ | 0 | 0.0786 | $7.223 \times 10^{-32}$ | 100 | 69.98 | 72.32 [a]) | 70.22 |
| | 5.171 | $\frac{1}{2}$ | $\frac{3}{2}$ | 2 | 0.0913 | $3.582 \times 10^{-32}$ | 100 | 16.12 | 16.87 [a]) | 16.15 |
| | 5.133 | $\frac{1}{2}$ | $\frac{5}{2}$ | 2 | 0.0913 | $2.0396 \times 10^{-32}$ | 100 | 13.77 | 10.74 [a]) | 13.34 |
| | 5.101 | $\frac{1}{2}$ | $\frac{7}{2}$ | 4 | 0.00395 | $0.384 \times 10^{-32}$ | 100 | 0.083 | 0.037 [a]) | 0.28 |
| | 5.036 | $\frac{1}{2}$ | $\frac{9}{2}$ | 4 | 0.00395 | $0.143 \times 10^{-32}$ | 100 | 0.038 | 0.013 [a]) | |
| $_{95}Am^{241} \rightarrow {}_{93}Np^{237}$ | 5.514 | $\frac{5}{2}$ | $\frac{5}{2}$ | 0 | 0.107 | $2.380 \times 10^{-30}$ | 81.60 | 86.30 | 85.45 [a]) | 86.03 |
| | | | | 2 | 0.112 | $1.434 \times 10^{-30}$ | 18.37 | | | |
| | | | | 4 | 0.00737 | $4.392 \times 10^{-31}$ | 0.02 | | | |
| | 5.471 | $\frac{5}{2}$ | $\frac{7}{2}$ | 2 | 0.112 | $7.999 \times 10^{-31}$ | 99.27 | 11.88 | 12.86 [a]) | 12.04 |
| | | | | 4 | 0.00737 | $2.451 \times 10^{-31}$ | 0.73 | | | |
| | | | | 6 | | | | | | |
| | 5.417 | $\frac{5}{2}$ | $\frac{9}{2}$ | 2 | 0.112 | $3.805 \times 10^{-31}$ | 95.62 | 2.05 | 1.67 [a]) | 1.89 |
| | | | | 4 | 0.00737 | $1.166 \times 10^{-31}$ | 4.38 | | | |
| | | | | 6 | | | | | | |

TABLE 1
(continued)

| Decay | $E$(MeV) [b] | $I_i$ | $I_f$ | $l$ | $\gamma_l^2(A-1)$ | $T_l(Z,A)$ | $\lambda_{I_f}^l$ % | $\lambda_{I_f}$ % | $\lambda_{I_f}$ % experimental | $\lambda_{I_f}$ % (Bohr-Fröman-Mottelson) |
|---|---|---|---|---|---|---|---|---|---|---|
| $_{95}Am^{241} \rightarrow {}_{93}Np^{237}$ | 5.352 | $\frac{5}{2}$ | $\frac{11}{2}$ | 4 | 0.00737 | $4.693 \times 10^{-32}$ | | 0.03 | 0.015 [a]) | 0.026 |
| | | | | 6 | | | | | | |
| | | | | 8 | | | | | | |
| $_{95}Am^{243} \rightarrow {}_{93}Np^{239}$ | 5.304 | $\frac{5}{2}$ | $\frac{5}{2}$ | 0 | 0.093 | $1.383 \times 10^{-31}$ | 79.66 | 85.38 | 86.9 | 86.11 |
| | | | | 2 | 0.1103 | $8.336 \times 10^{-32}$ | 20.33 | | | |
| | | | | 4 | | | | | | |
| | 5.262 | $\frac{5}{2}$ | $\frac{7}{2}$ | 2 | 0.1103 | $4.549 \times 10^{-32}$ | | 12.63 | 11.5 | 12.05 |
| | | | | 4 | | | | | | |
| | | | | 6 | | | | | | |
| | 5.207 | $\frac{5}{2}$ | $\frac{9}{2}$ | 2 | 0.1103 | $2.035 \times 10^{-32}$ | | 1.97 | 1.3 | 1.80 |
| | | | | 4 | | | | | | |
| | | | | 6 | | | | | | |
| $_{96}Cm^{243} \rightarrow {}_{94}Pu^{239}$ | 5.818 | $\frac{5}{2}$ | $\frac{5}{2}$ | 0 | 0.0697 | $4.149 \times 10^{-29}$ | 82.43 | 86.37 | 84.9 [a]) | 85.30 |
| | | | | 2 | 0.0688 | $2.507 \times 10^{-29}$ | 17.56 | | | |
| | | | | 4 | 0.000983 | $7.744 \times 10^{-30}$ | 0.005 | | | |
| | 5.774 | $\frac{5}{2}$ | $\frac{7}{2}$ | 2 | 0.0688 | $1.439 \times 10^{-29}$ | 99.83 | 11.61 | 13.24 [a]) | 12.79 |
| | | | | 4 | 0.000983 | $4.444 \times 10^{-30}$ | 0.16 | | | |
| | | | | 6 | 0.00701 | $7.014 \times 10^{-31}$ | 0.005 | | | |
| | 5.718 | $\frac{5}{2}$ | $\frac{9}{2}$ | 2 | 0.0688 | $7.029 \times 10^{-30}$ | 98.83 | 2.006 | 1.86 [a]) | 1.87 |
| | | | | 4 | 0.000983 | $2.171 \times 10^{-30}$ | 1.00 | | | |
| | | | | 6 | 0.00701 | $3.426 \times 10^{-31}$ | 0.17 | | | |

[a]) Percentage from the total intensity of the favoured decay.
[b]) Alpha-particle energy plus orbital electron screening correction.

Using the reduced widths of the favoured α transitions of even-even nuclei, as well as the penetrability factors of odd-mass nuclei, corrected with the aid of (19), we have computed the relative intensity $\lambda_{I_f}$ of every favoured transition

$$\lambda_{I_f} = \frac{P_{I_f}(A)}{\sum_{I_f} P_{I_f}(A)}, \tag{20}$$

the sum being extended to all levels of the favoured rotational band of the final nucleus.

We have also calculated for a given energy level the relative intensities $\lambda^1_{I_f}$ of an α-transition with different angular momenta.

The results are presented in table 1.

They indicate a somewhat smaller difference between theory and experiment in ref. [1]) than in the present paper; there is one exception, $U^{233}$, for which our results are closer to the experimental ones than those obtained in ref. [1]).

These features are a consequence of the constant value $c_2 = 0.7$ taken for $c_2$ in ref. [1]). Indeed, if we compare formula (18) with (1) and suppose $c_2 = 0.7$, there would result for a given level

$$\frac{\gamma_2^2(A-1)T_2(A)}{\gamma_0^2(A-1)T_0(A)} \approx 0.7. \tag{21}$$

But the calculated values are

| | $_{92}U^{233}$ | $_{94}Pu^{239}$ | $_{95}Am^{241}$ | $_{95}Am^{243}$ | $_{96}Cm^{243}$ |
|---|---|---|---|---|---|
| $\frac{\gamma_2^2(A-1)T_2(A)}{\gamma_0^2(A-1)T_0(A)}$ | 1.024 | 0 | 0.62 | 0.714 | 0.60 |

(22)

The mean value 0.7 used in ref. [1]) for $c_2$ is thus a good approximation for all nuclei excepting $U^{233}$ and $Pu^{239}$. For the last one, formula (21) may not be used, for in every transition of $Pu^{239}$ particles are emitted with a single value of the angular momentum. For $U^{233}$ the value 0.7 is too small. This explains the unsatisfactory result obtained in ref. [1]) for $U^{233}$.

## References

1) A. Bohr, P. O. Fröman and B. R. Mottelson, Mat. Fys. Medd. Dan. Vid. Selsk. **29**, No. 10 (1955)
2) R. G. Thomas, Prog. Theor. Phys. **12** (1954) 253
3) A. Bohr and B. R. Mottelson, Mat. Fys. Medd. Dan. Vid. Selsk. **27**, No. 16 (1953)
4) E. P. Wigner and L. Eisenbud, Phys. Rev. **72** (1947) 29
5) T. Teichman and E. P. Wigner, Phys. Rev. **87** (1952) 123
6) S. Yoshida, Prog. Theor. Phys. **12** (1954) 141
7) S. G. Nilsson, Mat. Fys. Medd. Dan. Vid. Selsk. **29**, No. 16 (1953)
8) J. O. Rasmussen, Phys. Rev. **113** (1959) 1593
9) G. Igo, Phys. Rev. Lett. **1** (1958) 72
10) J. O. Rasmussen, Phys. Rev. **115** (1959) 1675

7.C:9.A *Nuclear Physics* **26** (1961) 217—221; © *North-Holland Publishing Co., Amsterdam*
Not to be reproduced by photoprint or microfilm without written permission from the publisher

# A COMPARISON OF PION AND NUCLEON INTERACTIONS IN NUCLEAR EMULSIONS BETWEEN $10^{11}$ AND $10^{13}$ eV

F. A. BRISBOUT, C. GAULD, C. B. A. McCUSKER, J. MALOS, K. NISHIKAWA, L. S. PEAK
and
L. G. VAN LOON

*The Falkiner Nuclear Department, School of Physics, The University of Sydney, Sydney, Australia* †

Received 6 March 1961

**Abstract:** Using data obtained from a 10 l emulsion stack by the Sydney group and a 22 l stack by the Chicago group it is shown that at energies around 1000 GeV: a) the average number of shower particles in secondary jets (mainly produced by pions) is about half that in jets produced by protons, b) the spread of multiplicities in pion-nucleon encounters at a given energy is small, c) the spread of multiplicities in proton produced jets is considerable and in good agreement with the predictions of tunnel theory assuming a geometric interaction cross section for protons and d) the average number of heavy prongs in secondary jets (mostly produced by pions) decreases with increasing energy for about 15 at 6 GeV to about 3 at 5000 GeV.

## 1. Introduction

In two recent papers [1, 2]), the results of the study of two large stacks of nuclear emulsion flown to great heights have been presented. Taking these results together, a sufficient statistical sample can be obtained to clarify a number of points concerning nuclear interactions at energies around 1000 GeV which were previously in doubt and to make some new observations on this subject. Details of the flights, methods of scanning and methods of analysis are given in the papers quoted. These are sufficiently alike in the two cases for the data to be treated together.

## 2. Interaction Mean Free Path of Pions

Both groups have found an interaction mean free path for the secondary particles of jets which is considerably greater than the geometric value. The value given by the Chicago group is $41 \pm 8$ cm; that given by the Sydney group is $49^{+17}_{-10}$ cm. Combining the results, we find that in 2246 cm path length in the emulsion there were 53 interactions giving an interaction mean free path of 42.4 cm. This is to be compared with a value of 28 cm for a geometric interaction cross section.

† This work has been supported by the Nuclear Research Foundation and by the Office of Scientific Research of the Air Research and Development Command of the U.S.A.F.

## 3. The Average Number of Shower Particles

The Sydney group [1]) has pointed out that (possibly as a result of this long interaction mean free path of the pions) the average multiplicity of shower particles from pion and proton produced jets in the same energy range is very different. For a range of $\gamma_p$ from 300 to 2000 they find that $\bar{n}_s$ for the proton produced jets is 23.6 (at an average energy of 1010 GeV) and for pion produced jets it is 13.6 (for an average energy of 600 GeV). The Chicago results allow an independent confirmation of this feature at even higher energies. For the 57 primary jets, $\bar{n}_s$ is 22.5 at an average energy of 3500 GeV and for the 9 secondary jets of energy greater than 1000 GeV, it is 10.4 at an average energy of 2400 GeV, in very good agreement with the Sydney observation. The possibility that this difference is due to scanning bias has been discussed by the Sydney group and found to be unlikely. Further evidence that this is so, deduced from the combined results of both groups, is dealt with in sect. 4.

## 4. The Distribution in $n_s$

Fig. 1 shows the distribution of secondary jets in $n_s$. The sample is made up of the 19 secondary events from the Chicago group and 18 events from the

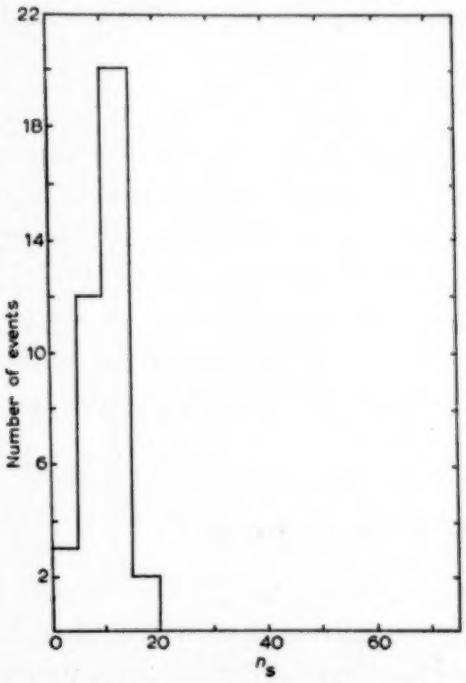


Fig. 1. The number of secondary jets of given $n_s$ plotted against $n_s$. The jets are those found in the 10 1 and 22 1 stacks with $E_0 > 300$.

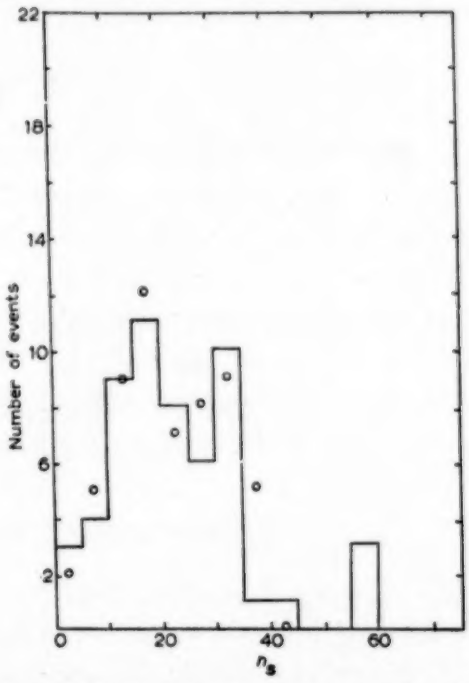


Fig. 2. The number of primary jets of given $n_s$ against $n_s$. The circles give the predictions of the tunnel theory for a $\gamma_p$ of 2000, normalized to the same total number of events. The three events with $n_s$ around 60 are not predicted by tunnel theory and may be due to deuteron primaries or the production of a secondary high $p_t$ early in the cascade.

Sydney group † with energies greater than 300 GeV. The separate distributions are similar. It can be seen that this distribution is very sharp. It can be well approximated by a Poissonian of mean value

$$\bar{n}_s = 11.1 \pm 0.4.$$

No events due to pions were found † with $n_s > 20$. Since the normal fluctuation of $\pi^{\pm}$ to $\pi^0$ mesons will certainly contribute to the spread in the $n_s$ value and since the variation in primary energy may possibly do so, this narrow distribution indicates that

a) at these energies most of the events involve only one nucleon in the struck nucleus (as far as meson production goes),

b) the spread in $n_s$ in pion-nucleon encounters at a given energy is small (this last feature was deduced by Roesler and McCusker for nucleon-nucleon encounter some time ago [3]).

The Chicago experiment was almost ideal for the study of proton initiated events. The large stack and long flight time ensured that a fair sized statistical sample was obtained; the high altitude that the beam incident on the stack was not greatly contaminated by pions, and the scanning procedure and steep cosmic ray energy spectrum that the events came from a fairly narrow energy band. The distribution in $n_s$ is shown in fig. 2. Also shown in fig. 2 are the predictions of the tunnel theory for the distribution expected from a mono-energetic proton beam of the same energy as the average energy of the Chicago events (3500 GeV). This distribution has been deduced from eq. 53 ref. [3]), assuming the target area in the emulsion to consist [4]) of CNO (26.5 %), Br (33 %) and Ag (40.5 %). The sharp cut off points in the theoretical curve (which are reproduced rather well in the experimental data) are due to the maximum tunnel lengths (corresponding to central collisions) in the light and heavy elements, respectively.

In ref. [1]), the Sydney group produced evidence suggesting that the large differerence in $\bar{n}_s$ in primary and secondary jets was not due to scanning bias. A comparison of figs. 1 and 2 confirms this. It seems improbable that a distribution of type 1 (assumed to be unbiased) could produce a distribution of type 2 by a scanning bias. One obvious feature of distribution 2 that could not arise in this way is the large fraction of events with $n_s > 20$ since there are none of these in distribution 1.

The comparison of the distributions also confirms the previous suggestion of the Sydney group that, at these energies, the interaction cross section of protons for meson production is greater than that of pions and probably close to geometric. This is supported by the good agreement of the tunnel theory's prediction and the observed distribution in $n_s$.

† One secondary jet from the Sydney group has been omitted. This was produced by a neutral primary, secondary to a primary jet produced by an $\alpha$ particle. It had both $N_h$ and $n_s$ anomalously high ($N_h = 22$, $n_s = 21$). There is good reason to believe that the primary was a neutron.

## 5. Average Number of Shower Particles versus Energy for Secondary Jets

Fig. 3 shows the variation of $\bar{n}_s$ with energy for the secondary jets from the 10 l and 22 l stacks. It can be seen that this can be well approximated by a straight line through the mean value for energies from 50 to 5000 GeV. The points are also consistent with a sufficiently slow increase in average multiplicity.

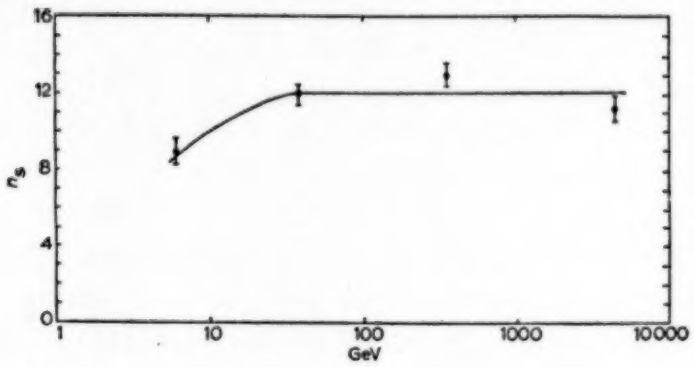


Fig. 3. The variation of the average number of shower particles for the secondary jets of the 10 and 22 l stacks plotted against energy.

## 6. Average Number of Heavy Prongs versus Energy for Secondary Jets

Tables 1 gives the average number of heavy prongs against the energy of the incident particle for the secondary jets of the Sydney and Chicago groups. It can be seen that there is good agreement between the sets of results.

TABLE 1

The variation in the number of black prongs per event for secondary jets against energy of the jet

| Range of $E_0$ | 0—10 | 10—100 | 100—1000 | > 1000 GeV |
|---|---|---|---|---|
| $\overline{N_h}$ (Sydney) | $\frac{14}{1} = 14.0$ | $\frac{122}{9} = 13.6$ | $\frac{133}{14} = 9.5$ | $\frac{33}{11} = 3.0$ |
| $\overline{N_h}$ (Chicago) | $\frac{179}{12} = 14.9$ | $\frac{279}{31} = 9.0$ | $\frac{150}{24} = 6.3$ | $\frac{21}{9} = 2.3$ |
| $\overline{N_h}$ (total) | $\frac{193}{13} = 14.8$ | $\frac{401}{40} = 10.0$ | $\frac{283}{38} = 7.4$ | $\frac{54}{20} = 2.7$ |

This result implies that as the primary energy increases, the energy communicated to the struck nucleus *decreases*. The number of black prongs is a rather sensitive test of the amount of energy given to the struck nucleus [5]). This energy is, in general, small compared to the primary energies with which we are dealing. Using the equation from ref. [5]), we find that the excitation energy changes from 670 MeV for 15 heavy prongs to 170 MeV for 3. Since the

average number of shower particles in these stars is only 11.1, and because of the form of the distribution in $n_s$, it is not likely that the increase in $N_h$ is due to a meson-producing cascade. However, elastic scattering of about 10 $\pi$-mesons could well communicate this rather small amount of energy. Then the reason for the increase in $N_h$ with decrease in primary energy would be either (a) the decrease in scattering angels as the energy increased, or (b) if the fireball model is correct, the decay of the fireball *inside* the nucleus at low energies and outside at high energies, or (c) possibly, both.

If the second of these mechanisms plays a large part then the study of the heavy prongs may enable us eventually to determine the velocity and half life of the fireball. This second mechanism would also mean that the decrease in $\bar{N}_h$ would happen at rather higher energies for proton produced jets.

## 7. Discussion

The results given suggest that

a) the pion-nucleon interaction cross section for meson production at about 1000 GeV is only one thrid of the geometric value,

b) as a result, pion-nucleus collisions at this energy are predominantly the collision of one pion and one nucleon,

c) the nucleon-nucleon cross section is appreciably greater than the pion-nucleon cross section and that, a as result, considerable cascading takes place inside the struck nucleus.

If the results of Brenner and Williams [6]) at 50 GeV and of the Chicago group at 250 GeV are accepted, this implies that the nucleon-nucleon cross section for meson production has increased by a factor of 2 to 3 between 250 GeV and 3500 GeV. On the other hand, the CERN group [7]) has recently found a total cross section as high as 40 mb for p-p collisions at 28.4 GeV.

We are very grateful to the members of the Chicago group for sending us their detailed results before publication. We wish to thank Professor H. Messel for the excellent laboratory facilities provided, Dr. A. J. Herz for supervising the balloon flying and processing of the 10 l stack and Miss Rosemary Roberts and her scanners for finding and helping to analyse our jets. One of us (L.S.P.) is indebted to the C.S.I.R.O. for a scholarship.

## References

1) F. A. Brisbout, C. Gauld, J. Lehane, C. B. A. McCusker, J. Malos, K. Nishikawa and L. G. van Loon, Nuclear Physics (to be published)
2) A. G. Barkow, B. Chamary, D. M. Haskin, P. L. Jain, F. Lehrman, M. W. Teucher and M. Schein, Phys. Rev. **122** (1961) 617
3) F. C. Roesler and C. B. A. McCusker, Nuovo Cim. **10** (1953) 127
4) M. Shapiro, Handbook of physics (Springer-Verlag, Berlin, 1958) p. 382 Vol. **45**
5) C. F. Powell, P. F. Fowler and D. H. Perkins, The study of elementary particles by the photo graphic method (Pergamon Press, London, (1959) p. 464
6) A. E. Brenner and R. W. Williams, Phys. Rev. **106** (1957) 1020
7) A. Ashmore, G. Cocconi, A. M. Diddens and A. M. Wetherell, Phys. Rev. Lett. **5** (1960) 576

8.B

*Nuclear Physics* **26** (1961) 222—229; © *North-Holland Publishing Co., Amsterdam*

Not to be reproduced by photoprint or microfilm without written permission from the publisher

# DERIVATION OF STRONG INTERACTIONS FROM A GAUGE INVARIANCE

Y. NE'EMAN

*Department of Physics, Imperial College, London*

Received 13 February 1961

**Abstract:** A representation for the baryons and bosons is suggested, based on the Lie algebra of the 3-dimensional traceless matrices. This enables us to generate the strong interactions from a gauge invariance principle, involving 8 vector bosons. Some connections with the electromagnetic and weak interactions are further discussed.

## 1. Introduction

Following Yang and Mills [1]), two new theories deriving the strong interactions from a gauge invariance principle have been published lately, by Sakurai [2]) and by Salam and Ward [3]). Sakurai's treatment is based on three separate gauges — isospin, hypercharge and baryonic charge — unrelated from the point of view of group-theory; Salam and Ward postulate one unified gauge, an 8-dimensional rotation gauge, combining isospin and hypercharge through Tiomno's [4]) representation.

One important advantage of the latter theory is the emergency of Yukawa-like terms, allowing for the production of single $\pi$ or K mesons. Such terms do not arise normally from the boson-currents, and it is through the reintroduction of the $\sigma$ scalar isoscalar meson [5]), and the assumption that it has a non vanishing vacuum expectation value, that they now appear in ref. [3]). On the other hand, boson-current terms with no $\sigma$ factor then lead to weak interactions, as it is the creation and re-absorption of these $\sigma$ mesons that generates the strong coupling. A 9-dimensional version, with a gauge based on restricted rotations, involves 13 vector bosons, of which only seven mediate the strong interactions; the remainder would generate weak interactions — though no way has been found to induce parity non conservation into these without affecting the strong interactions as well. The seven vector bosons of the strong interactions look like a K set and a $\pi$ set; in Sakurai's theory they are replaced by a $\pi$ set and two singlets.

The following treatment is an attempt to formulate a unified gauge, while reducing the number of vector bosons. It does, indeed, generate a set of 8 mediating fields, seven of which are similar to the above seven, the eighth is

rather like Sakurai's $B_y$ singlet. Still, one important factor is missed, namely, there is no room for the $\sigma$ meson, and thus there are no single-pion terms.

To minimise the number of parameters of the gauge, and thus the number of vector bosons it will generate, we have adopted the following method: we abandoned the usual procedure of describing fields as vector components in a Euclidean isospace, and replace it by a matrix-algebra manifold. Fields still form vectorial sets only in the space of the group operators themselves, invariance of the Lagrangians being achieved by taking the traces of product matrices.

We have also abandoned rotations and use a group first investigated by Ikeda, Ogawa and Ohnuki [6]) in connection with the construction of bound states in the Sakata model. Our present use of this group is in an entirely different context, as our assumptions with regard to the representation of the fermions do not follow the prescriptions of the model.

## 2. Matrix Formalism

We use an 8-dimensional linear vector space $P$ spanned by the semisimple Lie algebra of the $3\times3$ matrices $X_{ij}$ of ref. [6]). We have excluded the identity transformation and use as basis the 8 linearly independent $\mathbf{u}^i \in \mathbf{U}$ given by the following formulae:

$$\mathbf{U}\begin{cases} \mathbf{u}^1 = \frac{1}{2}\sqrt{2}(X_{(31)}-iX_{[31]}), & \mathbf{u}^4 = \frac{1}{2}\sqrt{2}(X_{(31)}+iX_{[31]}), \\ \mathbf{u}^2 = \frac{1}{2}\sqrt{2}(X_{(23)}-iX_{[23]}), & \mathbf{u}^3 = \frac{1}{2}\sqrt{2}(X_{(23)}+iX_{[23]}), \\ \mathbf{u}^5 = \frac{1}{2}\sqrt{2}(X_{(12)}+iX_{[12]}), & \mathbf{u}^6 = \frac{1}{2}\sqrt{2}(X_{(12)}-iX_{[12]}), \\ \mathbf{u}^7 = \frac{1}{2}(X_{11}-X_{22}), & \mathbf{u}^8 = \frac{1}{6}\sqrt{3}(X_{11}+X_{22}-2X_{33}), \end{cases} \tag{1}$$

$$X_{ij}^{\alpha\beta} = \tfrac{1}{2}\delta_{i\alpha}\delta_{j\beta}(1-i)+\tfrac{1}{2}\delta_{i\beta}\delta_{j\alpha}(1+i),$$

$$X_{(ij)} = \tfrac{1}{2}(X_{ij}+X_{ji}), \qquad X_{[ij]} = \tfrac{1}{2}(X_{ij}-X_{ji}),$$

the indices $\alpha$ and $\beta$ denoting the matrix elements. The $X_{ij}$ are hermitian, whereas the basis matrices $\mathbf{u}_i$ are not, with the exception of $\mathbf{u}^7$ and $\mathbf{u}^8$, both diagonal. $\mathbf{U}$ can contain only two linearly independent diagonal elements, and the 2-dimensional sub-space $P_\mathrm{d} \subset P$ spanned by the set of all diagonal elements can be represented by a real Euclidean 2-space. In this 2-space, $\mathbf{u}^7$ and $\mathbf{u}^8$ are orthogonal: not only do they commute with each other, as any $[\mathbf{u}'_\mathrm{d}, \mathbf{u}''_\mathrm{d}]=0$ for $\mathbf{u}'_\mathrm{d}, \mathbf{u}''_\mathrm{d} \subset P_\mathrm{d}$; each also commutes with a 3-rotation consrructed by taking the other as an $M_z$. In the set (1), $U_a$ $(\mathbf{u}^5, \mathbf{u}^6, \mathbf{u}^7)$ forms such a 3-rotation, and

$$[\mathbf{u}^8, \mathbf{u}^a] = 0. \tag{2}$$

We also use a basis $\mathbf{U}'$ differing from $\mathbf{U}$ only in $P_\mathrm{d}$,

$$\mathbf{U}'\begin{cases} \mathbf{u}^{i'} = \mathbf{u}^i, \qquad i = 1, 2, \ldots, 6, \\ \mathbf{u}^{7'} = -\frac{1}{2}(\mathbf{u}^7-\sqrt{3}\,\mathbf{u}^8), \\ \mathbf{u}^{8'} = \frac{1}{2}\sqrt{3}(\mathbf{u}^7+\frac{1}{3}\sqrt{3}\,\mathbf{u}^8), \end{cases} \tag{3}$$

where again $\mathbf{u}^{7'}$ and $\mathbf{u}^{8'}$ are orthogonal, $\mathbf{u}^{8'}$ commuting with the 3-rotation $U_b$ $(\mathbf{u}^2, \mathbf{u}^3, \mathbf{u}^{7'})$:

$$[\mathbf{u}^{8'}, \mathbf{u}^b] = 0. \tag{4}$$

We now define a metric $g_{ij}$ in $P$ space,

$$g_{ij} = \begin{vmatrix} & & & & & & & 1 \\ & & & & & & 1 & \\ & & & & & 1 & & \\ & & & & 1 & & & \\ & & & 1 & & & & \\ & & 1 & & & & & \\ & 1 & & & & & & \\ 1 & & & & & & & \end{vmatrix}, \tag{5}$$

such that

$$\sum_{i=1}^{8} g_{ij}\mathbf{u}^i = \mathbf{u}_j = \tilde{\mathbf{u}}^j. \tag{6}$$

Note that

$$2\mathrm{Tr}\{\tilde{\mathbf{u}}^i\,\mathbf{u}^j\} = 2\mathrm{Tr}\{\mathbf{u}^i\,\tilde{\mathbf{u}}^j\} = 1. \tag{7}$$

Thus

$$\mathbf{A}\cdot\mathbf{B} = 2\mathrm{Tr}\{\sum_{i,j=1}^{8} g_{ij}A^i\mathbf{u}^i B^j\mathbf{u}^j\} \equiv \sum_{i,j} g_{ij}A^iB^j \tag{8}$$

is a scalar product in $P$.

When using our algebra for unitary transformations, we shall take the hermitian set V as a basis for the infinitesimal operators,

$$\mathbf{V}\begin{cases} \mathbf{v}^{14} = \frac{1}{2}\sqrt{2}(\mathbf{u}^1+\mathbf{u}^4), & \mathbf{v}^{41} = \frac{1}{2}i\sqrt{2}(\mathbf{u}^1-\mathbf{u}^4), \\ \mathbf{v}^{23} = \frac{1}{2}\sqrt{2}(\mathbf{u}^2+\mathbf{u}^3), & \mathbf{v}^{32} = -\frac{1}{2}i\sqrt{2}(\mathbf{u}^2-\mathbf{u}^3), \\ \mathbf{v}^{56} = \frac{1}{2}\sqrt{2}(\mathbf{u}^5+\mathbf{u}^6), & \mathbf{v}^{65} = -\frac{1}{2}i\sqrt{2}(\mathbf{u}^5-\mathbf{u}^6), \\ \mathbf{v}^7 = \mathbf{u}^7, & \mathbf{v}^8 = \mathbf{u}^8, \end{cases} \tag{9}$$

so that

$$\sum_{k=1}^{8} A_V{}^k B_V{}^k = \sum_{i=1}^{8} A_U{}^i B_{U,i}, \tag{10}$$

i.e. the scalar product (8) is Euclidean in the $V$ system.

Under a unitary transformation $E^{(m_V)} = \exp(i\varepsilon^{m_V}\mathbf{v}^{m_V})$ ($m_V$ is the single or double index in V), the component $A^k\mathbf{u}^k$ transforms like

$$\sum_{l=1}^{8} \delta_{(m_V)}A^l\mathbf{u}^l = i\varepsilon^{m_V}A^k[\mathbf{v}^{m_V}, \mathbf{u}^k] = i\varepsilon^{m_V}A^k\sum_{l=1}^{8} f^l_{m_V,k}\mathbf{u}^l$$

and for

$$E = \exp(i\sum_{m_V}\varepsilon^{m_V}\mathbf{v}^{m_V}) \tag{11}$$

we get variations

$$\delta A^l = i \sum_{m_V} \varepsilon^{m_V} \sum_{k=1}^{8} f^l_{m_V,k} A^k. \tag{12}$$

The $f^l_{m_V,k}$ define an $8\times 8$ representation of our algebra in $P$ space,

$$C^{l,k}_{m_V} = f^l_{m_V,k}, \tag{13}$$

so that (12) becomes in $P$

$$\delta A^l = i \sum_{m_V=1}^{8} \varepsilon^{m_V} \sum_{k=1}^{8} C^{l,k}_{m_V} A^k,$$

or

$$\delta \mathbf{A} = i \sum_{m_V} \varepsilon^{m_V} C_{m_V} \mathbf{A} = i \sum_{i,j} g_{ij} \varepsilon^i C^j \mathbf{A}, \tag{14}$$

where we have returned to the basis **U** or **U′**.

## 3. Fields and Interactions

We define the quantum operators

$$\mathbf{I}(C_5, C_6, C_7), \qquad I_Z = C^7, \qquad Q = \tfrac{2}{3}\sqrt{3}\, C^{8\prime}, \qquad Y = \tfrac{2}{3}\sqrt{3}\, C^8, \tag{15}$$

and write the fields as vectors in P space

$$\begin{aligned} &\psi(\mathrm{p},\ \mathrm{n},\ \Xi^0,\ \Xi^-,\ \Sigma^+,\ \Sigma^-,\ \Sigma^0,\ \Lambda), \qquad \overline{\psi}(\overline{\Xi^-},\ \overline{\Xi^0},\ \bar{\mathrm{n}},\ \bar{\mathrm{p}},\ \overline{\Sigma^-},\ \overline{\Sigma^+},\ \overline{\Sigma^0},\ \bar{\Lambda}) \\ &\varphi(\mathrm{K}^+,\ \mathrm{K}^0,\ \overline{\mathrm{K}^0},\ \overline{\mathrm{K}}^-,\ \pi^+,\ \pi^-,\ \pi^0,\ \pi^{0\prime}), \qquad \overline{\varphi} = \varphi, \end{aligned} \tag{16}$$

or in matrix form

$$\psi = \tfrac{1}{2}\sqrt{2}\begin{vmatrix} \tfrac{1}{2}\sqrt{2}\,\Sigma^0 + \tfrac{1}{6}\sqrt{6}\,\Lambda & \Sigma^+ & \mathrm{p} \\ \Sigma^- & -\tfrac{1}{2}\sqrt{2}\,\Sigma^0 + \tfrac{1}{6}\sqrt{6}\,\Lambda & \mathrm{n} \\ \Xi^- & \Xi^0 & -\sqrt{\tfrac{2}{3}}\,\Lambda \end{vmatrix},$$

$$\overline{\psi} = \tfrac{1}{2}\sqrt{2}\begin{vmatrix} \tfrac{1}{2}\sqrt{2}\,\overline{\Sigma^0} + \tfrac{1}{6}\sqrt{6}\,\bar{\Lambda} & \overline{\Sigma^-} & \overline{\Xi^-} \\ \overline{\Sigma^+} & -\tfrac{1}{2}\sqrt{2}\,\overline{\Sigma^0} + \tfrac{1}{6}\sqrt{6}\,\bar{\Lambda} & \overline{\Xi^0} \\ \bar{\mathrm{p}} & \bar{\mathrm{n}} & -\sqrt{\tfrac{2}{3}}\,\bar{\Lambda} \end{vmatrix}, \tag{17}$$

$$\varphi = \tfrac{1}{2}\sqrt{2}\begin{vmatrix} \tfrac{1}{2}\sqrt{2}\,\pi^0 + \tfrac{1}{6}\sqrt{6}\,\pi^{0\prime} & \pi^+ & \mathrm{K}^+ \\ \pi^- & -\tfrac{1}{2}\sqrt{2}\,\pi^0 + \tfrac{1}{6}\sqrt{6}\,\pi^{0\prime} & \mathrm{K}^0 \\ \overline{\mathrm{K}^-} & \overline{\mathrm{K}^0} & -\sqrt{\tfrac{2}{3}}\,\pi^{0\prime} \end{vmatrix},$$

The free field Lagrangians are

$$\mathscr{L}_{\psi}{}^{0} = -\overline{\psi}\cdot(\gamma^{\mu}\partial_{\mu}+m_{\psi})\psi, \qquad \mathscr{L}_{\varphi}{}^{0} = -\tfrac{1}{2}(\partial^{\mu}\boldsymbol{\varphi}\cdot\partial_{\mu}\boldsymbol{\varphi}+m_{\varphi}{}^{2}\boldsymbol{\varphi}\cdot\boldsymbol{\varphi}). \quad (18)$$

We postulate the invariance of these Lagrangians under the unitary gauge transformation

$$E = \exp(i\sum_{m_{\nu}}\varepsilon^{m_{\nu}}(x)C^{m_{\nu}}) \quad (19)$$

and follow the now standardized technique of Yang and Mills [1]) and Utiyama [7]), recombining the $C$ set in terms of the basis **U** of (1).

The total Lagrangian becomes

$$\mathscr{L}_{\text{total}} = \mathscr{L}_{\psi}{}^{0}+\mathscr{L}_{\varphi}{}^{0}+\mathscr{L}_{\psi}{}^{g}+\mathscr{L}_{\varphi}{}^{g}+\mathscr{L}_{B}{}^{0}, \quad (20)$$

$$\mathscr{L}_{\psi}{}^{g} = -\sum_{i=1}^{8}\sum_{n=1}^{8}\bar{\psi}^{n}\gamma^{\mu}C_{i}\psi_{n}B_{\mu}{}^{i}, \quad (21)$$

$$\mathscr{L}_{\varphi}{}^{g} = -\sum_{\substack{i=1\\ j=1}}^{8}\sum_{n=1}^{8}(\partial_{\mu}\bar{\varphi}_{n}+C_{i}\bar{\varphi}_{n}B_{\mu}{}^{i})C_{j}\varphi^{n}B^{j\mu}. \quad (22)$$

The $B_{\mu}{}^{i}$ is a set of 8 vector bosons, with the following isobaric and strangeness qualities:

$$\begin{aligned} &B_{\mu}{}^{1}\to \mathrm{K}^{+}, \quad B_{\mu}{}^{2}\to \mathrm{K}^{0}, \quad B_{\mu}{}^{3}\to \overline{\mathrm{K}}{}^{0}, \quad B_{\mu}{}^{4}\to \overline{\mathrm{K}}{}^{-},\\ &B_{\mu}{}^{5}\to \pi^{+}, \quad B_{\mu}{}^{6}\to \pi^{-}, \quad B_{\mu}{}^{7}\to \pi^{0}, \quad B_{\mu}{}^{8}\to \pi^{0\prime}. \end{aligned} \quad (23)$$

We have here the same set of vector bosons Salam and Ward got out of the 8-dimensional rotation gauge — with an additional $\pi^{0\prime}$—like interaction. Denoting as in ref. [3]) the K-like set by $Z_{\mu}$,

$$Z_{\mu} = (Z_{\mu}{}^{+}, Z_{\mu}{}^{0}), \qquad \bar{Z}_{\mu} = (\bar{Z}_{\mu}{}^{-}, \bar{Z}_{\mu}{}^{0}),$$

the $\pi$-like one by $V_{\mu}{}^{i}$ with

$$V_{\mu}{}^{\pm} = \tfrac{1}{2}\sqrt{2}(V_{\mu}{}^{1}\pm iV_{\mu}{}^{2}), \qquad V_{\mu}{}^{0} = V_{\mu}{}^{3}$$

and the $\pi^{0\prime}$-like by $B_{\mu}{}^{8} = X_{\mu}{}^{0}$ we get

$$\mathscr{L}_{B}{}^{0} = -\tfrac{1}{4}(\mathbf{F}_{\mu\nu}\cdot\mathbf{F}^{\mu\nu}), \quad (24)$$

$$\mathbf{F}_{\mu\nu} = \mathbf{H}_{\mu\nu}+\mathbf{G}_{\mu\nu}, \quad (24')$$

$$\mathbf{H}_{\mu\nu} = \partial_{\mu}\mathbf{B}_{\nu}-\partial_{\nu}\mathbf{B}_{\mu}, \quad (24'')$$

$$\begin{aligned} G^{Z}_{\mu\nu} &= \tfrac{1}{2}\{Z_{\mu}(\mathbf{V}_{\nu}\cdot\boldsymbol{\tau}+\sqrt{3}\,X_{\nu}{}^{0})-(\mathbf{V}_{\mu}\cdot\boldsymbol{\tau}+\sqrt{3}\,X_{\mu}{}^{0})\tilde{}\,Z_{\nu}\},\\ G^{\bar{Z}}_{\mu\nu} &= -\tfrac{1}{2}\{\bar{Z}_{\mu}(\mathbf{V}_{\nu}\cdot\boldsymbol{\tau}+\sqrt{3}\,X_{\nu}{}^{0})\tilde{}-(\mathbf{V}_{\mu}\cdot\boldsymbol{\tau}+\sqrt{3}\,X_{\mu}{}^{0})\bar{Z}_{\nu}\},\\ G^{V}_{\mu\nu} &= i\mathbf{V}_{\mu}\wedge\mathbf{V}_{\nu}+\tfrac{1}{2}\{\bar{Z}_{\mu}\boldsymbol{\tau}Z_{\nu}-Z_{\mu}\boldsymbol{\tau}\bar{Z}_{\nu}\},\\ G^{X}_{\mu\nu} &= \tfrac{1}{2}\sqrt{3}\,\{\bar{Z}_{\mu}Z_{\nu}-Z_{\mu}\bar{Z}_{\nu}\}. \end{aligned} \quad (24''')$$

In the 3-space of the matrix elements of **U**, we have the set

$$\mathbf{B}_\mu = \tfrac{1}{2}\sqrt{2}\begin{vmatrix} \tfrac{1}{2}\sqrt{2}\,V_\mu^0+\tfrac{1}{6}\sqrt{6}\,X^0 & V_\mu^+ & Z_\mu^+ \\ V_\mu^- & -\tfrac{1}{2}\sqrt{2}\,V_\mu^0+\tfrac{1}{6}\sqrt{6}\,X_\mu^0 & Z_\mu^0 \\ Z_\mu^- & Z_\mu^0 & -\sqrt{\tfrac{2}{3}}\,X_\mu^0 \end{vmatrix}. \quad (25)$$

## 4. Discussion

The fermion and boson interaction Lagrangians provide us with the full set of known strong interactions (plus the $\pi^{0\prime}$ set) through the current-current-like 2nd order terms — but with no Yukawa-like simple processes for $\pi$ or K.

In its general features, our Lagrangian reflects a certain similarity with Sakurai's theory [2]). The $V_\mu$ is similar to the $B_T{}^\mu$ (isospin-current boson) of the latter, and the $X_\mu{}^0$ is similarly related to its $B_Y{}^\mu$ (the hypercharge-current boson singlet). On the other hand we have no $B_B{}^\mu$ (baryon-current singlet) and do have a $Z_\mu$ set which has no place in ref. [2]).

We note that we do get directly from our group structure a ratio between the couplings; for the $V$ and $X$ fields, this is $f_X = f_V\sqrt{3}$, a value that fits Sakurai's phenomenological conclusion (from KN and $\overline{\mathrm{K}}$N at low energies) that $(1/4\pi m_X{}^2)f_X{}^2 \approx (3/4\pi m_V{}^2)f_V{}^2$ if we assume the masses of be similar. Our $X^0$ field does not interact with the $(\Sigma, \Lambda)$ set, and $V$ does not interact with $\Lambda$, so that we get a split (N $\Xi$), $\Sigma$, $\Lambda$ but though the interactions of $X$ and $Z$ with N and $\Xi$ have opposite signs, lacking $B_B{}^\mu$ we cannot repeat here Sakurai's simple interpretation of the origin of the N-$\Xi$ mass split. The arguments explaining the $\pi$-N S-wave scattering exist in our gauge. We also note that $\mathscr{L}_B{}^0$ in (24) with its $G^i_{\mu\nu}G_i^{\mu\nu}$ provides us with effective mass terms (in the sense of the mass of $A_\mu{}^\pm$ in a former work [8]) of Salam and Ward) for $V_\mu$, $Z_\mu$ and $X_\mu{}^0$ (from $G^Z_{\mu\nu}$ and $G^{\bar{Z}}_{\mu\nu}$), whereas ref. [2]) lacks such terms for the singlets $B_Y$ and $B_B$. From $\mathscr{L}_\varphi{}^s$ we see that provided the masses are sufficient, there exist fast decays

$$Z \to \mathrm{K}+\pi,$$

$$V \to 2\pi \quad \text{or} \quad V \to \mathrm{K}+\overline{\mathrm{K}} \qquad \text{(the even } G \text{ combination)},$$

$$X \to \mathrm{K}+\overline{\mathrm{K}} \qquad \text{(odd } G \text{ combination)}.$$

Note the possibility that $m_X \approx m_V$.

From the point of view of the Lagrangian formalism, it seems preferable to us to have what is in fact one conservation law for a "charge" that behaves like a 2nd rank tensor in three dimensions, than three separate unrelated conservation laws; this is even more important in view of the necessity to bring in at some further stage the electromagnetic and the weak interactions. In Sakurai's theory, these seem to imply two new independently conserved

quantities $Q$ and $l$, though the relation $Q = I_Z + \frac{1}{2}Y$ seems to indicate that the interactions are not wholly independent (and so does the $|\Delta \mathbf{I}| = \frac{1}{2}$ rule of the weak interactions). We think that the "aesthetic' value of Sakurai's theory and the "Urschmiere" approach would be enhanced if there proved to be only one kind of "Urschmiere" instead of five.

Our gauge has not given us directly an additional electromagnetic and weak Lagrangian. Still, it is interesting to check the connection it may have with these. We can do that by using (3) and rewriting our gauge invariance and the vector bosons in that basis. We get

$$B_\mu^{8'} \to A_\mu, \tag{26}$$

$$\mathbf{B}'_\mu = \tfrac{1}{2}\sqrt{2} \begin{vmatrix} \sqrt{\tfrac{2}{3}}\, A_\mu & V_\mu^+ & Z_\mu^+ \\ V_\mu^- & \tfrac{1}{2}\sqrt{2}\, B_\mu^{7'} - \tfrac{1}{6}\sqrt{6}\, A_\mu & Z_\mu^0 \\ \bar{Z}_\mu^- & \bar{Z}_\mu^0 & -\tfrac{1}{2}\sqrt{2}\, B_\mu^{7'} - \tfrac{1}{6}\sqrt{6}\, A_\mu \end{vmatrix}. \tag{26'}$$

The interaction Lagrangian corresponding to (26) will be identical with the electromagnetic Lagrangian. It leads to the conditions

$$|\Delta \mathbf{I}| = 0,1 \qquad |\Delta I_Z| = 0, \qquad |\Delta Y| = 0, \tag{27}$$

though, of course, all quantum numbers are fully conserved when one adds the remaining interactions of $P_d$, mediated by $B_\mu^{7'}$. This last, with quantum numbers similar to (27), belongs with $B_\mu^2$ and $B_\mu^3$ (the $K^0$, $\bar{K}^0$-like vector bosons) to the subspace defined by $\mathbf{U}_b$ in (4). We note (4), from which we can see that $B_\mu^{8'}$ is the only matrix in $P_d$ orthogonal to the $\mathbf{U}_b$ set. If, following Salam and Ward's [3]) treatment of weak interactions, we assume that the $|\Delta \mathbf{I}| = \frac{1}{2}$ law results from a non zero vacuum expectation value for the field $K_1^0$, our system could mediate the weak interactions through this $B_\mu^2$, $B_\mu^3$ subset; thus the $\mathbf{U}_b$ subset is apparently responsible for the generation of weak interactions as a secondary effect, with non conservation of parity — but whatever the mechanism involved, it cannot affect the electromagnetic interactions, generated by an orthogonal gauge. Still, we have no suggestion to explain why the strong interactions, mediated by a **U** gauge, should be accompanied by weaker interactions involving a change of basis into **U**'.

One last remark, concerning the $\pi^{0'}$. From the group-structure aspect, it is related to the spinor-like subgroups (i.e. the K and not the $\pi$). From (2) we note that its matrix representation commutes with that of the pion. It has no direct interaction with the pions, while it does interact with all the kaons. If we assume a single parity for all the components of the $\varphi$ vector, it is a pseudoscalar particle, with a fast decay into $K^0 + \bar{K}^- + \pi^+$ (mediated by $Z_\mu$) or $K^+ + \bar{K}^- + \pi^0$ (through $Z_\mu$ again) etc., provided it has sufficient mass. On

the other hand, if it were scalar, it could do for the medium strong interactions what the vacuum decay of the $\sigma$ meson does for all strong interactions in ref. [3]). In fact it would then be identical with the $\sigma'$ particle suggested in a variant of ref. [3]).

I am indebted to Prof. A. Salam for discussions on this problem. In fact, when I presented this paper to him, he showed me a study he had done on the unitary theory of the Sakata model, treated as a gauge, and thus producing a similar set of vector bosons [9]).

Shortly after the present paper was written, a further version, utilizing the 8-representation for baryons, as in this paper, reached us in a preprint by Prof. M. Gell Mann.

## References

1) C. N. Yang and H. Mills, Phys. Rev. **96** (1954) 192
2) J. J. Sakurai, Ann. of Phys. **11** (1960) 1
3) A. Salam and J. C. Ward, Nuovo Cim. **19** (1961) 167
4) J. Tiomno, Nuovo Cim. **6** (1957) 1
5) J. Schwinger, Ann. of Phys. **2** (1957) 407
6) M. Ikeda, S. Ogawa, Y. Ohnuki, Progr. Theor. Phys. **22** (1959) 5, 719
7) R. Utiyama, Phys. Rev. **101** (1956) 1597
8) A. Salam and J. Ward, Nuovo Cim. **11** (1959) 4, 569
9) A. Salam and J. Ward, Nuovo Cim., to be published

8.B

*Nuclear Physics* **26** (1961) 230—232; © *North-Holland Publishing Co., Amsterdam*

Not to be reproduced by photoprint or microfilm without written permission from the publisher

# YUKAWA TERMS IN THE UNITARY GAUGE THEORY

Y. NE'EMAN

*Department of Physics, Imperial College London*

Received 24 March 1961

**Abstract:** Considering higher order graphs, Yukawa terms are shown to appear in the unitary gauge theory under certain CP assumptions.

## 1. Introduction

Three recent papers [1, 2, 3]) have derived the strong interactions from a 3-dimensional unitary gauge. Though the symmetries implied seem to fit most experimental facts, all three versions lack Yukawa terms, i.e. no single pions or kaons are emitted or absorbed.

In a former theory, Salam and Ward [4]) have shown that such terms appear in a gauge-theory if it contains a neutral meson with

$$\mathrm{CP} = 1. \tag{1}$$

Such an $x^0$ meson can then have

$$\langle x^0 \rangle_0 \neq 0, \tag{2}$$

so that terms like

$$x^0 \partial_\mu \pi B_i^\mu, \qquad \bar{\psi} \gamma_\mu \beta^i \psi B_i^\mu \tag{3}$$

give a Yukawa vector interaction mediated by the vector boson $B_i^\mu$ (here $\beta^i$ is the group operator).

## 2. The $\varrho^0$ Meson

Looking for an $x^0$ in the representations of the 3-unitary group, we first notice that there exists a one-dimensional representation given by the trace of the set. It could accommodate an $x^0$, but its scalar nature with respect to the group does not allow it to contribute to the interaction Lagrangian. Our answer therefore points to the isosinglet within the 8-representation, which we denoted in ref. [3]) by $\pi^{0\prime}$, otherwise known as $\rho^0$. For this meson to fulfil eq. (1) there are 3 possible choices. (A) The first choice is $\mathrm{C} = 1$ (as for the pions), $\mathrm{P} = 1$, i.e. the mesons' 8-vector does not have one parity for all its components. Such was also the case in refs. [4, 5]). In both studies, this was based on a group

structure allowing such a difference between the hypothetical sigma meson and the pions. In our case, the $\rho^0$ is also an isolated singlet.

In the formalism of ref. [3]), and with $((\mathbf{u}^i))$ denoting the linear envelope of vectors $\mathbf{u}^i$, namely subspaces of the algebra's 8-space $P$, we have

$$\rho^0 \in ((\mathbf{u}^8)), \tag{4}$$

$$\pi \in U_a = ((\mathbf{u}^5, \mathbf{u}^6, \mathbf{u}^7)), \tag{5}$$

$$[\mathbf{u}^8, \mathbf{u}^a] = 0, \qquad \mathbf{u}^a \in U_a. \tag{6}$$

On the other hand, we can form two other 3-rotation subspaces similar to $U_a$ with the kaons. Defining vectors

$$\mathbf{b}^0 = -\tfrac{1}{2}(\mathbf{u}^7 - \sqrt{3}\mathbf{u}^8), \qquad \mathbf{c}^0 = -\tfrac{1}{2}(\mathbf{u}^7 + \sqrt{3}\mathbf{u}^8), \tag{7}$$

we find

$$\mathrm{K}^0, \overline{\mathrm{K}}^0 \in U_b = ((\mathbf{u}^2, \mathbf{u}^3, \mathbf{b}^0)), \qquad \mathrm{K}^+, \overline{\mathrm{K}}^- \in U_c = ((\mathbf{u}^1, \mathbf{u}^4, \mathbf{c}^0)), \tag{8}$$

$$\rho^0 \in ((\mathbf{u}^8)) = ((\mathbf{b}^0 - \mathbf{c}^0)). \tag{9}$$

This defines a certain limited connection with the kaons; but assumption (A) is certainly allowed as long as the parity of the latter is undetermined.

Still, we should note that the analogy with refs. [4, 5]) may be too stretched, as these deal with 4-dimensional rotations (a semisimple algebra splitting into two ideals) whereas our gauge is given by a simple algebra with no ideals.

(B) The second choice one can make is the following: the $\rho^0$ is a complex field $\rho^0 = \frac{1}{2}\sqrt{2}(\rho_1{}^0 + i\rho_2{}^0)$ like the kaons, and $\rho_1{}^0$ is an $x^0$.

This would induce some changes in the formalism of ref. [3]) through putting

$$\overline{\varphi} \neq \varphi \tag{10}$$

in the $P$ 8-space. Still, as this is the case with the fermions, it could also happen here.

(C) The third possible choice is

$\mathrm{P} = -1$ (as for the pions),

$\mathrm{C} = -1$ (in opposition to the eigenvalue of the pions).

## 3. Discussion

If eq. (1) holds for $\rho^0 \in ((\mathbf{u}^8))$ while $\pi \in U_a$ has CP$=-1$ we should get opposite relative CP eigenvalues for the corresponding baryon bilinears. As these have $\mathrm{C} = 1$ both $S$ and $P$, this means opposite parities. ($S$ and $P$ are conventional scalar and pseudoscalar Fermion bilinears). Thus the assumption that $\rho^0$ is the $x^0$ of eq. (2) and (3) gives us a prediction for an odd relative $\Lambda - \Sigma$ parity.

It is also edifying to note the difference in the order of the diagrams leading

to Yukawa terms for the kaons and the pions respectively. Single kaons can be emitted as in eq. (3), mediated by $Z_\mu$ (the isospinor that may be identical with the observed K* according to Chan's calculation [6]) as in fig. 1.

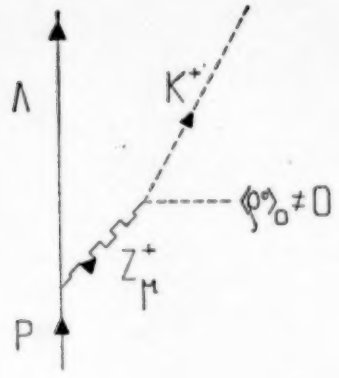


Fig. 1. Emission of a $K^+$ meson ($Z_\mu^+$ is a $K^+$-like vector boson).

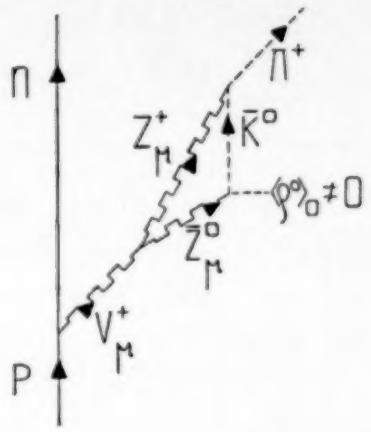


Fig. 2. Emission of a $\pi^+$ meson ($V_\mu^+$, $Z_\mu^+$, $Z_\mu^0$ are vector bosons behaving like $\pi^+$, $K^+$, $\bar{K}^0$ in isobaric space).

Because of eq. (6), there are no terms mixing $\rho^0$ and $\pi$ mesons in the 8-representation of the unitary group (as it is constructed from the Lie coefficients of the $\mathbf{u}^i$ basis). Thus, pion Yukawa terms appear only in higher order graphs, like the example in fig. 2. The possible effect on the ratio of the phenomenological couplings is interesting; $g_\pi > g_K$ would preclude the attribution of the strength itself to eq. (2) as was assumed in ref. [4]) namely terms with no $\rho^0$ would still be strongly coupled.

I would like to thank Prof. A. Salam for guidance, criticism and discussions of this problem.

## References

1) A. Salam and J. C. Ward, Nuovo Cim., to be published
2) M. Gell Mann, preprint
3) Y. Ne'eman, Nuclear Physics **26** (1961) 222
4) A. Salam and J. C. Ward, Nuovo Cim. **19** (1961) 167
5) J. Schwinger, Ann. Phys. **2** (1957) 407;
M. Gell Mann and Levy, Nuovo Cim. **16** (1960) 4, 705
6) C. H. Chan, Phys. Rev. Letters, to be published

2.I

*Nuclear Physics* **26** (1961) 233—249; © *North-Holland Publishing Co., Amsterdam*

Not to be reproduced by photoprint or microfilm without written permission from the publisher

# PHOTOPROTONS FROM CARBON

V. J. VANHUYSE

*Natuurkundig Laboratorium, Rijksuniversiteit, Gent, België*

and

W. C. BARBER

*High-Energy Physics Laboratory, Stanford University, Stanford, California* †

Received 21 February 1961

**Abstract:** Energy and angular distributions of protons ejected from $C^{12}$ targets bombarded by the beam of the Stanford Mark II accelerator have been measured by means of a magnetic spectrometer. The energy distributions, which are peaked at 6.0 MeV, show a structure that cannot be explained by a single resonance. Supposing that all transitions leave the residual nucleus in the ground state, the analysis of the proton distributions leads to a cross section which has a peak value of $(12.7 \pm 2.5)$ mb and values of $(41 \pm 9)$ MeV · mb and $(77 \pm 18)$ MeV · mb when integrated from 0 to 24 and 40 MeV, respectively. Except for the peak value, the cross section curve is very similar to that of the $^{12}C(\gamma, n)$ reaction. The angular distributions of the $(\gamma, p)$ and $(e, e'p)$ reactions have been measured for different proton energy groups at an electron energy of 40 MeV. Except for a $\cos\theta$ term, the distributions are in agreement with the independent particle picture of the giant resonance, p- to d-wave transitions being the important ones. The results are also a confirmation of the theory of electron induced reactions. Yield curves as a function of electron energy were measured up to 40 MeV, for different proton energy groups and at different angles. Analysis of the yield curves leads to differential cross sections as a function of photon energy. The main property of these cross sections is to support to some extent the assumption of exclusively ground state transitions.

## 1. Introduction

The photodisintegration of $C^{12}$ in the giant-resonance region has been the subject of many investigations. The review article by De Sabbata [1]) summarizes most of the work done until 1958 in the study of the principal modes of disintegration, $B^{11}+p$ and $C^{11}+n$. Investigations reported since 1958 include that on photoprotons by Penner and Leiss [2]) and studies of the inverse reaction $B^{11}+p \rightarrow C^{12}+\gamma$ by Gemmell *et al.* [3]) and Gove *et al.* [4]). Several questions remain unsettled, the main ones relating to possible fine structure in the giant resonance and to the relative magnitudes of the $(\gamma, n)$ and $(\gamma, p)$ cross sections.

Our measurements used the Stanford Mark II linear electron accelerator [5]) as a source of photons and a magnetic spectrometer as a proton analyzer. In all our experiments, the electron beam traversed the target so that protons were produced by the direct interaction of the electrons as well as by bremsstrahlung

† Work supported by the Office of Naval Research, the U.S. Atomic Energy Commission and the Air Force Office of Scientific Research.

from the material upstream from the target and from the target itself. By varying the material ahead of the target we were able to obtain information on both the C ($\gamma$, p) B and C(e, e' p) B reactions, and to compare them. Our apparatus permitted measurements in greater detail and with greater statistical accuracy than previous C ($\gamma$, p) experiments (most of which were done with nuclear emulsions), and we believe they help to clarify or at least make more quantitative some of the questions mentioned above.

## 2. Apparatus

The apparatus has been described in detail in a previous article [6]). The electrons of the Mark II were energy analysed by a two-magnet achromatic deflection system. The number of incident electrons was monitored by a secondary-emission monitor, which was calibrated on a Faraday-cup. The energy of the electrons was variable from 10 to 44 MeV. The protons were momentum analysed and detected by means of a magnetic double focusing spectrometer, which contained eight KI (Tl) scintillation counters, located in the output focal plane. This permitted simultaneous measurement of different energy intervals. The energy resolution of the different counters varied from 2.5% in the norrowest channel to 5.5 % in the widest. The spectrometer, which was rotatable around the target, had an acceptance solid angle of about 0.01 sr. The number of detected protons $N_p$ per unit monitor response $V$ in a specific counter can be written as

$$\frac{N_p}{V} = [\Delta E_p \Delta\Omega C] n_t \operatorname{cosec} \varphi \int_0^{E_0} \frac{d^2\sigma(\theta, k, E_0)}{d\Omega dE_p} n(E_0, k, t) dk, \qquad (1)$$

where $\Delta E_p$ is the proton energy spread detected by the counter resulting from its finite width, $\Delta\Omega$ the solid angle subtended by the counter, $C$ the number of electrons required to produce unit monitor response, $n_t$ the number of target nuclei per cm$^2$, $\varphi$ the target angle; $d^2\sigma/d\Omega dE_p$ is a differential cross section to produce a proton at an angle $\theta$ and energy $E_p$ by photons of energy $k$, and $n(E_0, k, t)$ is the number of photons per unit energy interval (real and virtual effective when one electron of energy $E_0$ traverses the target characterized by $t$. From eq. (1), one can deduce

$$Y \equiv \int_0^{E_0} \frac{d^2\sigma(\theta, k, E_p)}{d\Omega dE_p} n(E_0, k, t) dk = \frac{N_p \sin \varphi}{V E_p n_t} \left[\frac{\Delta E_p}{E_p} \Delta\Omega C\right]^{-1}. \qquad (2)$$

As explained in ref. [6]), by studying protons from the photodisintegration of the deuteron, the value of the square bracket for counter 7 was found to be

$$\frac{\Delta E_p}{E_p} \Delta\Omega C = [9.52 \pm 1.4] \times 10^9. \qquad (3)$$

The values of the product $(\Delta E_p/E_p)\Delta\Omega$ for the other counters relative to counter 7 were obtained by measuring the same flat portion of a proton energy spectrum with each counter.

The targets were polystyrene sheets. Three different thicknesses were used 24.46 mg/cm², 7.7 mg/cm² and 2.39 mg/cm².

## 3. Results

The results are illustrated by the figs. 1 to 13. In all cases the indicated errors are standard deviations determined from counter statistics.

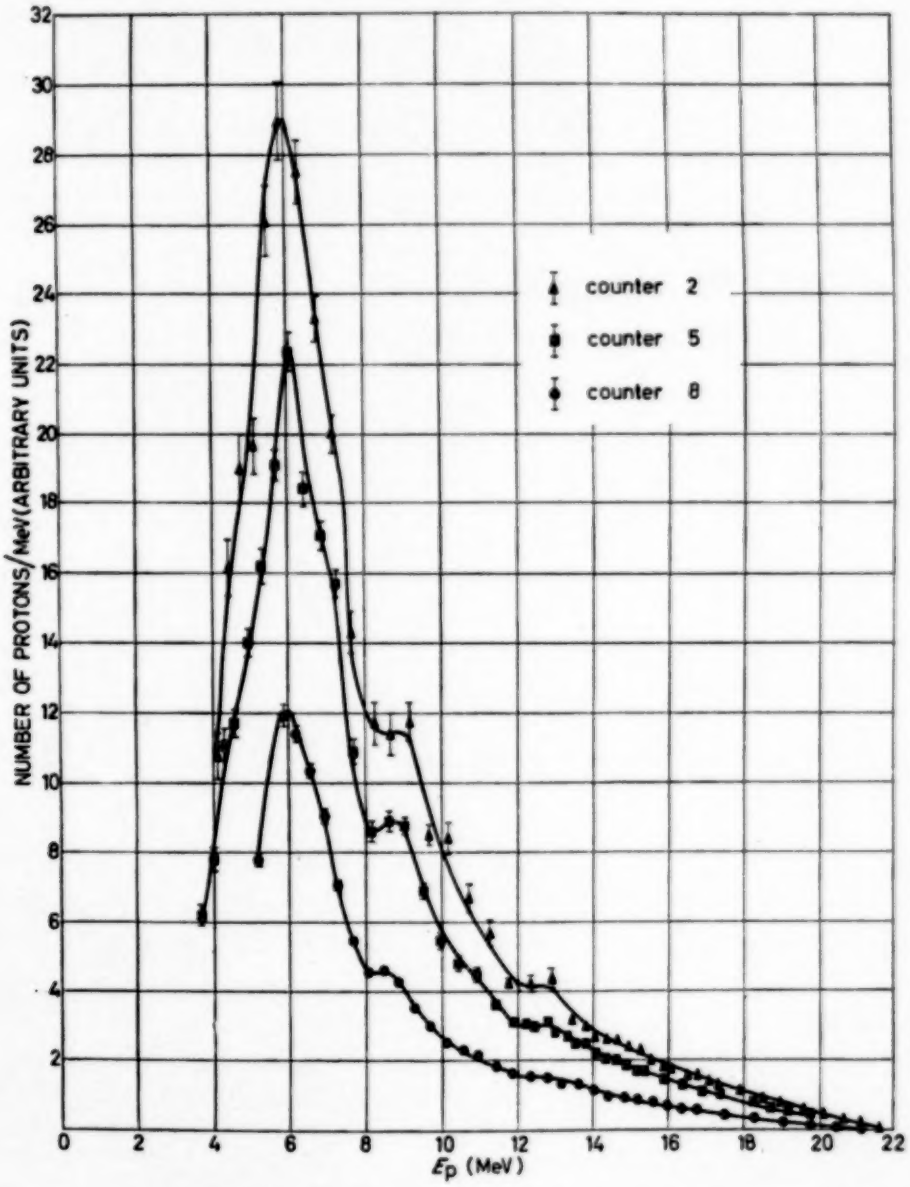


**Fig. 1.** Energy distributions at $\theta = 75°$ for $E_0 = 40$ MeV for three different counters. The curves are drawn arbitrarily.

The energy distributions for $\theta_{lab} = 75°$, shown in fig. 1, were taken with $E_0 = 40$ MeV and with an 0.0127 cm Pb radiator in the primary beam. The background, which turned out to be small, was measured by removing the target and not the radiator. This was done in all the experiments where the radiator was used. The energy spread of the primary electrons $\Delta E_0$, was $0.02\ E_0$. Most of the points were obtained with the 7.7 mg/cm² target placed in such a way that the angle between the normal of the target and the line from the target to the spectrometer entrance was 15°. For the higher energy

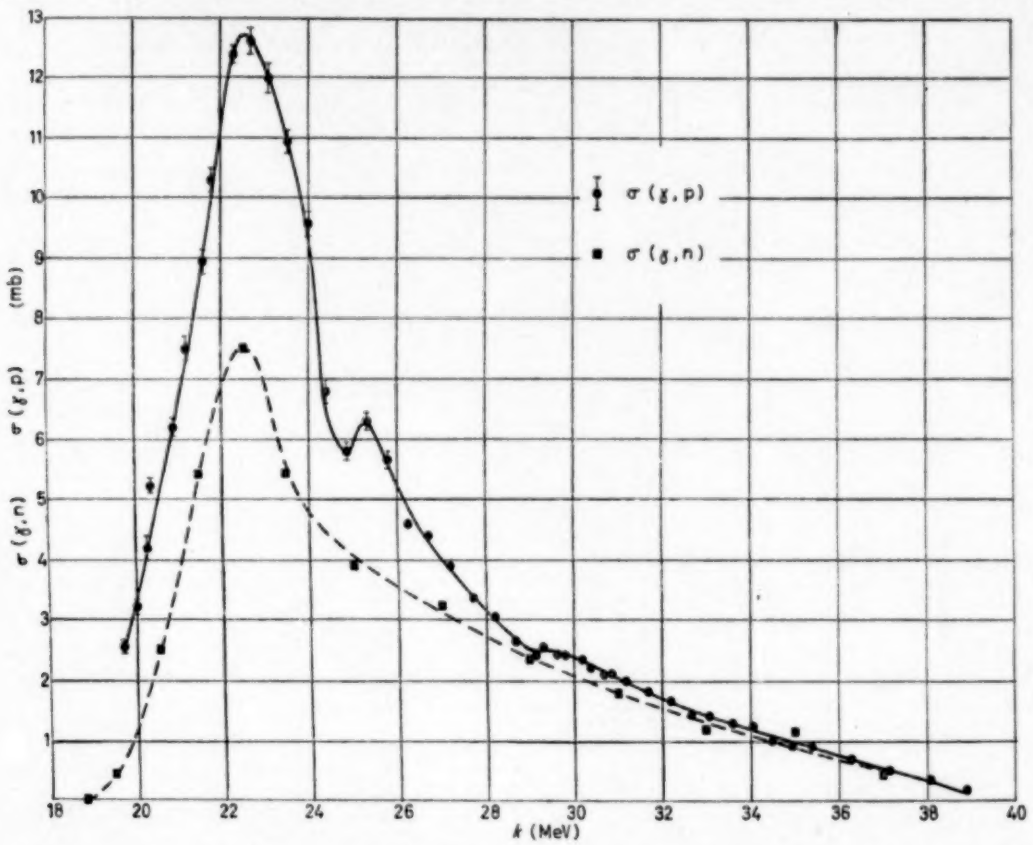


Fig. 2. Cross section of $C^{12}$ ($\gamma$, p) assuming 100 % of transitions leave $B^{11}$ in ground state and cross section of $C^{12}$ ($\gamma$, n) from photon difference method.

protons, the target was 24.46 mg/cm² thick, and the just mentioned angle was 20°. This was kept so in all the other measurements. The correction for energy-loss in the target was made, assuming that all protons traversed half of the effective target. In fig. 1, the closely-spaced points are the ones where the thicker target was used. Supposing that all transitions leave the residual nucleus in the ground state, we obtained from the energy distribution for counter 7 the total cross section $\sigma(k)$ as a function of photon energy (fig. 2). In that case $dE_p = \frac{11}{12}dk$ and (2) reduces to

$$\frac{d\sigma}{d\Omega} = \frac{11}{12}\frac{N_p \sin\varphi}{n(E_0, k, t)VE_p n_t}\left[\frac{\Delta E_p}{E_p}\Delta\Omega C\right]^{-1}, \qquad (4)$$

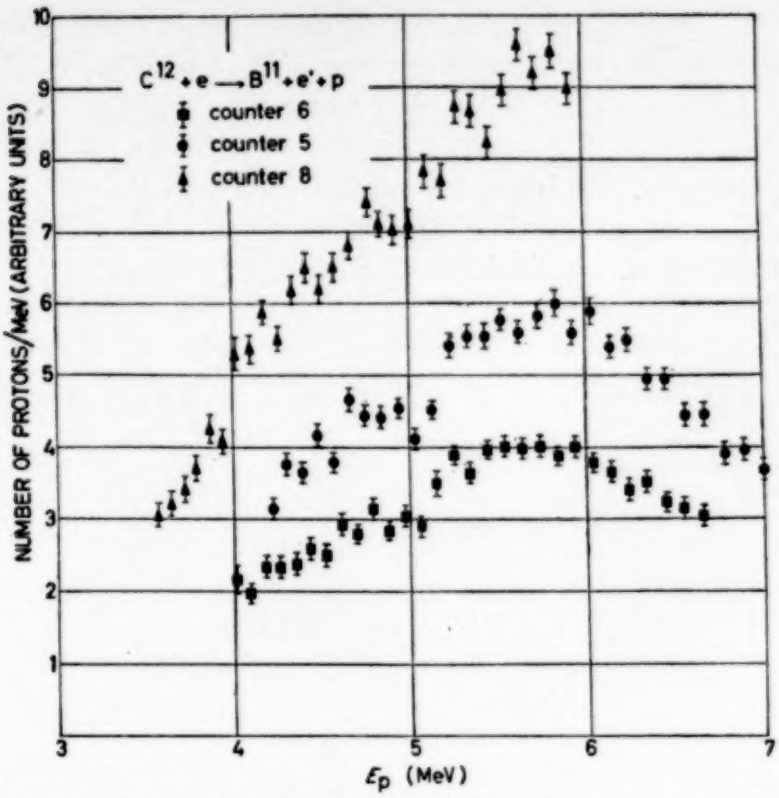


Fig. 3. Energy distributions at $\theta_{lab} = 105°$ for $E_0 = 26$ MeV for three different counters. (Thin C H target).

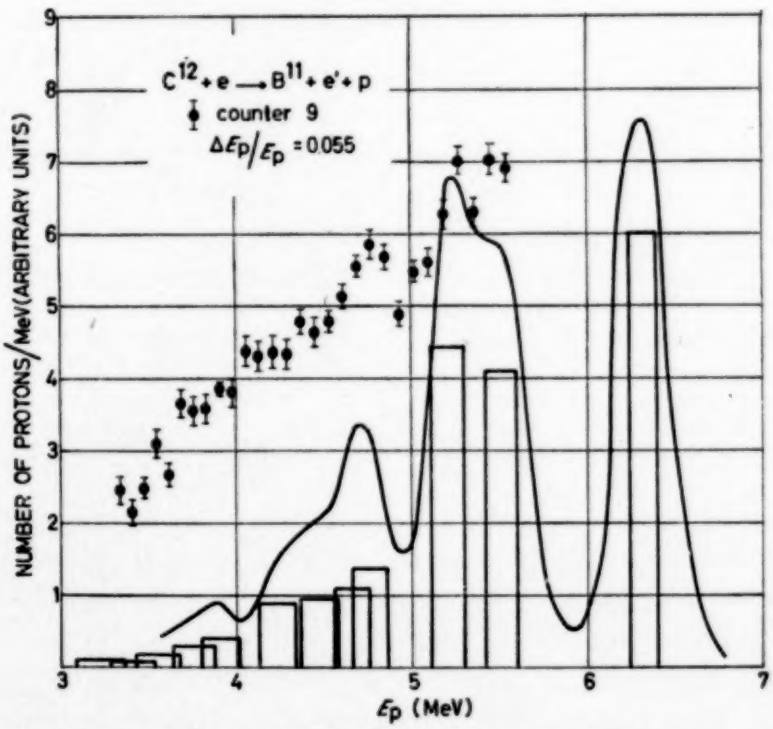


Fig. 4. Energy distribution at $\theta_{lab} = 105°$ for $E_0 = 26$ MeV. The solid curve shows what should be expected if the "breaks" in $\sigma$ ($\gamma$, n) given by Katz are supposed to be the same in $\sigma$ ($\gamma$, p) and if only the ground state transitions are present.

from which $\sigma(k)$ is easily found if the angular distribution $f(\theta)$ is known. In determining $\sigma(k)$ we took for all protons $f(\theta) = 1+0.25\cos\theta+1.35\sin^2\theta$.

Figs. 3 and 4 show the energy distribution for $E_0 = 26$ MeV for four different counters under an angle $\theta_{lab} = 105°$ and with the 2.39 mg/cm² target in place. No radiator was used. The backward angle was chosen in order to reduce the background as much as possible. No target thickness corrections or recoil corrections were made. The incident electron energy spread $\Delta E_0$ was 1 % of $E_0$.

Angular distributions were measured with and without the Pb radiator for two different spectrometer settings. The energy spread of the primary electrons

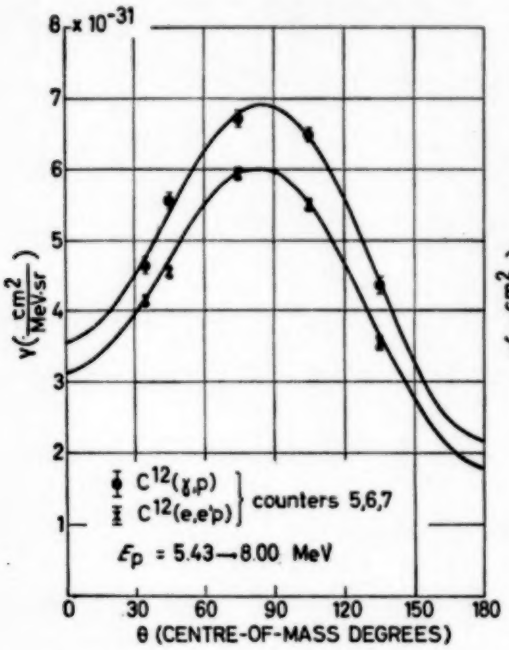


Fig. 5. Angular distributions for $E_0 = 40$ MeV of a proton energy group from $C^{12}$ (e, e'n) and $C^{12}$ ($\gamma$, n) reactions. The curves represent least-square fits to the data. Circles: $2.86\,[1+0.25\cos\theta+1.42\sin^2\theta+0.00\sin^2\theta\cos\theta]\times10^{-31}$ cm²/MeVsr. Crosses: $2.49\,[1+0.27\cos\theta+1.40\sin^2\theta+0.04\sin^2\theta\cos\theta]\times10^{-31}$ cm²/MeVsr.

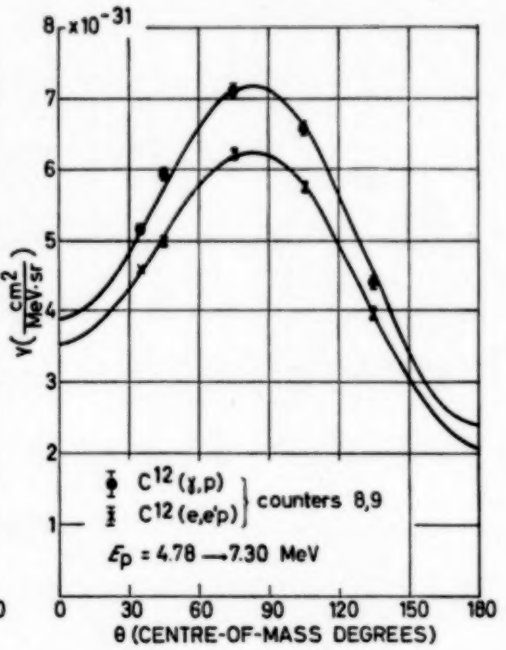


Fig. 6. Angular distribution for $E_0 = 40$ MeV of a proton energy group from $C^{12}$ (e, e' n) and $C^{12}$ ($\gamma$, n) reactions. The curves represent least square fits to the data. Circles: $3.12\,[1+0.24\cos\theta+1.30\sin^2\theta+0.08\sin^2\theta\cos\theta]\times10^{-31}$ cm²/MeVsr. Crosses: $2.83\,[1+0.26\cos\theta+1.20\sin^2\theta-0.04\sin^2\theta\cos\theta]\times10^{-31}$ cm²/MeVsr.

was 2 %. The number of real photons was rather negligible in the case that no radiator was used, so that we were able to find the angular distributions for the (e, e' p) reaction directly and for the ($\gamma$, p) reaction by suitable subtraction of the numbers obtained with and without radiator. We must note, however, that a small correction, resulting from the fact that the electrons lose some energy in the radiator was not made. The weighted averages of the values of $Y$ (eq. 2) for some counters were used to make the plots of figs. 5, 6 and 7.

We used the thick 24.46 mg/cm² target in the angular distribution measurement. This made the original energy spread of the protons which are measured in one counter rather big, so that successive counters overlap. For finding the given limiting values for $E_p$, we took into account the energy loss in the effective target and the width of the counter. For the measurements the current in the spectrometer was slightly changed for the different angles so that protons, cor-

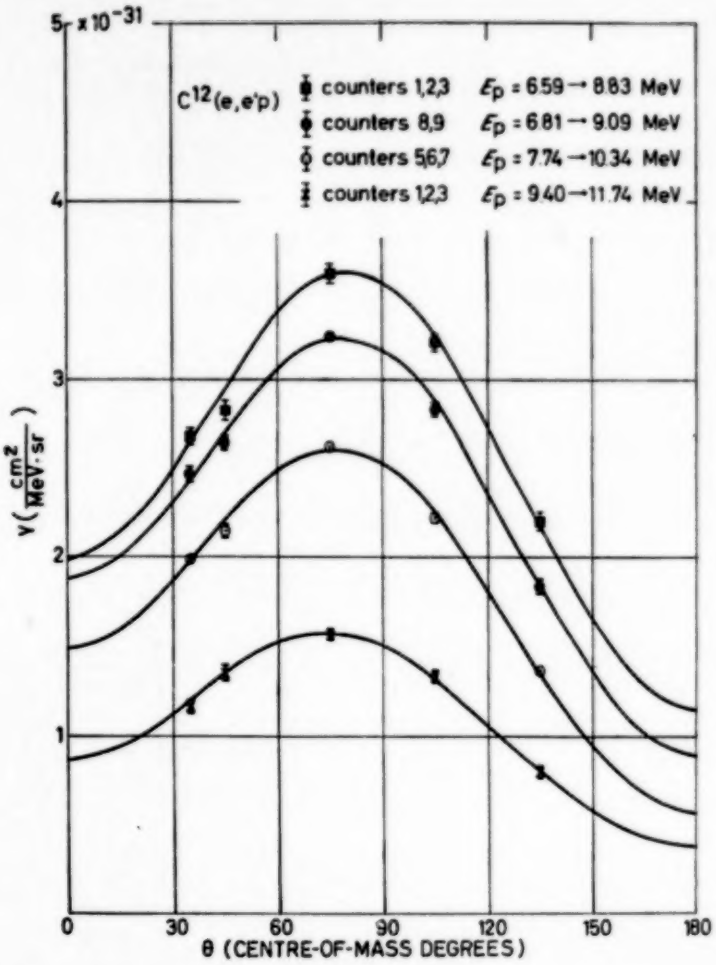


Fig. 7. Angular distributions for $E_0 = 40$ MeV of different proton energy groups from the $C^{12}$ (e, e'p) reaction.

Squares: $1.57[1+0.27\cos\theta+1.27\sin^2\theta+0.12\sin^2\theta\cos\theta]\times10^{-31}$ cm²/MeV.sr.
Full circles: $1.39[1+0.35\cos\theta+1.26\sin^2\theta+0.17\sin^2\theta\cos\theta]\times10^{-31}$ cm²/MeV.sr.
Open circles: $1.03[1+0.44\cos\theta+1.44\sin^2\theta+0.25\sin^2\theta\cos\theta]\times10^{-31}$ cm²/MeV.sr.
Crosses: $0.63[1+0.40\cos\theta+1.41\sin^2\theta+0.41\sin^2\theta\cos\theta]\times10^{-31}$ cm²/MeV.sr.

responding to the same centre-of-mass energy, were detected at each angle. The absorption of a photon of such an energy that a ground state transition occurred was supposed. This made the value of $E_p$ that must be used for computing $Y$ dependent on the angle. We want to point out that the finite acceptance angle of the spectrometer introduces a small error in the angular distribution if the latter

is anisotropic. For our spectrometer, where the ratio of height to width of the rectangular mouth was 2.5, one finds, for instance, that a real angular distribution $1+1.5\sin^2\theta$ would be measured as $1+1.49\sin^2\theta$.

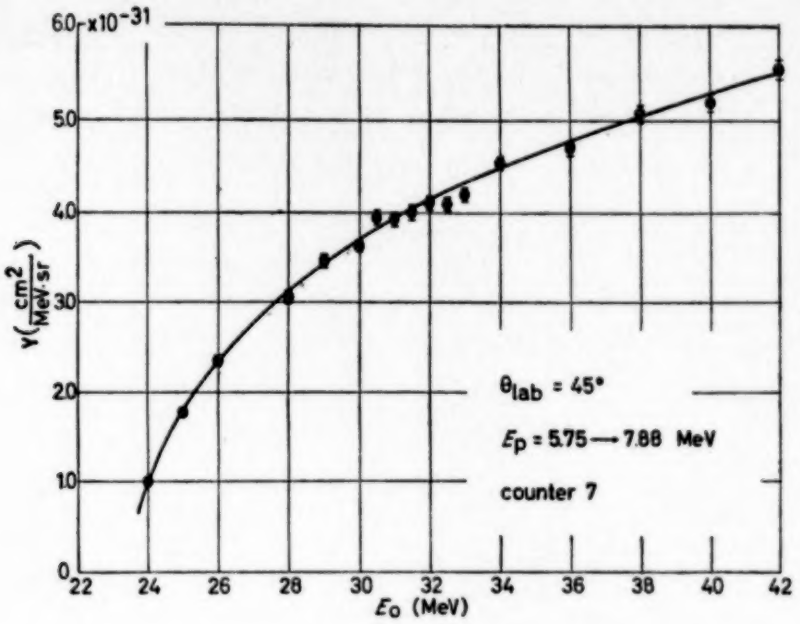


Fig. 8. Excitation of an energy group of protons at 45° as a function of primary electron energy.

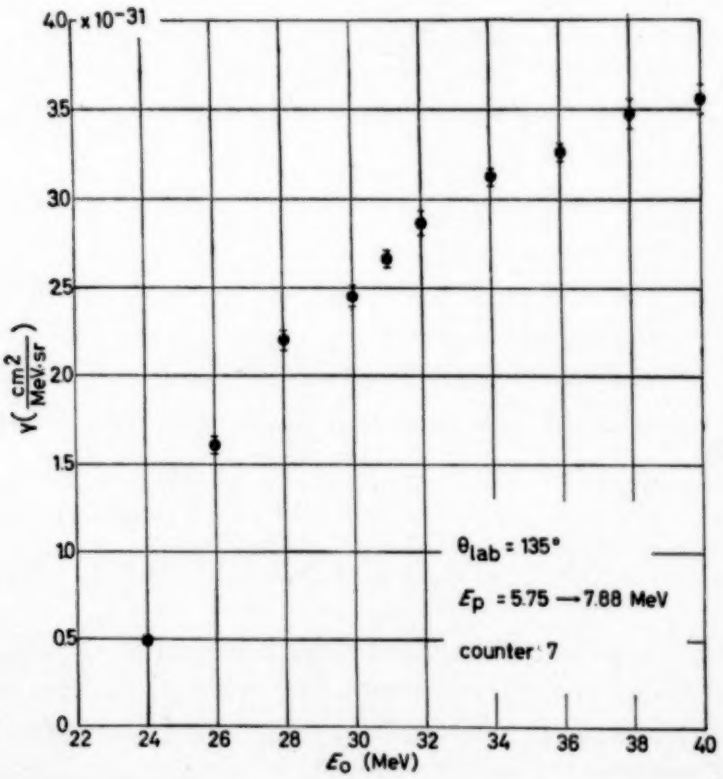


Fig. 9. Excitation of an energy group of protons at 135° as a function of primary electron energy.

Excitation functions were taken with the 24.46 mg/cm² target at two different spectrometer settings. In each case the Pb radiator was placed in the

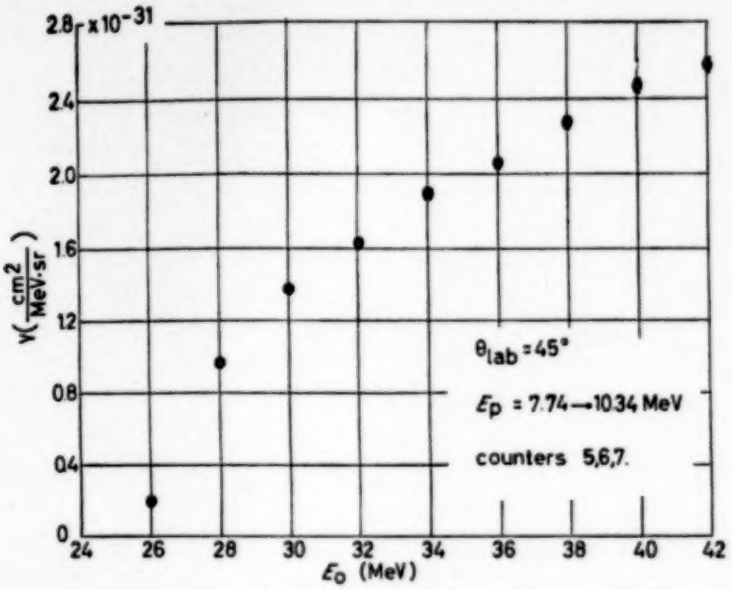


Fig. 10. Excitation of an energy group of protons at 45° as a function of primary electron energy.

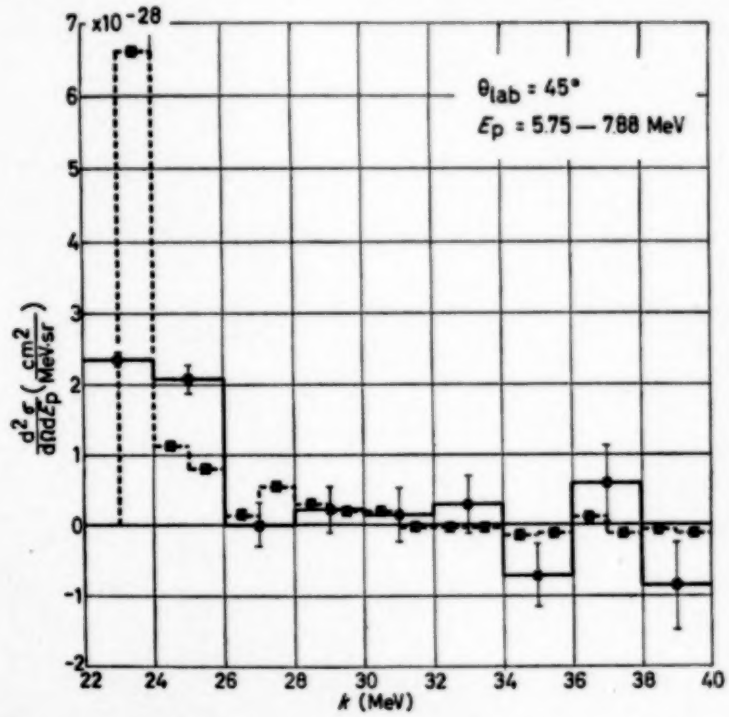


Fig. 11. Differential cross section for producing protons of a given energy group at 45°. The 2 MeV steps histogram is derived by a photon difference analysis of fig. 8, using the experimental points. The 1 MeV steps histogram is derived by a photon difference analysis using the smooth curve of fig. 8.

electron beam and $\Delta E_0/E_0$ was 0.01. As examples, figs. 8 and 9 show the results obtained from counter 7 for $\theta_{lab} = 45°$ and 135°, respectively, for a proton

group near the maximum of the energy distribution, while fig. 10 shows the result for the weighted average of counters 5, 6 and 7 for a higher energy group

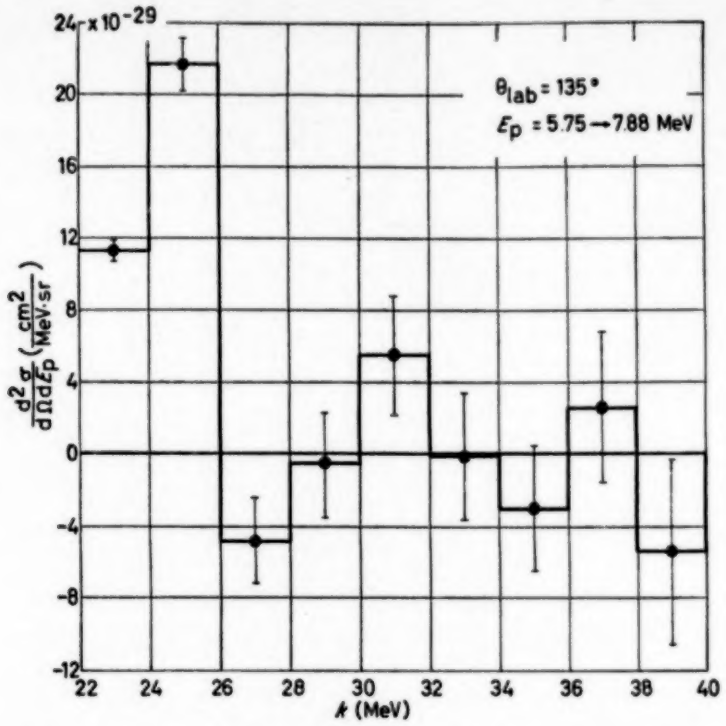


Fig. 12. Differential cross section for producing protons of a given energy group at 135°. The histogram is derived from a photon difference analysis of fig. 9 using the experimental points.

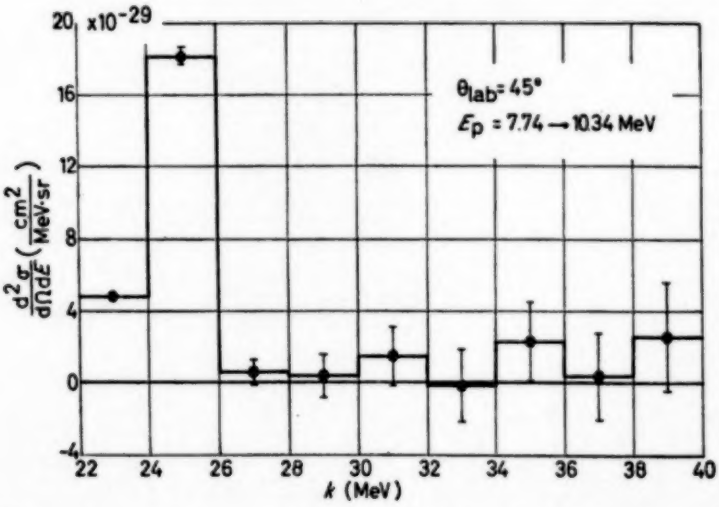


Fig. 13. Differential cross section for producing protons of a given group at 45°. The histogram is derived from a photon difference analysis of fig. 10 using the experimental points.

at $\theta_{lab} = 45°$. The indicated proton energies contain all corrections except this resulting from the momentum transfer due to the absorption of the photon by the nucleus.

From the excitation functions, cross sections were obtained (figs. 11-13) by means of a photon difference analyses. The indicated errors are those resulting from the standard deviations in the excitation function. Most of the measured points in the excitation function were taken at two MeV intervals and two MeV steps were used in the analysis. In fig. 11, a one MeV step analyses is also shown. This was made from the smooth curve in fig. 8 which was drawn arbitrary through the points. As the effective photon spectrum, we took the sum of the bremsstrahlung spectrum produced in the windows and in the radiator (the number of real photons produced in the target is negligible) and the electric dipole virtual photon spectrum [7]). The use of only the electric dipole virtual photon spectrum is a good approximation because not much of other types of transitions are involved. From the one-MeV-step cross section of fig. 11, we obtain

$$\frac{\mathrm{d}\sigma}{\mathrm{d}\Omega} = \tfrac{11}{12}\int \frac{\mathrm{d}^2\sigma}{\mathrm{d}\Omega \mathrm{d}E_\mathrm{p}}\,\mathrm{d}k = (8.7\pm 1.7)\times 10^{-28}\ \mathrm{cm^2/sr}, \qquad (5)$$

which leads to a total cross section of $11.2\pm 2.2$ mb if the experimental angular distribution $1+0.25\cos\theta+ 1.35\sin^2\theta$ is used. The two MeV analysis leads to a total cross section of $10.6\pm 2.1$ mb. These values do not represent the peak cross section but an average value for the proton energy interval 5.75 to 7.88 MeV which spans the peak. The indicated errors are estimated to be 20 % (sect. 4.3).

## 4. Discussion

### 4.1. ENERGY DISTRIBUTIONS

The proton energy distribution taken at 40 MeV rises steeply to a peak value at 6.0 MeV. The first part of the right side of the narrow peak is steep also. Two small secondary peaks were observed with all the counters in the high energy tail: a first one at about 8.9 MeV and a second smaller bump near 13 MeV. The tail extends to 22 MeV. Since the threshold energy for $C^{12}$ ($\gamma$, p) is 15.95 MeV, this means that groundstate transitions must be present up to the end point energy of 40 MeV. The secondary peaks must come from excited states of $C^{12}$ with an energy of at least 25.5 MeV and 30 MeV, respectively. The form of the curves drawn on figs. 1 and 2 also suggest the possibility of an unresolved peak near 6.8 MeV. It should be remarked that the place of the peaks and bumps in the energy distribution is slightly dependent on the energy of the electrons producing the bremsstrahlung. There is a remarkable agreement with the energy distribution measured with a 35 MeV bremsstrahlung spectrum by Livesey [8]). Although the statistics are not very good, his histogram shows clearly the main peak at 6.0 MeV and smaller ones at 6.7 and 9.0 MeV. There is also an excellent agreement with the results of the study of the inverse reaction $B^{11}$ (p, $\gamma_0$) $C^{12}$, using monoenergetic protons and looking for ground-

state transition gamma rays. The yield curve measured by Gemmell *et al.* [3]) shows the peak cross section at a proton energy at 7.2 MeV which corresponds to 7.2 MeV $\times (\frac{11}{12})^2 = 6.05$ MeV in our experiment. They do not go high enough in proton energy to be able to see the other peaks. Gove, Batchelor and Litherland [4, 9]), who did the same experiment, found their main peak at 7.1 MeV, and a smaller one at 10.5 MeV. In the (p, $\gamma$) case these energies correspond to 5.97 MeV and 8.82 MeV, respectively. Furthermore the form of their yield curve suggests the possibility of an unresolved peak at about 8.3 MeV, which is in agreement with our unresolved peak of 6.8 MeV.

The energy distribution at $E_0 = 26$ MeV (fig. 3) was taken in order to look for fine structure in the energy region from 4 to 7 MeV. Such fine structure is present in the result of the Pennsylvania group [10]). They used a polyethylene target that was slightly thinner than ours (2 mg/cm$^2$) and $E_0 = 25$ MeV. Their statistics are rather poor. As is clear from figs. 3 and 4, we did not find resolved peaks, but alternating plateaus and rising portions, indicating that the energy distribution cannot be explained by a single resonance. The small dip at about 5 MeV corresponds with the dip found by Cohen *et al.* [10]). The dip at about 5.8 MeV found by them is not visible on our results. The yield curve for $B^{11}$ (p, $\gamma$) $C^{12}$ groundstate gamma rays given by Gemmell, Morton and Titterton [3]) shows similarity with our results. Although their resolution is good, they find only very small peaks at 21.4 and 22.1 MeV excitation of the $C^{12}$ nucleus, but the curve is otherwise smooth. Their first peak should correspond to about 4.9 MeV in fig. 3. The agreement is rather good. Their second one is not visible in our results. Neither are these results compatible with the data of Katz [11]), for the "breaks" in the $C^{12}$ ($\gamma$, n) yield curve if one expects to find the corresponding peaks in $C^{12}$ ($\gamma$, p). This is well illustrated by fig. 4. The solid curve shows what should be expected if one starts from Katz' breaks and values of the cross section of the corresponding resonances which are given in table 1, except for low energies.

TABLE 1

Breaks in the $C^{12}$ ($\gamma$, n) $C^{11}$ yield curve

| Break energy $E_1$(MeV) | $\sigma^i_{\gamma n}\,dE$ (MeV · mb) | Break energy $E_1$(MeV) | $\sigma^i_{\gamma n}\,dE$ (MeV · mb) |
|---|---|---|---|
| 19.57 | 0.064 | 20.90 | 0.60 |
| 19.76 | 0.057 | 21.08 | 0.69 |
| 19.92 | 0.11 | 21.22 | 0.87 |
| 20.13 | 0.19 | 21.58 | 2.7 |
| 20.29 | 0.26 | 22.02 | 2.5 |
| 20.62 | 0.56 | 22.88 | 3.8 |

After subtraction of the threshold energy from the break energy, recoil corrections were made. Neglecting the width of the levels with respect to the energy-

loss in the target, the latter defines the width of the rectangles of fig. 4, whose surface is proportional to the product of $\sigma_{\gamma n}^{i}$ and the number of virtual photons per energy interval at the corresponding photon energy. This gives the result one should obtain with an apparatus with infinite energy resolution. The complete experimental energy resolution curve for counter 9, given in ref. [6]), was used to find the solid curve. The agreement with the measured points is not good at all except for the place of the 5 MeV dip. It may be possible that more breaks are found in the $C^{12}$ ($\gamma$, n) yield curve since Katz' publication. If however, the break experiments are consistent, the early ones should give the same gross distribution as later ones, which discover still finer structure. Thus, we think it is not sure that more breaks will explain the discrepancy. The penetrability of a proton through the Coulomb and angular momentum barriers, being larger than the penetrability of a neutron through the angular momentum barrier alone (for the same $k$), the width of the proton level will be larger. It is however questionable whether the difference will be sufficient in order to give an explanation for the disagreement with the experiment.

### 4.2. ANGULAR DISTRIBUTIONS

The experimental angular distributions (figs. 5, 6 and 7) are approximately the same whether the reaction is induced by electrons or by real bremsstrahlung. The multiple scattering of electrons in the radiator produces a root-mean-square spread of about 4° in the angle of incidence of the bremsstrahlung. The scattering of the electrons in the directly induced reaction results in an angular distribution for the products which is somewhat more isotropic than would be produced by a beam of photons. Bosco and Fubini [12]) have calculated this effect for the case of electric-dipole transitions. Their result can be extended to show that if the reaction induced by photons has the angular distribution

$$\frac{\mathrm{d}\sigma_\gamma}{\mathrm{d}\Omega_N} = \alpha+\beta \sin^2\theta, \tag{6}$$

it will appear as

$$\frac{\mathrm{d}\sigma_e}{\mathrm{d}\Omega_N} = C\left[\alpha+\frac{E/E_0}{[(E_0/E)+(E/E_0)]\lambda-2}\beta+\left\{1-\frac{(\frac{3}{2})(E/E_0)}{[(E_0/E)+(E/E_0)]\lambda-2}\right\}\right]\beta \sin^2\theta], \tag{7}$$

when induced by electrons †. In eqs. (6) and (7), $\lambda = \ln [2E_0E/m(E_0-E)]$, where $E_0$ and $E$ are the initial and final electron energies, respectively, $m$ is the electron rest energy, $C$ a constant, the subscript N refers to the nuclear particle detected in the experiment and terms of order $m/E$ have been neglected in comparison with unity. If we represent the electron-induced angular distribution by

$$\mathrm{d}\sigma_e/\mathrm{d}\Omega_N = a+b \sin^2\theta, \tag{8}$$

† We are indebted to W. R. Dodge for pointing out a sign error in eq. (6) of Bosco and Fubini's paper and for integrating their result over final electron angels so that it corresponds to the condition of our experiment.

we find for the case of the carbon giant resonance, with $E_0 = 40$ MeV and $E = 17$ MeV,

$$\frac{b}{a} = \frac{0.943\ (\beta/\alpha)}{1+0.038\ (\beta/\alpha)}. \tag{9}$$

This smearing of the electron-induced angular distribution toward isotropy is about the same as the smearing of the bremsstrahlung-induced distribution by multiple scattering of electrons in the radiator, and thus it is to be expected that the experimental angular distributions are the same.

The angular distributions derived from our experiment are in good agreement with those observed by Penner and Leiss [2]) for the $C^{12}$ ($\gamma$, p) reaction, and by Gove *et al* [9]) for the $B^{11}$ (p, $\gamma_0$) reaction. This is shown by table 2 where the

TABLE 2

Comparison of angular distributions observed in C(e, e' p), C($\gamma$, p) and $B^{11}$ (p, $\gamma_0$) reactions

| Experiment | Excitation energy (MeV) | $C_0$ | $C_1$ | $C_2$ |
|---|---|---|---|---|
| Average of data given by crosses on figs. 5 and 6 after correction | 22 to 23 | 1 | 0.14±0.02 | −0.50±0.03 |
| Penner and Leiss [2]) C($\gamma$, p) | 22.1 | 1 | 0.09±0.02 | −0.56±0.04 |
| Gove *et al.* [9]) $B^{11}$ (p, $\gamma_0$) | 22.5 | 1 | 0.12±0.03 | −0.69±0.05 |
| Full circles on fig. 7, after correction | 25 | 1 | 0.26±0.04 | −0.49±0.06 |
| Penner and Leiss [2]) | 25.3 | 1 | 0.27±0.04 | −0.59±0.06 |
| Gove *et al.* [9]) | 25.5 | 1 | 0.29±0.06 | −0.57±0.09 |

angular distributions are expressed in a series of Legendre polynomials $f(\theta) = \sum_l C_l P_l$ (cos $\theta$). In representing our results in table 2, we have corrected the electron-induced angular distributions given by figs. 5, 6 and 7 for the small amount of smearing caused by experimental angular resolution and for the electron effect given by eq. (9). The agreement between the angular distributions observed in the C($\gamma$, p) reaction and those derived from observations on the C(e, e'p) reaction is a confirmation of the theory of electron-induced nuclear reactions. The similarity of the angular distributions in the $B^{11}$ (p, $\gamma_0$) and the C($\gamma$, p) reactions is a confirmation of detailed balancing.

The cos $\theta$ term in the angular distribution can result only from mixing of final states of different parity. The results (figs. 5, 6 and 7 and table 2) show that the amount of mixing increases as the excitation energy is increased. Except for the cos $\theta$ term, the angular distribution is in good agreement with the independent particle picture of the giant resonance. In carbon, p- to d-wave transitions are the important ones in producing the resonance. In this case the angular distribution predicted [13]) in the *L-S* coupling limit, $1+1.5\ \sin^2\theta$, is in best agreement with the experiments.

### 4.3. ABSOLUTE CROSS SECTION

The cross section (fig. 2), which is based on our measured energy and angular distributions together with the assumption that all protons are the result of transitions leaving the residual nucleus in the ground state, has a peak value of $(12.7\pm2.5)$ mb and values of $41\pm9$ MeV · mb and $77\pm18$ MeV · mb when integrated to 24 and 40 MeV, respectively. We have assigned a possible 20 % standard error to the results based on estimated errors of 15 % in determining the constants of the spectrometer and detectors (eq. (2)) and uncertainties of about 5 % in our knowledge of the effective photon spectrum and in our extrapolation of the angular distributions. The assumption of exclusively ground state transitions is supported to some extent by the excitation-function analysis, which showed that protons in the energy group from 5.8 to 7.9 MeV are produced with an average cross section of about 11 mb, a result in good agreement with fig. 2. The presence of transitions to excited final states would tend to make our estimate of the integrated cross sections too low.

Our results are in fair agreement with that of Penner and Leiss [2]), who found $8.1\pm2.4$ mb for the peak cross section leading to ground state transitions only, under the assumption that the full width at half-maximum of the giant resonance is 3.6 MeV. They found that the contribution of transitions to excited final states of $B^{11}$ to the cross section in the neighbourhood of the giant resonance maximum was only of the order of 10 %.

An early determination of the C($\gamma$, p) cross section from a bremsstrahlung yield curve by Halpern and Mann [14]) gave a very narrow resonance (1.7 MeV) with a maximum value of $4\pi(\mathrm{d}\sigma_{90°}/\mathrm{d}\Omega)$ equal to $(34\pm8)$ mb, and an integrated value

$$4\pi\int_0^{24\ \mathrm{MeV}}\frac{\mathrm{d}\sigma_{90°}}{\mathrm{d}\Omega}\times\mathrm{d}E=63\ \mathrm{MeV}\cdot\mathrm{mb}.$$

A later measurement from the same laboratory[10]) determined the proton energy distribution at 90° and gave about 18 mb for the peak cross section and 56 MeV · mb for the cross section integrated to 24 MeV if the angular distributions were isotropic. The latter workers remarked that the earlier determination contained an over-correction for absorption of protons in the target which accounted for the discrepancy in the integrated cross sections. If the latter measurements are corrected for an angular distribution of the form $1+1.5\sin^2\theta$, the results,

$$\sigma_{\mathrm{peak}}=14.7\ \mathrm{mb}\ \text{and}\ \int_0^{24\ \mathrm{MeV}}\sigma\mathrm{d}E=46\ \mathrm{MeV}\cdot\mathrm{mb},$$

are in agreement with ours.

The only study of the inverse reaction yielding an absolute cross section was that of Gemmell *et al.* [3]). This gave a value of $(2.7\pm0.5)\times10^{-28}\mathrm{cm}^2$ for the peak cross section for the $B^{11}$ (p, $\gamma_0$) reaction leading to the ground state

of $C^{12}$. If this value, which was derived from 90° measurements under the assumption of an isotropic angular distribution, is combined with the principle of detailed balancing, a result $(29\pm5)$ mb is obtained for the peak value of the $C^{12}$ $(\gamma, p)$ $B^{11}$ ground state reaction. After correction for the angular distribution, this value becomes $(24\pm4)$ mb, which is still considerably higher than any of the recent $C(\gamma, p)$ experiments. (The apparent agreement with the early experiment [14]) is illusory because the narrow width observed in that case was not observed in the $B^{11}(p, \gamma_0)$ experiment.) This disagreement between measurements of the reaction and its inverse cannot be reconciled by consideration of other than ground state transitions. Gemmell *et al.* [3]) were able to resolve the ground-state $\gamma$-ray from all others, and hence their experiment should be the exact inverse of that of Penner and Leiss [2]). Our result and that of Cohen *et al.* [10]) included the possibility of transitions leaving excited states of $B^{11}$, but these can cause only an increase in yield of protons and hence a further discrepancy with the inverse-reaction result. In view of the good agreement between the reaction and its inverse shown by the energy and angular distributions, it is disconcerting that the absolute cross sections do not agree. The determination of absolute cross sections is, however, subject to experimental errors which are difficult to evaluate, and we feel that more experiments are required to resolve this important problem.

The energy at the peak of the cross section curve of fig. 2, can be situated at $(22.5\pm0.2)$ MeV, which is in excellent agreement with the result of Gemmell *et al.* [3]), who found $(22.55\pm0.1)$ MeV.

On fig. 2 we have also plotted the $C^{12}(\gamma, n)C^{11}$ cross section obtained by Barber, George and Reagan [15]), using a photon difference analysis of a yield curve. It is remarkable that there is good agreement between the two cross sections (as one should expect from charge symmetry of nuclear forces, $C^{12}$ being a self conjugate nucleus), as far as the place of the peak and the high energy tail is concerned. The large difference in amplitude at the left part of the diagram can partly be explained by the difference in threshold energy which is 15.95 MeV for $(\gamma, p)$ and 18.72 MeV for $(\gamma, n)$. This causes a difference in penetrability of the potential barriers. As is seen from the angular distribution the ejected protons are d-protons. The same holds for the neutrons which have also an angular distribution that is compatible with $1+1.5\sin^2\theta$ (ref. [16])). For a given $k$ and supposing ground state transitions in both cases, the energy of the protons will be 2.77 MeV larger than the energy of the neutrons, and the penetrability of the Coulomb barrier plus the angular momentum barrier for $E_p = k - 15.95$ MeV will be larger than the penetrability of the angular momentum barrier alone for $E_n = k - 18.72$ MeV.

In addition to the barrier effect there is a possible large effect due to the isobaric spin mixing. Radicati [17]) and Gell-Mann and Telegdi [18]) have shown that for any radiation the selection rule $\Delta T = 0, \pm1$ holds; however electric

dipole transitions between states of the same isobaric spin are forbidden (except for very small contributions from higher order terms in the $E_1$ operator). This means that for $C^{12}$ the dipole state is a $T = 1$ state. Coulomb interactions will relax partially the selection rules and small amounts of the $T = 0$ state can be admixed to the $T = 1$ state. Barker and Mann [19]) have pointed out that such an admixture of about 1 % is sufficient to have $\sigma(\gamma, p) = 2\sigma(\gamma, n)$ for $C^{12}$. This includes already a factor 1.3 due to the difference in barrier penetrability.

We should like to thank W. R. Dodge for aiding us in the operation of the equipment and in the analysis of the experimental results. One of us (VJV) wishes to acknowledge the support of the Belgian Interuniversity Institute for Nuclear Science which made his stay at Stanford possible, and to thank Professor W. K. H. Panofsky for his hospitality in making the facilities of the High-Energy Physics Laboratory available to him.

## References

1) V. De Sabbata, Nuovo Cim. **11** (1959) 225
2) S. Penner and J. E. Leiss, Phys. Rev. **114** (1959) 1101
3) D. S. Gemmell, A. H. Morton and E. W. Titterton, Nuclear Physics **10** (1959) 33
4) H. E. Gove, A. E. Litherland and R. Batchelor, Phys. Rev. Lett. **3** (1959) 177
5) R. F. Post and N. S. Shiren, Rev. Sci. Instr. **26** (1955) 205
6) W. C. Barber and V. J. Vanhuyse, Nuclear Physics **16** (1960) 381
7) R. H. Dalitz and D. R. Yennie, Phys. Rev. **105** (1957) 1598
8) S. L. Livesey, Ca. J. Phys. **35** (1957) 987
9) H. E. Gove, private communication to W. C. Barber
10) L. Cohen, A. K. Mann, B. J. Batton, K. Reibel, W. E. Stephens and E. J. Winhold, Phys. Rev. **104** (1956) 108
11) L. Katz, Washington Photonuclear Conf. (May 1958)
12) B. Bosco and S. Fubini, Nuovo Cim. **9** (1958) 350
13) A. K. Mann, W. E. Stephens and D. H. Wilkinson, Phys. Rev. **97** (1955) 1184
14) J. Halpern and A. K. Mann, Phys. Rev. **83** (1951) 370
15) W. C. Barber, W. D. George and D. D. Reagan, Phys. Rev. **98** (1955) 73
16) V. Emma, C. Milone and A. Rubbino, Phys. Rev. **118** (1960) 1297
17) L. A. Radicati, Phys. Rev. **87** (1952) 521
18) M. Gell-Mann and V. L. Telegdi, Phys. Rev. **91** (1953) 169
19) F. C. Barker and A. K. Mann, Phil. Mag. **5** (1957) 2

1.D.2:
1.E.4

*Nuclear Physics* **26** (1961) 250—258; © *North-Holland Publishing Co., Amsterdam*
Not to be reproduced by photoprint or microfilm without written permission from the publisher

# ENERGY LOSS OF PROTONS IN RARE EARTH OXIDES AND REDUCED TRANSITION PROBABILITIES FOR $2^+ \rightarrow 0^+$ TRANSITIONS IN EVEN ROTATIONAL NUCLEI

G. GOLDRING and Z. VAGER

*Department of Physics, The Weizmann Institute of Science, Rehovoth, Israel*

Received 23 February 1961

**Abstract:** Measurements of $\gamma$ ray yields from thick targets of rare earth oxides bombarded by protons were combined with lifetime measurements to determine reduced E2 transition probabilities in $2^+ \rightarrow 0^+$ rotational transitions. The rate of energy loss of the protons in the target was determined by a measurement of the absorption of the $\gamma$ rays in the target material at different proton energies yielding the mean penetration of the protons into the target.

## 1. Introduction

The thick target yield of $\gamma$ rays following Coulomb excitation is one of the simplest ways of determining the Coulomb excitation cross section. There are however two weak links in the chain of calculations leading from the measured yield values to the reduced electromagnetic transition probabilities.

The total conversion coefficients $\alpha$ for the electrons accompanying the $\gamma$ radiation are not yet known with certainty as there are still some doubts about the accuracy of the calculated values, furthermore the rate of energy loss by the protons in the target material $\mathrm{d}E/\mathrm{d}x$ is known in only a very approximate fashion. In the present experiment these difficulties were overcome by combining the results of three different measurements: a) a yield measurement for $2^+$ rotational states, b) a previous [1]) measurement of the mean lives of these states and c) a measurement of the absorption of the $\gamma$ rays in the target material. This last measures the mean depth inside the target at which the reactions occur and is equivalent to a measurement of $\mathrm{d}E/\mathrm{d}x$. Both a) and b) depend on the reduced E2 transition probabilities $B(\mathrm{E2})$ and on the conversion coefficients $\alpha$ but in different combinations. These two measurements, therefore, allow a complete experimental determination of both $B(\mathrm{E2})$ and $\alpha$.

## 2. Description of the Method

The cross section for electric quadrupole Coulomb excitation by protons is given by [2])

$$\sigma(E) = 4.819 \times 10^{-24} \frac{E_{\mathrm{MeV}} - \Delta E_{\mathrm{MeV}}}{Z} B(\mathrm{E2}) f_{\mathrm{E2}}(\eta_1, \xi) \mathrm{cm}^2,$$

where $E$ is the energy of the protons in MeV, $Z$ is the atomic number of the target nucleus and $\Delta E$ is the transition energy. The quantity $f_{E2}(\eta_1, \xi)$ is a known function of $E$ and is tabulated in ref. [2]). The reduced transition probability for exitation $B(E2)$ is in units of $e^2 \cdot 10^{-48}$ cm$^4$.

The yield of $\gamma$ rays per bombarding proton from a thick target is given by

$$Y(E) = \frac{N}{1+\alpha}\int_0^E \frac{\sigma(E')\mathrm{d}E'}{\kappa(E')}, \tag{1}$$

where $\alpha$ is the total conversion coefficient, $\kappa$ is the energy loss per unit path length of the protons in the target material and $N$ is the density of the target nuclei. The yield $Y(E)$ is given in ref. [2]) in the form

$$Y(E) = \frac{1}{1+\alpha}\sigma(E)\frac{EN}{\kappa(E)}\frac{\delta E}{E}. \tag{2}$$

The "effective" target thickness $\delta E$ is defined by this equation, and is given explicitly in ref. [2]). The calculations in ref. [2]) are based on the assumption that

$$\kappa(E) \propto E^{-0.55}. \tag{3}$$

With this assumption the only important information about $\kappa(E)$ for the evaluation of the integral (1) is therefore the value of the function at the bombarding energy. In what follows, we write eq. (2) in the form

$$Y(E) = \frac{B(E2)}{1+\alpha}\frac{E}{\kappa(E)}F(E), \tag{4}$$

where $F(E)$ is given by

$$F(E) = 4.819\,\frac{E_{\mathrm{MeV}} - \Delta E_{\mathrm{MeV}}}{Z} f_{E2}(\eta_1, \xi) N \frac{\delta E}{E}.$$

The function $\kappa(E)$ is known only very approximately in the range of energies and atomic numbers encountered in the present experiment, and the situation is aggravated by the fact that the target materials are compound materials and not monoatomic substances.

The conventional method for measuring $\kappa$ (the determination of the energy loss caused by the passage of protons through thin foils) is not practical in this case, and therefore a different method was applied in which the absorption of the $\gamma$ rays in the target material is used to measure distances.

The experimental arrangement is shown schematically in fig. 1. Two counters are placed near the target, one (the "front counter") at an angle $\vartheta$ to the beam and the other (the "back counter") at an angle $\pi+\vartheta$. The values of the angular distribution function at these two angles are equal, as the angular distribution is expressed in Legendre polynomials of even order.

If a source of $\gamma$ rays is located at a depth $x$ from the surface of the target, the $\gamma$ rays emitted in the direction of the back counter will be absorbed in a layer of thickness $x/\cos\vartheta$, whereas those emitted in the direction of the front counter will be absorbed in a layer of thickness $(l-x)/\cos\vartheta$. The ratio of counts in the front counter to the counts in the back counter, denoted by $r$, is therefore a function of $x$. In particular, if the $\gamma$ rays are produced in a reaction with cross section $\sigma(E)$, then $\sigma$ can also be expressed as a function of $x$ and we get

$$r = \frac{\int_0^\infty \sigma(x)\mathrm{e}^{-k'x}\mathrm{d}x}{\int_0^\infty \sigma(x)\mathrm{e}^{-k'(l-x)}\mathrm{d}x},$$

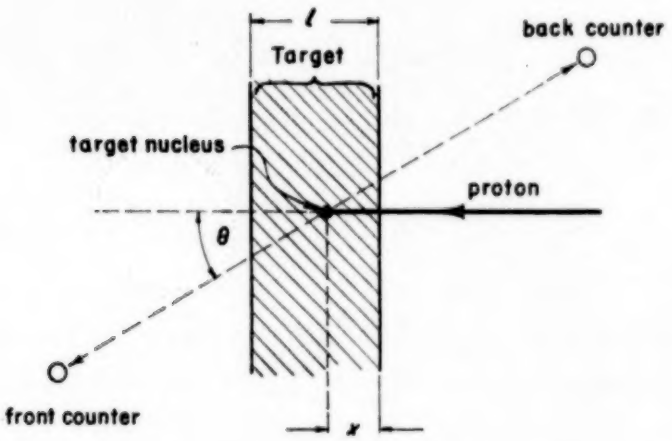


Fig. 1. Experimental arrangement for mean penetration measurement.

where $k'$ is given by $k' = k/\cos\vartheta$ and $k$ is the absorption coefficient for the $\gamma$ rays in the target material. If the exponents are expanded in $k'x$, we have up to the second order $r = \mathrm{e}^{k'l}(1-2k'\bar{x}+2k'^2\bar{x}^2)$, where the mean penetration $\bar{x}$ is

$$\bar{x} = \int_0^\infty x\sigma(x)\mathrm{d}x \Big/ \int_0^\infty \sigma(x)\mathrm{d}x. \tag{5}$$

The measurement of $r$ is carried out at two different proton energies $E_1$ and $E_2$ and we define the double ratio $R(E_1, E_2)$

$$R(E_1, E_2) = \frac{r(E_1)}{r(E_2)} \tag{6}$$

$$= \frac{(\text{counts in front counter at high energy})}{(\text{counts in back counter at high energy})} : \frac{(\text{counts in front counter at low energy})}{(\text{counts in back counter at low energy})}.$$

To second order in $k'\bar{x}$, we get

$$2k'[\bar{x}(E_1)-\bar{x}(E_2)] = \log R(E_1, E_2). \tag{7}$$

The penetration $\bar{x}(E_1)$ for protons of a few MeV is only of the order of

$20\text{mg} \cdot \text{cm}^{-2}$, but $k'$ may be quite large ($\approx 6\ \text{cm}^2 \cdot \text{g}^{-1}$) because some of the $\gamma$ transition energies are very close to the K absorption edge, and therefore it is possible to obtain ratios $R$, which are appreciably different from unity.

Eq. (5) may be written

$$x(E) = \frac{1}{Y(E_0)} \int_0^{Y(E_0)} x \mathrm{d}Y.$$

This expression can be evaluated if the dependence of $Y$ on $E$ is known. For the function $Y(E)$ of eq. (4), with $\kappa(E) \propto E^{-\varepsilon}$, we get

$$\bar{x}(E_1) - \bar{x}(E_2) = \frac{E_1}{\kappa(E_1)} Q(E_1, E_2), \tag{8}$$

$$Q(E_1, E_2) = \frac{1}{1+\varepsilon} \left\{ 1 - \left(\frac{E_2}{E_1}\right)^{2+\varepsilon} - \frac{1}{E_1^{2+\varepsilon}} \left[ \frac{E_1}{f(E_1)} \int_0^{f(E_1)} E^{1+\varepsilon} \mathrm{d}f - \frac{E_2}{f(E_2)} \int_0^{f(E_2)} E^{1+\varepsilon} \mathrm{d}f \right] \right\},$$

where $f(E) = F(E) \cdot E^{1+\varepsilon}$.

From eq. (7) we get

$$\frac{E_1}{\kappa(E_1)} = \frac{\log R(E_1, E_2)}{2k' Q(E_1, E_2)}. \tag{9}$$

We can now combine eqs. (9) and (4); thus we have

$$\frac{2k' Y(E)}{\log R(E_1, E_2)} = \frac{F(E)}{Q(E_1, E_2)} \frac{B(\text{E2})}{1+\alpha}. \tag{10}$$

The left hand side of this equation contains the measured quantities $Y(E)$, $R(E_1, E_2)$ and the absorption coefficient $k' = k/\cos\vartheta$. The right hand side contains the quantities of physical interest, $B(\text{E2})/(1+\alpha)$ and the known numerical function $F(E)/Q(E_1, E_2)$.

We note that $Q(E_1, E_2)$ as defined in (8) depends on $\varepsilon$ and therefore the calculated value of $\kappa(E)$ also depends on $\varepsilon$. However, this dependence is of the same order as the dependence of $F$ (the calculated yield) on $\varepsilon$. Moreover, if $F(E)$ and $Q(E_1, E_2)$ are calculated with the same value of $\varepsilon$ and if $E$ is equal to or somewhat smaller than $E_1$, then the ratio $F/Q$ depends less on $\varepsilon$ than either $F$ or $Q$. This means that if the quantity $B(\text{E2})/(1+\alpha)$ is evaluated from the combined measurements of $Y$ and $R$ (eq. (9)), the error caused by assuming an incorrect function for $\kappa(E)$ is less severe than if the evaluation were carried out from the *single* measurement $Y$ using eq. (3) and the *correct* value of $\kappa(E)$ at the bombarding energy.

## 3. Description of the Measurements

Measurements of $R(E_1, E_2)$ were carried out at proton energies of 3.18 MeV and 1.8 MeV with the counters positioned at 54° and 180°+54° to the proton

beam. $R(E_1, E_2)$ was determined for two transitions, the 89 keV transition in $Gd^{156}$ and the 95 keV transition in $Ho^{165}$. The targets were in oxide form $Gd_2O_3$ and $Ho_2O_3$.

The results of these measurements are given in table 1, together with direct

TABLE 1

Mean penetration measurements

| Nucleus | transition energy in keV | $R$(3.18 MeV; 1.8 MeV) as in eq. (6) | absorption coefficient $k$ | $\kappa$(3.18 MeV) from $R$, eq. (9) | $\kappa$(3.18 MeV) adjusted | $\kappa$(extrapolated from ref.[4])) |
|---|---|---|---|---|---|---|
| $Gd^{156}$ | 89 | 1.213±0.046 | 3.58±0.10 | 39.3±8.4 | 38±5 | 45.3 |
| $Ho^{165}$ | 95 | 1.228±0.037 | 3.54±0.10 | 36.0±5.9 | 37±5 | 43.9 |

$R$ is the double ratio as defined in eq. (6).
$k$ is the absorption coefficient for $\gamma$ radiation in the target material.
The sixth column gives values $\kappa$ adjusted with the assumption $\kappa \propto Z^{-\frac{1}{2}}$.

measurements of the total absorption coefficients for the $Gd^{156}$ radiation in $Gd_2O_3$ and the $Ho^{165}$ radiation in $Ho_2O_3$. The absorbers for these measurements were prepared by dissolving the oxides in dilute nitric acid. The values of $\kappa$(3.18 MeV) in the sixth column of table 1 are the pooled values of the two measurements assuming a dependence [4]) $\kappa \propto Z^{-\frac{1}{2}}$. For comparison, we also list $\kappa$(3.18 MeV) extrapolated from measurements on Ag and Au [4]) and corrected for the fractional amount of oxygen in the target. The agreement is seen to be quite good considering the rather large uncertainty in the extrapolation. Nevertheless, as the dependence of $\kappa$ of the oxide targets on energy may well be different from $\propto E^{-0.55}$, the measured value of $\kappa$ must be regarded as an "effective" value which is appropriate for the relation (4) but may be different from the "true" value of $\kappa$ at the same energy. Because of the unknown dependence of $\kappa$ on energy, it is also conceivable that the effective $\kappa$ for either relation (4) or (8) may be slightly dependent on $Z\Delta E$, because this quantity governs the steepness of the cross section as a function of energy. For this reason, we limit ourselves in the yield determinations to transitions with $Z\Delta E$ values close to those of the $Gd^{156}$ and $Ho^{165}$ transitions for which the mean penetration measurements were carried out.

In the $\gamma$ yield measurements, even nuclei ranging from Sm to Hf were investigated. The targets were in oxide form and were bombarded by 2.75 MeV protons.

The angular distribution of these radiations is given rather accurately [2, 3]) by

$$W(\vartheta) = 1 + A_2 P_2(\cos\vartheta).$$

The counter was therefore placed at an angle $\vartheta_1 = 54°$ for which $P_2(\cos\vartheta_1) = 0$ so that

$$2\pi \int W(\vartheta) \sin\vartheta \mathrm{d}\vartheta = 4\pi W(\vartheta_1).$$

The yield measurements were corrected for absorption of the $\gamma$ rays in the target material. This correction could be determined directly from the mean penetration measurements, and it was found to be quite appreciable, in some cases up to 17%.

Our Hf targets were of low isotopic enrichment, and the yield values are therefore given in table 2 as a mean of the two isotopes $Hf^{178}$ and $Hf^{180}$. A small correction to $\kappa$ was introduced in this case to account for the different composition of these targets, HfO as compared to the $Gd_2O_3$ and $Ho_2O_3$ targets in which $\kappa$ was measured.

## 4. Discussion

The results of the yield measurements are summarized in table 2. In the fifth column of table 2 are listed the values of the quantities $B(E2)/(1+\alpha)$. These are derived by means of eq. (10) from the yield measurements and the double ratio measurements of $R$ as given in table 1. Eq. (10) could be applied strictly only to $Gd^{156}$. For other nuclei, the assumption was made that $\kappa$ is proportional to $Z^{-\frac{1}{2}}$. The values $B(E2)(1+\alpha)$ in the sixth column were derived from mean life measurements according to the relation

$$B(E2)(1+\alpha) = (2452\tau E^5)^{-1}, \tag{11}$$

where $B(E2)$ is given in units of $e^2 \cdot 10^{-48}cm^4$, the mean life $\tau$ in ns and $E$ in MeV. Available data on $\tau$ from delayed $\gamma$ coincidence work are also included in table 1 (column 4). The listed values are weighted means of the various measurements.

The two quantities $B(E2)/(1+\alpha)$ and $B(E2)(1+\alpha)$ determine $B(E2)$ and $\alpha$. The values of $B(E2)$ are compared in table 2 with values derived from inelastic proton scattering experiments[5]) and the total conversion coefficients are compared to values calculated from the tables of Rose[6]) according to $\alpha_{calc} = \alpha_K + 1.3\alpha_L$, where the addition of $0.3\alpha_L$ is supposed to represent the contributions from higher shells (as in ref. [5])). For most of the transitions the agreement in both the $B(E2)$ and the $\alpha$ comparisons is quite good, and there does not appear to be a significant systematic difference between the two $B(E2)$ values compared. We therefore conclude that the three independent measurements, the proton inelastic scattering cross section, the $\gamma$ yield and the mean life of the excited states, determine *consistently* the $B(E2)$ values and the total conversion coefficients of these transitions. The mean measured value of $1+\alpha$ for all the transitions investigated is larger by about 4 % than the mean of the values of Rose. This may well be due to a systematic error in one of the experiments, e.g. in the measurement of $dE/dx$. Such an error would in any case be well inside the estimated experimental errors.

We now confidently expect the conversion coefficients to be adequately represented by Rose's values also in other similar transitions, and the $B(E2)$

TABLE 2

Summary of results

| 1 | 2 | 3 | 4 | 5 | 6 | 7 | 8 | 9 | 10 | 11 |
|---|---|---|---|---|---|---|---|---|---|---|
| nucleus | transition energy in keV | yield of $\gamma$ per $10^7$ protons, $Y$ (2.75 MeV) | mean life $\tau$ in $10^{-9}$ sec. | $B(E2)/(1+\alpha)$ from $Y$ and $R$ eq. (10) | $B(E2)\cdot(1+\alpha)$ from eq. (11) | $1+\alpha$ from $\tau$ cols. 5, 6 | $1+\alpha_{calc}$ from ref. [6]) | $B(E2)$ from cols. 5, 6 | $B(E2)$ from $\tau$ and $\alpha_{calc}$ | $B(E2)$ from ref. [5]) |
| $Nd^{150}$ | 131 | | 2.22±0.10[1]) | | 4.76±0.21 | | 1.84 | | 2.6±0.1 | |
| $Sm^{152}$ | 121.9 | | 2.07±0.07[1, 10]) | | 7.34±0.25 | | 2.18 | | 3.4±0.1 | 3.40±0.15 |
| $Sm^{154}$ | 82.0 | 1.23±0.10 | 3.95±0.35[1]) | 0.59±0.09 | 27.9 ±2.5 | 6.9±0.6 | 5.93 | 4.1±0.4 | 4.7±0 4 | 4.61±0.20 |
| $Gd^{154}$ | 123.1 | | 1.71±0.05[1, 10, 13]) | | 8.45±0.29 | | 2.20 | | 3.8±0.1 | 3.43±0.30 |
| $Gd^{156}$ | 89.0 | 1.37±0.10 | 3.01±0.15[1, 11, 14]) | 0.73±0.11 | 24.3 ±1.2 | 5.8±0.5 | 4.84 | 4.2±0.4 | 5.0±0 3 | 4.57±0.27 |
| $Gd^{158}$ | 79.5 | 1.19±0.10 | 3.60±0.3[1]) [b]) | 0.64±0.10 | 35.3 ±3.0 | 7.4±0.6 | 6.86 | 4.8±0.4 | 5.2±0.2 | 5.44±0.25 |
| $Gd^{160}$ | 75.3 | | 3.64±0.20[1]) | | 46.4 ±2.6 | | 8.48 | | 5.5±0.3 | 5.80±0.25 |
| $Dy^{162}$ | 80.7 | 1.17±0.10 | 3.20±0.20[1]) | 0.70±0.11 | 37.4 ±2,3 | 7.3±0.6 | 6.81 | 5.1±0.4 | 5.5±0.3 | 5.11±0.15 |
| $Dy^{164}$ | 73.4 | | 3.49±0.35[1]) | | 54.9 ±5.5 | | 9.61 | | 5.7±0.6 | 5.64±0 25 |
| $Er^{166}$ | 80.6 | 1.38±0.15 | 2.61±0.25[1]) | 0.88±0.15 | 46.0 ±4.4 | 7.2±0.7 | 7.55 | 6.4±0.6 | 6.1±0.6 | 5.66±0.25 |
| $Er^{168}$ | 80.0 | 1.38±0.15 | 2.65±0.25[1]) | 0.90±0.15 | 46.9 ±4.4 | 7.2±0.7 | 7.72 | 6.5±0.6 | 6.1±0.6 | 5.72±0.20 |
| $Yb^{176}$ | 82.2 | 0.90±0.10 | 2.90±0.15[15]) | 0.65±0.10 | 37.6 ±1.9 | 7.6±0.6 | 7.64 | 5.0±0.4 | 4.9±0.3 | 5.78±0.20 |
| $Hf^{178, 180}$ [a]) | 93.2 | 0.87±0.10 | 2.45±0.15[1, 10]) | 0.76±0.13 | 23.6 ±1.4 | 5.6±0.5 | 5.67 | 4.2±0.4 | 4.2±0.3 | |
| $W^{182}$ | 100.1 | | 1.97±0.12[1, 10]) | | 20.6 ±1.3 | | 4.80 | | 4.3±0.3 | |
| $W^{184}$ | 111.1 | | 1.88±0.09[1, 12]) | | 12.8 ±0.61 | | 3.55 | | 3.6±0.2 | |
| $W^{186}$ | 122.5 | | 1.61±0.10[1]) | | 9.19 ±0.57 | | 2.74 | | 3.4±0.2 | |

$\alpha_{calc}$ in column 8 is the sum $\alpha_K+1.3\alpha_L$ · $B(E2)$ values are given in units of $e^2\cdot10^{-48}cm^4$. The errors are standard errors of the mean.

a) Mean value for both isotopes.

b) Preliminary results from recent measurements in this laboratory.

values can then be determined directly from the mean lives. The $B$(E2) values derived in this way are listed in table 2 in the tenth column. The overall agreement between these values and the inelastic scattering results was already pointed out in ref [5]).

Measurements of $\gamma$ yields similar to those described here have been carried out before for the same transitions [7–9]). On the whole, the measured $B$(E2) values show rather large discrepancies as compared to the present work (even after elimination of $\alpha$), differences of 50 % being quite common. As the details of measurement and analysis of the yield measurements are basically the same in all these experiments including the present one, we assume that these large discrepancies are due to incorrect estimates of the energy loss of the bombarding particles in the target material.

The dependence of the reduced E2 transition probability on neutron and proton numbers at both ends of the region of strong deformation shows some distinct features which are summarized in table 3. At the onset of the rotational

TABLE 3

The dependence of $B$(E2) on $Z$ and $N$ *at* the beginning and end of the rotational region

| | $\frac{1}{B(\mathrm{E2})}\left(\frac{\partial B(\mathrm{E2})}{\partial Z}\right)_N$ | $\frac{1}{B(\mathrm{E2})}\left(\frac{\partial B(\mathrm{E2})}{\partial N}\right)_Z$ |
|---|---|---|
| beginning | 0.05 (0) | 0.15 (0.15) |
| end | −0.03 (−0.035) | −0.04 (−0.04) |

The quantities listed are the relative changes of $B$(E2) for a change of $Z$ or $N$ by one unit, (derived from comparisons between neighbouring even nuclei differing in $Z$ or $N$ by two units), and the values are averages of the values for isotopes of Nd, Sm and Gd (beginning), and Hf and W (end). The values in parenthesis are the corresponding values for the moment of inertia $\mathcal{I}$: $(1/\mathcal{I})(\partial\mathcal{I}/\partial Z)_N$ and $(1/\mathcal{I})\ (\partial\mathcal{I}/\partial N)_Z$.

region, the $B$(E2) values are seen to be only weakly dependent of $Z$ at constant $N$ but strongly dependent on $N$. This striking behaviour is discussed at length in ref. [5]). It is interesting to note that this behaviour matches exactly the way in which the rotational region makes its appearance, namely at the "break" in neutron number 90 and quite independent of $Z$. At the end of the rotational region, one finds that the $B$(E2) values decrease rather slowly with either $N$ or $Z$ and here again we note that this behaviour closely resembles the dying away of the rotational structure which, unlike the abrupt change at $N = 90$, here goes gradually through an intermediate transition region, the gradual transition taking place for either increasing $N$ or $Z$.

We are greatly indebted to Dr. Y. Wolfson for his cooperation in the design and the early stages of the experiment. Our thanks are due to Mrs. D. Kedem for her help in the analysis of the data.

## References

1) M. Birk, G. Goldring and Y. Wolfson, Phys. Rev. **116** (1960) 730
2) K. Alder *et al.*, Rev. Mod. Phys. **28** (1956) 432
3) G. Goldring and R. P. Scharenberg, Phys. Rev. **110** (1958) 701
4) Handbuch der Physik **34** (1958)
5) B. Elbeck *et al.*, Nuclear Physics **19** (1960) 523
6) M. E. Rose, Internal conversion coefficients (North Holland Publishing Co. Amsterdam, 1958)
7) N. P. Heydenburg and G. M. Temmer, Phys. Rev. **100** (1955) 150
8) H. Mark and G. T. Paulissen, Phys. Rev. **100** (1955) 813
9) N. P. Heydenburg and G. M. Temmer, Phys Rev. **104** (1956) 981
10) A. W. Sunyar, Phys. Rev. **98** (1955) 653
11) O. Nathan, Nuclear Physics **5** (1958) 401
12) E. Bodenstedt *et al.*, Nuclear Physics **15** (1960) 239
13) R. Stiening and M. Deutsch, private communication
14) R. E. Bell and M. H. Jørgensen, Nuclear Physics **12** (1959) 413

7.C

*Nuclear Physics* **26** (1961) 259—279; © *North-Holland Publishing Co., Amsterdam*

Not to be reproduced by photoprint or microfilm without written permission from the publisher

# ELECTRON-PROTON BREMSSTRAHLUNG

R. A. BERG and C. N. LINDNER

*Institute of Theoretical Physics, Department of Physics, Stanford University, Stanford, California* †

Received 16 January 1961

**Abstract:** The electron-proton bremsstrahlung cross section is calculated in first Born approximation, neglecting radiative corrections to the electron. As an extension of an earlier calculation, the proton Compton effect contribution is analyzed in its most general form. It involves twelve form factors of three invariants, $f_j(\nu_1, \nu_2, \nu_3)$, where $j = 1, \ldots, 12$. The cross section is stated explicitly in terms of these twelve functions and the two form factors of one invariant describing the proton vertex. The contributions to the $f_j$ from (a) the single nucleon intermediate state, (b) the one-meson, one-nucleon intermediate state and (c) the neutral pion exchange, are calculated. These three contributions are expected to be the major effects when the energies involved are in the range of present experimental interest. To order $(1/M)^2$, only three combinations of these twelve $f_j$ will contribute to the cross section. When only (a) and (b) are considered, only two of these three combinations are independent. Some numerical values for a bremsstrahlung coincidence experiment are presented.

## 1. Introduction

In a previous paper [1]) we derived the bremsstrahlung cross section with the following assumptions:

(1) local vector interaction of the electron $(\gamma_\mu)$;

(2) vector and tensor interaction of the proton, with structure as described by the Hofstadter form factors $F_1\gamma_\mu + (\mu_p F_2/2M)\sigma_{\mu\nu}q^\nu$;

(3) lowest order perturbation theory, as represented by the Bethe-Heitler diagrams (fig. 2(a)) and the two Compton diagrams with single photon exchange (fig. 3(a)), both in first Born approximation;

(4) approximations of zero magnetic moment and the static limit in the interference and Compton contributions.

As we remarked, the form factors for charge and moment distributions completely describe the proton vertex part but are inadequate for a complete description of the Compton part.

In sect. 2 we analyze the virtual Compton effect amplitude in its most general form, with one photon real and the other virtual. This amplitude will be described by twelve form factors of three invariants. The case when both photons are real is described by six form factors of two invariants. In sect. 3 we calculate the bremsstrahlung cross section in first Born approximation, leaving the form factors unspecified. In sect. 4 we expand the cross section in

† Supported in part by the U. S. Air Force through the Air Force Office of Scientific Research.

powers of momentum/proton mass, written symbolically as $1/M$, and show that only three combinations of the twelve Compton form factors contribute when leading terms are considered. In sect. 5 we consider three contributions to the virtual Compton effect:

(a) The single nucleon intermediate state, for which the $f_j$ are expressible in terms of the electric and magnetic form factors for the proton vertex.

(b) The one-pion, one-nucleon intermediate state, for which unitarity of the $S$-matrix enables us to write the imaginary part of the $f_j$ from this intermediate state in terms of the matrix elements for pion photoproduction by real and virtual photons. We consider the three combinations of the twelve form factors in the $1/M^2$ approximation. The real contribution generated by this intermediate state is then derived by assuming subtracted dispersion relations to hold (with a cut-off above the experimentally known region).

(c) Neutral pion exchange, which contributes to one of the twelve form factors.

Some numerical results are given for these various contributions to the bremsstrahlung cross section for a coincidence process.

## 2. Virtual Proton Compton Effect Amplitude

Consider the proton Compton effect amplitude in fig. 1, where $\mu$ is the index of the virtual photon with momentum $r$, while the real photon has momentum $k$ and is in polarization state $e$. The two real protons have momentum $Q_1$, $Q_2$.

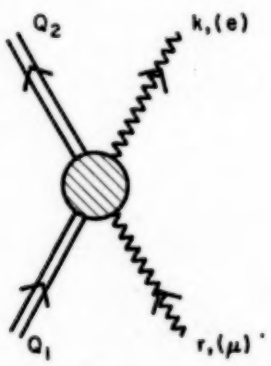


Fig. 1. Virtual Compton amplitude for the proton. The momentum and the polarization state of the virtual photon are $r$, $\mu$, those of the real photon $k$, $e$.

The matrix element corresponding to this amplitude is $\bar{U}_2 M^{\mu\nu} e_\nu U_1$. In a manner similar to that of Prange [2]), we define four orthogonal four-vectors, $A_\mu$, $B_\mu$, $C_\mu$ and $D_\mu$, which we denote by $\eta_\mu^{(\sigma)}$ ($\sigma = 1, \ldots, 4$), i.e. $\eta_\mu^{(1)} = A_\mu \ldots$ $\eta_\mu^{(4)} = D$. The matrix element can then be expanded in terms of this basis:

$$M_{\mu\nu} = \sum_{\rho,\sigma=1}^{4} \eta_\mu^{(\rho)} C^{\rho\sigma} \eta_\nu^{(\sigma)}, \tag{1.1}$$

where $C^{\rho\sigma}$ is some combination of $\gamma$-matrices, and is therefore a matrix in the spinor indices. We define our basis as follows (metric: $(ab) = a^0 b^0 - \mathbf{a}\cdot\mathbf{b}$):

$$\begin{aligned} &K_\mu \equiv \tfrac{1}{2}(r+k)_\mu, \qquad Q_\mu \equiv \tfrac{1}{2}(r-k)_\mu, \qquad R_\mu \equiv \tfrac{1}{2}(Q_1+Q_2)_\mu, \\ &A_\mu \equiv K_\mu, \qquad\qquad C_\mu \equiv R_\mu - \frac{(RK)}{K^2}K_\mu - \frac{(RB)}{B^2}B_\mu, \\ &B_\mu \equiv Q_\mu - \frac{(QK)}{K^2}K_\mu, \quad D_\mu = \varepsilon_{\mu\nu\alpha\beta}A^\nu B^\alpha C^\beta. \end{aligned} \tag{1.2}$$

Since $k$ is a real photon, we can impose the Lorentz condition $(ke) = 0$, so that e.g. $\eta_\nu^{(2)}$ can be eliminated. In addition, gauge invariance requires that

$$M_{\mu\nu}k^\nu = 0, \qquad r^\mu M_{\mu\nu} = 0, \tag{1.3}$$

enabling us to eliminate $\eta_\nu^{(1)}$ and to express $C^{2\sigma}$ in terms of $C^{1\sigma}$:

$$C^{2\sigma} = \frac{2(3K^2+Q^2)K^2}{(K^2-Q^2)^2}C^{1\sigma} \equiv xC^{1\sigma}. \tag{1.4}$$

Assuming parity conservation and making use of the fact that $M_{\mu\nu}$ operates between two free particle Dirac spinors to eliminate all the $\gamma$-combinations except $1, \gamma_5, \mathbf{K} = \gamma^\mu K_\mu, \mathbf{D} = \gamma^\mu D_\mu$, we have

$$\begin{aligned} M_{\mu\nu} = {} & \frac{C_\mu C_\nu}{MC^2}\left[f_1 + \frac{1}{M}\mathbf{K}f_2\right] + \frac{D_\mu D_\nu}{MD^2}\left[f_3 + \frac{1}{M}\mathbf{K}f_4\right] \\ & + \frac{M(C_\mu D_\nu + D_\mu C_\nu)}{D^2}\left[\gamma_5 f_5 + \frac{1}{M^3}\mathbf{D}f_6\right] + \frac{M(C_\mu D_\nu - C_\nu D_\mu)}{D^2}\left[\gamma_5 f_7 + \frac{1}{M^3}\mathbf{D}f_8\right] \\ & + \frac{MA'_\mu C_\nu}{A^2C^2}\left[f_9 + \frac{1}{M}\mathbf{K}f_{10}\right] + \frac{M^3A'_\mu D_\nu}{A^2D^2}\left[\gamma_5 f_{11} + \frac{1}{M^3}\mathbf{D}f_{12}\right], \end{aligned} \tag{1.5}$$

where

$$A_\mu' \equiv A_\mu + xB_\mu.$$

The twelve complex dimensionless form factors are functions of three invariants, which we take to be the dimensionless quantities,

$$\begin{aligned} &\nu_1 \equiv \frac{(RK)}{M^2} = \frac{(kQ_1)+(KQ_2)}{2M^2}, \qquad \nu_2 \equiv \frac{Q^2-K^2}{2M^2} = \frac{(KQ_1)-(KQ_2)}{2M^2}, \\ &\nu_3 = \frac{(QK)}{M^2} = \frac{r^2}{4M^2}. \end{aligned} \tag{1.6}$$

Then we get

$$x = (\nu_3 - \nu_2)(2\nu_3 - \nu_2)/\nu_2^2.$$

We have taken $M_{\mu\nu}$ with overall dimension of $1/M$, since this is what occurs naturally in considering the single-nucleon intermediate state.

Since one photon is real and the other is virtual, we cannot use crossing symmetry for the photon. Crossing symmetry for the proton, however, still holds:

$$C^{-1}M^{\mathrm{T}}_{\mu\nu}(Q_1 \leftrightarrow -Q_2)C = M_{\mu\nu}, \tag{1.7}$$

and requires

$$\begin{aligned} f_j(\nu_1, \nu_2, \nu_3) &= f_j(-\nu_1, \nu_2, \nu_3) \quad \text{for} \quad j = 1, 3, 5, 6, 7, 8, 10, \\ f_j(\nu_1, \nu_2, \nu_3) &= -f_j(-\nu_1, \nu_2, \nu_3) \quad \text{for} \quad j = 2, 4, 9, 11, 12. \end{aligned} \tag{1.8}$$

In the limiting case when $r$ is taken to be a real photon ($\nu_3 \to 0$), we have crossing symmetry for both photons and protons, and therefore $f_5 = f_8 = 0$. The Lorentz condition on $r$ then enables us to eliminate $f_{9,10,11,12}$, and we are left with six form factors of two invariants [2]).

## 3. Bremsstrahlung and Pair-Production Cross Sections

The virtual Compton effect amplitude is now used to express the cross section for bremsstrahlung (and pair-production) of electrons on protons, in terms of the twelve $f_j$ and the two-proton vertex form factors. The proton vertex is taken as

$$\bar{U}(Q_2)\left[\gamma^\mu F_{1\mathrm{p}}(q^2) + \frac{\mu_\mathrm{p}}{4M} F_{2\mathrm{p}}(q^2)(\mathbf{q}\gamma^\mu - \gamma^\mu \mathbf{q})\right] U(Q_1) \equiv \bar{U}_2 \Gamma^\mu(q) U_1, \tag{2.1}$$

where $q^2 = (Q_2 - Q_1)^2 = 4M^2(\nu_2 + \nu_3)$.

The matrix element of fig. 2 is then

$$\begin{aligned} \text{M.E.} = {} & \frac{\text{const.}}{q^2}\bar{u}_2\left[\mathbf{e}\frac{1}{m - \mathbf{p}_2 - \mathbf{k}}\gamma^\mu + \gamma^\mu \frac{1}{m - \mathbf{p}_1 + \mathbf{k}}\mathbf{e}\right] u_1 \times \bar{U}_2 \Gamma_\mu(q) U_1 \\ & - \frac{\text{const.}}{r^2}\bar{u}_2 \gamma^\mu u_1 \times \bar{U}_2 M_{\mu\nu} e^\nu U_1, \end{aligned} \tag{2.2}$$

where the constant is equal to

$$\frac{-i\alpha^{\frac{3}{2}} mM}{\pi^2 \sqrt{4\omega\varepsilon_1\varepsilon_2 E_1 E_2}}.$$

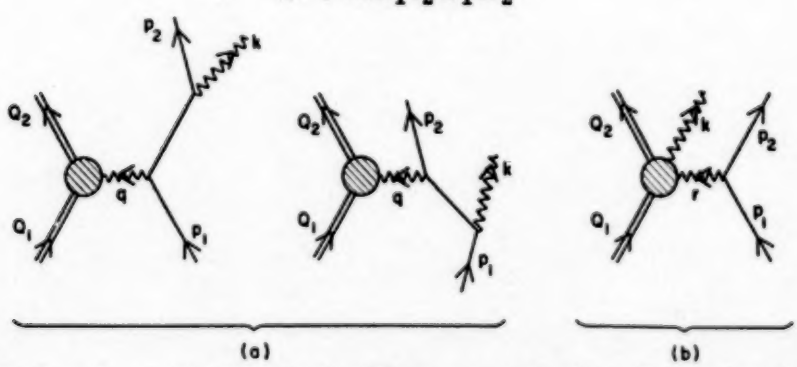


Fig. 2. (a) Electron bremsstrahlung in first Born approximation. (b) Proton bremsstrahlung.

Summing over final and averaging over initial spins and polarizations we get

$$\mathrm{d}\sigma = \frac{\delta^4(p_1+Q_1-p_2-Q_2-k)}{\sqrt{(p_1Q_1)^2-m^2M^2}}\,\frac{\alpha r_0^2 m^2}{4\pi^2 M^2}\,[Y_{\mathrm{I}}+Y_{\mathrm{II}}+Y_{\mathrm{III}}]\,\frac{\mathrm{d}^3\mathbf{p}_2\mathrm{d}^3\mathbf{Q}_2\mathrm{d}^3\mathbf{K}}{\varepsilon_2 E_2 k}. \quad (2.3)$$

The term $Y_{\mathrm{I}}$ is the contribution from the bremsstrahlung of the electron alone, $Y_{\mathrm{III}}$ is the contribution of the bremsstrahlung of the proton alone, and $Y_{\mathrm{II}}$ is the interference between the two. The quantities $Y$ are complicated and are given in terms of five invariants ($v_j$, $j = 1 \ldots 5$), and the fourteen functions $f_j\,(v_1v_2v_3)$, $F_{1,2}\,(v_2+v_3)$. (Refer to Appendix A for definitions and comments on the notation.)

### 3.1. ELECTRON BREMSSTRAHLUNG (BETHE-HEITLER) TERM

$$\begin{aligned} Y_{\mathrm{I}} = \frac{2M^4}{q^4}\Bigg[&\mathscr{F}_1(q^2)\left\{-\frac{\lambda_1}{\lambda_2}-\frac{\lambda_2}{\lambda_1}-\frac{m^2q^2}{2\lambda_1^2}-\frac{m^2q^2}{2\lambda_2^2}-\frac{r^2q^2}{2\lambda_1\lambda_2}\right\} \\ &+\mathscr{F}_2(q^2)\left\{-\frac{m^2}{2M^2}\left(\frac{\mu_1+\mu_4}{\lambda_2}-\frac{\mu_2+\mu_3}{\lambda_1}\right)^2-\frac{q^2}{4M^2}\left(\frac{(\mu_1+\mu_4)^2+(\mu_2+\mu_3)^2}{\lambda_1\lambda_2}\right)\right. \\ &\left.+\frac{m^2q^2}{\lambda_1\lambda_2}\left(1-\frac{q^2}{4M^2}\right)\right\}+\mathscr{F}_3(q^2)\left\{\left(\frac{m^2}{\lambda_1}-\frac{m^2}{\lambda_2}\right)-\tfrac{1}{2}\left(\frac{m^2}{\lambda_1}-\frac{m^2}{\lambda_2}\right)^2\right\}\Bigg], \end{aligned} \quad (2.4)$$

where

$$\begin{aligned} &\mathscr{F}_1(q^2) \equiv F_{1\mathrm{p}}^2+\tfrac{1}{4}(F_{1\mathrm{p}}^2+4F_{1\mathrm{p}}F_{2\mathrm{p}}\mu_{\mathrm{p}}+F_{2\mathrm{p}}^2\mu_{\mathrm{p}}^2)\frac{q^2}{M^2}+\frac{\mu_{\mathrm{p}}^2F_{2\mathrm{p}}^2}{16}\left(\frac{q^2}{M^2}\right)^2, \\ &\mathscr{F}_2(q^2) \equiv F_{1\mathrm{p}}^2-\frac{\mu_{\mathrm{p}}^2q^2}{4M^2}F_{2\mathrm{p}}^2, \qquad \mathscr{F}_3(q^2) \equiv (F_{1\mathrm{p}}+\mu_{\mathrm{p}}F_{2\mathrm{p}})^2\frac{q^2}{M^2}. \end{aligned} \quad (2.5)$$

### 3.2. INTERFERENCE TERM

$$\begin{aligned} Y_{\mathrm{II}} = \frac{8M^4}{q^2r^2(4v_4^2-v_2^2)}\Bigg[&(f_1, f_2)y_1+(f_3, f_4)y_2+(f_9, f_{10})y_3 \\ &+(F_{1\mathrm{p}}+\mu_{\mathrm{p}}F_{2\mathrm{p}})\frac{q^2}{M^2}\sum_{n=1}^{6}Z_n\,\mathrm{Re}\,(f_{2n})\Bigg], \end{aligned}$$

$$(f_i, f_j) \equiv F_{1\mathrm{p}}(q^2)\,\mathrm{Re}\,(f_i+v_1f_j)+\frac{\mu_{\mathrm{p}}q^2}{4M^2}F_{2\mathrm{p}}(q^2)\,\mathrm{Re}\,(f_i), \quad (2.6)$$

$$\begin{aligned} &y_1 = 2\alpha_1[\alpha_1\alpha_3(v_2v_5-v_1v_4)+2v_4^2+v_2v_3], \\ &y_2 = 2\alpha_2[v_2v_5-v_1v_4]-v_2^2\alpha_1, \\ &y_3 = -(4v_3/v_2^2)[\alpha_1\alpha_3\{v_1v_2(v_2+v_3)-2v_4(v_1v_4-v_2v_5)\}+v_4(4v_4^2-v_2^2)], \\ &\alpha_1 = v_5+v_1v_4(2v_3+v_2)/v_2^2, \qquad \alpha_3 = v_2^2[v_2^2+(v_2+v_3)(v_1^2-v_2^2)]^{-1}, \\ &\alpha_2 = M^{-2}D^{-2}(SD)^2 = \alpha_2(v_1, v_2, v_3, v_4, v_5), \end{aligned}$$

$$Z_1 = \nu_2\nu_4\alpha_1{}^2\alpha_3, \qquad Z_2 = \nu_2\nu_4\alpha_2, \qquad Z_3 = \tfrac{1}{4}\alpha_1[2\nu_2(2\alpha_2+\nu_2+\nu_3)+4\nu_4{}^2-\nu_2{}^2],$$
$$Z_4 = \tfrac{1}{4}\alpha_1[4\nu_4{}^2-\nu_2{}^2-2\nu_2\nu_3], \qquad Z_5 = -\alpha_1\alpha_3\nu_3(4\nu_4{}^2-\nu_2{}^2)/\nu_2, \tag{2.6}$$
$$Z_6 = -(\nu_3\nu_4/\nu_2)(2\alpha_2+(4\nu_4{}^2-\nu_2{}^2)/\nu_2).$$

(See Appendix 1 for explicit form of $\alpha_2$.)

### 3.3. PROTON BREMSSTRAHLUNG TERM

$$Y_{\mathrm{III}} = -\frac{4M^4}{r^4}\left[\frac{4\nu_3{}^2\alpha_3}{\nu_2{}^4}(4\nu_4{}^2-\nu_2{}^2)J_1+(\nu_3+\alpha_1{}^2\alpha_3)J_2 \right.$$
$$\left. +(\nu_3+\alpha_2)J_3-(8\nu_3\nu_4\alpha_1\alpha_3/\nu_2{}^2)J_4\right],$$

$$J_1 \equiv [9,10,11,12] \equiv |f_9+\nu_1 f_{10}|^2+(\nu_2+\nu_3)\{|f_{12}|^2-|f_9|^2-\nu_2{}^{-2}|f_{11}|^2\}$$
$$+\frac{\nu_1{}^2(\nu_2+\nu_3)^2}{\nu_2{}^2}|f_{12}|^2-\nu_2{}^2\left\{|f_{10}|^2+\left(\frac{\nu_2+\nu_3}{\nu_2}\right)^2|f_{12}|^2\right\}, \tag{2.7}$$

$$J_2 \equiv [1,2,5+7,6+8], \qquad J_3 \equiv [3,4,5-7,\ 6-8],$$

$$J_4 \equiv \mathrm{Re}\left\{(f_1+\nu_1 f_2)(\bar{f}_9+\nu_1\bar{f}_{10})+(\nu_2+\nu_3)(\bar{f}_{12}(f_6+f_8)-f_1\bar{f}_9-\nu_2{}^{-2}\bar{f}_{11}(f_5+f_7))\right.$$
$$\left.+\frac{\nu_1{}^2(\nu_2+\nu_3)^2}{\nu_2{}^2}(f_6+f_8)\bar{f}_{12}-\nu_2{}^2\left(f_2\bar{f}_{10}+\left(\frac{\nu_2+\nu_3}{\nu_2}\right)^2(f_6+f_8)\bar{f}_{12}\right)\right\}.$$

### 3.4. PAIR PRODUCTION

Making use of the substitution rule [3]), we have for the related process of pair production (summed and averaged over spins and polarizations)

$$\mathrm{d}\sigma_{\mathrm{pair}} = \frac{\delta^4(k+Q_1-Q_2-p_+-p_-)\alpha r_0{}^2m^2}{4\pi^2M^2\ (kQ_1)}[Y_{\mathrm{I}}^{\mathrm{p}}+Y_{\mathrm{II}}^{\mathrm{p}}+Y_{\mathrm{III}}^{\mathrm{p}}]\frac{\mathrm{d}^3\mathbf{Q}_2}{E_2}\frac{\mathrm{d}^3\mathbf{p}_+}{\varepsilon_+}\frac{\mathrm{d}^3\mathbf{p}_-}{\varepsilon_-}, \tag{2.8}$$

where

$$Y^{\mathrm{p}} = -Y(k\to -k, p_1\to -p_+, p_2\to p_-).$$

### 3.5. APPLICATION TO OTHER PROCESSES

No assumption has been made about the energies and masses involved, and the formulae above could therefore be applied to processes such as muon-proton bremsstrahlung, muon pair production in the field of a proton, etc. Since the various form factors are unspecified, the formulae are also directly applicable to such processes as electron-neutron, lepton-hyperon, etc. bremsstrahlung and pair production.

## 4. Expansion of the Cross Section in Powers of $1/M$

By an expansion in $1/M$ we mean an expansion in the ratio of the momentum involved to the proton mass. The expansion in $1/M$ then consists of two parts:

the expansion of the kinematic terms ($\nu_1$, $\alpha_1$, $y_1$, etc.) and the expansion of the $f_j$. The kinematic terms have the behaviour, in leading order,

$$\begin{aligned} &\nu_{1,5} \approx M^{-1}, \quad \nu_{2,3,4} \approx M^{-2}, \quad \alpha_1 \approx M^{-1}, \quad \alpha_2 \approx M^{-2}, \quad \alpha_3 \approx 1, \\ &y_{1,2} \approx M^{-5}, \quad y_3, Z_6 \approx M^{-4}, \quad Z_{1,2} \approx M^{-6}, \quad Z_{3,4,5} \approx M^{-5}. \end{aligned} \tag{3.1}$$

E.g., for $\nu_1$ (momenta in lab. system; electron relativistic) we have

$$\nu_1 \equiv \frac{(kQ_1)+(kQ_2)}{2M^2} = \frac{p_1-p_2}{M} - \frac{(\mathbf{p}_1-\mathbf{p}_2)\cdot\mathbf{Q}_2}{2M^2} + \ldots.$$

The behaviour of the $f_j$ in a $1/M$ expansion is determined as follows:

$$f_1+\frac{1}{M}\mathbf{K}f_2 = \frac{M}{C^2}C^\mu C^\nu M_{\mu\nu}, \qquad f_3+\frac{1}{M}\mathbf{K}f_4 = \frac{M}{D^2}D^\mu D^\nu M_{\mu\nu}, \qquad \text{etc.} \tag{3.2}$$

Since $A, B \approx 1$ and $C, D \approx M$, we see that the $f_j$ must have the following expansions:

$$\begin{aligned} &f_{2,4} \approx M^2 \times AM^{-\alpha}, \qquad f_{1,3,6,8,10} \approx M \times AM^{-\alpha}, \\ &f_{9,12} \approx 1 \times AM^{-\alpha}, \qquad f_{5,7} \approx M^{-1} \times AM^{-\alpha}, \\ &f_{11} \approx M^{-2} \times AM^{-\alpha}, \end{aligned} \tag{3.3}$$

where $AM^{-\alpha}$ denotes the leading term in any contribution to $M_{\mu\nu}$ in a $1/M$ expansion (the contribution may be the single-nucleon intermediate state, the one-nucleon intermediate state, etc., each with possibly different values of $A$ and $\alpha$). Let us now consider $Y_{II}$. We assume that the energies are such that the following conditions hold:

$$\frac{\mu_p q^2}{4M^2} F_{2p}(q^2) \ll F_{1p}(q^2), \tag{3.4a}$$

$$(F_{1p}+\mu_p F_{2p})\frac{q^2}{M^2} \ll F_{1p}. \tag{3.4b}$$

Condition (3.4a) implies that the bracket symbol $(f_i, f_j)$ may be approximated by

$$(f_i, f_j) \approx F_{1p}(q^2)\,\mathrm{Re}(f_i+\nu_1 f_j). \tag{3.5}$$

Consider the kinematic coefficients of Re $(f_2)$

$$\left[F_{1p}(q^2)\nu_1 y_1 + (F_{1p}+\mu_p F_{2p})\frac{q^2}{M^2}\right] \mathrm{Re}\,(f_2). \tag{3.6}$$

Condition (3.4b) implies then (since $\nu_1 y_1$ and $Z_1$ both have the same $1/M^6$ behaviour) that we may neglect $Z_1(F_{1p}+\mu_p F_{2p})q^2/M^2$ in comparison with

$F_{1p}\nu_1 y_1$; likewise for $y_{2,3}$. Consider the Re $(f_6)$ term

$$(F_{1p}+\mu_p F_{2p})\frac{q^2}{M^2}Z_3 \text{ Re } (f_3).$$

By comparing this with, e.g., the term $F_{1p}y_1 \text{Re}(f_1+\nu_1 f_2)$ we have by condition (3.4b)

$$\begin{aligned} &F_{1p}(y_1^0 M^{-5}+\ldots)(f_1^0 M^{-\alpha+1}+\nu_1^0 M^{-1} f_2^0 M^{-\alpha+2}+\ldots) \gg \\ &(F_{1p}+\mu_p F_{2p})\frac{q^2}{M^2}(Z_3^0 M^{-5}+\ldots)(f_6^0 M^{-\alpha+1}+\ldots), \end{aligned} \tag{3.7}$$

where $y_1^0 M^{-5}+\ldots, \nu_1^0 M^{-1}+\ldots, Z_3^0 M^{-5}+\ldots, f_1^0 M^{-\alpha+1}+\ldots$ are the respective expansions of $y_1$, $\nu_1$, $Z_3$ and $f_1$ in $1/M$. The coefficients $(y_1^0, \nu_1^0, \ldots)$ of the leading orders in the expansions are all comparable quantities.

Thus, $Y_{II}$, under the conditions (3.4) can be expressed as

$$Y_{II} = \frac{8M^4}{q^2\nu^2(4\nu_4^2-\nu_2^2)}F_{1p}(q^2)[y_1 \text{ Re } (b_1)+y_2 \text{ Re } (b_2)+y_3 \text{ Re } (b_3)], \tag{3.8}$$

where $b_1$ is the leading term of $f_1+\nu_1 f_2$ in a $1/M$ expansion, $b_2$ the leading term of $f_3+\nu_1 f_4$ in a $1/M$ expansion, and $b_3$ = leading term of $f_9+\nu_1 f_{10}$ in a $1/M$ expansion.

Note that each $b_j$ is a sum of all contributions to the process, but that we can take the leading terms in $1/M$ for each contribution. The various intermediate states will of course contribute different powers of $1/M$ as their leading terms, and some will dominate over others, depending on the energy ranges involved, interaction strengths, etc.

For $Y_{III}$, we see by inspection of the $J_{1,2,3,4}$ and by considerations similar to the above, that under the conditions

$$\nu_2+\nu_3 \ll 1, \qquad \nu_2^2 \ll \nu_1^2, \tag{3.9}$$

we may write

$$J_1 = |b_3|^2, \qquad J_2 = |b_1|^2, \qquad J_3 = |b_2|^2, \qquad J_4 = \text{Re}(b_1 b_2^*). \tag{3.10}$$

Thus both $Y_{II}$ and $Y_{III}$, under conditions (3.4a), (3.4b) and (3.9) may be written in terms of three form factors $b_{1,2,3}$ instead of twelve. The conditions are basically kinematic in nature.

For the energy regions of interest here, electron scattering experiments indicate $F_{1p} \approx F_{2p}$, so that condition (3.4b) will imply condition (3.4a); condition (3.4b) is then the following:

$$q^2 \ll M^2(1+\mu_p)^{-1}.$$

## 5. Evaluation of the Form Factors $f_j$

The causal amplitude $M_{\mu\nu}$ must be well behaved in the physical region. Represented as a contraction of the two photons (with the equal-time commutator dropped)

$$uM_{\mu\nu}u = \int \mathrm{d}^4 Z\, \mathrm{e}^{\mathrm{i}rZ}\langle Q_2|\theta(Z_0)[j_\mu(\tfrac{1}{2}Z), j_\nu(-\tfrac{1}{2}Z)]|Q_1\rangle, \tag{4.1}$$

it yields the statement of unitarity

$$2\,\mathrm{Im}(u^*M_{\mu\nu}u) = \sum_n \langle Q_2|j_\mu|n\rangle\langle n|j_\nu|Q_1\rangle, \tag{4.2}$$

as well as a dispersion relation with respect to the variable $\nu_1$,

$$\mathrm{Re}\,(u^*M^{\mu}{}_{\nu}u) = \frac{1}{\pi}\,\mathrm{P}\int \frac{\mathrm{Im}(u^*M_{\mu\nu}u)}{\nu'_1-\nu_1}\,\mathrm{d}\nu'_1, \tag{4.3}$$

within a limited domain of $\nu_2$ and $\nu_3$, and with appropriate subtractions. These statements are formal, the dispersion relations applying only to the scalar form factors $f_j$. We do not prove these statements in this paper, but assume them to be true.

### 5.1. SINGLE NUCLEON INTERMEDIATE STATE

The contribution from the pole in (4.2) occurs in the non-physical region (fig. 3(a)) so that the corresponding $f_j$ are real. These terms dominate the cross

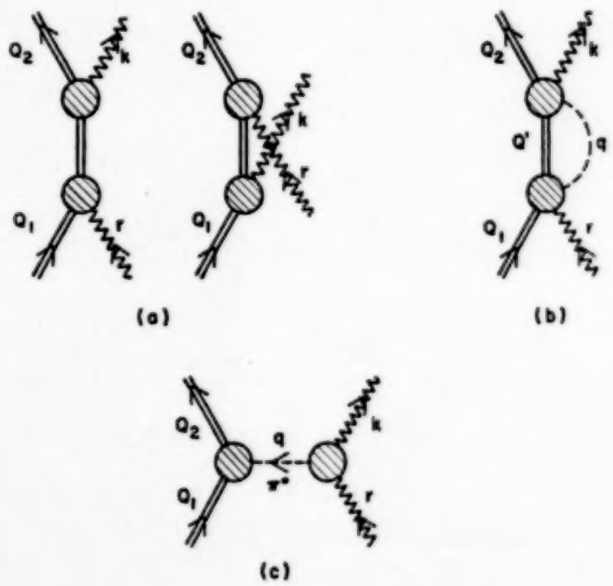


Fig. 3. (a) Single-nucleon intermediate state. (b) One-meson, one-nucleon intermediate state. (c) Neutral pion exchange.

section in the low energy region and become exact in the limit of zero photon energy [4]):

$$M_{\mu\nu} = \left[F_1(r^2)\gamma_\mu + \frac{\mu_p F_2(r^2)}{4M}(\mathbf{r}\gamma_\mu - \gamma_\mu \mathbf{r})\right] \frac{1}{M - Q_2 + k}\left[\gamma_\nu + \frac{\mu_p}{2M}\gamma_\nu \mathbf{k}\right]$$
$$+\text{crossed term.}$$

Here $\mu_p$ is the proton's anamalous magnetic moment, and $F_{1,2}$ are the proton vertex form factors evaluated at the momentum transfers indicated. Expanding the various terms with respect to the basis $A$, $B$, $C$, $D$ of sect. 2, making use of the fact that $M_{\mu\nu}$ operates between two free proton Dirac spinors, and writing $M_{\mu\nu}$ in the form of (1.1), we find (using the abbreviation $F_{1,2} = F_{1,2}(r^2)$)

$$f_1 = -\frac{2\nu_2 F_1}{\nu_1^2 - \nu_2^2} + \frac{2\nu_3 \mu_p F_2}{\nu_2}, \qquad f_2 = \frac{-\nu_1 F_1}{\nu_1^2 - \nu_2^2} - \frac{2\nu_1\nu_3(F_1 + \mu_p F_2)}{\nu_2(\nu_1^2 - \nu_2^2)},$$

$$f_3 = F_1 - (1+\mu_p)(F_1 + \mu_p F_2), \qquad f_4 = \frac{(1+\mu_p)(F_1 + \mu_p F_2)\nu_1}{\nu_1^2 - \nu_2^2},$$

$$f_5 = \tfrac{1}{2}\mu_p(F_1 - F_2)\nu_2\left[\frac{(\nu_2+\nu_3)(\nu_1^2-\nu_2^2)+\nu_2^2}{(\nu_2+\nu_3)(\nu_1^2-\nu_2^2)}\right],$$

$$f_6 = -\frac{\nu_2(2F_1 + \mu_p(F_1+F_2))}{2(\nu_1^2-\nu_2^2)} + \tfrac{1}{2}\mu_p^2 F_2 + \frac{\nu_2\nu_3(F_1-F_2)\mu_p}{2(\nu_2+\nu_3)(\nu_1^2-\nu_2^2)},$$

$$f_7 = \tfrac{1}{2}\nu_2 f_3 + \frac{\nu_2^3(2F_1 + \mu_p(F_1+F_2))}{2(\nu_2+\nu_3)(\nu_1^2-\nu_2^2)} - \frac{\mu_p^2 F_2 \nu_2 \nu_3}{2(\nu_2+\nu_3)}, \tag{4.4}$$

$$f_8 = \frac{\mu_p(F_1-F_2)\nu_2}{2(\nu_1^2-\nu_2^2)} + \frac{\mu_p^2 F_2 \nu_3}{2(\nu_2+\nu_3)} + \frac{\nu_2\nu_3(2F_1 + \mu_p(F_1+F_2))}{2(\nu_2+\nu_3)(\nu_1^2-\nu_2^2)},$$

$$f_9 = \nu_1 \mu_p F_2\left(\tfrac{1}{2} + \frac{\nu_2}{\nu_1^2-\nu_2^2} + \frac{\nu_3}{\nu_2}\right),$$

$$f_{10} = -\left(1 + \frac{\nu_3}{\nu_2}\right)(F_1 + \mu_p F_2) - \frac{\nu_2}{\nu_1^2-\nu_2^2}(F_1 + \mu_p F_2) + \frac{\nu_1^2 \mu_p F_2}{2(\nu_1^2-\nu_2^2)},$$

$$f_{11} = -\tfrac{1}{2}\nu_1\nu_2 F_2(\mu_p + \mu_p^2)\left(1 + \frac{\nu_2^2}{(\nu_1^2-\nu_2^2)(\nu_2+\nu_3)}\right),$$

$$f_{12} = \mu_p(1+\mu_p)F_2 \frac{\nu_1\nu_2^2}{2(\nu_2+\nu_3)(\nu_1^2-\nu_2^2)} + \tfrac{1}{2}\nu_1\mu_p^2 F_2.$$

The single-nucleon contribution to the three form-factor combinations of sect. 4 are

$$b_1 = -F_1(r^2)\left[1 + \frac{2\nu_2}{\nu_1^2} + \frac{2\nu_3}{\nu_2}\right], \qquad b_2 = F_1(r^2), \qquad b_3 = \tfrac{1}{2}\nu_1(b_1 - b_2). \tag{4.5}$$

Since no $\mu_p$ appears in the $b_j$ above, our analysis indicates that $Y_{II}^{S.N.}$ and $Y_{III}^{S.N.}$ (including order $1/M^2$) from the single nucleon state (S.N.) will have no $\mu_p$ terms [5]).

The expressions obtained above for the $f_j$ agree with those of Walecka [6]) in the real photon limit $\nu_3 \to 0$.

Referring to sect. 4, we see that the next higher order of approximation for $Y_{II}$ in a $1/M$ expansion will include terms of the type $y_1^0 \,\mathrm{Re}\,(b_1^{(1)})$, $y_1^1 \,\mathrm{Re}(b_1^{(0)})$, $(\mu_p q^2/4M^2)F_2 \,\mathrm{Re}(f_1)$, $(F_1+\mu_p F_2)(q_2/M^2)Z_1 \,\mathrm{Re}(f_2)$, etc., where $b_1^{(0)}$ is the leading term and $b_1^{(1)}$ is the next higher order term in the expansion of $f_1+\nu_1 f_2$ in $1/M$. (i.e. $y_1 = M^{-5}(y_1^0+y_1^1+\ldots) = M^{-5}+M^{-6}+\ldots$). Since inspection of the single nucleon $f_j$ shows that they drop down by two orders of $1/M$ (i.e. $f_1 \approx 1+M^{-2}+M^{-3}+\ldots$), we see that the next higher order of the single nucleon $b_{1,2,3}^{S.N.}$ is always down by two orders of $1/M$ from the leading term of $b_{1,2,3}^{S.N.}$. However, $y_j$ drops down by only one order of $1/M$: $y_1 \approx M^{-5}+M^{-6}+\ldots$ but the next higher order of $Y_j$ is multiplied by $b_j^{(0)}$, containing no power of $\mu_p$. We may symbolically summarize our result as follows:

$$Y_{II}^{S.N.} \approx (1/M+1/M^2)+\left(\frac{\mu_p,\ \mu_p^2}{M^3}\right)+\ldots. \tag{4.6}$$

A similar analysis for $Y_{III}$ gives

$$Y_{III}^{S.N.} \approx (1/M^2+1/M^3)+\left(\frac{\mu_p,\ \mu_p^2}{M^4}\right)+\ldots. \tag{4.7}$$

This shows that when we consider the next approximations in a $1/M$ expansion to $Y_{II}^{S.N.}$ and $Y_{III}^{S.N.}$ using the anomalous moments, we must consider $\mu_p$ terms together with $\mu_p^2$ terms. The $\mu_p$-term cannot be consistently considered alone in $Y_{II}^{S.N.}$ for example, while neglecting the $\mu_p^2$ term (as has been done in a related treatment of the problem [7])).

### 5.2. MESON-NUCLEON INTERMEDIATE STATE

#### 5.2.1. *Imaginary parts of the $b_j$*

We expect the meson-nucleon intermediate state to be the most important of the remaining terms of (4.2) at energies of present experimental interest. The absorptive part of fig. 3(b) is readily evaluated from a knowledge of the real and virtual photoproduction amplitudes. Specifically, we have

$$\begin{aligned} &2\,\mathrm{Im}(u^* M_{\mu\nu} u) \\ &\quad = \int \mathrm{d}^4 q \int \mathrm{d}^4 Q' \delta(q^2-\mu^2)\delta(Q'^2-M^2)\delta^4(Q'+q-Q_1-r)\delta^4(k+Q_2-Q'-q) \\ &\quad \times \langle Q_2|j_\mu^\dagger|Q'q\rangle\langle Q'q|j_\nu|Q_1\rangle. \end{aligned} \tag{4.8}$$

For the analysis of the real photoproduction amplitude, we rely on the work of Chew *et al.* [8]), while for the corresponding virtual processes, we follow Fubini *et al.* [9]), and Dalitz and Yennie [10]). We note the following:

(a) These amplitudes may be represented by an invariant form factor analysis similar to that for the virtual Compton amplitude. However, it has been found convenient to use a multipole representation in the pion-nucleon centre-of-mass system. For the virtual process we have (using $r+Q_1 \to Q'+q$, where $r$ is the momentum of the initial virtual photon, and $q$ that of the meson)

$$\begin{aligned} M = {} & (\mathrm{E1T})i\left(\boldsymbol{\sigma}\cdot\boldsymbol{\varepsilon} - \frac{1}{\mathbf{r}^2}\boldsymbol{\sigma}\cdot\mathbf{r}\,\boldsymbol{\varepsilon}\cdot\mathbf{r}\right) - (\mathrm{M1})\left(\frac{\boldsymbol{\sigma}\cdot\mathbf{q}\;\boldsymbol{\sigma}\cdot\mathbf{r}\times\boldsymbol{\varepsilon}}{|r|\,|q|}\right) \\ & - (\mathrm{M3})\left(\frac{3\mathbf{q}\cdot\mathbf{k}\times\boldsymbol{\varepsilon} - \boldsymbol{\sigma}\cdot\mathbf{q}\;\boldsymbol{\sigma}\cdot\mathbf{r}\times\boldsymbol{\varepsilon}}{|\mathbf{q}||\mathbf{r}|}\right) + (\mathrm{E1L})i\left(\boldsymbol{\sigma}\cdot\mathbf{r}\,\frac{\boldsymbol{\varepsilon}\cdot\mathbf{r}}{\mathbf{r}^2}\right) \\ & + \frac{(\mathrm{E2T})i}{2|\mathbf{r}||\mathbf{q}|}\left(\boldsymbol{\sigma}\cdot\mathbf{r}\;\boldsymbol{\varepsilon}\cdot\mathbf{q} + \boldsymbol{\sigma}\cdot\boldsymbol{\varepsilon}\;\mathbf{r}\cdot\mathbf{q} - \frac{2}{\mathbf{r}^2}\boldsymbol{\sigma}\cdot\mathbf{r}\;\boldsymbol{\varepsilon}\cdot\mathbf{r}\,\mathbf{r}\cdot\mathbf{q}\right) \\ & + (01)i\left(\frac{\boldsymbol{\sigma}\cdot\mathbf{q}\;\boldsymbol{\varepsilon}\cdot\mathbf{r}}{|\mathbf{q}||\mathbf{r}|}\right) + \frac{(\mathrm{E2L})i}{|\mathbf{r}||\mathbf{q}|}\left(\frac{\boldsymbol{\sigma}\cdot\mathbf{r}\;\boldsymbol{\varepsilon}\cdot\mathbf{r}\,\mathbf{r}\cdot\mathbf{q}}{\mathbf{r}^2} - \frac{\boldsymbol{\sigma}\cdot\mathbf{q}\;\boldsymbol{\varepsilon}\cdot\mathbf{r}}{3}\right), \end{aligned} \tag{4.9}$$

while in the corresponding expression for the real process, $(k+Q_2 \to Q'+q)$, the gauge condition $(ek) = 0$ is invoked. The static multipoles are understood to operate between appropriate Pauli spinors. If gauge invariance is maintained, there is no loss of covariance in such a representation.

(b) For the Compton process, both $\pi^+$ and $\pi^0$ intermediate states must be considered. By the Watson theorem, the multipoles above have the phases of the pion scattering multipoles, so that this contribution to the Compton process is to be expressed in terms of the scattering phase shifts.

The general expression for Im $(f_j)$ in terms of the various multipoles is rather complicated. The calculation is carried out in terms of the multipoles for s and p wave production. For the energies of present interest ($r_0$, $k < 500$ MeV in the lab. system) the higher multipoles of this absorptive process are not accessible to observation. There is no reason to believe, however, that they will not generate dispersive effects that may be comparable to those considered here. Lack of information precludes further consideration of them here, however.

For the dominant behaviour of the photoproduction and electroproduction processes, we in fact restrict our attention to the following multipole contributions, where T and L refer to the transverse and longitudinal components of the electric dipole amplitude, respectively:

$$\begin{aligned} &\text{for} \quad \pi^+\text{:} \quad \mathrm{E1T} = \mathrm{E1L} \equiv \mathrm{E1} = \frac{g}{2M}\sqrt{2}\,\frac{2M}{W+M}, \\ &\qquad (\mathrm{M3})_+ = \frac{g}{2M}\,\frac{|\mathbf{k}|\mu}{|\mathbf{q}|^2}\,e^{i\delta_{33}}\sin\delta_{33}\left[\frac{(\mu_p-\mu_n)\mu}{12Mf_r^2}\right]\sqrt{2}, \\ &\text{for} \quad \pi^0\text{:} \quad (\mathrm{M3})_0 = \sqrt{2}(\mathrm{M3})_+. \end{aligned} \tag{4.10}$$

Here, $\delta_{33}$ is the phase shift for the ($T = \frac{3}{2}$, $J = \frac{3}{2}$) pion-nucleon resonance, $\mu_p$ and $\mu_n$ are the proton and neutron anomalous moments, and $W$ is the energy of the proton plus meson in the proton-meson centre-of-mass system. An additional contribution for $\pi^+$ is the photomeson current which contains all multipoles. For higher energies, for which these terms are large, a more elaborate treatment is necessary, as we have neglected them here.

In this approximation then, the contributions to $\mathrm{Im}(f_j)$ are given in terms of $|\mathrm{E1}|^2$ and $|\mathrm{M3}|^2$. It was shown in sect. 4. in fact, that keeping the leading terms in a $1/M$ expansion, only three combinations of the twelve $f_j$ contribute to the cross section. The contributions to the imaginary parts of these three $b_j$ from the one-meson, one-nucleon intermediate state turn out to be

$$\begin{aligned}
\mathrm{Im}(b_1^M) &= -\frac{\sqrt{\nu_1^2-\nu_0^2}}{4\pi}\left[\left(1+\frac{2\nu_3}{\nu_2}\right)\left(|\mathrm{E1}|^2+\frac{2\nu_1}{\sqrt{\nu_1^2-4\nu_3}}|\mathrm{M3}|^2\right)+\frac{2\nu_2}{\nu_1^2}|\mathrm{E1}|^2\right],\\
\mathrm{Im}(b_2^M) &= \frac{\sqrt{\nu_1^2-\nu_0^2}}{4\pi}\left[\left(|\mathrm{E1}|^2+\frac{2\nu_1}{\sqrt{\nu_1^2-4\nu_3}}|\mathrm{M3}|^2\right)+\frac{2\nu_2}{\nu_1^2}\left(\frac{2\nu_1|\mathrm{M3}|^2}{\sqrt{\nu_1^2-4\nu_3}}\right)\right], \qquad (4.11)\\
\mathrm{Im}(b_3^M) &= \tfrac{1}{2}\nu_1\,\mathrm{Im}(b_1^M-b_2^M), \qquad |\mathrm{M3}|^2 \equiv |\mathrm{M3}|_+^2+|\mathrm{M3}|_0^2,\\
q &= M\sqrt{\nu_1^2-\nu_0^2}.
\end{aligned}$$

For estimating these expressions we divide the $\nu_1$ region into three parts, (1) $0 < \nu_1 < \nu_0$, where $\nu_0$ is the (centre-of-mass) threshold for pion production, (2) $\nu_0 < \nu_1 < \nu_R$, where $\nu_R$ is the resonance and (3) $\nu_R < \nu_1 < \nu_M$, where $\nu_M$ is some cut-off for $\nu_1$ used in the dispersion relations below. Both $|\mathrm{E1}|^2$ and $|\mathrm{M3}|^2$ are zero in the region (1) below the threshold. We take

$$|\mathrm{M3}|^2 = \frac{g^2}{4M^2}\frac{|\mathbf{k}||\mathbf{r}|}{q^4}\sin^2\delta_{33}\left(\frac{2\mu^4(\mu_p-\mu_n)(\mu_p F_{2p}(\gamma^2)-\mu_n F_{2n}(\gamma^2))}{144M^2 f_r^4}\right). \qquad (4.12)$$

Using the effective range approximation for $\sin\delta_{33}$ (noting that, in the $1/M^2$ approximation we are taking, $k \approx M\nu_1$, $\gamma \approx M\sqrt{\nu_1^2-4\nu_3}$), we make the following approximations:

$$\frac{kr\mu^2}{q^4}\sin^2\delta_{33} \approx \begin{cases} \left(\dfrac{M^4}{8\mu^4}\right)\nu_1(\nu_1^2-\nu_0^2)\sqrt{\nu_1^2-4\nu_3} & (\nu_0 < \nu_1 < \nu_R),\\ \dfrac{(1.3)\mu^3}{M^3}\dfrac{\sqrt{\nu_1^2-4\nu_3}}{\nu_1(\nu_1^2-\nu_0^2)^{\frac{1}{2}}} & (\nu_R < \nu_1 < \nu_M), \end{cases}$$

$$|\mathrm{E1}|^2 \approx \begin{cases} \dfrac{2f^2}{\mu^2}F_{1p}(\gamma^2) & (\nu_0 < \nu_1 < \nu_R),\\ \dfrac{2f^2}{\mu^2}\sqrt{\dfrac{\nu_1^2}{\nu_1^2-\nu_0^2}}F_{1p}(\gamma^2)\times(0.6) & (\nu_R < \nu_1 < \nu_M). \end{cases} \qquad (4.13)$$

The imaginary parts of the $b_j$ coming from one-meson, one-nucleon intermediate state are then

$$\begin{aligned}
\operatorname{Im} b_1^M(\nu_1, \nu_2, \nu_3) &= -\left(1+\frac{2\nu_3}{\nu_2}\right) L_1(\nu_1) - 2\nu_2 L_2(\nu_1), \\
\operatorname{Im} b_2^M(\nu_1, \nu_2, \nu_3) &= L_1(\nu_1) + 2\nu_2 L_3(\nu_1), \\
\operatorname{Im} b_3^M(\nu_1, \nu_2, \nu_3) &= \tfrac{1}{2}\nu_1 \operatorname{Im}(b_1^M - b_2^M),
\end{aligned} \tag{4.14}$$

where (using $y \equiv \nu_1/\nu_0$, $g_r^2 = 4M^2 f_r^2/\mu^2 = M^2 f^2/\pi\mu^2 \approx 14$) we have introduced

$$\begin{aligned}
L_1(\nu_1) &= \frac{\nu_0}{4\pi}\sqrt{y^2-1}\, M^2|\mathrm{E1}|^2 + \frac{\nu_0}{2\pi} y \frac{\sqrt{y^2-1}}{\sqrt{y^2 - 4\nu_3/\nu_0^2}} M^2|\mathrm{M3}|^2, \\
L_2(\nu_1) &= \frac{1}{4\pi\nu_0}\frac{\sqrt{y^2-1}}{y^2} - M^2|\mathrm{E1}|^2, \\
L_3(\nu_1) &= \frac{1}{(\nu_0 y)^2} L_1 - L_2.
\end{aligned} \tag{4.15}$$

*5.2.2 Real parts of the $b_j^M$*

We now assume dispersion relations to hold in the invariant $\nu_1$. This statement is a conjecture based on previous work on the real Compton effect [11]). We do not concern ourselves with its range of validity for the virtual Compton effect. We take a cut-off in the range of integration above the experimentally known region. We consider first the unsubtracted dispersion relations and show that the real parts of the $b_j^M$ derived from them do not give the proper Thomson theorem limit ($b_j^M(0, 0, 0) = 0$). Subtracted dispersion relations are then assumed. We are unable to say anything about the subtraction constants thus introduced. This remains an unsolved aspect of the problem.

Unsubtracted dispersion relations

We state (without proof) the following relation:

$$\operatorname{Re} b_{1,2}^M(\nu_1\nu_2\nu_3) = \frac{2}{\pi}\mathrm{P}\int_{\nu_0}^{\nu_M} \frac{x\,\mathrm{d}x}{(x^2-y^2)} \operatorname{Im} b_{1,2}^M(\nu_0\chi, \nu_2\nu_3). \tag{4.16}$$

Then, by (4.14) we have

$$\operatorname{Re} b_3^M(\nu_1, \nu_2, \nu_3) = \tfrac{1}{2}\nu_1 \operatorname{Re}(b_1^M - b_2^M). \tag{4.17}$$

Hence the contribution to $\operatorname{Re} b_j^M$ is

$$\begin{aligned}
\operatorname{Re} b_1^M &= -\left(1+\frac{2\nu_3}{\nu_2}\right) H_1(\nu_1) - 2\nu_2 H_2(\nu_1), \\
\operatorname{Re} b_2^M &= H_1(\nu_1) + 2\nu_2 H_3(\nu_1), \\
\operatorname{Re} b_3^M &= \tfrac{1}{2}\nu_1 \operatorname{Re}(b_1^M - b_2^M),
\end{aligned} \tag{4.18}$$

where

$$H_j(\nu_1) = \frac{2}{\pi} \mathrm{P} \int_{\nu_0}^{\nu_M} \left( \frac{\nu'_1}{\nu'^2_1 - \nu_1^2} \right) L_j(\nu'_1) \mathrm{d}\nu'_1. \tag{4.19}$$

Consider now the *real* proton Compton effect. In our notation, the cross section in the centre-of-mass system is

$$\frac{\mathrm{d}\sigma}{\mathrm{d}\Omega} = \frac{\alpha^2}{2(E+\omega)^2} \Big[ |f_1+\nu_1 f_2|^2 + |f_3+\nu_1 f_4|^2 - \nu_2 \{ |f_1|^2 + |f_3|^2 + \nu_2 |f_2|^2 + \nu_2 |f_4|^2 \} + (\nu_1^2 - \nu_2^2 - \nu_2) |f_6|^2 - \frac{1}{\nu_2} |f_7|^2 \Big], \tag{4.20}$$

where $\omega$ and $E$ are the photon and proton energies respectively. The six form factors are taken at the value $\nu_3 = 0$. In the $1/M$ expansion, we have

$$\frac{\mathrm{d}\sigma}{\mathrm{d}\Omega} = \frac{\alpha^2}{2(E+\omega)^2} [|b_1|^2 + |b_2|^2] + (\text{higher order terms in } 1/M). \tag{4.21}$$

We now add the single-nucleon contribution to Re $b_j^M$ and take the Thomson limit $(\omega \to 0)$:

$$\begin{aligned} \nu_1 &= \frac{1}{2M^2} [E\omega - \omega^2 \cos\theta + E\omega + \omega^2] \to \frac{\omega}{M}, \\ \nu_2 &= \frac{1}{2M^2} [E\omega - \omega^2 \cos\theta - E\omega - \omega^2] \to -\frac{\omega^2}{2M^2} (1+\cos\theta). \end{aligned} \tag{4.22}$$

Then we have

$$b_1 = -[H_1(0)+1] - \frac{2\nu_2}{\nu_1^2} [1], \qquad b_2 = [H_1(0)+1]. \tag{4.23}$$

Therefore using $2\nu_2/\nu_1^2 = -(1+\cos\theta)$, we get

$$\begin{aligned} \frac{\mathrm{d}\sigma}{\mathrm{d}\Omega} &\xrightarrow{\omega \to 0} \frac{\alpha^2}{2M^2} [(1+H_1(0))^2 + (1+H_1(0) + 2\nu_2/\nu_1^2)^2] \\ &= \frac{\alpha^2}{2M^2} [(1+H_1(0))^2 + (H_1(0) - \cos\theta)^2]. \end{aligned} \tag{4.24}$$

The Thomson limit is, however,

$$\frac{\mathrm{d}\sigma}{\mathrm{d}\Omega} = \frac{\alpha^2}{2M^2} (1+\cos^2\theta). \tag{4.25}$$

Since $H_1(0) \neq 0$, the unsubtracted dispersion relations do not give the Thomson limit. We therefore use the subtracted dispersion relations.

## Subtracted Dispersion Relations

We assume one subtraction for $b_{1,2}$ and two subtractions for $b_3$, resulting in

$$\begin{aligned}
&\text{Re } b_{1,2}^{M}(\nu_1, \nu_2, \nu_3) - \text{Re } b_{1,2}^{M}(0, \nu_2, \nu_3) = \frac{2}{\pi} \text{P} \int \frac{\mathrm{d}\nu'_1 \, \nu_1^2}{\nu'_1(\nu_1'^2 - \nu_1^2)} \text{Im } b_{1,2}^{M}(\nu'_1, \nu_2, \nu_3), \\
&\text{Re } b_3^{M}(\nu_1, \nu_2, \nu_3) - \text{Re } b_3^{M}(0, \nu_2, \nu_3) - \nu_1 \text{ Re } b_3^{M'}(0, \nu_2, \nu_3) \qquad (4.26) \\
&\qquad = \frac{2}{\pi} \text{P} \int \frac{\nu_1^3 \, \mathrm{d}\nu'_1}{\nu'_1(\nu_1'^2 - \nu_1^2)} \text{Im } b_3(\nu'_1, \nu_2, \nu_3).
\end{aligned}$$

The behaviour of the $b_j^{\text{S.N.}}$ for $\nu_1 \to \infty$ suggests the additional subtraction for $b_3$. We know in the Thomson limit that Re $b_j^M$ (0, 0, 0) = 0, but we can say nothing about the constants for arbitrary parameters $\nu_2$ and $\nu_3$. Our subsequent treatment assumes that they are not important. To this extent the relation

$$\text{Re } b_3^{M} = \tfrac{1}{2}\nu_1 \text{ Re } (b_1^{M} - b_2^{M}) \qquad (4.27)$$

remains valid.

Then

$$\begin{aligned}
\text{Re } b_1^{M} &= -\left(1 + \frac{2\nu_3}{\nu_2}\right)[y^2 H_1] - 2\nu_2 [y^2 H_2], \\
\text{Re } b_2^{M} &= [y^2 H_1] + 2\nu_2 [y^2 H_3], \qquad (4.28) \\
\text{Re } b_3^{M} &= \tfrac{1}{2}\nu_1 \text{ Re } (b_1^{M} - b_2^{M}),
\end{aligned}$$

where we now redefine

$$H_j(\nu_1) = \frac{2}{\pi} \text{P} \int \frac{\mathrm{d}x}{x(x^2 - y^2)} L_j. \qquad (4.29)$$

These results may be summarized as follows (adding on the single-nucleon contribution):

$$\begin{aligned}
b_1 &= -\left(1 + \frac{2\nu_3}{\nu_2}\right)[F_{1p}(r^2) + y^2 H_1 + iL_1] - \frac{2\nu_2}{\nu_1^2}[F_{1p}(r^2) + y^2 \nu_1^2 H_2 + i\nu_1^2 L_2], \\
b_2 &= [F_{1p}(r^2) + y^2 H_1 + iL_1] + \frac{2\nu_2}{\nu_1^2}[y^2 \nu_1^2 H_3 + i\nu_1^2 L_3], \qquad (4.20) \\
b_3 &= \tfrac{1}{2}\nu_1 (b_1 - b_2).
\end{aligned}$$

Again, the functions $H$ and $L$ contain the form factors $F_{1p}(r^2)$, $F_{2p}(r^2)$, and $F_{2n}(r^2)$. Assuming that these are equal in the range of interest, the form factor becomes a common factor in each of these expressions. Numerical values for $H$ and $L$ are given in fig. 4 for values of $\nu_1$ near the meson production threshold.

At the meson threshold $\nu_1 = 0.161 + \nu_2$ and at the resonance $\nu_1 = 0.317 + \nu_2$. In the spirit of our approximation, we would neglect $\nu_2$ in these relations. However, $L$ and $H$ are sensitive functions of $\nu_1$, therefore, we must use a

definition of $\nu_1$ (as argument of these functions) which yields the value 0.150 at threshold, in accordance with our graphs of $L$ and $H$: we use $\nu_{1M} \equiv (W-M)/$

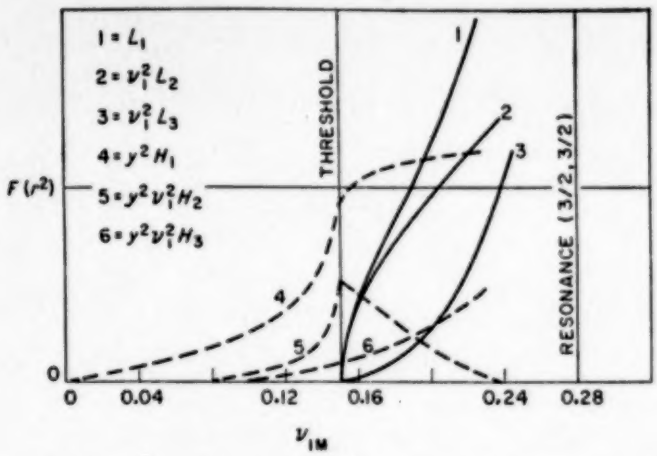


Fig. 4. Contributions of the one-meson, one nucleon-intermediate state. Solid lines show the imaginary contributions to $b_j^M$, dotted lines the real contributions to $b_j^M$.

$M$, where $W$ is the total energy of proton plus photon in the proton-photon centre-of-mass system. (The numerical values of table 1 are obtained with this convention.)

TABLE 1

Calculated cross section (in $10^{-35}$ cm² MeV · sr²)

| $\theta$ | $M^{-1}(W-M)$ | $Y_I$ | $Y_{II}^{S.N.}$ | $Y_{II}^{S.N,M}$ | $Y_{III}^{S.N.}$ | $Y_{III}^{S.N,M}$ |
|---|---|---|---|---|---|---|
| 30° | 0.218 | 634 | −8.7 | −22 | 0.022 | 0.13 |
| 90° | 0.177 | 2.37 | −0.06 | −0.16 | 0.6004 | 0.005 |
| 150° | 0.150 | 0.351 | −0.002 | −0.002 | 0.00004 | 0.0004 |

### 5.3. NEUTRAL PION EXCHANGE CONTRIBUTION

A contribution [12]) to the $f_j$ comes from fig. 3(c). The $\pi^0$ decay matrix element has the form (with $q \to k+r$)

$$\text{M.E.} = \frac{i(2\pi)^4}{(2\pi)^{\frac{3}{2}}\sqrt{8\mu\omega_k\omega_r}} f(r^2=0,\ k^2=0,\ q^2=\mu^2)(\varepsilon^{\mu\nu\alpha\beta} r_\alpha k_\beta)\varepsilon_\mu^{(1)}\varepsilon_\nu^{(2)},$$
$$\frac{1}{\tau_0} = \frac{\mu^3}{16\pi}|f|^2. \tag{4.31}$$

A crude perturbation theory estimate gives $f \approx ge^2/M$. The matrix element of fig. 3(c) is then

$$\bar{U}_2\gamma_5\Gamma(q^2)U_1\varepsilon_{\mu\nu\alpha\beta}r^\alpha k^\beta f(r^2, k^2=0, q^2)\frac{iM}{(2\pi)^2\sqrt{4\omega_r\omega_k E_1 E_2}}. \tag{4.32}$$

Expanding in terms of the set $A$, $B$, $C$, $D$, we find that we have only a contribution for $f_7$,

$$f_7^{(\pi^0)} = \frac{2g\, f(r^2, 0, q^2)\Gamma(q^2)M^3}{e^2(\mu^2 - q^2)}\, \nu_2^2. \tag{4.33}$$

Then, assuming $\tau_0 = 5\times 10^{-17}$ sec, $\Gamma(q^2) \approx 1$ and $f(r^2, 0, q^2) \approx f(0, 0, \mu^2)$, we get

$$|f_7^{(\pi^0)}|^2 \approx \left| \frac{120\nu_2^2}{1 - 180\,(\nu_2 + \nu_3)} \right|^2. \tag{4.34}$$

Although $f_7$ seemingly goes to zero as $\nu_2 \to 0$ (an experimentally possible situation), it will actually give a non-zero effect in this limit in $Y_{III}$ because of the presence of $\nu_2$ in the denominator of the expressions involved. These spurious poles of $\nu_2$ all cancel in the limit.

For these cases of table 1, the $\pi^0$ contribution to $f_7$ is considerably smaller than the $f_7$ of the single nucleon state (about 10 %). In the spirit of our approximation, $f_7$ is to be neglected and therefore we may neglect the $\pi_0$ exchange contribution to $Y_{III}$.

## 6. Numerical Results

We present some numerical results for a hypothetical bremsstrahlung coincidence experiment, in which $\mathrm{d}\sigma/\mathrm{d}\Omega_{p_2}\, \mathrm{d}\Omega_k \mathrm{d}k$ is measured. Let us denote by $\varphi$ the angle between $\mathbf{k}\times\mathbf{p}_1$ and $\mathbf{k}\times\mathbf{p}_2$, by $\theta_0$ the angle between $\mathbf{k}$ and $\mathbf{p}_1$ and by $\theta$ the angle between $\mathbf{k}$ and $\mathbf{p}_2$ (see ref. [7])). Table 1 gives the cross section, using the $1/M$ expansion of sect. 4, in units of $10^{-35}$ cm$^2$/MeV · sr$^2$ for $\varphi = 0$, $\theta_0 = 6°$, and $\theta = 30°$, $90°$, $150°$. The superscript S.N. refers to the single nucleon contribution alone, and the superscript S.N., M refers to the single nucleon and the nucleon plus meson contributions taken together. As indicated before, we assume $F_{1p} = F_{2p} = F_{2n}$ and $F_{1n} = 0$. From the table we see that the nucleon-meson intermediate state has a significant effect on $Y_{II}$ and $Y_{III}$, even at the threshold for pion production (case 3, $\theta = 150^0$).

The $1/M$ approximation must be used with care, since the proton anomalous moment terms from the single nucleon intermediate state may contribute significantly in some cases because of the large value of $\mu_p$ ($\mu_p = 1.79$). The conditions (3.4a), (3.4b) and (3.9) of sect. 4 must be satisfied for our $1/M$ expansion to hold.

## 7. Conclusions

We have presented a calculation of electron-proton bremsstrahlung and pair production in first Born approximation, neglecting radiative corrections to the electron, and taking the proton part of the amplitude as described by a set of two plus twelve form factors. No approximations regarding the size of the masses or recoil were made, so that the results are applicable to other processes,

e.g. muon-proton bremsstrahlung. By assuming that one can make a kinematic expansion in $1/M$, considerable simplification was obtained in the formulae. The contributions to the form factors from the single-nucleon intermediate state (the "pole" of dispersion theory) were treated in generality, making no assumptions about a $1/M$ expansion. The meson-nucleon intermediate state contribution was treated in the $1/M$ approximation. It contributes significantly to the interference and proton parts of the cross section, dominating the single nucleon contribution near and above the meson production threshold.

We wish to thank Professors S. D. Drell, N. Byers and J. D. Walecka for stimulating discussions and comments. We also wish to thank the Western Data Processing Center for the use of their IBM 709 computer.

One of us (CNL) wishes to acknowledge the support of an Eastman Kodak Fellowship during part of this work.

## Appendix 1.

### NOTATION

For the virtual Compton effect, momentum conservation ($r+Q_1 = k+Q_2$) reduces the number of invariants required to three, which we selected as $\nu_1$, $\nu_2$ and $\nu_3$. For the bremsstrahlung process, the electron vertex introduces the vector $S = \frac{1}{2}(p_1+p_2)$, whose projections on the basis $A$, $B$, $C$, $D$ can be expressed in terms of two additional invariants which we select as

$$\nu_4 \equiv \frac{(SA)}{M^2} = \frac{\lambda_1+\lambda_2}{4M^2} = \frac{(kp_1)+(kp_2)}{4M^2}, \qquad \nu_5 = \frac{(SR)}{M^2} = \frac{((p_1+p_2)(Q_1+Q_2))}{4M^4}.$$

The cross section is then a function of these five invariants.

The Bethe-Heitler term $Y_I$ has been given in our previous notation, which we can express in terms of the $\nu$'s as follows:

$$\begin{aligned}
\lambda_1 &\equiv (kp_1) = M^2(2\nu_4-\nu_2), & \mu_1 &\equiv (p_1Q_1) = M^2[\nu_5+\nu_4-\nu_3-\tfrac{1}{2}(\nu_2-\nu_1],\\
\lambda_2 &\equiv (kp_2) = M^2(2\nu_4+\nu_2), & \mu_2 &\equiv (p_2Q_2) = M^2[\nu_5-\nu_4-\nu_3-\tfrac{1}{2}(\nu_2+\nu_1)],\\
\Lambda_1 &\equiv (kQ_1) = M^2(\nu_1+\nu_2), & \mu_3 &\equiv (p_2Q_1) = M^2[\nu_5+\nu_4+\nu_3+\tfrac{1}{2}(\nu_2-\nu_1)],\\
\Lambda_2 &\equiv (kQ_2) = M^2(\nu_1-\nu_2), & \mu_4 &\equiv (p_1Q_2) = M^2[\nu_5-\nu_4+\nu_3+\tfrac{1}{2}(\nu_2+\nu_1)],\\
r^2 &\equiv (p_1-p_2)^2 = 4M^2\nu_3, & q^2 &\equiv (Q_2-Q_1)^2 = 4M^2(\nu_2+\nu_3).
\end{aligned}$$

In addition we have

$$\begin{aligned}
(SD) &= \tfrac{1}{2}\varepsilon_{\alpha\beta\mu\nu}p_1{}^{\alpha}p_2{}^{\beta}Q_1{}^{\mu}Q_2{}^{\nu} = \tfrac{1}{4}M\mathbf{Q}_2^{\text{lab}}\cdot(\mathbf{p}_1\times\mathbf{p}_2)^{\text{lab}},\\
\alpha_2 &\equiv \frac{(SD)^2}{M^2D^2} = \left(\frac{m^2}{M^2}-\nu_3\right)+\frac{M^6}{D^2}[-(\nu_2\nu_5+\nu_1\nu_4)^2\\
&\qquad +4\nu_3(\nu_4{}^2-\nu_1\nu_4\nu_5)-4\nu_3\nu_4{}^2(\nu_2+\nu_3)],\\
D^2 &= M^6[\nu_2{}^2+(\nu_2+\nu_3)(\nu_1{}^2-\nu_2{}^2)] = M^6\nu_2{}^2/\alpha_3.
\end{aligned}$$

## Appendix 2.

### THE TERMS $Y_{II}^{S.N.}$ AND $Y_{III}^{S.N.}$ WITH $\mu_p = 0$

In the single-nucleon intermediate state approximation (with $\mu_p = 0$), we have

$$
\begin{aligned}
Y_{II}^{S.N.} = \frac{M^4 F_1(r^2) F_1(q^2)}{2q^2 r^2} \Bigg[ & \left\{ \left( 2 + \frac{2m^2}{M^2} \right) \frac{q^2+r^2}{M^2} + \frac{8(\mu_1\mu_2+\mu_3\mu_4)}{M^4} \right\} \left\{ \frac{M^2}{\lambda_1} \left( \frac{\mu_1}{\Lambda_1} - \frac{\mu_4}{\Lambda_2} \right) \right. \\
& \left. - \frac{M^2}{\lambda_2} \left( \frac{\mu_3}{\Lambda_1} - \frac{\mu_2}{\Lambda_2} \right) \right\} + \frac{4(\mu_1\mu_2-\mu_3\mu_4)}{M^4} \left( \frac{M^2}{\Lambda_2} - \frac{M^2}{\Lambda_1} + \frac{M^2}{\lambda_2} - \frac{M^2}{\lambda_1} \right) \\
& - 4 \left( \frac{\mu_1\lambda_2\Lambda_2}{M^2\lambda_1\Lambda_1} + \frac{\mu_4\lambda_2\Lambda_1}{M^2\lambda_1\Lambda_2} + \frac{\mu_3\lambda_1\Lambda_2}{M^2\lambda_2\Lambda_1} + \frac{\mu_2\lambda_1\Lambda_1}{M^2\lambda_2\Lambda_2} \right) \\
& + \left( \frac{4\lambda_1\mu_2\mu_3}{M^4\lambda_2} - \frac{4\lambda_2\mu_1\mu_4}{M^4\lambda_1} \right) \left( \frac{M^2}{\Lambda_1} + \frac{M^2}{\Lambda_2} \right) + 4 \left( \frac{\Lambda_1\mu_2\mu_4}{M^4\Lambda_2} - \frac{\Lambda_2\mu_1\mu_3}{M^4\Lambda_1} \right) \left( \frac{M^2}{\lambda_1} + \frac{M^2}{\lambda_2} \right) \\
& - \frac{2(r^2+2m^2)(\Lambda_1+\Lambda_2)}{M^4} \left( \frac{M^2}{\lambda_1} + \frac{M^2}{\lambda_2} \right) - \frac{2(q^2+2M^2)(\lambda_1+\lambda_2)}{M^4} \left( \frac{M^2}{\Lambda_1} + \frac{M^2}{\Lambda_2} \right) \\
& + \frac{2r^2}{M^2} \left( \frac{\mu_2+\mu_3}{\lambda_2} - \frac{\mu_1+\mu_4}{\lambda_1} \right) + \frac{2q^2}{M^2} \left( \frac{\mu_2+\mu_4}{\Lambda_2} - \frac{\mu_1+\mu_3}{\Lambda_1} \right) \\
& + \frac{4}{M^2} (\mu_1+\mu_2+\mu_3+\mu_4) \left\{ 3 + \frac{M^2}{\Lambda_1} - \frac{M^2}{\Lambda_2} + \frac{m^2}{\lambda_1} - \frac{m^2}{\lambda_2} \right\} \Bigg],
\end{aligned}
$$

$$
\begin{aligned}
Y_{III}^{S.N.} = \frac{M^4 F_1^2(r^2)}{2r^4} \Bigg[ & \left( \frac{r^2+4m^2}{2M^2} \right) \left( - \frac{2\Lambda_1}{\Lambda_2} - \frac{2\Lambda_2}{\Lambda_1} - \frac{M^2 r^2}{\Lambda_1^2} - \frac{M^2 r^2}{\Lambda_2^2} - \frac{r^2 q^2}{\Lambda_1 \Lambda_2} \right) \\
& - 2 \left( \frac{\mu_1+\mu_3}{\Lambda_2} - \frac{\mu_2+\mu_4}{\Lambda_1} \right)^2 - \frac{r^2}{M^2} \left( \frac{(\mu_1+\mu_3)^2+(\mu_2+\mu_4)^2}{\Lambda_1\Lambda_2} \right) \\
& + \frac{4m^2 r^2}{\Lambda_1\Lambda_2} \left( 1 - \frac{r^2}{4m^2} \right) + \frac{r^2}{M^2} \left\{ \left( \frac{4M^2}{\Lambda_1} - \frac{4M^2}{\Lambda_2} \right) - 2 \left( \frac{M^2}{\Lambda_1} - \frac{M^2}{\Lambda_2} \right)^2 \right\} \Bigg].
\end{aligned}
$$

The usefulness of taking the magnetic moment as zero is discussed in subsect. 5.1. The invariants are defined in Appendix 1. This differs from our previous result [1]) in that no approximation regarding the static limit is made here. Similar results have been obtained elsewhere [7]).

## References


1) R. A. Berg and C. N. Lindner, Phys. Rev. **112** (1958) 2072
2) R. E. Prange, Phys. Rev. **110** (1958) 240
3) J. M. Jauch and F. Rohrlich, Theory of Photons and Electrons (Addison-Wesley, Reading, Mass,, 1955) p. 161

4) Bethe, Schweber and de Hoffmann, Mesons and Fields (Row-Peterson, Evanston, 1955) Vol. I, p. 364
5) J. D. Bjorken, S. D. Drell and S. C. Frautschi, Phys. Rev. **112** (1958) 1409
6) J. D. Walecka, Stanford Institute of Theoretical Physics Tech. Note, no. 8 (1959)
7) P. S. Isaev and I. S. Zlatev, Nuclear Physics **16** (1960) 608
8) G. Chew, Y. Nambu, F. Low and M. Goldberger, Phys. Rev. **106** (1957) 1345
9) S. Fubini, Y. Nambu and V. Wataghin, Phys. Rev. **111** (1958) 329
10) R. H. Dalitz and D. R. Yennie, Phys. Rev. **105** (1957) 1598
11) L. I. Lapidus and Chou Kuang-Chao, JETP **10** (1960) 1213
12) M. Jacob and J. Matthews, Phys. Rev. **117** (1960) 854

8.A

*Nuclear Physics* **26** (1961) 280—285; © *North-Holland Publishing Co., Amsterdam*

Not to be reproduced by photoprint or microfilm without written permission from the publisher

# RELATIVE MEASUREMENTS ON THE LONGITUDINAL POLARIZATION OF BETA RAYS FROM $Na^{24}$, $Mn^{56}$, $Sb^{122}$, $Ho^{166}$ AND $Au^{198}$

R. SOSNOWSKI, Z. WILHELMI and J. WOJTKOWSKA †

*Institute of Nuclear Research, Polish Academy of Sciences, Warsaw*

Received 7 February 1961

**Abstract:** The longitudinal polarization of electrons from $\beta$-decay of $Na^{24}$, $Mn^{56}$, $Sb^{122}$, $Ho^{166}$ and $Au^{198}$ was compared. The degree of polarization was measured by the asymmetry in the electron scattering in a thin gold foil. Longitudinal electron polarization was changed into transverse polarization by means of crossed electric and magnetic fields. The measurements were carried out for the electrons with $v/c = 0.85$. The results for the asymmetry are as follows:
$11.0\pm0.9$ % ($Na^{24}$), $11.1\pm0.8$ % ($Mn^{56}$), $10.1\pm0.3$ % ($Sb^{122}$), $10.4\pm0.2$ % ($Ho^{166}$) and $9.3\pm0.3$ % ($Au^{198}$). The results suggest that the longitudinal polarization is not identical for the measured beta transitions.

The measurements made so far on the longitudinal electron polarization from a beta-decay are in general consistent with the assertion that the polarization is equal to $-v/c$ (see e.g. ref. [1])), which has been predicted from the present approved theory of weak interactions [2, 3]). The accuracy of these measurements is not greater than a few per cent and the possibility of introducing systematic errors makes it difficult to compare the results obtained by various authors. Therefore measurements carried out in similar conditions for a greater number of isotopes are particularly valuable. The results by A. J. Alikhanov *et al.* [4]), R. E. Spivak and L. A. Mikaelian [5]) and J. S. Geiger *et al.* [6]) should be specially mentioned here. In the first of the above experiments it was found that the longitudinal electron polarization (from $Sr^{90}+Y^{90}$, $Tm^{170}$, $Sm^{153}$, $Lu^{177}$, $Re^{186}$ and $Au^{198}$) was independent of the emitting nucleus and was equal to $-v/c$. Results obtained by R. E. Spivak and L. A. Mikaelian showed that for some isotopes, particularly for those with a higher atomic number, the departure of the polarization from $-v/c$ could be as large as 10 %. The results of J. S. Geiger *et al.*, although not so significant, seem to indicate the same.

The work reported here was undertaken to compare the electron polarization from $Na^{24}$, $Mn^{56}$, $Sb^{122}$, $Ho^{166}$ and $Au^{198}$ in as far as possible identical experimental conditions. The choice of isotopes of highly different atomic numbers was aimed at correlating any departure of the polarization from $-v/c$ with the value of $Z$ or $A$.

† This work was presented at a nuclear physics conference in Balatonõsod, Hungary, September, 1960.

The polarization was measured by determining the asymmetry in the electron scattering in a thin gold foil. Since such polarization analyzer is sensitive only

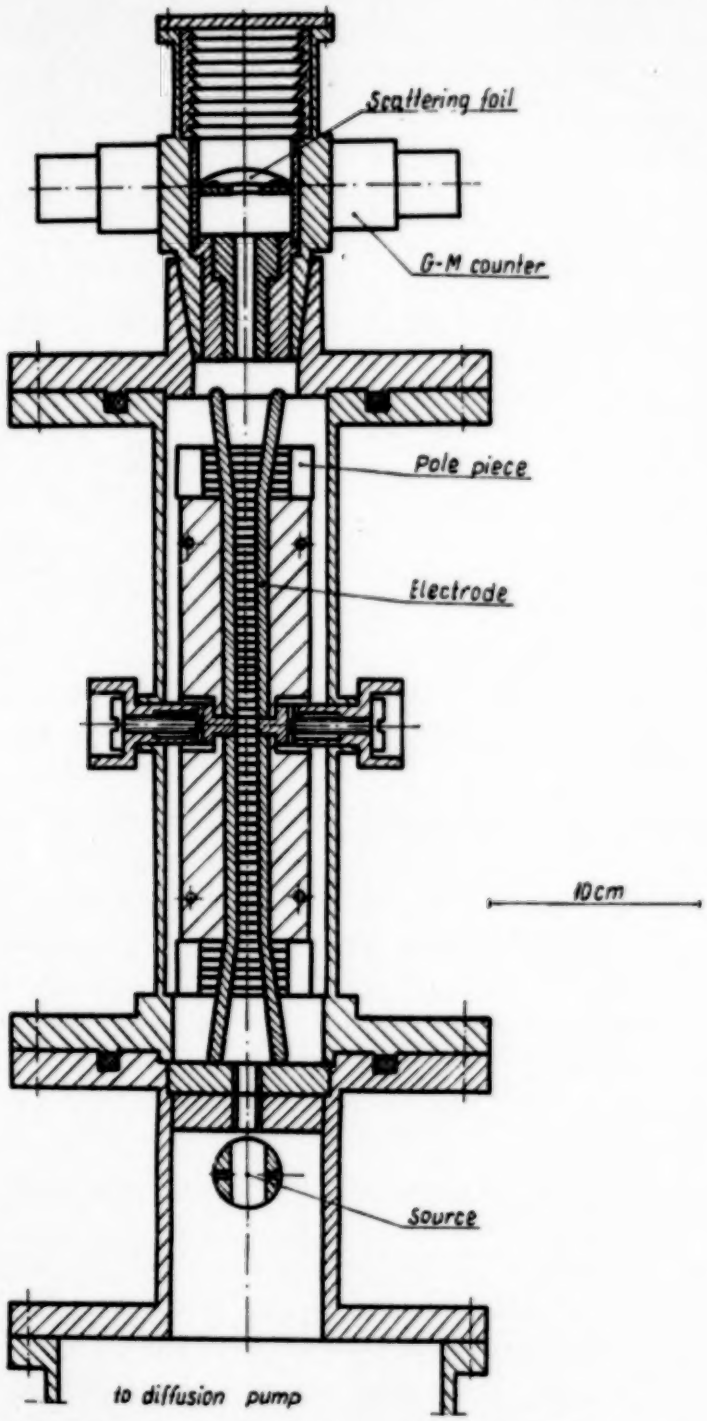


Fig. 1. Cross-section of the apparatus.

to the transverse polarization, the longitudinal electron polarization was transformed into the transverse one by means of crossed magnetic and electric fields. Fig. 1 is a cross section of the apparatus. The electron beam striking the scatter-

er was collimated by two collimators. One of them was placed directly above the source and cut off the electrons scattered by the walls of the apparatus close to the source. The results obtained with a point source of $Ho^{166}$ indicated that the background due to these electrons was $0.001 \pm 0.002$ of the activity of the source. The beam collimated by the first collimator was passed through an area limited by electrodes and pole shoes of an electromagnet. The electrodes were transversely grooved and covered with an aluminium foil 3 mg/cm² thick, to reduce electron scattering. Similarly, the surface of the pole shoes was covered with a layer of lucite transversely grooves.

The crossed fields used for changing the type of polarization simultaneously selected the electrons of a given velocity. For all the isotopes the measurements of the asymmetry of the electron scattering were made for electrons whose velocities were equal to $v/c = 0.85 \pm 0.09$. The edge effect of the magnetic field was taken into consideration by using specially formed electrodes. This made it possible to maintain a constant ratio of fields along the axis of the apparatus.

As a polarization analyzer a gold foil 1 mg/cm² thick was used. It was inclined at 60° to the beam axis. The inside walls of the apparatus in the vicinity of the foil were covered by a layer of lucite which was grooved in such a way that it absorbed effectively the scattered electrons as well as the secondary electrons produced by gamma radiation. The electrons scattered at 90° were registered by means of G. M. counters in coincidence. These counters and the gold foil itself could be rotated round the beam axis. The measurement of the asymmetry consisted in determining the intensity of electron scattering in two directions perpendicular to the plane defined by the beam axis and the direction of the transverse polarization. The number of scattered electrons was obtained from the counting rate with the scatterer in and with the scatterer out. The number of secondary electrons knocked out from the thin gold foil at 90° to the beam direction was negligible and therefore the intensity of scattering could be obtained from the difference in the counting rates with the scatterer in and with the scatterer out.

The thickness of all the sources used in this experiment was 1 mg/cm² within 15 % accuracy, their surface was $1 \times 2$ cm². They were placed between two aluminium foils 1.4 mg/cm² thick. The active sources of $Na^{24}$, $Mn^{56}$, $Sb^{122}$ and $Au^{198}$ were obtained by activating the layers of NaCl and metal manganese, antimony and gold evaporated onto aluminium foil in the neutron beam of $10^{13}/\text{cm}^2 \cdot \text{sec}$. A thin layer of holmium was prepared by quick evaporation of holmium chloride onto an Al foil. The activities for the individual sources varied from 5 mCur for $Na^{24}$ to 30 mCur for $Au^{198}$. In spite of these great differences the counting rates for all the sources were approximately identical (within a factor 2), because the background due to the secondary electrons was much higher for the less active sources ($Na^{24}$ and $Mn^{56}$).

In table 1 the results are summarized together with the characteristic data for $\beta$-transitions under consideration.

TABLE 1

Experimental results

| Isotope | Type of transition | $E_{max}$ (keV) | $E_{max}$ mean (keV) | Asymmetry (%) |
|---|---|---|---|---|
| $Na^{24}_{11}$ | $4^+ \rightarrow 4^+$ | 1400 | 1400 | 11.0±0.9 |
| $Mn^{56}_{25}$ | $3^+ \rightarrow 2^+$<br>$3^+ \rightarrow 2^+$<br>$3^+ \rightarrow 2^+$ | 2860 (50 %)<br>1050 (30 %)<br>700 (20 %) | 1890 | 11.1±0.8 |
| $Sb^{122}_{51}$ | $2^- \rightarrow 0^+$<br>$2^- \rightarrow 2^+$ | 1970 (30 %)<br>1400 (63 %) | 1570 | 10.1±0.3 |
| $Ho^{166}_{67}$ | $0^- \rightarrow 2^+$<br>$0^- \rightarrow 0^+$ | 1854 (52 %)<br>1744 (47 %) | 1800 | 10.4±0.2 |
| $Au^{198}_{79}$ | $2^- \rightarrow 0^+$ | 960 | 960 | 9.3±0.3 |

Although identical conditions of measurement were aimed at, there were several factors which may have influenced the results and consequently may have been different for various isotopes. The following are the most important ones:

1) the shape of the beta spectrum (maximum energy),
2) gamma spectrum associated with beta transitions,
3) the material of the source,
4) the activity of the source.

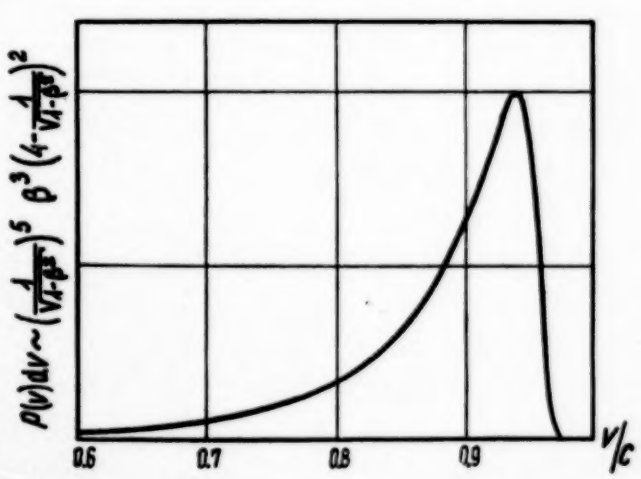


Fig. 2. Beta spectrum shape in the velocity distribution for $E_{max} = 1500$ keV.

The effect of the first factor cannot be very essential. The shape of the beta spectrum in the velocity distribution is shown in fig. 2. For all the isotopes under investigation the point representing $v/c = 0.85$ was on the rising part of

the curve. Therefore the spectrum of the electrons striking the scatterer should be similar in spite of low resolution. In order to check this conclusion one has to prove whether or not the measured asymmetry depends on energy. One can expect that for the transitions of higher energy the asymmetry in the scattering at 90° will be smaller [7]). Fig. 3 shows something rather to the contrary. It may be, therefore, concluded that the differences in the asymmetries obtained cannot be caused by the difference in the beta spectra.

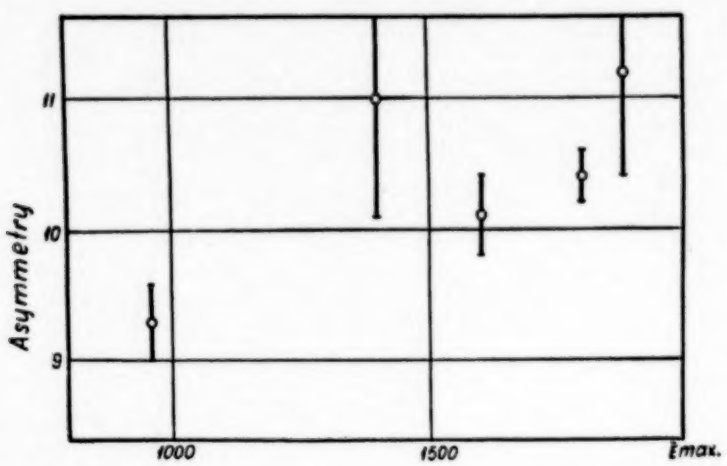


Fig. 3. The asymmetry dependence on the mean maximum energy.

The effect from gamma radiation was taken into account by measuring the background from each source, i.e. the counting rate with the gold foil taken away. In a separate measurement with an NaCl source and electrons deflected by electric and magnetic fields acting in the same direction it was found that the introduction of the gold foil did not change the number of secondary electrons reaching the counters.

All the sources used were approximately 1 mg/cm$^2$ thick. If the depolarization effect in the source were proportional to thickness, its contribution to each source would be identical. However, if this assumption were not valid, it would follow from refs. [5, 8]) that the depolarization in 1 mg/cm$^2$ sources was small and the differences in the depolarization were of a higher order.

As was mentioned, the activities of the sources were different. If these differences had caused differences in the counting rates, the results would have been connected with the error due to the dead-time of the counters. The weaker sources, however, had a much higher gamma background and the counting rates were not very much different from source to source. Dead-time corrections had to be introduced only for $Au^{198}$.

It follows that unless the results obtained have a systematic error, they will indicate that the electron polarization is not constant for all the isotopes. For the hypothesis that the polarization is constant the $\chi^2$-parameter takes on a

value 12.37. For $\alpha = 0.02$ this hypothesis should be discarded. In assuming, e.g., a linear decrease in polarization with $Z$, for $P = 1 - 0.002 \times Z$ determined by the least-square method, we obtain $\chi^2 = 5.85$. Therefore, this hypothesis is much more probable and cannot be discarded even for $\alpha = 0.05$.

## References

1) J. Smorodinski, U.F.N. **67** (1959) 43
2) R. P. Feynman and H. Gell-Mann, Phys. Rev. **109** (1958) 193
3) E. C. Sudarshan and R. E. Marshak, Phys. Rev. **109** (1958) 1860
4) A. J. Alikhanov et al., Nuclear Physics **7** (1958) 655
5) L. A. Mikaelian and P. E. Spivak, JETP **37** (1959) 1168, **39** (1960) 574
6) J. S. Geiger *et al.*, Phys. Rev. **112** (1958) 1684
7) N. Sherman, Phys. Rev. **103** (1956) 1601
8) H. De Wáard *et al.*, Proc. Rehovoth Conf. Nucl. Structure (1958) p. 388

1.C

*Nuclear Physics* **26** (1961) 286—305; © *North-Holland Publishing Co., Amsterdam*

Not to be reproduced by photoprint or microfilm without written permission from the publisher

# GENERALIZED SELF-CONSISTENT-FIELD AND RANDOM-PHASE APPROXIMATIONS FOR MULTI-PHASE SYSTEMS

D. E. McCUMBER †

*Institute for Theoretical Physics, University of Copenhagen, Denmark*

Received 1 March 1961

**Abstract:** A formalism is presented which provides a basis for a rigorous unified quantal treatment of an extensive class of thermodynamic multi-phase many-particle systems. The thermodynamic phases considered are those associated with special spectral forms of the particle density operator, a type of hole-particle pairing operator. Fundamental to the formalism is the recognition that in self-bound systems characterized by a single "cluster", especially those whose position is not localized by external forces, the relevant particle density is that measured relative to the centre of mass. From a consistency requirement, derived equivalently from a generalized Hartree self-consistent-field approximation or from a type of random-phase approximation, an intrinsically non-linear integral equation is obtained whose solutions define a static background potential characteristic of the various phases.

## 1. Introduction

Attempting to derive the quantitative statistical properties of multi-phase many-particle systems from first principles, one soon discovers that mathematical techniques appropriate to a weakly correlated phase fail when they are applied to phases which exhibit strong correlations. As a consequence of this not unreasonable result, which is related to certain momentum transfer properties, the derivation of a single unified scheme for the treatment of multi-phase systems has remained a major problem in spite of recent advances made in the quantal treatment of other features of many-particle systems ††. In this work we discuss a formalism, based upon the special spectral characteristics of a hole-particle pairing operator, which provides a convenient basis for a unified discussion of the desired type.

Multi-phase classical systems have been discussed extensively in the literature. Most treatments are based upon the analysis of the (non-quantal) partition function for the canonical or grand canonical ensemble and in some cases upon various density correlation functions †††. When the container enclosing the many-particle system is uniformly occupied by a single-thermodynamic

† National Science Foundation Postdoctoral Fellow.

†† For a detailed discussion of one approach with references to prior developments see ref. [1]).

††† See ref. [2]) and the review article of ref. [3]).

phase, these methods — and their quantal analogues — yield accurate estimates of the bulk properties of the thermodynamic phase. The various approximation schemes, which can be elaborately extended by including more and more "diagrams", fail when two or more phases exist simultaneously or when the many-particle system through "condensation" or "self-binding" occupies only a fraction of the available volume. While it is practical in some instances to analyse system properties by means of "Monte-Carlo" numerical techniques [4]), it is clearly desirable to have a formalism which permits a systematic functional analysis. In the present work we recognize that a suitable formalism can be developed for self-bound systems characterized by a single "cluster" if one observes that the relevant particle density is not that obtained by averaging over the whole volume but is rather that measured relative to the centre of mass. That the centre of mass (operator) — and an axis orientation operator in non-spherically-symmetric systems — plays a fundamental role in the description of self-bound systems is the essential feature upon which the present work is based.

Statistical approaches based upon the grand canonical ensemble through the partition function

$$Z(\alpha, \beta) \equiv e^{-W(\alpha, \beta)} \equiv \mathrm{Tr}\ (e^{-\alpha N - \beta H}) = \sum_N \sum_E e^{-\alpha N} e^{-\beta E}\ \mathrm{Tr}\ (P_N P_E) \quad (1.1a)$$

and the weighted expectation value

$$\langle \mathcal{O} \rangle \equiv e^{+W(\alpha, \beta)}\ \mathrm{Tr}\ (e^{-\alpha N - \beta H} \mathcal{O}) \quad (1.1b)$$

are subject to two basic instabilities, one having its origin in the physics of the situation and the other in the mathematical approximations employed. Although we are primarily interested in the latter class of instabilities, it is important to have a qualitative understanding of the physical instabilities. In this regard we observe that the functions (1.1) strictly converge only in the half planes

$$\mathrm{Re}\ \beta > 0, \qquad \mathrm{Re}\ \alpha > \mathrm{Re}\ \alpha_0, \quad (1.2a)$$

where

$$\alpha_0 = -\beta \liminf_{N \to \infty} \left\{ \frac{\mathrm{Tr}\ (P_N H)}{N\ \mathrm{Tr}\ (P_N)} \right\}. \quad (1.2b)$$

The long-range attractive two-particle interactions in $H$ generate a negative contribution to $\mathrm{Tr}(P_N H)$ of order $N^2$. Taken by itself, this would destroy the convergence of (1.1). In most discussions of the grand ensemble in the literature it is assumed that $\alpha_0$ remains finite as a consequence, say, of F-D statistics or of short-range volume exclusion effects. In general such arguments are either inaccurate or irrelevant. The usual mathematical techniques employed in treating the functions (1.1) are insensitive to the very-large-$N$ components.

As a consequence, it is sufficient for all practical purposes to demand only that representations of the functions (1.1), as power series in the fugacity $e^{-\alpha}$, converge asymptotically for the $N$-region of interest. Systems for which this is the case we shall call *physically stable*, irrespective of the very-large-$N$ dependence of the ratio (1.2b). We shall say that systems are *physically unstable* if divergencies predicted in the range of physical interest are not inhibited or if their inhibitions arise from pathological phenomena well beyond the $N$-region of interest. In order that a system be physically stable it is of course necessary that attractive $N^2$-effects saturate to a linear dependence upon $N$ as a consequence of repulsive interactions, of local lessening of the attractions, or of F-D statistical effects. However, we wish to emphasize that such saturation is physically meaningful only if it occurs for reasonable values of $N$ and further that formal convergence imposed by pathological very-short-range repulsions is not strictly necessary.

These remarks also indicate the origin of an important class of mathematical instabilities associated with the grand ensemble: if the approximations utilized in the treatment of physically stable systems having long-range attractive forces are such that the saturation-producing forces are not included in the proper proportion, the resulting approximate forms of (1.1) will exhibit non-physical singularities.

When the system under discussion displays several different phases, the functions (1.1) belonging to a large but finite system exhibit nearly singular behaviour at those $(\alpha, \beta)$ values appropriate to the phase transition points. To a rather high degree of accuracy those functions may be approximated in each phaseregion by different analytic forms. It is clear that the approximations appropriate to a particular phase region may be quite different from those appropriate to another region. Unfortunately, it is also true that from the forms appropriate to one phase it is difficult even to infer what a suitable approximation for treating an adjacent phase might be. It is the purpose of the present work to present a single unified formalism which is appropriate to the separate thermodynamic phases generated from long-range forces. Underlying the final results is a non-linear integral equation whose stable solutions (for physically stable systems) in the various phase regions characterize the particle density relative to the system centre of mass and form the basis for the treatment of the separate phases. The formalism displays in a natural manner the analytic segmentation noted above.

In this work we shall restrict our considerations to the bulk properties of a multi-particle system composed of a single type of particle confined within an arbitrarily large volume $V$. Although in the limit $V \to \infty$ such bulk properties do not depend upon the boundary conditions, we assume for simplicity that the system is confined to a rectangular box on the surface of which periodic boundary conditions obtain. We further assume that the system is governed

by the Hamiltonian, number-conserving but spatially variant (through the single-particle potential $u(\mathbf{k})$),

$$H = \sum_{\mathbf{p}} \varepsilon_{\mathbf{p}} \psi_{\mathbf{p}}^{\dagger} \psi_{\mathbf{p}} + \sum_{\mathbf{k}} u(\mathbf{k}) \sum_{\mathbf{p}} \psi_{\mathbf{p}+\frac{1}{2}\mathbf{k}}^{\dagger} \psi_{\mathbf{p}-\frac{1}{2}\mathbf{k}} + \tfrac{1}{2} \sum_{\mathbf{k}} v(\mathbf{k}) \sum_{\mathbf{p}} \sum_{\mathbf{p}'} \psi_{\mathbf{p}+\frac{1}{2}\mathbf{k}}^{\dagger} \psi_{\mathbf{p}'-\frac{1}{2}\mathbf{k}}^{\dagger} \psi_{\mathbf{p}'+\frac{1}{2}\mathbf{k}} \psi_{\mathbf{p}-\frac{1}{2}\mathbf{k}}, \tag{1.3}$$

where $\psi$ and $\psi^{\dagger}$ are annihilation and creation fields satisfying the usual B-E or F-D commutation relations and $\varepsilon_{\mathbf{p}} = p^2/2m$. If we define

$$\rho_{\mathbf{p}}{}^{\mathbf{k}}(t) \equiv \psi_{\mathbf{p}-\frac{1}{2}\mathbf{k}}^{\dagger}(t) \psi_{\mathbf{p}+\frac{1}{2}\mathbf{k}}(t) = (\rho_{\mathbf{p}}{}^{-\mathbf{k}}(t))^{\dagger},$$

$$\rho^{\mathbf{k}}(t) \equiv \sum_{\mathbf{p}} \rho_{\mathbf{p}}{}^{\mathbf{k}}(t) = \int d\tau\, e^{-i\mathbf{k}\cdot\mathbf{r}} \rho(\mathbf{r}, t) = \int d\tau\, e^{-i\mathbf{k}\cdot\mathbf{r}} \psi^{\dagger}(\mathbf{r}, t) \psi(\mathbf{r}, t),$$

then by straightforward application of the commutation relations we obtain the following equations of motion ($\hbar = 1$):

$$i \frac{\partial}{\partial t} \psi_{\mathbf{p}} = \varepsilon_{\mathbf{p}} \psi_{\mathbf{p}} + \sum_{\mathbf{k}} \{u(\mathbf{k}) + \tfrac{1}{2}[v(\mathbf{k}) + v(-\mathbf{k})] \rho^{\mathbf{k}}\} \psi_{\mathbf{p}-\mathbf{k}}, \tag{1.4a}$$

$$-i \frac{\partial}{\partial t} \psi_{\mathbf{p}}^{\dagger} = \varepsilon_{\mathbf{p}} \psi_{\mathbf{p}}^{\dagger} + \sum_{\mathbf{k}} \psi_{\mathbf{p}+\mathbf{k}}^{\dagger} \{u(\mathbf{k}) + \tfrac{1}{2}[v(\mathbf{k}) + v(-\mathbf{k})] \rho^{\mathbf{k}}\}, \tag{1.4b}$$

$$\begin{aligned} i \frac{\partial}{\partial t} \rho_{\mathbf{p}}{}^{\mathbf{k}} = {} & (\varepsilon_{\mathbf{p}+\frac{1}{2}\mathbf{k}} - \varepsilon_{\mathbf{p}-\frac{1}{2}\mathbf{k}}) \rho_{\mathbf{p}}{}^{\mathbf{k}} + \sum_{\mathbf{k}''} u(\mathbf{k}'') [\rho_{\mathbf{p}-\frac{1}{2}\mathbf{k}''}^{\mathbf{k}-\mathbf{k}''} - \rho_{\mathbf{p}+\frac{1}{2}\mathbf{k}''}^{\mathbf{k}-\mathbf{k}''}] \\ & + \sum_{\mathbf{k}''} \tfrac{1}{2}[v(\mathbf{k}) + v(-\mathbf{k})] \sum_{\mathbf{p}''} \psi_{\mathbf{p}''-\frac{1}{2}\mathbf{k}''}^{\dagger} [\rho_{\mathbf{p}-\frac{1}{2}\mathbf{k}''}^{\mathbf{k}-\mathbf{k}''} - \rho_{\mathbf{p}+\frac{1}{2}\mathbf{k}''}^{\mathbf{k}-\mathbf{k}''}] \psi_{\mathbf{p}''+\frac{1}{2}\mathbf{k}''}. \end{aligned} \tag{1.5}$$

For simplicity we assume in what follows that the interaction is sufficiently regular, so that $t$-matrix techniques are not necessary and that the dominant effects are of the long-range "polarization" type such as are commonly associated with the random-phase approximation.

In the following section we discuss the closely related Hartree self-consistent-field (SCFA) and random-phase (RPA) approximations which are appropriate respectively to equations (1.4) and (1.5) in the low-density weak-interaction limit. We there observe that the RPA is equivalent to the introduction of an effective Hamiltonian whose non-Hermitian character is ultimately responsible for the instability of the approximations as the system changes phase. Noting a limited parallel between this behaviour and that which occurs in the superconductor, we introduce in the third section physically important hole-particle "pairing" operators whose dominant zero-frequency components we utilize in the following section to extract those important components of an expectation value which were excluded from the ordinary SCFA and RPA through an over-simplified treatment of momentum properties. The generalized approximations which we obtain are characterized by a static collective back-

ground deriving from the time-independent component of the particle density measured relative to the centre of mass. The different thermodynamic phases are identified by the different admissible forms of the collective background.

In the fifth section we demonstrate that the generalized RPA conserves particle number and has the appropriate momentum conservation properties. In the sixth section we note an important relationship that exists between the generalized approximations of the fourth section and certain external-field forms of the usual SCFA and RPA, forms which have been frequently utilized by other authors in computing properties of self-bound systems.

In a final section we consider self-consistency criteria imposed by our previous assumptions. For physically stable systems the resulting intrinsically non-linear integral equations determine the parameters characteristic of the static background configurations and hence of the thermodynamic phase.

## 2. Self-Consistent-Field and Random-Phase Approximations

If one uses eqs. (1.4) and (1.5) to study, for example, the frequency spectra of the retarded commutators †

$$G_1(\mathbf{p}, \mathbf{p}'; t, t')_0 \equiv (-i)\langle[\psi_{\mathbf{p}}(t), \psi^{\dagger}_{\mathbf{p}'}(t')]_{\mp}\rangle\theta(t-t'), \tag{2.1}$$

$$\mathscr{D}(\mathbf{k}, \mathbf{p}; \mathbf{k}'; t-t')_0 \equiv (-i)\langle[\rho_{\mathbf{p}}{}^{\mathbf{k}}(t), \rho^{-\mathbf{k}'}(t')]\rangle\theta(t-t'), \tag{2.2}$$

where $\langle \ldots \rangle$ is defined in eqs. (1.1), one finds

$$\begin{aligned}\omega G_1(\mathbf{p}, \mathbf{p}'; \omega)_0 = \delta(\mathbf{p}, \mathbf{p}') + \varepsilon_{\mathbf{p}} G_1(\mathbf{p}, \mathbf{p}'; \omega)_0 + \sum_{\mathbf{k}} u(\mathbf{k}) G_1(\mathbf{p}-\mathbf{k}, \mathbf{p}'; \omega)_0 \\ + \sum_{\mathbf{k}} w(\mathbf{k})\{(-i)\langle[\rho^{\mathbf{k}}\psi_{\mathbf{p}-\mathbf{k}}(t), \psi^{\dagger}_{\mathbf{p}'}(t')]_{\mp}\rangle\}(\omega)_0;\end{aligned} \tag{2.3}$$

$$\begin{aligned}\omega\mathscr{D}(\mathbf{k}, \mathbf{p}; \mathbf{k}'; \omega)_0 = IH + \Delta^{\mathbf{k}}\varepsilon_{\mathbf{p}}\mathscr{D}(\mathbf{k}, \mathbf{p}; \mathbf{k}'; \omega)_0 \\ + \sum_{\mathbf{k}''} u(\mathbf{k}'')[\mathscr{D}(\mathbf{k}-\mathbf{k}'', \mathbf{p}-\tfrac{1}{2}\mathbf{k}''; \mathbf{k}'; \omega_0 - \mathscr{D}(\mathbf{k}-\mathbf{k}'', \mathbf{p}+\tfrac{1}{2}\mathbf{k}''; \mathbf{k}'; \omega)_0] \\ + \sum_{\mathbf{k}''} w(\mathbf{k}'') \sum_{\mathbf{p}''} \{(-i)\langle[\psi^{\dagger}_{\mathbf{p}''-\frac{1}{2}\mathbf{k}''}(\rho^{\mathbf{k}-\mathbf{k}''}_{\mathbf{p}-\frac{1}{2}\mathbf{k}''} - \rho^{\mathbf{k}-\mathbf{k}''}_{\mathbf{p}+\frac{1}{2}\mathbf{k}''})\psi_{\mathbf{p}''+\frac{1}{2}\mathbf{k}''}(t), \rho^{-\mathbf{k}'}(t')]\rangle\}(\omega)_0.\end{aligned} \tag{2.4}$$

For simplicity in notation we have introduced

$$\Delta^{\mathbf{k}}\varepsilon_{\mathbf{p}} \equiv \varepsilon_{\mathbf{p}+\frac{1}{2}\mathbf{k}} - \varepsilon_{\mathbf{p}-\frac{1}{2}\mathbf{k}}, \qquad w(\mathbf{k}) \equiv \tfrac{1}{2}[v(\mathbf{k}) + v(-\mathbf{k})],$$

and we have represented the $\omega$-independent inhomogeneous terms of (2.4) simply by IH. If we assume that the last functions on the right-hand side of (2.3) and (2.4) may be factored by means of a suitable many-particle analogue of Wick's theorem [1]) into a sum of products of a simple expectation value times the

† For a brief discussion of spectral representation and of the special importance of retarded commutators of the type (2.1) with their relation to time-ordered functions see ref. [8]).

Green's function appearing on the left-hand side of each equation, we obtain, to within correlation effects of order $v$,

$$\omega G_1(\mathbf{p}, \mathbf{p}'; \omega)_0 = \delta(\mathbf{p}, \mathbf{p}') + \varepsilon_{\mathbf{p}} G_1(\mathbf{p}, \mathbf{p}'; \omega)_0 + \sum_{\mathbf{k}''} \{u(\mathbf{k}'') + w(\mathbf{k}'')\langle \rho^{\mathbf{k}''}\rangle\} G_1(\mathbf{p}-\mathbf{k}'', \mathbf{p}'; \omega)_0, \quad (2.5)$$

$$\begin{aligned}(\omega - \Delta^{\mathbf{k}}\Sigma_{\mathbf{p}})\mathscr{D}(\mathbf{k}, \mathbf{p}; k'; \omega)_0 &= IH + \sum_{\mathbf{k}''} \{u(\mathbf{k}'') + w(\mathbf{k}'')\langle \rho^{\mathbf{k}''}\rangle\} \\ &\times [\mathscr{D}(\mathbf{k}-\mathbf{k}'', \mathbf{p}-\tfrac{1}{2}\mathbf{k}''; \mathbf{k}'; \omega)_0 - \mathscr{D}(\mathbf{k}-\mathbf{k}'', \mathbf{p}+\tfrac{1}{2}\mathbf{k}''; \mathbf{k}'; \omega)_0] \quad (2.6) \\ &+ \sum_{\mathbf{k}''} w(\mathbf{k}'')\langle \rho_{\mathbf{p}-\frac{1}{2}\mathbf{k}''}^{\mathbf{k}-\mathbf{k}''} - \rho_{\mathbf{p}+\frac{1}{2}\mathbf{k}''}^{\mathbf{k}-\mathbf{k}''}\rangle \sum_{\mathbf{p}''} \mathscr{D}(\mathbf{k}'', \mathbf{p}''; \mathbf{k}'; \omega)_0.\end{aligned}$$

In writing these equations, we have for simplicity neglected exchange terms which enter by virtue of the double sum $(\mathbf{k}, \mathbf{p}'')$ in (2.3), (2.4). If the interaction is of sufficiently long range, the exchange contributions are small and, if desired, one can often approximate their short-range contributions by a change in $w(\mathbf{k})$. [The difference between the direct and exchange terms arises mathematically from the fact that the $\mathbf{p}''$-sum in (2.5) and (2.6) is unweighted while the equivalent exchange summation would be weighted by $w(\mathbf{p}'')$. If $v$ is long range, a $w(\mathbf{p}'')$ weighting eliminates all but relatively few terms from the sum.] Equation (2.5) will be recognized as the SCFA and (2.6) as the RPA †.

With respect to the limits of applicability of (2.5) and (2.6), let us note that (2.6) corresponds in essence to the replacement of (1.5) by

$$\begin{aligned}[\rho_{\mathbf{p}}^{\mathbf{k}}, H_{\mathrm{eff}}] &= \Delta^{\mathbf{k}}\varepsilon_{\mathbf{p}}\rho_{\mathbf{p}}^{\mathbf{k}} + \sum_{\mathbf{k}''} [u(\mathbf{k}'') + w(\mathbf{k}'')\langle \rho^{\mathbf{k}''}\rangle](\rho_{\mathbf{p}-\frac{1}{2}\mathbf{k}''}^{\mathbf{k}-\mathbf{k}''} - \rho_{\mathbf{p}+\frac{1}{2}\mathbf{k}''}^{\mathbf{k}-\mathbf{k}''}) \\ &+ \sum_{\mathbf{k}''} w(\mathbf{k}'')\langle \rho_{\mathbf{p}-\frac{1}{2}\mathbf{k}''}^{\mathbf{k}-\mathbf{k}''} - \rho_{\mathbf{p}+\frac{1}{2}\mathbf{k}''}^{\mathbf{k}-\mathbf{k}''}\rangle \rho^{\mathbf{k}''},\end{aligned} \quad (2.7)$$

where $\langle \rho^{\mathbf{k}}\rangle$ is a number. If one *formally* assumes that the operators $\rho, \rho^{\dagger}$ satisfy the canonical commutation relations,

$$[\rho_{\mathbf{p}}^{\mathbf{k}}, (\rho_{\mathbf{p}'}^{\mathbf{k}'})^{\dagger}] = \delta(\mathbf{k}, \mathbf{k}')\delta(\mathbf{p}, \mathbf{p}'),$$

then (2.7) implies an effective Hamiltonian of the form

$$\begin{aligned}H_{\mathrm{eff}} = \sum_{\mathbf{p}}\sum_{\mathbf{p}'}\sum_{\mathbf{k}}\sum_{\mathbf{k}'} &\{\Delta^{\mathbf{k}}\varepsilon_{\mathbf{p}}\delta(\mathbf{k}, \mathbf{k}')\delta(\mathbf{p}, \mathbf{p}') + [u(\mathbf{k}-\mathbf{k}') + w(\mathbf{k}-\mathbf{k}']\langle \rho^{\mathbf{k}-\mathbf{k}'}\rangle] \\ &\times [\delta(\mathbf{p}-\mathbf{k}; \mathbf{p}-\mathbf{k}') - \delta(\mathbf{p}+\mathbf{k}; \mathbf{p}+\mathbf{k}')] + w(\mathbf{k}')\langle \rho_{\mathbf{p}-\frac{1}{2}\mathbf{k}'}^{\mathbf{k}-\mathbf{k}'} - \rho_{\mathbf{p}+\frac{1}{2}\mathbf{k}'}^{\mathbf{k}-\mathbf{k}'}\rangle\}(\rho_{\mathbf{p}}^{\mathbf{k}})^{\dagger}(\rho_{\mathbf{p}'}^{\mathbf{k}'}).\end{aligned} \quad (2.8)$$

† That the two approximations are closely related is readily apparent if one recognizes that with $\delta u(\mathbf{k}, t)$ a small time-dependent perturbation of the single-particle potential $u(\mathbf{k})$,

$$\mathscr{D}(\mathbf{k}, \mathbf{p}; \mathbf{k}'; t-t') = \pm \frac{\delta G_1(\mathbf{p}+\frac{1}{2}\mathbf{k}, \mathbf{p}-\frac{1}{2}\mathbf{k}; t, t^+)}{\delta u(\mathbf{k}', t')}.$$

Applying this relation to (2.5), one obtains (2.6) directly. Cf. also ref. [10]).

The $\omega$-plane singularities of (2.6) coincide with the eigenvalues of the effective Hamiltonian (2.8).

The most important feature of $H_{eff}$ from our present viewpoint is that it is not Hermitian [6]). When the coefficients $w(\mathbf{k})\ \langle \rho_{\mathbf{p}-} - \rho_{\mathbf{p}+} \rangle$ are small relative to the coefficients of the first two (Hermitian) terms, this feature is of small consequence. The eigenvalues remain real and their values reflect the small modifications appropriate to $v(\mathbf{k})$. However, when the interaction, weighted by the particle density, becomes large, $H_{eff}$ may be dominated by the non-Hermitian components and the eigenvalues may become complex. Such breakdowns of the RPA are well known for $v(\mathbf{k})$ attractive †.

It is interesting to observe that a similar breakdown, which could also be viewed as resulting from the replacement of $H$ by a non-Hermitian $H_{eff}$, occurs in the simplest treatment of short-range pairing forces in superconductors. There an instability develops for low-temperature systems whenever the attractive pairing interaction becomes larger than a certain critical value [7]). As shall become apparent shortly, the parallel with the superconductor extends further and, coupled with physical considerations, ultimately suggests a satisfactory solution to the difficulties.

The breakdown in the RPA associated with the transition to complex eigenvalues in $H_{eff}$ reflects a type of physical instability which we may associate with a thermodynamic phase change. The remarks of the preceding paragraphs suggest that, as a first effort to stabilize the mathematics and thereby to describe the second phase, one should replace (2.5) and (2.6) by equations which include the neglected Hermitian complements implicit in (2.3) and (2.4). The difficulties inherent in this approach — as in the corresponding approach to the superconductor — stem from the fact that the Hermitian complements appear to be inextricably bound in correlated non-linear expressions. In the present case this reflects itself in the fact that, when the single operator $\rho^{\mathbf{k}}$ with $\mathbf{k} \neq 0$ is factored from an expectation value of a product of operators, the momentum-transfer characteristics of the operator product are altered ††. When $u(\mathbf{k}) = 0$ or when the $u(\mathbf{k}) \neq 0$ components are dominated by the interaction terms so that expectation values conserve (or nearly conserve) momentum, this feature is particularly important, and the simple factorization implicit in (2.5) and (2.6) does not generally account for the most important contributions of the original functions. By exploiting the spectral characteristics of the operator which measures the particle density relative to the system centre of mass, we shall find that it is possible to circumvent the momentum-transfer difficulties and to establish generalizations of (2.5) and (2.6) which more closely reflect the dominant features of the correlated functions of (2.3) and (2.4).

† See *note added in proof* at the end of this paper.

†† In the superconductor the commutation properties with $N$ are changed.

## 3. Hole-Particle Pairing Operators and Linear-Momentum Generators

In the superconductor the operator combination

$$\mathscr{P}_{\mathrm{pp}} \equiv \sum_{\mathbf{2}} v(1,-1;\,2,\,-2)\psi_2\psi_{-2} \tag{3.1}$$

and its adjoint appear in several non-linear correlated expressions. Those expressions are subsequently simplified by the assumption (verified by a self-consistency requirement, which also serves to fix the gap $\Delta$) that the matrix elements of $\mathscr{P}_{\mathrm{pp}}$, taken with respect to the relevant strongly paired multi-particle states, are dominated by the single frequency $\omega = 2\mu$. Essential to such an argument is the observation that the $\omega = 2\mu$ dominance is strongly enhanced by a B-E type of weight function in the spectral representation of the matrix elements.

Somewhat more precisely, it is known that any Green's function formed from time-ordered products of field operators $\psi$, $\psi^\dagger$ weighted as in (1.1) can be separated into different analytic time components which are related by various periodicity and commutation relations [1, 5]). Assuming that the commutation properties are sufficiently well behaved, it is sufficient to restrict our considerations to two special sets of functions: those in which the operator combination of interest is entirely to the left and those in which it is entirely to the right. If $\mathscr{P}$ represents the operator of particular interest and $\mathscr{O}$ a particular configuration of all the other operators (for some fixed values of their indices), two special cases are

$$g(\tau)_+ = (-i)\langle\mathscr{P}(\tau)\mathscr{O}\rangle, \qquad g(\tau)_- = (-i)(-1)^m\langle\mathscr{O}\mathscr{P}(\tau)\rangle.$$

If we define the $(\alpha, \beta)$-dependent spectral function $A(\omega)^{\alpha\beta}$ in such a way that

$$g(\tau)_0 = g(\tau)_+ - g(\tau)_- = (-i)\int \frac{\mathrm{d}\omega}{2\pi} A(\omega)^{\alpha\beta}\,\mathrm{e}^{-i\omega\tau},$$

it is easy to verify that

$$g(\tau)_+ = (-i)\int \frac{\mathrm{d}\omega}{2\pi} A(\omega)^{\alpha\beta} \frac{\mathrm{e}^{\beta(\omega-\mu m)}}{\mathrm{e}^{\beta(\omega-\mu m)} - (\pm 1)^m}\,\mathrm{e}^{-i\omega\tau}, \tag{3.2a}$$

$$g(\tau)_- = (-i)\int \frac{\mathrm{d}\omega}{2\pi} A(\omega)^{\alpha\beta} \frac{(\pm 1)^m}{\mathrm{e}^{\beta(\omega-\mu m)} - (\pm 1)^m}\,\mathrm{e}^{-i\omega\tau}, \tag{3.2b}$$

where $\mu = -\alpha/\beta$ is the chemical potential. The integer $m$ is defined by $[\mathscr{P}, N] = m\mathscr{P}$ and the upper and lower signs refer to the B-E and F-D cases, respectively. For the operator (3.1), $m = 2$ and the heavy B-E weighting in the neighbourhood of $\omega = 2\mu$ follows immediately from (3.2). Hence, a sufficient condition that the superconductor pairing approximation be valid is that

the function $A(\omega)^{\alpha\beta}$ give a finite contribution in the neighbourhood of $\omega = 2\mu$ and, implicitly, that the remaining $A(\omega)^{\alpha\beta}$ contributions generate short-lived correlations such as are characteristic of a branch line (in contrast to a sharply defined pole).

It is clear from a consideration of the M-B limit for which $\mu \to -\infty$ that the $\omega = 2\mu$ dominance of $\mathscr{P}_{pp}$ is essentially a low-temperature phenomenon. The RPA breakdown is considerably more general; it occurs, for example, even in the M-B treatments of gas-liquid condensation. We may conclude that any admissible B-E condensation treatment of the phase change accompanying the RPA breakdown cannot be based upon the particle-particle pairing operator (3.1) but must be based upon a type of hole-particle operator $\mathscr{P}$ which commutes with $N$.

To facilitate the introduction of a suitable operator $\mathscr{P}$, it is convenient first to define a group of linear momentum generators

$$\pi_{\mathbf{K}} = e^{i\mathbf{K}\cdot\bar{\mathbf{R}}}, \tag{3.3}$$

where $\bar{\mathbf{R}}$ is the centre-of-mass operator

$$\bar{\mathbf{R}} = \int d\tau\, \mathbf{r}\, \rho(\mathbf{r}) \Big/ \int d\tau\, \rho(\mathbf{r}). \tag{3.4}$$

The generator (3.3) has the commutation properties

$$\begin{aligned} &\pi_{N\mathbf{K}}\psi_{\mathbf{p}} = \psi_{\mathbf{p}+\mathbf{K}}\pi_{N\mathbf{K}}, \qquad \pi_{N\mathbf{K}}\psi_{\mathbf{p}}^{\dagger} = \psi_{\mathbf{p}+\mathbf{K}}^{\dagger}\pi_{N\mathbf{K}}, \\ &[\pi_{\mathbf{K}}, \rho(r)] = [\pi_{\mathbf{K}}, \rho^{\mathbf{k}}] = 0, \quad [\pi_{\mathbf{K}}, N] = 0, \quad [\pi_{\mathbf{K}}, \mathbf{P}] = -\mathbf{K}\pi_{\mathbf{K}}, \\ &[\pi_{\mathbf{K}}, H] = \left\{\frac{K^2}{2mN} - \frac{2\mathbf{K}\cdot\mathbf{P}}{2mN}\right\}\pi_{\mathbf{K}} = \pi_{\mathbf{K}}\left\{-\frac{K^2}{2mN} - \frac{2\mathbf{K}\cdot\mathbf{P}}{2mN}\right\}, \end{aligned} \tag{3.5}$$

which follow directly from the fundamental field commutation relations. In addition, we have

$$\pi_{\mathbf{K}'}\pi_{\mathbf{K}''} = \pi_{\mathbf{K}'+\mathbf{K}''}, \qquad \pi_0 = 1, \qquad (\pi_{\mathbf{K}})^{\dagger} = (\pi_{\mathbf{K}})^{-1} = \pi_{-\mathbf{K}}. \tag{3.6}$$

Using the generators (3.3) and the operator (3.4), we introduce an operator

$$\rho(\mathbf{r}+\bar{\mathbf{R}}_{op}), \tag{3.7a}$$

which measures particle density relative to the centre of mass. Somewhat more precisely, in terms of the commuting operators $\rho^{\mathbf{k}}$, $\pi_{\mathbf{k}}$ we define the Fourier transform of (3.7a) to be

$$\int d\tau\, \rho(\mathbf{r}+\bar{\mathbf{R}}_{op})\, e^{-i\mathbf{k}\cdot\mathbf{r}} \equiv e^{i\mathbf{k}\cdot\bar{\mathbf{R}}}\rho^{\mathbf{k}} = \pi_{\mathbf{k}}\rho^{\mathbf{k}}. \tag{3.7b}$$

We assert that the operator (3.7) and, to a more limited extent, the separate component operators

$$\pi_{\mathbf{k}}\rho_{\mathbf{p}}^{\ \mathbf{k}} \tag{3.8}$$

are suitable pairing operators $\mathscr{P}$ for the treatment of phase changes associated with SCFA and RPA instabilities. In contrast to the simple density operator $\rho^k$ used in the approximations of the preceding section, the operators (3.7), (3.8) commute with **P** and therefore preserve the momentum transfer characteristics of any operator product from which they are factored.

There are of course many operators other than (3.7) and (3.8) which commute with $N$ and which therefore might appear to be suitable $\mathscr{P}$-operators from spectral-*weight*-function considerations alone. In this regard one must determine from supplementary physical considerations whether the operator choice is such that finite contributions to the spectral-function sum rules,

$$i^n \left\langle \left[ \frac{\partial^n}{\partial \tau^n} \mathscr{P}(\tau), \mathscr{O} \right] \right\rangle \Big|_{\tau=0} = \int_{-\infty}^{\infty} \frac{d\omega}{2\pi} \omega^n A(\omega),$$

arise from the neighbourhood of the weight-function pole: it is necessary to select that operator which is physically relevant. In those situations where condensed thermodynamic phases are characterized by a single "cluster", the various phases are clearly to be distinguished by the different time-independent configurations of the particle density relative to the centre of mass. It is for this reason that we have chosen to consider primarily the operator (3.7). The present formalism is of course only applicable to thermodynamic multi-phase systems which are indeed characterized by density distributions relative to the centre of mass. In a subsequent article we shall discuss the generalizations appropriate to those cases where the density distributions about the centre of mass are not spherically symmetric and an angular reference is required to supplement the position reference (3.4).

Paralleling the pp-pairing case, we assume that, if the $\alpha$, $\beta$-dependent multi-particle spectra associated with matrix elements of the hole-particle pairing operators contain $\omega = 0$ components, those components dominate completely. We shall neglect the $\omega \neq 0$ corrections both when there is an $\omega = 0$ component and when there is none. Presumably such corrections are small. Actually they are ultimately responsible for the fact that phase transitions in (1.1) for finite systems are analytic in $(\alpha, \beta)$ at the transition points and in gas-liquid systems for the fact that the $p$-$V$ curve is strictly monotonic. Neglecting the $\omega \neq 0$ terms, we shall find that the phase transitions are sharp and non-analytic. Since in multi-particle systems described by (1.1) the dominant frequencies associated with the various collective modes are $(\alpha, \beta)$-dependent, the frequency to be associated with one pairing mode may shift to zero while that associated with another may shift from zero, as $(\alpha, \beta)$ changes. The resulting change in the static ($\omega = 0$) properties of the system constitutes a thermodynamic phase change †. It is obvious that this process will occur mathematically in a contin-

† Cf. the relation in the superconductor between the $(\alpha, \beta)$-dependent exciton spectrum and the different stable pairing configurations [6]).

uous fashion only if in the transition region one takes into account all relevant modes, those with $\omega = 0$ and those for which $\omega$ may shift to zero.

If $C^{\mathbf{k}}$ is that component of the operator (3.7b) associated with the $\omega = 0$ spectral-weight-function pole and if $C^{\mathbf{k}}(\mathbf{p})$ is the corresponding component of (3.8), then

$$C_{\mathbf{k}} = \sum_{\mathbf{p}} C_{\mathbf{k}}(\mathbf{p}), \tag{3.9a}$$

$$[C_{\mathbf{k}}(\mathbf{p}), H] = [C_{\mathbf{k}}(\mathbf{p}), N] = [C_{\mathbf{k}}(\mathbf{p}), \mathbf{P}] = 0. \tag{3.9b}$$

If $\mathcal{O}$ is any operator, then with $\langle \ldots \rangle$ defined in (1.1) we have

$$\langle \mathcal{O} \rangle = e^{W(\alpha,\beta)} \sum_N \sum_E e^{-\alpha N} e^{-\beta E} \langle EN\xi' | \mathcal{O} | EN\xi' \rangle;$$

i.e. $\langle \mathcal{O} \rangle$ is a function only of those components of $\mathcal{O}$ which commute with $N$ and $H$. Applying this result to the hole-particle pairing operators, we find

$$\langle \pi_{\mathbf{k}} \rho^{\mathbf{k}} \rangle = \langle C_{\mathbf{k}} \rangle \equiv \Gamma_{\mathbf{k}} = \Gamma^*_{-\mathbf{k}}, \tag{3.10a}$$

$$\langle \pi_{\mathbf{k}} \rho_{\mathbf{p}}{}^{\mathbf{k}} \rangle = \langle C_{\mathbf{k}}(\mathbf{p}) \rangle \equiv \gamma_{\mathbf{k}}(\mathbf{p}), \tag{3.10b}$$

where we have introduced the convenient parameters $\gamma_{\mathbf{k}}(\mathbf{p})$ and $\Gamma_{\mathbf{k}}$.

## 4. Generalized Self-Consistent-Field and Random-Phase Approximations.

Considering initially a generalization of the SCFA, we may use the operator $C_{\mathbf{k}}$ defined in the previous section to write the first of equations (1.4) in the form

$$i \frac{\partial}{\partial t} \psi_{\mathbf{p}} = \varepsilon_{\mathbf{p}} \psi_{\mathbf{p}} + \sum_{\mathbf{k}} [u(\mathbf{k}) + w(\mathbf{k}) C_{\mathbf{k}} \pi_{-\mathbf{k}}] \psi_{\mathbf{p}-\mathbf{k}} + \sum_{\mathbf{k}} w(\mathbf{k}) [\rho^{\mathbf{k}} - C_{\mathbf{k}} \pi_{-\mathbf{k}}] \psi_{\mathbf{p}-\mathbf{k}}. \tag{4.1}$$

A similar form obtains for the adjoint equation. The primary assumption underlying the present approach is that, when (4.1) is used in an equation of the type (2.3), the last term on the right-hand side of eq. (4.1) may be treated as a small perturbation. We also assume that fluctuation and potential-correlation effects are small in the matrix elements of interest and that it is a reasonable approximation simply to factor $C_{\mathbf{k}}$ from such matrix elements. If for given $(\alpha, \beta)$ two or more different thermodynamic phases contribute to (1.1) in comparable proportions, we shall require that the $N, H$ weight function in (1.1) be supplemented by a concentration weight function capable of distinguishing the separate phases. With this restriction and the previous assumptions it is clear that the parameters (3.10) will characterize the thermodynamic phase under consideration. In the last section of this paper we discuss self-consistency criteria which serve to fix those parameters.

For simplicity we shall restrict our attention to those cases for which the energy levels of the system are closely spaced and for which the exchange effects of the neighbouring fields $\psi$, $\psi^\dagger$ on $C_\mathbf{k}$ are negligible. This restriction is completely equivalent to that usually employed in treating pp-pairing in superconductors and is not essential. [Cf. discussion of (4.4) below.] When the relevant energy levels are not closely spaced and the contribution of a single level is a significant fraction of the total, one must proceed with greater care. This situation parallels that encountered in the application of the superconductor formalism to the short-range pairing forces in nuclei. The finite spacing of the nuclear single-particle levels generates important modifications in the effective gap to be associated with different matrix elements [9]). In this introductory work we shall neglect such effects.

Within the above qualifications we may easily derive from eq. (4.1) a generalized SCFA appropriate to the class of functions

$$g_1(\mathbf{K}, \mathbf{p}; \mathbf{K}', \mathbf{p}'; t-t')_0 \equiv (-i)\langle[(\pi_\mathbf{k}\psi_\mathbf{p})(t), (\pi_{\mathbf{k}'}\psi_{\mathbf{p}'})^\dagger(t')]_\mp\rangle\theta(t-t'). \quad (4.2)$$

(The function (2.1) is that special case of (4.2) for which $\mathbf{K} = \mathbf{K}' = 0$.) Thus, neglecting the last term on the right-hand side of (4.1), we have †

$$\begin{aligned}
&\omega g_1(\mathbf{K}, \mathbf{p}; \mathbf{K}', \mathbf{p}'; \omega)_0 - \delta(\mathbf{p}, \mathbf{p}')\langle\pi_{\mathbf{K}-\mathbf{K}'}\rangle - \langle[\pi_\mathbf{K}, \psi^\dagger_{\mathbf{p}'}]\pi_{-\mathbf{K}'}\psi_\mathbf{p} + \pi_\mathbf{K}\psi^\dagger_{\mathbf{p}'}[\psi_\mathbf{p}, \pi_{-\mathbf{K}'}]\rangle \\
&\quad = \varepsilon_\mathbf{p} g_1(K, p; K', p'; \omega)_0 + \sum_\mathbf{k} u(\mathbf{k}) g_1(\mathbf{K}, \mathbf{p}-\mathbf{k}; \mathbf{K}', \mathbf{p}'; \omega)_0 \\
&\quad + \left\{(-i)\left\langle\left[\left(\left(\frac{K^2}{2mN} - \frac{2\mathbf{K}\cdot\mathbf{P}}{2mN}\right)\pi_\mathbf{K}\psi_\mathbf{p}\right)(t), (\pi_{\mathbf{K}'}\psi_{\mathbf{p}'})^\dagger(t')\right]\right\rangle\right\}(\omega)_0 \\
&\quad + \sum_\mathbf{k} w(\mathbf{k})\{(-i)\langle[(C_\mathbf{k}\pi_{\mathbf{K}-\mathbf{k}}\psi_{\mathbf{p}-\mathbf{k}})(t), (\pi_{\mathbf{K}'}\psi_{\mathbf{p}'})^\dagger(t')]\rangle\}(\omega)_0 \qquad (4.3) \\
&\quad \approx \sum_\mathbf{k}\{\varepsilon_\mathbf{p}\delta(\mathbf{k}) + u(\mathbf{k})\} g_1(\mathbf{K}, \mathbf{p}-\mathbf{k}; \mathbf{K}', \mathbf{k}'; \omega)_0 \\
&\quad + \sum_\mathbf{k} w(\mathbf{k}) \Gamma_\mathbf{k} g_1(\mathbf{K}-\mathbf{k}, \mathbf{p}-\mathbf{k}; \mathbf{K}', \mathbf{k}'; \omega)_0.
\end{aligned}$$

Consistent with our assumptions, we assert that the time-ordered analogue of (4.3) has the same time-periodicity properties as the $G_1$-function. Because the operator $\pi_{-\mathbf{k}}$ appears in one term but not in the other, the $u(\mathbf{k})$ and $w(\mathbf{k})\,\Gamma_\mathbf{k}$ terms of (4.4) are quite different — a result which differs qualitatively from (2.5).

It is clear from (4.3) that, in so far as they apply to that equation, the arguments of the preceding section are nothing more or less than a justifica-

† In the last line of eq. (4.3) and in subsequent equations we have neglected the contribution of terms of the type $\pm K^2/2m\langle N\rangle$ to the Green's function frequencies. Such terms, which represent the kinetic energy of the centre of mass, introduce no essential modifications into the subsequent arguments, although certain algebraic complications result from the fact that in the simplest approximations $K^2/2m\langle N\rangle$ appears with opposite signs for the two terms of the commutators of (4.2) and of (4.6).

tion for the factorization

$$\langle(\rho^{\mathbf{k}''}\pi_{\mathbf{k}''}\rho^{\mathbf{k}-\mathbf{k}''}\pi_{\mathbf{k}-\mathbf{k}''})(t)(\rho^{\mathbf{k}'}\pi_{\mathbf{k}'})^\dagger(t')\rangle \approx \langle\rho^{\mathbf{k}''}\pi_{\mathbf{k}''}\rangle\langle(\rho^{\mathbf{k}-\mathbf{k}''}\pi_{\mathbf{k}-\mathbf{k}''})(t)(\rho^{\mathbf{k}'}\pi_{\mathbf{k}'})^\dagger(t')\rangle. \quad (4.4a)$$

This approximation is the centre-of-mass analogue of the factorization

$$\langle(\rho^{\mathbf{k}''}\rho^{\mathbf{k}-\mathbf{k}''})(t)\rho^{-\mathbf{k}'}(t')\rangle \approx \langle\rho^{\mathbf{k}''}\rangle\langle\rho^{\mathbf{k}-\mathbf{k}''}(t)\rho^{-\mathbf{k}'}(t')\rangle \quad (4.4b)$$

used in (2.5). Corresponding to the various higher-order forms of (4.4b), there exist straightforward extensions of (4.4a) which include exchange, $t$-matrix and similar correlation effects. In essence, one would consider in place of the usual $\psi$, $\psi^\dagger$ formalism [1]) a formalism based upon the "centre-of-mass fields"

$$\varphi_{\mathbf{k}} \equiv \psi_{\mathbf{k}}\pi_{\mathbf{k}}, \qquad \varphi_{\mathbf{k}}^\dagger \equiv \pi_{-\mathbf{k}}\psi_{\mathbf{k}}^\dagger.$$

In such a formalism, complicated somewhat by the usually negligible commutators $[\psi_{\mathbf{k}}, \pi_{\mathbf{k}'}]$, the analogue of the Hartree-Fock factorization

$$\begin{aligned}\langle(\psi_1(t_1)\psi_2(t_2)\psi_{2'}^\dagger(t'_2)\psi_{1'}^\dagger(t'_1))_+\varepsilon\rangle \\ \approx \langle(\psi_1(t_1)\psi_{1'}^\dagger(t'_1))_+\varepsilon\rangle\langle(\psi_2(t_2)\psi_{2'}^\dagger(t'_2))_+\varepsilon\rangle \\ \pm\langle(\psi_2(t_2)\psi_{1'}^\dagger(t'_1))_+\varepsilon\rangle\langle(\psi_1(t_1)\psi_{2'}^\dagger(t'_2))_+\varepsilon\rangle\end{aligned}$$

would be essentially the same expression but with $\psi$, $\psi^\dagger$ everywhere replaced by $\varphi$, $\varphi^\dagger$. As shall become clear when the consistency conditions are discussed in the last section, the $\psi$, $\psi^\dagger$ and $\varphi$, $\varphi^\dagger$ formalisms do *not* differ significantly except in the self-bound case.

The generalization of the RPA analogous to (4.3) for the SCFA follows from a consideration of

$$\begin{aligned}&\sum_{\mathbf{k}''} w(\mathbf{k}'')\sum_{\mathbf{p}''}\rho_{\mathbf{p}''}^{\mathbf{k}''}\pi_{\mathbf{k}}(\rho_{\mathbf{p}-\frac{1}{2}\mathbf{k}''}^{\mathbf{k}-\mathbf{k}''}-\rho_{\mathbf{p}+\frac{1}{2}\mathbf{k}''}^{\mathbf{k}-\mathbf{k}''}) \\ &= \sum_{\mathbf{k}''} w(\mathbf{k}'')\{C_{\mathbf{k}''}\pi_{\mathbf{k}-\mathbf{k}''}[\rho_{\mathbf{p}-\frac{1}{2}\mathbf{k}''}^{\mathbf{k}-\mathbf{k}''}-\rho_{\mathbf{p}+\frac{1}{2}\mathbf{k}''}^{\mathbf{k}-\mathbf{k}''}]+\rho^{\mathbf{k}''}\pi_{\mathbf{k}''}[C_{\mathbf{k}-\mathbf{k}''}(\mathbf{p}-\tfrac{1}{2}\mathbf{k}'')-C_{\mathbf{k}-\mathbf{k}''}(\mathbf{p}+\tfrac{1}{2}\mathbf{k}'')] \\ &\qquad -C_{\mathbf{k}''}[C_{\mathbf{k}-\mathbf{k}''}(\mathbf{p}-\tfrac{1}{2}\mathbf{k}'')-C_{\mathbf{k}-\mathbf{k}''}(\mathbf{p}+\tfrac{1}{2}\mathbf{k}'')]\} \quad (4.5) \\ &+\sum_{\mathbf{k}''} w(\mathbf{k}'')\{\pi_{\mathbf{k}''}\rho^{\mathbf{k}''}-C_{\mathbf{k}''}\}\{[\pi_{\mathbf{k}-\mathbf{k}''}\rho_{\mathbf{p}-\frac{1}{2}\mathbf{k}''}^{\mathbf{k}-\mathbf{k}''}-C_{\mathbf{k}-\mathbf{k}''}(\mathbf{p}-\tfrac{1}{2}\mathbf{k}'')] \\ &\qquad -[\pi_{\mathbf{k}-\mathbf{k}''}\rho_{\mathbf{p}+\frac{1}{2}\mathbf{k}''}^{\mathbf{k}-\mathbf{k}''}-C_{\mathbf{k}-\mathbf{k}''}(\mathbf{p}+\tfrac{1}{2}\mathbf{k}'')]\},\end{aligned}$$

which expression contains the essential two-particle components of (1.5). Our primary assumption here is that, when (4.5) is used in equations of the type (2.4), the last term on the right-hand side of (4.5) constitutes a small perturbation. With this assumption and additional assumptions analogous to those introduced in treating (4.1), we may easily derive a generalized RPA appropriate to the class of functions

$$\mathscr{L}(\mathbf{K}, \mathbf{k}, \mathbf{p}; \mathbf{K}', \mathbf{k}'; t-t')_0 \equiv (-i)\langle[(\pi_{\mathbf{K}}\rho_{\mathbf{p}}^{\mathbf{k}})(t), (\pi_{\mathbf{K}'}\rho^{\mathbf{k}'})^\dagger(t')]\rangle\theta(t-t'). \quad (4.6)$$

(The function (2.2) is that special case of (4.6) for which $\mathbf{K} = \mathbf{K}' = 0$.) Thus,

we have

$$
\begin{aligned}
&(\omega-\Delta^{\mathbf{k}}\varepsilon_{\mathbf{p}})\mathscr{L}(\mathbf{K},\mathbf{k},\mathbf{p};\mathbf{K}',\mathbf{k}';\omega)_0 \\
&\quad=[\langle\pi_{\mathbf{K}-\mathbf{K}'}\rho_{\mathbf{p}-\frac{1}{2}\mathbf{k}'}^{\mathbf{k}-\mathbf{k}'}\rangle-\langle\pi_{\mathbf{K}-\mathbf{K}'}\rho_{\mathbf{p}+\frac{1}{2}\mathbf{k}'}^{\mathbf{k}-\mathbf{k}'}\rangle+\langle\pi_{\mathbf{K}-\mathbf{K}'}(\rho_{\mathbf{p}+\mathbf{K}'/\langle N\rangle}^{\mathbf{k}}-\rho_{\mathbf{p}}^{\mathbf{k}})\rho^{-\mathbf{k}'}\rangle] \\
&\quad+\sum_{\mathbf{k}''}\{u(\mathbf{k}'')[\mathscr{L}(\mathbf{K},\mathbf{k}-\mathbf{k}'',\mathbf{p}-\tfrac{1}{2}\mathbf{k}'';\mathbf{K}',\mathbf{k}';\omega)_0 \\
&\qquad\qquad-\mathscr{L}(\mathbf{K},\mathbf{k}-\mathbf{k}'',\mathbf{p}+\tfrac{1}{2}\mathbf{k}'';\mathbf{K}',\mathbf{k}';\omega)_0] \qquad (4.7)\\
&\quad+\omega(\mathbf{k}'')\Gamma_{\mathbf{k}''}[\mathscr{L}(\mathbf{K}-\mathbf{k}'',\mathbf{k}-\mathbf{k}'',\mathbf{p}-\tfrac{1}{2}\mathbf{k}'';\mathbf{K}',\mathbf{k}';\omega)_0 \\
&\qquad\qquad-\mathscr{L}(\mathbf{K}-\mathbf{k}'',\mathbf{k}-\mathbf{k}'',\mathbf{p}+\tfrac{1}{2}\mathbf{k}'';\mathbf{K}',\mathbf{k}';\omega)_0]\} \\
&\quad+\sum_{\mathbf{k}''}w(\mathbf{k}'')[\gamma_{\mathbf{k}-\mathbf{k}''}(\mathbf{p}-\tfrac{1}{2}\mathbf{k}'')-\gamma_{\mathbf{k}-\mathbf{k}''}(\mathbf{p}+\tfrac{1}{2}\mathbf{k}'')]\sum_{\mathbf{p}''}\mathscr{L}(\mathbf{K}+\mathbf{k}''-\mathbf{k},\mathbf{k}''\mathbf{p}'';\mathbf{K}',\mathbf{k}';\omega)_0.
\end{aligned}
$$

Consistent with our assumptions, we assert that the time-ordered analogue of (4.7) has the same time-periodicity properties as the $\mathscr{D}$-function. The second term on the right-hand side of (4.7) is the direct analogue of the last term in (4.3). The last term of (4.7), which has no analogue in (4.3), is the generalization of the collective RPA term of (2.6) and differs from that term through the $\pi_{\mathbf{k}}$-weighting.

The $C_{\mathbf{k}}$ contributions to (4.3) and (4.7) generate a type of self-consistent single-particle static background potential of strength $w(\mathbf{k}'')\,\Gamma_{\mathbf{k}''}$. This interpretation is corroborated by the observation that $\Gamma$ measures relative to the centre of mass the strength of the time-invariant component of the spatial density (pairing) operator. Although it is clear that the replacement of the pairing operator (3.7) in (4.1) and (4.5) by the operator $C_{\mathbf{k}}$ is physically justifiable, it is not immediately obvious that the subsequent replacement in (4.5) (in order to generate the dynamic collective components of (4.7)) of the separate component operators (3.8) by $C_{\mathbf{k}}(\mathbf{p})$ is equally admissible. In this regard we remark that, while the relevant matrix elements of (3.8) may exhibit a relatively sharp spectral component at some $(\mathbf{k},\mathbf{p})$-dependent non-zero frequency in addition to the postulated component at $\omega=0$, the latter frequency is $(\mathbf{k},\mathbf{p})$-independent and therefore contributes *coherently* in equations of the type (4.7). (An equivalent coherence argument is implicit in any discussion attempting to justify the neglect of the $\omega\neq 0$ components of (3.7).)

## 5. Conservation Properties of the Generalized Random-Phase Approximation

In a previous work [5]) we discussed the importance of the conservation properties satisfied by the inhomogeneous forms of Boltzmann-like equations such as (4.7). It is useful to verify that eq. (4.7) does indeed satisfy the criteria outlined in that work for number conservation and momentum conservation.

Using the algebraic identity

$$\sum_{\mathbf{p}}(a+\mathbf{b}\cdot\mathbf{p})[f(\mathbf{p}-\mathbf{q})-f(\mathbf{p}+\mathbf{q})]=\mathbf{b}\cdot\mathbf{q}\sum_{\mathbf{p}}f(\mathbf{p}) \qquad (5.1)$$

with the homogeneous form of (4.7), we find

$$\begin{aligned}
\omega \sum_{\mathbf{p}} (a+\mathbf{b}\cdot\mathbf{p})\mathscr{L}(\mathbf{K}=0,\mathbf{k}=0,\mathbf{p};\mathbf{K}',\mathbf{k}';\omega)_0 \\
&= \left\{ i\frac{\partial}{\partial t}(-i)\langle[(aN+bP)(t),(\pi_{\mathbf{K}'}\rho^{\mathbf{k}'})^\dagger(t')]\rangle \right\}(\omega)_0 \\
&= \sum_{\mathbf{k}''} \mathbf{b}\cdot\mathbf{k}'' u(\mathbf{k}'') \sum_{\mathbf{p}} \mathscr{L}(0,-\mathbf{k}'',\mathbf{p};\mathbf{K}',\mathbf{k}';\omega)_0 \qquad (5.2) \\
&+ \sum_{\mathbf{k}''} \mathbf{b}\cdot\mathbf{k}'' w(\mathbf{k}'') \sum_{\mathbf{p}} \{\Gamma_{\mathbf{k}''}\mathscr{L}(-\mathbf{k}'',-\mathbf{k}'',\mathbf{p};\mathbf{K}',\mathbf{k}';\omega)_0 \\
&\qquad + \Gamma_{-\mathbf{k}''}\mathscr{L}(\mathbf{k}'',\mathbf{k}'',\mathbf{p};\mathbf{K}',\mathbf{k}';\omega)_0\} \\
&= \sum_{\mathbf{k}''} \mathbf{b}\cdot\mathbf{k}'' u(\mathbf{k}'') \sum_{\mathbf{p}} \mathscr{L}(0,-\mathbf{k}'',\mathbf{p};\mathbf{K}',\mathbf{k}';\omega)_0,
\end{aligned}$$

since $w(-\mathbf{k}) = w(\mathbf{k})$. These results are in agreement with the relations

$$i\frac{\partial}{\partial t}N(t) = [N,H] = 0,$$

$$i\frac{\partial}{\partial t}\mathbf{P}(t) = [\mathbf{P},H] = 0, \quad \text{if} \quad u(\mathbf{k}\neq 0) = 0.$$

## 6. Special Relations between Solutions

In sect. 4 we introduced a set of generalized functions $g_1$, $\mathscr{L}$ having the same periodicity properties as the functions $G_1$, $\mathscr{D}$ of sect. 2. It is an important fact that under certain circumstances the approximate spectral forms defined for $g_1$, $\mathscr{L}$ by the generalized equations (4.3), (4.7) coincide (numerically) with the approximate forms defined for $G_1$, $\mathscr{D}$ by the more familiar equations (2.5), (2.6). Trivial identities of course occur if in both equations $u(\mathbf{k})$, $\Gamma_{\mathbf{k}}$, $\gamma_{\mathbf{k}}(\mathbf{p})$ are all zero for $\mathbf{k}\neq 0$ or if $w(\mathbf{k}) = 0$. However, the following situation is *not* trivial.

In (2.5) let us take $w(\mathbf{k}) = 0$, while in (4.3) we take $u(\mathbf{k}) = 0$ and set $\mathbf{K} = \mathbf{k}$. Solving the resulting form of (2.5), we obtain a functional of $u(\mathbf{k})$

$$G_1(\mathbf{p},\mathbf{p}';\omega)_0 = F_1(\mathbf{p},\mathbf{p}';\omega;u(\mathbf{k})). \qquad (6.1a)$$

This may be identified with the solution of (4.3)

$$g_1(\mathbf{p},\mathbf{p};\mathbf{p}',\mathbf{p}';\omega)_0 = F_1(\mathbf{p},\mathbf{p}';\omega;w(\mathbf{k})\Gamma_{\mathbf{k}}). \qquad (6.1b)$$

As a consequence of this relation and the identity of the periodicity properties it follows from (3.10) that, when the quantity $u(\mathbf{k})$ in (6.1a) equals the quantity $w(\mathbf{k})\Gamma_{\mathbf{k}}$ in (6.1b), we have

$$\langle\rho_{\mathbf{p}}{}^{\mathbf{k}}\rangle|_{(6.1a)} = \langle\pi_{\mathbf{k}}\rho_{\mathbf{p}}{}^{\mathbf{k}}\rangle|_{(6.1b)} = \gamma_{\mathbf{k}}(\mathbf{p})|_{(6.1b)}. \qquad (6.2)$$

If, using these facts, we take $w(\mathbf{k}) = 0$ in the (self-consistent) $u(\mathbf{k})$-term of

(2.6) but retain $w(\mathbf{k}) \neq 0$ in the last term, while in (4.7) we take $u(\mathbf{k}) = 0$ and set $\mathbf{K} = \mathbf{k}$, we may solve the resulting equations to obtain

$$\mathscr{D}(\mathbf{k}, \mathbf{p}; \mathbf{k}'; \omega)_0 = F_2(\mathbf{k}, \mathbf{p}; \mathbf{k}'; \omega; u(\mathbf{k}), w(\mathbf{k})), \tag{6.3a}$$

$$\mathscr{L}(\mathbf{k}, \mathbf{k}, \mathbf{p}; \mathbf{k}', \mathbf{k}'; \omega)_0 = F_2(\mathbf{k}, \mathbf{p}; \mathbf{k}'; \omega; w(\mathbf{k})\Gamma_{\mathbf{k}}, w(\mathbf{k})). \tag{6.3b}$$

These results are important because they permit us to identify the combination $w(\mathbf{k})\Gamma_{\mathbf{k}}$ with a type of real external field and because they justify the usual external-field approach conventionally used in treating self-bound systems such as nuclei. That this identification is not trivial is apparent if one notes that the real external field $u(\mathbf{k})$ is part of $H$ and consequently appears in the exponential weight factor of (1.1) while, in contrast, $w\Gamma$ does not directly appear in the weighting exponential.

## 7. Self-Consistency Conditions

In deriving the expressions of sect. 4 ,we assumed that the relevant matrix elements of the pairing operators of sect. 3 had $\omega$-plane singularities at $\omega = 0$ proportional to $\Gamma_{\mathbf{k}}$ or $\gamma_{\mathbf{k}}(\mathbf{p})$, as appropriate. It follows that the results (4.3), (4.7) are self-consistent only if they admit the existence of such singularities. The equations generated by this self-consistency requirement are particularly important since they serve to define the set of parameters $\{\Gamma_{\mathbf{k}}, \gamma_{\mathbf{k}}(\mathbf{p})\}$ characterizing the various phases.

Let us consider first the consistency relations implied by (4.3) when $g_1$ is used with (3.10) to determine the parameters $\Gamma_{\mathbf{k}}$. Introducing a spectral function $A(\mathbf{K}, \mathbf{k}; \mathbf{K}', \mathbf{k}'; \omega)^{\alpha\beta}$ such that

$$g_1(\mathbf{K}, \mathbf{k}; \mathbf{K}', \mathbf{k}'; \omega)_0 = \int \frac{\mathrm{d}\bar{\omega}}{2\pi} \frac{A(\mathbf{K}, \mathbf{k}; \mathbf{K}', \mathbf{k}'; \bar{\omega})^{\alpha\beta}}{\omega - \bar{\omega} + i\varepsilon}, \quad \varepsilon = 0^+, \tag{7.1a}$$

we have from the general theory [1, 5]) that

$$\begin{aligned} \langle \pi_{\mathbf{K}} \psi_{\mathbf{k}} \psi^{\dagger}_{\mathbf{k}'} \pi_{\mathbf{K}'} \rangle &= \langle \pi_{\mathbf{K}} (\psi^{\dagger}_{\mathbf{k}'} \psi_{\mathbf{k}} \pm \delta(\mathbf{k}, \mathbf{k}')) \pi_{-\mathbf{K}'} \rangle \\ &= \int \frac{\mathrm{d}\omega}{2\pi} \frac{\mathrm{e}^{\beta(\omega-\mu)}}{\mathrm{e}^{\beta(\omega-\mu)} \mp 1} A(K, k; K', k'; \omega)^{\alpha\beta}. \end{aligned} \tag{7.1b}$$

Using (7.1) with (3.10), we obtain the consistency relation

$$\gamma_{\mathbf{k}}(\mathbf{p}) = \int \frac{\mathrm{d}\omega}{2\pi} \frac{\mathrm{e}^{\beta(\omega-\mu)}}{\mathrm{e}^{\beta(\omega-\mu)} \pm 1} A(\mathbf{k}, \mathbf{p}+\tfrac{1}{2}\mathbf{k}; 0, \mathbf{p}-\tfrac{1}{2}\mathbf{k}; \omega)^{\alpha\beta} \mp \delta(\mathbf{k}), \tag{7.2}$$

which must be satisfied by the parameters $\Gamma_{\mathbf{k}} = \Sigma_{\mathbf{p}} \gamma_{\mathbf{k}}(\mathbf{p})$ of (4.3). It is to be noted that obtaining a "clustered" solution for $\gamma_{\mathbf{k}}(\mathbf{p})$ is not mathematically trivial. For example with $u(\mathbf{k} \neq 0) = 0$ finite-order perturbation calculations about the point $v = 0$ generate only the solutions $\gamma_{\mathbf{k}}(\mathbf{p}) = 0, \mathbf{k} \neq 0$. This is more apparent if we express the $g_1$ consistency relation in an alternative form.

Subtracting (4.3) from the equivalent adjoint equation, we obtain

$$\begin{aligned}0 = {} & \Delta^{\mathbf{k}}\varepsilon_{\mathbf{p}}g_1(\mathbf{K}, \mathbf{p}+\tfrac{1}{2}\mathbf{k}; \mathbf{K}', \mathbf{p}-\tfrac{1}{2}\mathbf{k}; \omega)_0 \\ & + \sum_{\mathbf{k}''} u(\mathbf{k}'')[g_1(\mathbf{K}, \mathbf{p}-\mathbf{k}''+\tfrac{1}{2}\mathbf{k}; \mathbf{K}', \mathbf{p}-\tfrac{1}{2}\mathbf{k}; \omega)_0 \\ & \qquad - g_1(\mathbf{K}, \mathbf{p}+\tfrac{1}{2}\mathbf{k}; \mathbf{K}', \mathbf{p}+\mathbf{k}''-\tfrac{1}{2}\mathbf{k}; \omega)_0] \\ & + \sum_{\mathbf{k}''} w(\mathbf{k}'')\Gamma_{\mathbf{k}''}[\gamma_{\mathbf{K}-\mathbf{k}''}(\mathbf{p}-\tfrac{1}{2}\mathbf{k}''; \mathbf{k}-\mathbf{k}'') - \gamma_{\mathbf{K}-\mathbf{k}''}(\mathbf{p}+\tfrac{1}{2}\mathbf{k}''; \mathbf{k}-\mathbf{k}'')].\end{aligned}$$

Using (7.1) and neglecting the small commutator $[\rho^{\mathbf{k}}_{\mathbf{p}\pm\frac{1}{2}\mathbf{k}''}, \pi_{-\mathbf{k}''}]$, we find from this

$$\begin{aligned}0 = {} & \Delta^{\mathbf{k}}\varepsilon_{\mathbf{p}}\gamma_{\mathbf{K}}(\mathbf{p}; \mathbf{k}) + \sum_{\mathbf{k}''} u(\mathbf{k}'')[\gamma_{\mathbf{K}}(\mathbf{p}-\tfrac{1}{2}\mathbf{k}''; \mathbf{k}-\mathbf{k}'') - \gamma_{\mathbf{K}}(\mathbf{p}+\tfrac{1}{2}\mathbf{k}''; \mathbf{k}-\mathbf{k}'')] \\ & + \sum_{\mathbf{k}''} w(\mathbf{k}'')\Gamma_{\mathbf{k}''}[\gamma_{\mathbf{K}-\mathbf{k}''}(\mathbf{p}-\tfrac{1}{2}\mathbf{k}''; \mathbf{k}-\mathbf{k}'') - \gamma_{\mathbf{K}-\mathbf{k}''}(\mathbf{p}+\tfrac{1}{2}\mathbf{k}''; \mathbf{k}-\mathbf{k}'')],\end{aligned} \tag{7.3}$$

where we have defined

$$\gamma_{\mathbf{K}}(\mathbf{p}; \mathbf{k}) \equiv \langle \pi_{\mathbf{K}}\rho_{\mathbf{p}}{}^{\mathbf{k}}\rangle, \qquad \Gamma_{\mathbf{K}}(\mathbf{k}) \equiv \langle \pi_{\mathbf{K}}\rho^{\mathbf{k}}\rangle = \sum_{\mathbf{p}} \gamma_{\mathbf{K}}(\mathbf{p}; \mathbf{k}). \tag{7.4}$$

The parameters (3.10) are special cases of the parameters (7.4). For $u(\mathbf{k} \neq 0) = 0$ equation (7.3) becomes

$$\begin{aligned}0 = {} & \Delta^{\mathbf{k}}\varepsilon_{\mathbf{p}}\gamma_{\mathbf{K}}(\mathbf{p}; \mathbf{k}) + \sum_{\mathbf{k}''} w(\mathbf{k}'')\Gamma_{\mathbf{k}''} \\ & \times [\gamma_{\mathbf{K}-\mathbf{k}''}(\mathbf{p}-\tfrac{1}{2}\mathbf{k}''; \mathbf{k}-\mathbf{k}'') - \gamma_{\mathbf{K}-\mathbf{k}''}(\mathbf{p}+\tfrac{1}{2}\mathbf{k}''; \mathbf{k}-\mathbf{k}'')],\end{aligned} \tag{7.5a}$$

and momentum conservation requires that

$$\gamma_{\mathbf{K}}(\mathbf{p}; \mathbf{k}) = \delta(\mathbf{K}, \mathbf{k})\gamma_{\mathbf{K}}(\mathbf{p}). \tag{7.5b}$$

With $w(\mathbf{k} \neq 0) = 0$, (7.5) admits only the $\mathbf{k} \neq 0$ solutions: $\gamma_{\mathbf{k}}(\mathbf{p}) = 0$, $\Gamma_{\mathbf{k}} = 0$. Moreover, on account of the non-linear character of the interaction term, it is clear that *all* perturbative corrections to the zero-order solutions are zero. Non-zero solutions can only result if the consistency equations are treated as intrinsically non-linear equations.

It is also to be noted that (7.2) is somewhat more restrictive than (7.3). Equation (7.3) always admits the trivial solution $\gamma_{\mathbf{k}}(\mathbf{p}) = \Gamma_{\mathbf{k}} = 0$. For a solution of that form (7.2) reduces simply to an equivalent expression based upon the Hartree equation (2.5), whose solutions are known to exhibit instabilities. The notion of solution stability is most suitably discussed in terms of the generalized RPA (4.7). As was noted in sect. 2, the breakdown of the usual RPA is associated with the transition from real to complex frequencies in the spectral representation of the $\mathscr{D}$-function (2.2). For any given set of parameters (3.10) a similar situation occurs when the generalized approximations (4.3) and (4.7) fail — the frequency spectrum of the $\mathscr{L}$-function computed from (4.7) becomes complex. We shall therefore stipulate that only those solutions $\{\gamma_{\mathbf{k}}(\mathbf{p}), \Gamma_{\mathbf{k}}\}$ are admissible for which the $\mathscr{L}$-function spectrum of (4.7) is real. The transition of the spectral singularities of the $\mathscr{L}$-function from real to complex values as $(\alpha, \beta)$ changes is to be associated with a thermodynamic

phase transition from an initial phase characterized by one set of parameters (3.10) to another phase with parameters such that the spectral singularities of (4.7) are real.

To obtain an alternative derivation of the self-consistency relations, we may proceed directly from an equation of the type (4.7). Basic to our various approximations was the assumption that the operators (3.7), (3.8) contained $N$, $H$-commuting components of strength proportional to the parameters $\Gamma_{\mathbf{k}}$, $\gamma_{\mathbf{k}}(\mathbf{p})$, respectively. The presence of such a component will reflect itself in the spectrum of the function †

$$\mathscr{L}(K,k,p;K',k';t-t')_+ \equiv (-i)\langle(\pi_{\mathbf{K}}\rho_{\mathbf{p}}^{\mathbf{k}})(t)(\pi_{\mathbf{K}'}\rho^{\mathbf{k}'})^\dagger(t')\rangle = (-i)\int\frac{d\omega}{2\pi}\frac{e^{\beta\omega}A(\mathbf{K},\mathbf{k},\mathbf{p};\mathbf{K}',\mathbf{k}';\omega)e^{-i\omega(t-t')}}{e^{\beta\omega}-1}, \quad (7.6a)$$

where $A(\omega \neq 0)$ is here the spectral function for the commutator (4.6). Consistent with our previous assumptions we allege that

$$\frac{e^{\beta\omega}A(\mathbf{K},\mathbf{k},\mathbf{p};\mathbf{K}',\mathbf{k}';\omega)}{e^{\beta\omega}-1} = \gamma_{\mathbf{K}}(\mathbf{p};\mathbf{k})\Gamma_{\mathbf{K}'}(\mathbf{k}')^*\delta(\omega)+\frac{e^{\beta\omega}}{e^{\beta\omega}-1}A(\omega\neq 0), \quad (7.6b)$$

where we have used the parameters (7.4). Taking

$$\{(-i)\langle(C_{\mathbf{k}''}[C_{\mathbf{k}-\mathbf{k}''}(\mathbf{p}-\tfrac{1}{2}\mathbf{k}'')-C_{\mathbf{k}-\mathbf{k}''}(\mathbf{p}+\tfrac{1}{2}\mathbf{k}'')]\pi_{\mathbf{K}-\mathbf{k}})(t)(\pi_{\mathbf{K}'}\rho^{\mathbf{k}'})^\dagger(t')\rangle\}(\omega) = \Gamma_{\mathbf{k}''}[\gamma_{\mathbf{k}-\mathbf{k}''}(\mathbf{p}-\tfrac{1}{2}\mathbf{k}'')-\gamma_{\mathbf{k}-\mathbf{k}''}(\mathbf{p}+\tfrac{1}{2}\mathbf{k}'')]\langle\pi_{\mathbf{K}-\mathbf{k}}\rangle\Gamma_{\mathbf{K}'}(\mathbf{k}')^*\delta(\omega), \quad (7.7)$$

a term which does not appear in the $\omega \neq 0$ expression (4.7), we easily obtain the analogue of (4.7) for the function (7.6),

$$\begin{aligned}(\omega-\Delta^{\mathbf{k}}\varepsilon_{\mathbf{p}})\mathscr{L}(\mathbf{K},\mathbf{k},\mathbf{p};\mathbf{K}',\mathbf{k}';\omega)_+ &= \sum_{\mathbf{k}''}\{u(\mathbf{k}'')[\mathscr{L}(\mathbf{K},\mathbf{k}-\mathbf{k}'',\mathbf{p}-\tfrac{1}{2}\mathbf{k}'';\mathbf{K}',\mathbf{k}';\omega)_+ \\ &\quad -\mathscr{L}(\mathbf{K},\mathbf{k}-\mathbf{k}'',\mathbf{p}+\tfrac{1}{2}\mathbf{k}'';\mathbf{K}',\mathbf{k}';\omega)_+] \\ &\quad +w(\mathbf{k}'')\Gamma_{\mathbf{k}''}[\mathscr{L}(\mathbf{K}-\mathbf{k}'',\mathbf{k}-\mathbf{k}'',\mathbf{p}-\tfrac{1}{2}\mathbf{k}'';\mathbf{K}',\mathbf{k}';\omega)_+ \\ &\quad -\mathscr{L}(\mathbf{K}-\mathbf{k}'',\mathbf{p}+\tfrac{1}{2}\mathbf{k}'';\mathbf{K}',\mathbf{k}';\omega)_+]\} \\ &\quad +\sum_{\mathbf{k}''}w(\mathbf{k}'')[\gamma_{\mathbf{k}-\mathbf{k}''}(\mathbf{p}-\tfrac{1}{2}\mathbf{k}'')-\gamma_{\mathbf{k}-\mathbf{k}''}(\mathbf{p}+\tfrac{1}{2}\mathbf{k}'')] \\ &\quad \times\{\sum_{\mathbf{p}''}\mathscr{L}(\mathbf{K}+\mathbf{k}''-\mathbf{k},\mathbf{k}'',\mathbf{p}'';\mathbf{K}',\mathbf{k}';\omega)_+-\Gamma_{\mathbf{k}''}\langle\pi_{\mathbf{K}-\mathbf{k}}\rangle\Gamma_{\mathbf{K}'}(\mathbf{k}')^*\delta(\omega)\}.\end{aligned} \quad (7.8)$$

In order that the assumed spectral form of (7.6) be consistent with (7.8) for $\omega = 0$, we must have

$$\begin{aligned}0 &= \Delta^{\mathbf{k}}\varepsilon_{\mathbf{p}}\gamma_{\mathbf{K}}(\mathbf{p};\mathbf{k})+\sum_{\mathbf{k}''}u(\mathbf{k}'')[\gamma_{\mathbf{K}}(\mathbf{p}-\tfrac{1}{2}\mathbf{k}'';\mathbf{k}-\mathbf{k}'')-\gamma_{\mathbf{K}}(\mathbf{p}+\tfrac{1}{2}\mathbf{k}'';\mathbf{k}-\mathbf{k}'')] \\ &\quad +\sum_{\mathbf{k}''}w(\mathbf{k}'')\Gamma_{\mathbf{k}''}[\gamma_{\mathbf{K}-\mathbf{k}''}(\mathbf{p}-\tfrac{1}{2}\mathbf{k}'';\mathbf{k}-\mathbf{k}'')-\gamma_{\mathbf{K}-\mathbf{k}''}(\mathbf{p}+\tfrac{1}{2}\mathbf{k}'';\mathbf{k}-\mathbf{k}'')] \\ &\quad +\sum_{\mathbf{k}''}w(\mathbf{k}'')[\gamma_{\mathbf{k}-\mathbf{k}''}(\mathbf{p}-\tfrac{1}{2}\mathbf{k}'')-\gamma_{\mathbf{k}-\mathbf{k}''}(\mathbf{p}+\tfrac{1}{2}\mathbf{k}'')][\Gamma_{\mathbf{K}+\mathbf{k}''-\mathbf{k}}(\mathbf{k}'')-\Gamma_{\mathbf{k}''}\langle\pi_{\mathbf{K}-\mathbf{k}}\rangle].\end{aligned} \quad (7.9)$$

† Cf. (3.2). As has been discussed in ref [5]), the $\omega = 0$ component is not specified by the commutator (4.6). Since it is precisely that component which is relevant to consistency considerations, we must introduce in place of (4.6) one of the separate components such as (7.6a).

When $u(\mathbf{k} \neq 0) = 0$, (7.9) reduces to (7.5). In the more general case (7.9) is identical with (7.3) for $\mathbf{K} = \mathbf{k}$ while, when $\mathbf{K} \neq \mathbf{k}$, the last term of (7.9) includes additional higher-order correlation effects not taken into account in (7.2) and (7.3).

The $u(\mathbf{k} \neq 0) = 0$ case may be interpreted by means of the equivalence relations of sect. 6. In this regard we observe from (7.2) that the effective potential $w\Gamma$ seen by a particular particle of the self-bound system incorrectly includes the contribution arising from that particle itself. In physical systems such as crystals for which the mean separation is of the order of the range of the interparticle force, this error is important and must be taken into account, although it is less important in those systems for which the mean separation is less than the force range. The incorrect treatment of such "self-energy" effects results from the too simple factorization (4.4) used in the present paper. By including $t$-matrix and other correlation effects we could eliminate errors of this type.

One may ask whether there exist different sets $\{\Gamma_{\mathbf{k}}, \gamma_{\mathbf{k}}\}$ which are simultaneously admissible solutions of the consistency equations. We assert that in an accurate treatment such solutions do exist for those special values of $(\alpha, \beta)$ which characterize the thermodynamic multi-phase regions. When such simultaneously stable solutions do exist, the partition function (1.1) is to be approximated by a weighted average over all stable configurations, the weighting being equal to the concentration of each phase. (Compare the discussion preceding (4.2) where we emphasized that in the equations of sect. 4 each phase must be treated separately. The weighted multi-phase average is performed only after the sect. 4 computations have been completed.) In general, for simultaneously admissible stable solutions the stability criterion will be barely met and a small change in $(\alpha, \beta)$ will usually eliminate at least one of the solutions. "Critical points" are characterized by those multi-phase values of $(\alpha, \beta)$ for which two simultaneously admissible solutions merge into one.

We wish to emphasize that approximations of the type presented in this paper are least accurate, as representations of the equilibrium situation, for $(\alpha, \beta)$ in the neighbourhood of the phase transiton points. The reason for this is clear if one recalls that our approximations were based upon the assumption that by virtue of a singular equilibrium weight function of the B-E type a single spectral component dominates various matrix elements. In such an approximation scheme a single spectral component is given its equilibrium weighting while the remaining components are neglected completely. By neglecting those components, we essentially replace the equilibrium $\beta$-dependent weight function by a weight function appropriate to a metastable ensemble. The distinction is of course important only when the stable and metastable weight functions, so to speak, are considerably different — when the frequency

of one or more of the neglected components approaches the singularity of the equilibrium weight function, the situation which obtains in the neighbourhood of the phase transition points. It is clear therefore that we cannot expect to compute a smooth equilibrium phase-transition characteristic unless we include, with their *equilibrium* weighting, all spectral components in the neighbourhood of the weight-function singularity. Such a computation would involve a set of coupled intrinsically non-linear equations, each of complexity comparable to the consistency equations presented in this section.

I am indebted to Prof. G. Brown, Prof. P. C. Martin, Prof. B. Mottelson, Dr. V. Ambegaokar, and Dr. L. Kadanoff for helpful comments relative to multi-phase systems. I am also grateful to Profs. N. and A. Bohr for the hospitality extended to me at the Institute for Theoretical Physics, Copenhagen.

*Note added in proof:* In section 2 we admit only representations of the expectation value $\langle \rho^{\mathbf{k}} \rangle$ which for $\mathbf{k} = 0$ vanish continuously as $u(\mathbf{k} = 0) \to 0$. Such functions reflect the correct invariance properties implicit in (1.1b) when $[H, \mathbf{P}] = 0$. If we evaluate $\langle \rho^{\mathbf{k}} \rangle$ from the $G_1$ of (2.5), treating the coupled equations as a non-linear system, we find that there *do* exist additional stable non-physical solutions which correspond for $u(\mathbf{k}) = 0$ to the "external-potential" solutions of sect. 6. As representations of $\langle \rho^{\mathbf{k}} \rangle$ such solutions violate the momentum conservation properties of (1.1b). Moreover, they do not reflect the real physical distinction between a self-consistent field and an external potential. [Cf. eqs. (2.5), (2.6) with (4.3), (4.7).] They are not suitable for describing, for example, the centre-of-mass oscillations of the composite self-bound system in a shallow external well.

## References

1) P. C. Martin and J. Schwinger, Phys. Rev. **115** (1959) 1342
2) H. D. Ursell, Proc. Camb. Phil. Soc. **23** (1927) 685;
J. G. Kirkwood, Jour. Chem. Phys. **3** (1935) 300;
J. E. Mayer and M. G. Mayer, Statistical Mechanics (J. Wiley and Sons, New York, 1940);
M. Born and H. S. Green, Proc. Roy. Soc. **188** (1946) 10
3) E. Salpeter, Ann. Phys. **5** (1958) 183
4) J. R. Ehrman, L. D. Fosdick, and D. C. Handscomb, Jour. Math. Phys. **1** (1960) 547
5) D. E. McCumber, Supp. Nuovo Cim. **17** (1960) 8
6) G. E. Brown, J. A. Evans and D. J. Thouless, Nuclear Physics **24** (1961) 1
7) L. P. Kadanoff and P. C. Martin, Phys. Rev. (to be published)
8) A. Bardasis and J. R. Schrieffer, Phys. Rev. **124** (1961) 1050
9) V. G. Soloviev, Dubna Publication D-545 (1960)
10) D. J. Thouless, Nuclear Physics **21** (1960) 225

1.D.1:
2.C

*Nuclear Physics* **26** (1961) 306—320; © *North-Holland Publishing Co., Amsterdam*
Not to be reproduced by photoprint or microfilm without written permission from the publisher

# REDUCED WIDTHS FOR NUCLEON CLUSTERS IN SHELL MODEL

Yu. F. SMIRNOV and D. CHLEBOWSKA †

*Nuclear Physics Research Institute, Moscow State University, Moscow, USSR*

Revceived 8 December 1960

**Abstract:** The reduced widths of nucleon clusters for certain low levels of p-shell nuclei are calculated on the basis of the shell-model. The results of the calculation are in good agreement with experiment. In certain cases when the nature of the excited state is not uniquely determined, the comparison with experiment of the reduced widths of nucleon clusters for different variants of the structure of the wave functions makes it possible to eliminate non-uniqueness. The formal problems involved in calculation techniques are treated in detail. Simple expressions for the fractional parentage coefficients are given for the separation of several nucleons.

## 1. Introduction

In a number of investigations in recent years it has been established that the model of independent particles takes into account the clustering of nucleons in nuclei to an essential degree and that in the structure of the wave functions of this model there appear some features of the α-particle model and the model of resonating group structure [1]). In particular it was shown that the wave function $|s^4 p^4\rangle$ of $Be^8$ is an anti-symmetrized product of the wave functions of two α-clusters by the wave function of their relative motion. The wave function $|s^4 p^2\rangle$ of $Li^6$ is a product of the wave functions of a deuteron and an α-cluster by the function of their relative motion, etc. These properties of the shell model served as a basis for a method of calculating the reduced widths for the emission of nucleon clusters from light nuclei, proposed in ref. [2]). Calculated by this method, the reduced widths for several simple nuclei proved to be in good agreement with experiment. Yet the calculation techniques were treated in this paper very briefly and a number of essentials was omitted. In the present paper we calculate the reduced widths for more complex nuclei, compare the results with experiment and offer a sufficiently detailed exposition of the calculation techniques for the reduced widths.

Wigner and Teichman [3]) pointed out that the reduced widths can be useful for the analysis of the structure of nuclear states. Lane [4]) obtained an expression for the reduced nucleon width in the shell model in *LS*, *jj* and intermediate coupling. Thus in *LS* coupling the reduced width for the emission of a nucleon from the nucleus whose incomplete shell is described by the configuration

† On leave from the Theoretical Physics Institute of the Academy of Sciences of Poland.

$|l^n L_1 S_1 J_1 T_1\rangle$, by a transition to the final state $|l^{n-1} L_2 S_2 J_2 T_2\rangle$, is equal to

$$\theta^2_{\text{nucleon}} = \tfrac{2}{3} n \langle l^n L_1 S_1 T_1 | l^{n-1} L_2 S_2 T_2\rangle^2 U^2(L_2 S_2 j \tfrac{1}{2}; J_2 S_1) \times U^2(l L_2 J_1 S_1; L_1 j)(T_2 T_{2z} \tfrac{1}{2}\tau | T_1 T_{1z})^2. \quad (1)$$

Here the reduced width $\theta^2$ is measured in units of the Wigner limit $\frac{3}{2}\hbar^2/\mu a$ ($\mu$ is the reduced mass of the decay products of the compound nucleus, $a$ the radius of the channel surface), $\langle l^n L_1 S_1 T_1 | l^{n-1} L_2 S_2 T_2\rangle$ is the fractional parentage coefficient [4]), $j$ is the channel spin, $l$ is the orbital momentum of the outgoing nucleon, $U(abcd; ef)$ are the Racah coefficients [5]) and $(T_2 T_{2z} \frac{1}{2}\tau | T_1 T_1)$ is the coefficient of vector addition.

From eq. (1) it is clear that the reduced width for the emission of an $\alpha$-particle must be proportional to the square of the fractional parentage coefficient for the separation of four nucleons in a state with zero spin and zero isobaric spin

$$\langle l^n L_1 S_1 T_1 | l^{n-4} L_2 S_2 T_2, l^4 \Lambda\ S = 0 \quad T = 0\rangle.$$

This fact is mentioned in passing in the paper by Lane and Wilkinson [6]). An elaborate derivation of the formula for the reduced width for an $\alpha$-particle is performed in ref. [2]). The general formula for the reduced widths for emission of a cluster of $m$ nucleons ($m = 1, 2, 3, 4$) from a nucleus with atomic number $A$, the incomplete shell of which is in the state $|l^n [f_1] L_1 S_1 J_1 T_1\rangle$, by a transition to the state $|l^{n-m} [f_2] L_2 S_2 J_2 T_2\rangle$, is of the form

$$\theta^2_{m\Lambda J_1 J_2} = \tfrac{2}{3}\left(\frac{A}{A-m}\right)^N \binom{n}{m} \sum_{L_3 J_3} \langle l^n [f_1] L_1 S_1 T_1 | l^{n-m} [f_2] L_2 S_2 T_2;\ l^m [f_3] L_3 S_3 T_3\rangle^2 \times K_m^2(N\Lambda, L_3) U^2(S_1 L_2 J_1 L_3; J_3 L_1) U^2(L_2 S_2 J_3 S_3; J_2 S_1)(T_2 T_{2z} T_3 T_{3z} | T_1 T_{1z})^2. \quad (2)$$

This formula was obtained using oscillator shell functions under the assumption that all preceding shells, with the exception of the last $l^n$, are filled. Let us explain the notations in eq. (2); $[f_i]$ is a symbol of Young's scheme [5]), $J_3$ is the channel spin, $\Lambda$ is the orbital momentum of the outgoing particle and

$$\binom{n}{m}$$

is the binomial coefficient taking into account the identity of nucleons. The coefficient $K_m^2$ $(N\Lambda, L_3)$ represents a statistical weight of the product $\psi_{N\Lambda}$ $(\mathbf{R}_m)$ $\psi_m$ (*internal*) in the function $|l^m [f_3] L_3 S_3 T_3\rangle$, where $\psi_{N\Lambda}$ $(\mathbf{R}_m)$ is the oscillator function of the centre-of-mass motion of the cluster of $m$ nucleons and $\psi_m$ (*internal*) is the function of the internal motion of this aggregate. The factor $(A/A-m)^N$ gives a correction taking into account the motion of the general centre of mass. In eq. (1) this correction is not taken into account because it scarcely differs from unity.

Eq. (2) is a generalization of eq. (1). It is clear that for calculating the reduced width one must be able to determine the fractional parentage coefficients $\langle l^n | l^{n-m}; l^m \rangle$ and the factor $K_m\,(N\Lambda, L_3)$ and for more complex configurations it is necessary to modify the correction for the motion of the general centre of mass. In section 2 of the present paper we consider the methods of obtaining all these factors. In section 3 we make an analysis of the reduced widths of certain nuclear levels of the p-shell.

## 2. Elements of Formalism

### 2.1. FRACTIONAL PARENTAGE COEFFICIENTS

The formula for the nucleon reduced width (1) contains fractional parentage coefficients for the separation of one particle. There is already extensive literature (see ref. [5])) on the properties and methods of calculation of these fractional parentage coefficients. For the case of $LS$-coupling tables of these coefficients are given for the p-shell by Jahn and Van Wieringen, and for the configurations $d^3$, $d^4$ by Jahn [7, 8]). For the case of $jj$-coupling, the coefficients have been calculated for $j = \frac{3}{2}$ and $\frac{5}{2}$ by Edmonds and Flowers [8]).

We are chiefly interested in the reduced widths for deuterons, tritons ($He^3$) and $\alpha$-particles. Therefore we need the coefficients for separation of two, three and four particles. A general method of calculating the coefficients for separation of an arbitrary number of particles was evolved by Jahn [9]), but this method is inconvenient for specific applications since it requires rather cumbersome calculations. Therefore we shall consider specifically all three types of fractional parentage coefficients necessary to us.

(i) $\langle l^n | l^{n-2}, l^2 \rangle$.

These coefficients are expressed in a simple way [8]) through the coefficients $\langle l^n | l^{n-1} \rangle$ and $\langle l^{n-1} | l^{n-2} \rangle$:

$$\begin{aligned}\langle l^n \alpha LST | l^{n-2} \alpha_1 L_1 S_1 T_1, l^2 L_0 S_0 T_0 \rangle \\ = \sum_{\alpha_2 L_2 S_2 T_2} \langle l^n \alpha LST | l^{n-1} \alpha_2 L_2 S_2 T_2 \rangle \langle l^{n-1} \alpha_2 L_2 S_2 T_2 | l^{n-2} \alpha_1 L_1 S_1 T_1 \rangle \\ \times U(L_1 l L l; L_2 L_0) U(S_1 \tfrac{1}{2}\, S \tfrac{1}{2}; S_2 S_0) U(T_1 \tfrac{1}{2}\, T \tfrac{1}{2}; T_2 T_0).\end{aligned} \tag{3}$$

For the p-shell there is a complete table of the coefficients for separation of two particles [10]).

(ii) $\langle l^n | l^{n-3}, l^3 \rangle$.

These coefficients can be expressed through $\langle l^n | l^{n-1} \rangle$, $\langle l^{n-1} | l^{n-3}, l^2 \rangle$ and $\langle l^3 | l^2 \rangle$ with the aid of a formula analogous to (3). Using the definition of the

coefficients $\langle l^3|l^2\rangle$,

$$|l^3[f_3]L_3S_3T_3\rangle = \sum_{L_0S_0T_0} \langle l^3[f_3]L_3S_3T_3|l^2L_0S_0T_0\rangle \times |l^2L_0S_0T_0, l : L_3S_3T_3\rangle,$$

we have in complete analogy with (3)

$$\begin{aligned}&\langle l^n[f_1]\alpha_1L_1S_1T_1|l^{n-3}[f_2]\alpha_2L_2S_2T_2, l^3[f_3]\alpha_3L_3S_3T_3\rangle \\ &\quad = \sum_{\substack{[f_4]\alpha_4L_4S_4T_4 \\ L_0S_0T_0}} \langle l^n[f_1]\alpha_1L_1S_1T_1|l^{n-1}[f_4]\alpha_4L_4S_4T_4\rangle \\ &\quad \times \langle l^{n-1}[f_4]\alpha_4L_4S_4T_4|l^{n-3}[f_2]\alpha_2L_2S_2T_2, l^2L_0S_0T_0\rangle \langle l^3[f_3]\alpha_3L_3S_3T_3|l^2L_0S_0T_0\rangle \\ &\quad \times U(L_2L_0Ll; L_4L_3)U(S_2S_0S\tfrac{1}{2}; S_4S_3)U(T_2T_0T\tfrac{1}{2}; T_4T_3).\end{aligned} \tag{4}$$

(iii) $\langle l^n|l^{n-4}, l^4\rangle$.

These coefficients can be expressed by means of $\langle l^n|l^{n-2}, l^2\rangle$, $\langle l^{n-2}|l^{n-4}, l^2\rangle$ and $\langle l^4|l^2, l^2\rangle$. Using the definition of the coefficients $\langle l^4|l^2, l^2\rangle$,

$$\begin{aligned}|l^4[f_3]\alpha_3L_3S_3T_3\rangle = \sum_{\substack{L_0S_0T_0 \\ L_{00}S_{00}T_{00}}} &\langle l^4[f_3]\alpha_3L_3S_3T_3|l^2L_0S_0T_0, l^2L_{00}S_{00}T_{00}\rangle \\ &\times |l^2L_0S_0T_0, l^2L_{00}S_{00}T_{00} : L_3S_3T_3\rangle,\end{aligned}$$

we obtain by analogy with (3) and (4)

$$\begin{aligned}&\langle l^n[f_1]\alpha_1L_1S_1T_1|l^{n-4}[f_2]\alpha_2L_2S_2T_2, l^4[f_3]\alpha_3L_3S_3T_3\rangle \\ &\quad = \sum_{\substack{[f_4]\alpha_4L_4S_4T_4 \\ L_0S_0T_0L_{00}S_{00}T_{00}}} \langle l^n[f_1]\alpha_1L_1S_1T_1|l^{n-2}[f_4]\alpha_4L_4S_4T_4, l^2L_{00}S_{00}T_{00}\rangle \\ &\quad \times \langle l^{n-2}[f_4]\alpha_4L_4S_4T_4|l^{n-4}[f_2]\alpha_2L_2S_2T_2, l^2L_0S_0T_0\rangle \\ &\quad \times \langle l^4[f_3]\alpha_3L_3S_3T_3|l^2L_0S_0T_0, l^2L_{00}S_{00}T_{00}\rangle U(L_2L_0LL_{00}; L_4L_3) \\ &\quad \times U(S_2S_0SS_{00}; S_4S_3)U(T_2T_0TT_{00}; T_4T_3).\end{aligned}$$

2.2. COEFFICIENTS $K_m(N\Lambda, L_3)$

As has been pointed out above, the square of these coefficients represents a statistical weight of the product $\psi_{N\Lambda}(\mathbf{R}_m)\psi_m$ (*internal*) in the function $|l^m[f_3]\alpha_3L_3S_3T_3\rangle$. For finding these coefficients it is obviously necessary to isolate the motion of the centre-of mass of the entire cluster and choose the coefficient of the corresponding term. As functions of the internal motion of clusters we take the following:

for a deuteron

$$\psi_{\mathrm{d}}\,(intern)\,\psi_{00}(\mathbf{R}_2) = |\mathrm{s}^2[2]\; L = 0\; S = 1\; T = 0\rangle \equiv \psi_2^{\mathrm{shell}},$$

for a triton ($He^3$)

$$\psi_{\mathrm{t}}\,(intern)\,\psi_{00}(\mathbf{R}_3) = |\mathrm{s}^3[3]\; L = 0\; S = \tfrac{1}{2}\; T = \tfrac{1}{2}\rangle \equiv \psi_3^{\mathrm{shell}}, \tag{6}$$

and for an $\alpha$-particle

$$\psi_{\alpha}\,(intern)\,\psi_{00}(\mathbf{R}_4) = |\mathrm{s}^4[4]\; L = 0\; S = 0\; T = 0\rangle \equiv \psi_4^{\mathrm{shell}}.$$

The selection of internal functions for more complex aggregate, is similar. For example, for a fragment $Be^7$ we assume

$$\psi_{Be^7}^{ground}(intern)\psi_{00}(\mathbf{R}_7) = |s^4p^3[3]\, L=1\, S=\tfrac{1}{2}\, J=\tfrac{3}{2}\, T=\tfrac{1}{2}\rangle \equiv \psi_7^{shell}. \quad (7)$$

In all configurations on the right-hand sides the centre-of-mass moves only in the lowest state $\psi_{00}(\mathbf{R})$ since these configurations contain no more than one incomplete shell. From eqs. (6) and (7) as well as from the definition of the coefficients $K_m(N\Lambda, L_3)$ it follows that

$$K_m(N\Lambda, L_3) = \langle l^m[f_3]\, L_3 S_3 T_3 \left| \frac{\psi_{N\Lambda}(\mathbf{R}_m)}{\psi_{00}(\mathbf{R}_m)} \right| \psi_m^{shell} \rangle. \quad (8)$$

The expression $\psi_{N\Lambda}(\mathbf{R}_m)/\psi_{00}(\mathbf{R}_m)$ is a polynomial of degree $N$ in $\mathbf{R}_m = \sum_i \mathbf{r}_i/m$. With the aid of the fractional parentage coefficients one can calculate the matrix element on the right-hand side of eq. (8) and find the required coefficient.

In a number of cases it is possible not to use the general formula (8) but to calculate $K_m\,(N\Lambda, L_3)$ in a simpler way with the aid of the Talmi coefficients. Let us for example consider the function $\psi = |l^2[2] L_3\, S_3 = 1\, T_3 = 0\rangle$. This function can be re-written as a product of the orbital and spin-isobaric parts

$$\psi = |l^2 L_3 > \chi_{S=1\ T=0}. \quad (9)$$

The product of orbital functions of two nucleons can be transformed into the centre-of-mass system via the Talmi transformation [11])

$$|(nl)^2 L_3\rangle = \sum_{N\Lambda\nu\lambda M\mu} \langle nlnl : L_3 | N\Lambda\nu\lambda : L_3\rangle (\Lambda M\lambda\mu | L_3 M_3) \times \psi_{N\Lambda M}(\mathbf{R}_2)\psi_{\nu\lambda\mu}(\mathbf{r}_{12}). \quad (10)$$

Here $n$ is the main quantum number of each nucleon, $\langle n_1 l_1 n_2 l_2 : L | N\Lambda\nu\lambda : L\rangle$ is the Talmi coefficient, $\mathbf{r}_{12} = \mathbf{r}_1 - \mathbf{r}_2$, and $(\Lambda M\lambda\mu | L_3 M_3)$ is the vector addition coefficient. From the first equation (6) it is clear that

$$\psi_d(intern) \equiv \psi_{000}(\mathbf{r}_{12})\chi_{S=1\ T=0}.$$

Hence from eqs. (9) and (10) it follows that

$$K_d(N\Lambda, L_3) = \langle nlnl : L_3 | N\Lambda, 00 : L_3\rangle.$$

From the properties of the Talmi coefficients we have

$$L_3 = \Lambda, \qquad N = 2n.$$

Thus we finally obtain

$$K_d(NL_3, L_3) = \langle nlnl : L_3 | NL_3\, 00 : L_3\rangle. \quad (11)$$

If we deal with nucleons of different shells, e.g. the function $|l_1 l_2 : L_3\rangle \chi_{S=1\ T=0}$,

then, taking into account the symmetry of the orbital function

$$|l_1 l_2 : L_3\rangle = \frac{1}{\sqrt{2}} \sum_{m_1 m_2} (l_1 m_1 l_2 m_2 | L_3 M_3)\{\psi_{n_1 l_1 m_1}(1)\psi_{n_2 l_2 m_2}(2) + \psi_{n_1 l_1 m_1}(2)\psi_{n_2 l_2 m_2} \quad (1)\},$$

we obtain similarly

$$K_d(n_1 + n_2\, L_3,\, L_3) = \sqrt{2}\langle n_1 l_1 n_2 l_2 : L_3 | n_1 + n_2\, L_3,\, 00 : L_3\rangle. \qquad (12)$$

For convenience we give below (eq. (21)) the general formula for the Talmi coefficients entering into eqs. (11) and (12).

Now let us consider the function $|l^3[3] L_3 S_3 = \frac{1}{2}\, T_3 = \frac{1}{2}\rangle$. It is known that the function belonging to a Young scheme [3] can also be written as a product of the orbital and spin-isobaric parts

$$|l^3[3] L_3\, S_3 = \tfrac{1}{2}\, T_3 = \tfrac{1}{2}\rangle = |l^3[3] L_3\rangle\, \chi_{S=\frac{1}{2}\, T=\frac{1}{2}}. \qquad (12')$$

Now let us isolate the motion of the centre-of-mass in the orbital part. Using the orbital fractional parentage coefficients it can be written

$$|l^3[3] L_3 M_3\rangle = \sum_{L_0} \langle l^3[3] L_3 | l^2 L_0\rangle |l^2 L_0,\, l : L_3 M_3\rangle. \qquad (13)$$

Let us pass to the centre-of-mass system of the first two nucleons:

$$|l^2 L_0\rangle = \sum_{N\Lambda\nu\lambda} \langle nlnl : L_0 | N\Lambda\nu\lambda : L_0\rangle\, |N\Lambda(\mathbf{R}_2),\, \nu\lambda(\mathbf{r}_{12}) : L_0\rangle. \qquad (14)$$

Now let us consider the product of the function of the centre-of-mass of the first two nucleons by the function of the third nucleon

$$\psi_{N\Lambda M}(\mathbf{R}_{12})\psi_{nlm}(\mathbf{r}_3)$$

and pass to new variables: the coordinates of the general centre-of-mass $\mathbf{R}_3 = \frac{2}{3}\mathbf{R}_{12} + \frac{1}{3}\mathbf{r}_3$ and $\boldsymbol{\rho} = \mathbf{R}_{12} - \mathbf{r}_3$. In fact this will be the transition to the centre-of-mass system for a particle of mass 2 corresponding to the function $\psi_{N\Lambda M}(\mathbf{R}_{12})$ and for particle no. 3 of mass 1. Both of them are moving in the oscillator potential of frequency $\omega$. This transition is effected using the Talmi coefficients for particles with different masses. The theory of these coefficients is set down in ref. [12]) which also contains the general formula for these coefficients. They are designated similarly to the Talmi coefficients used before, viz. by

$$\langle n_1 l_1 n_2 l_2 : L | \mu_1 \mu_2 | N\Lambda\nu\lambda : L\rangle, \qquad (15)$$

where $\mu_1$ and $\mu_2$ are the masses of the first and second particles respectively. The usual Talmi coefficients correspond to $\mu_1 = \mu_2 = 1$. Using the coefficients

(15) one may write

$$|N\Lambda(\mathbf{R}_{12}), nl(\mathbf{r}_3) : LM\rangle = \sum_{N'\Lambda'\nu'\lambda'} \langle N\Lambda nl : L|2, 1|N'\Lambda'\nu'\lambda' : L\rangle |N'\Lambda'(\mathbf{R}_3), \nu'\lambda'(\boldsymbol{\rho}) : L\rangle. \quad (16)$$

It can readily be seen from (6) that the function $\psi_t$ (*intern*) corresponds to $\nu = \lambda = \nu' = \lambda' = 0$. Hence with the aid of (13), (14) and (16) we obtain

$$K_t(N\Lambda, L_3) = \delta_{N,3n}\delta_{\Lambda,L_3} \sum_{L_0} \langle l^3[3]L_3|l^2L_0\rangle \times \langle nlnl : L_0|1, 1|2nL_0, 00 : L_0\rangle \langle 2nL_0, nl : L_3|2, 1|3nL_3, 00 : L_3\rangle. \quad (17)$$

If the three isolated nucleons belong to different shells it is not difficult to introduce the necessary changes into eq. (17), similarly to the transition from (11) to (12). For $\alpha$-particles the motion of the centre-of-mass can be isolated by two methods. The first consists in isolating the centre-of-mass of nucleons nos. 1, 2 and nos. 3, 4 separately. Then the motion of the general centre-of-mass is determined from the product of the wave functions of these centres-of-mass. The transitions similar to those which led to eq. (17) then yield

$$\begin{aligned} K_\alpha(N\Lambda, L_3) = \delta_{N,4n}\delta_{\Lambda,L_3} \sum_{L',L''} &\langle l^4[4]L_3|l^2L', l^2L''\rangle \\ &\times \langle nlnl : L'|1, 1|2nL', 00 : L'\rangle \langle nlnl : L''|1, 1|2nL'', 00 : L''\rangle \\ &\times \langle 2nL', 2nL'' : L_3|2, 2|4nL_3, 00 : L_3\rangle. \end{aligned} \quad (18)$$

In the second method the centre-of-mass of the first three nucleons is isolated using eq. (17) and then the general centre of mass is determined from the product of the function of the centre-of-mass of the three nucleons by the function of the last nucleon. Thus we have

$$\begin{aligned} K_\alpha(N\Lambda, L_3) = \delta_{N,4n}\delta_{\Lambda,L_3} \sum_{L'} &\langle l^4[4]L_3|l^3[3]L'\rangle \\ &\times K_t(3nL', L')\langle 3nL', nl : L_3|3, 1|4nL_3, 00 : L_3\rangle. \end{aligned} \quad (19)$$

Eqs. (17), (18) and (19) contain *only the orbital parts* of the fractional parentage coefficients.

If one of the four particles belongs to another shell, then, taking account of the symmetry of the orbital part of the wave function,

$$\begin{aligned} |l^3[3]L_3\, S_3 = \tfrac{1}{2}\, T_3 = \tfrac{1}{2}, l' : \Lambda\, S = 0\, T = 0\rangle \\ = \tfrac{1}{2}(1 - \sum_{i=1}^{3} P_{i4})|l^3[3]L_3\, S_3 = \tfrac{1}{2}\, T_3 = \tfrac{1}{2}(\mathbf{r}_1\mathbf{r}_2\mathbf{r}_3),\ l'(\mathbf{r}_4) : \Lambda\, S = 0\, T = 0\rangle, \end{aligned}$$

where $P_{ik}$ is the operator of the permutation of nucleons with the numbers $i$ and $k$, we obtain a somewhat modified eq. (19):

$$K_\alpha(N\Lambda, \Lambda) = 2K_t(3nL_3, L_3)\langle 3nL_3, nl : \Lambda|3, 1|4n\Lambda, 00 : \Lambda\rangle. \quad (20)$$

In conclusion of this subsection we give the formula for the Talmi coefficients entering into eqs. (11), (12), (17) and (20):

$$\langle n_1 l_1 n_2 l_2 : \Lambda | \mu_1 \mu_2 | n_1+n_2 \Lambda, 00 : \Lambda \rangle$$

$$= (-1)^{\frac{1}{2}(\Lambda+l_1+l_2)} 2^{\frac{1}{2}(l_1+l_2-\Lambda)} \sqrt{\frac{(\frac{1}{2}(n_1+n_2-\Lambda))!(\Lambda+n_1+n_2+1)!!}{(\frac{1}{2}(n_1-l_1))!(\frac{1}{2}(n_2-l_2))!(n_1+l_1+1)!!(n_2+l_2+1)!!}}$$

$$\times \frac{\mu_1^{\frac{1}{2}n_1} \mu_2^{\frac{1}{2}n_2}}{(\mu_1+\mu_2)^{\frac{1}{2}(n_1+n_2)}} (l_1 0 l_2 0 | \Lambda 0) \sqrt{\frac{(2l_1+1)(2l_2+1)}{(2\Lambda+1)}}. \qquad (21)$$

It will be noted that in ref. [12]) and in the present work the main quantum numbers $n$ of the oscillator functions are designated differently. In the present work the eigenvalue of the energy is

$$E_n = (n+\tfrac{3}{2})\hbar\omega$$

whereas in ref. [12]) it was

$$E_n = (2n+l+\tfrac{3}{2})\hbar\omega.$$

In the model of independent particles the centre-of mass of the nucleus does not remain at rest but oscillates in the oscillator potential with the same frequency as individual nucleons. If all shells except the last are filled, the centre of mass of the nucleus moves in the lowest state $\psi_{00}(\mathbf{R})$, as was shown in ref. [13]). If the configuration is more complex, the wave function may contain an admixture of higher excited states of the motion of the centre-of-mass (known as "spurious" states).

If the configurations of the initial and final nucleus are such that their centres-of-mass move in the lowest state, then, as was established in ref. [2]), it is necessary, in calculating the reduced width, to take into account only the state of the outgoing particles in which their general centre-of-mass moves in the same lowest state. Taking account of this fact leads to the appearance in eq. (2) of the factor

$$\langle 00N\Lambda : \Lambda | A-m, m | 00N\Lambda : \Lambda \rangle^{-2}. \qquad (22)$$

The formula for this Talmi coefficient is similar to (21) and gives the value $A/(A-m)^N$ for the factor (22). If the configurations are complicated it is necessary to take a certain mixture of several configurations to eliminate the admixture of spurious states. In the general case the construction of regular functions is performed by diagonalizing the Hamiltonian of the centre-of-mass

$$H_{\text{c.m.}} = -\frac{\hbar^2}{2M} \Delta_R + \tfrac{1}{2} M\omega^2 R^2.$$

2.3. $jj$-COUPLING

For the case of $jj$-coupling the general principle of calculation of the reduced width remains the same. The expression for $\theta_m^2$ similar to eq. (2) will contain the fractional parentage coefficients for separation of 2,3 etc. particles in $jj$-coupling. For describing the internal motion of clusters we again take the wave functions (6). Now it is necessary to isolate, from the functions of separated particles in $jj$-coupling the components with internal motion described by the functions (6). For this purpose it is necessary to pass from $jj$-coupling to $LS$-coupling.

The expression for the deuteron width will contain the coefficient $\langle j^2 J\, T = 0 | l^2 L\, S = 1\, J\, T = 0\rangle$. The latter can be simply expressed through the $9j$-symbol:

$$\langle j^2 J\, T = 0 | l^2 L\, S = 1\, J\, T = 0\rangle = \begin{Bmatrix} l & l & L \\ \frac{1}{2} & \frac{1}{2} & 1 \\ j & j & J \end{Bmatrix} (2j+1)\sqrt{3(2L+1)}. \quad (23)$$

The calculations of $9j$-symbols in this formula offers no difficulties since in ref. [15]) there are simple formulas for them. Using the fractional parentage coefficients in $LS$ and $jj$ coupling and eq. (23) it is possible to pass from $jj$ to $LS$ coupling for three or four particles as well:

$$\langle j^3 \alpha JT | l^3 \beta LST : J\rangle = \sum_{L_0 S_0 L_0 T_0} \langle j^3 \alpha JT | j^2 J_0 T_0\rangle \langle l^3 \beta LST | l^2 L_0 S_0 T_0\rangle \quad (24)$$

$$\times \begin{Bmatrix} L_0 & S_0 & J_0 \\ l & \frac{1}{2} & j \\ L & S & J \end{Bmatrix} \begin{Bmatrix} l & l & L_0 \\ \frac{1}{2} & \frac{1}{2} & S_0 \\ j & j & J_0 \end{Bmatrix} (2j+1)\sqrt{(2L_0+1)(2S_0+1)(2J_0+1)(2j+1)(2L+1)(2S+1)},$$

$$\langle j^4 \alpha JT | l^4 \beta LST : J\rangle = \sum_{\substack{L_0 S_0 J_0 T_0 \\ L_{00} S_{00} J_{00} T_{00}}} \langle j^4 \alpha JT | j^2 J_0 T_0, j^2 J_{00} T_{00}\rangle$$

$$\times \langle l^4 \beta LST | l^2 L_0 S_0 T_0, l^2 L_{00} S_{00} T_{00}\rangle \begin{Bmatrix} l & l & L_0 \\ \frac{1}{2} & \frac{1}{2} & S_0 \\ j & j & J_0 \end{Bmatrix} \begin{Bmatrix} l & l & L_{00} \\ \frac{1}{2} & \frac{1}{2} & S_{00} \\ j & j & J_{00} \end{Bmatrix} \quad (25)$$

$$\times \begin{Bmatrix} L_0 & S_0 & J_0 \\ L_{00} & S_{00} & J_{00} \\ L & S & J \end{Bmatrix} (2j+1)^2$$

$$\times [(2L_0+1)(2S_0+1)(2L_{00}+1)(2S_{00}+1)$$

$$\times (2J_0+1)(2J_{00}+1)(2L+1)(2S+1)]^{\frac{1}{2}}.$$

Effecting the transition to $LS$ coupling we isolate the motion of the centre of mass of a cluster by eqs. (11), (12), (17) and (20). As a result the expression for the reduced width for the emission of a cluster of $m$ nucleons from the nucleus with an incomplete shell in the state $|j^n \alpha_1 J_1 T_1\rangle$ by a transition to the state

$|j^{n-m}\alpha_2 J_2 T_2\rangle$ has the form

$$\theta^2_{mAJ_1J_3} = \tfrac{2}{3}\left(\frac{A}{A-m}\right)^N \binom{n}{m} \sum_{J_4}\{\sum_{\alpha_3 J_3 L_3} \langle j^n\alpha_1 J_1 T_1|j^{n-m}\alpha_2 J_2 T_2, j^m\alpha_3 J_3 T_3\rangle$$
$$\times\langle j^m\alpha_3 J_3 T_3|l^m[f_0]L_3 S_0 T_0\rangle K_m(N\Lambda, L_3)U(\Lambda L_0 J_3 S_0; L_3 J_0) \qquad (26)$$
$$\times U(\Lambda J_0 J J_2; J_3 J_4)\}^2.$$

Here $J_4$ is the channel spin and $L_0$, $S_0$, $J_0$ are the orbital momentum, spin and total internal momentum of the cluster contained in the cluster wave function $|s^4p^{m-4}L_0S_0J_0T_0\rangle$. The fractional parentage coefficients in $jj$-coupling are calculated by eqs. (3), (4) and (5), where $l$, $L$ should be replaced by the correspinding $j$, $J$ everywhere, the designations of the spin dropped and the Racah coefficients containing spins discarded.

Using eqs. (2) and (26) it is possible to calculate the reduced width also for the case of intermediate coupling but we shall not quote this expression because it is too cumbersome. It should be emphasized once again that eqs. (2) and (26) are obtained for nuclear states which have only one incomplete shell. If there are several incomplete shells, and admixture of "spurious" states should be taken into account.

## 3. Results of Calculations

In ref. [2]) the reduced width for nucleon clusters was calculated for the case of several simple nuclei. In the present paper an analysis is made of the available experimental data on the reduced widths for nucleon clusters in the region of the p-shell nuclei at not too high excitations. ($\lesssim$ 10 MeV). Admittedly the amount of these data is at present not large, in particular because in many cases nucleon clusters in low states of nuclei are bound. The reduced widths for such levels can be determined from the cross-sections of direct reactions and there are already determinations of this kind [16]). It should be noted, however, that the question of deriving the reduced widths from the experimental cross sections of direct reactions has not yet been sufficiently worked out. Many values of reduced widths for highly excited states of nuclei have been measured, but the question of the structure of their wave functions is still quite unclear.

The basic results of our calculations are given in table 1. The experimental values of the reduced widths are taken from the survey of ref. [17]). We shall comment in detail on some results.

### 3.1. THE NUCLEUS $Li^5(He^5)$

Of interest is the second excited level of energy 16.7 MeV which manifests itself in the reactions $H^3$(d, n) $He^4$, $He^3$(d, p)$He^4$. The deuteron reduced width of this level is equal in order of magnitude to one Wigner unit and the nucleon

TABLE 1

Results of calculations of reduced transition widths

| Nucleus | $E^*$ (MeV) | $J^\pi, T$ | Wave function | Decay mode | $A$ | $\theta^2_{\text{theor}}$ | $\theta^2_{\text{exp}}$ | $R$ (fm) |
|---|---|---|---|---|---|---|---|---|
| $He^5$ | 16.69 | $\frac{3}{2}^+, \frac{1}{2}$ | $s^3\, L_1=0\, S_1=\frac{1}{2}\, T_1=\frac{1}{2}$, $p^2\, L_2=0$, $S_2=1\, T_2=0$: $J=\frac{3}{2}\, T=\frac{1}{2}$ | $H^3+d$ | 0 | 0.9 | 1.0 (0.7) | 5 (7) |
| $Li^5$ | 16.81 | $\frac{3}{2}^+, \frac{1}{2}$ | | $He^3+d$ | 0 | | 1.4 (0.7) | |
| $Li^6$ | 0 | $1^+, 0$ | $p^2[2]\ L=0\ S=1\ T=0\ J=1$ | $He^4+d$ | 0 | 0.75 | 0.51, 0.3–0.45 | 5 |
| | 2.183 | $3^+, 0$ | $p^2[2]\ L=2\ S=1\ T=0\ J=3$ | | 2 | 0.75 | 0.8 | 3.5 |
| | 4.52 | $2^+, 0$ | $p^2[2]\ L=2\ S=1\ T=0\ J=2$ | | 2 | 0.75 | 1.0 | |
| | 4.9–5.8 | $1^+, 0$ | $p^2[2]\ L=2\ S=1\ T=0\ J=1$ | | 2 | 0.75 | 0.2–1.0 | |
| $Li^7$ | 0 | $\frac{3}{2}^-, \frac{1}{2}$ | $p^3[3]\ L=1\ S=\frac{1}{2}\ T=\frac{1}{2}\ J=\frac{3}{2}$ | $He^4+H^3$ | 1 | 0.8 | (≈1.0) | 2.8 |
| | 0.48 | $\frac{1}{2}^-, \frac{1}{2}$ | $p^3[3]\ L=1\ S=\frac{1}{2}\ T=\frac{1}{2}\ J=\frac{1}{2}$ | | 1 | 0.8 | (≈1.0) | 2.8 |
| | 4.63 | $(\leq\frac{7}{2}^-, \frac{1}{2})$ | $p^3[3]\ L=3\ S=\frac{1}{2}\ T=\frac{1}{2}\ J=\frac{7}{2}$ | | 3 | 0.8 | 0.5±0.2 | |
| $Be^7$ | 4.53 | $\frac{7}{2}^-, \frac{1}{2}$ | $p^3[3]\ L=3\ S=\frac{1}{2}\ T=\frac{1}{2}\ J=\frac{7}{2}$ | $He^4+He^3$ | 3 | 0.8 | 0.36 | 4.4 |
| $Li^7$ | 7.47 | $\frac{5}{2}^-, \frac{1}{2}$ | $p^3[3]\ L=3\ S=\frac{1}{2}\ T=\frac{1}{2}\ J=\frac{5}{2}$ | $He^4+H^3$ | 3 | 0.8 | 0.04, 0.014, 0.017 | |
| $Be^7$ | 7.18 | $(\frac{5}{2}^-), \frac{1}{2}$ | $p^3[21]\ L=1\ S=\frac{3}{2}\ T=\frac{1}{2}\ J=\frac{5}{2}$ | $He^4+He^3$ | | 0 | 0.095 | |
| | 0 | $0^+, 0$ | $p^4[4]\ L=0\ S=0\ T=0$ | | 0 | 1 | 0.75 (0.15) | 444 (5.7) |

| | | | | | | | | |
|---|---|---|---|---|---|---|---|---|
| $Be^7$ | 7.18 | $(\frac{3}{2}^-), \frac{1}{2}$ | $p^3[21]$ $L=1$ $S=\frac{1}{2}$ $T=\frac{1}{2}$ $J=\frac{3}{2}$ | $He^4+He^3$ | 1 | 0 | 0.095 | |
| $Be^8$ | 0 | $0^+, 0$ | $p^4[4]$ $L=0$ $S=0$ $T=0$ | $He^4+He^4$ | 0 | 1 | 0.75 (0.15) | 444 (5.7) |
| | 2.92 | $2^+, 0$ | $p^4[4]$ $L=2$ $S=0$ $T=0$ | | 2 | 1 | 0.7 (0.4) | 5 (3.5) |
| | 11.8 | $4^+, 0$ | $p^4[4]$ $L=4$ $S=0$ $T=0$ | | 4 | 1 | 1.3 | 4.44 |
| $B^{10}$ | 6.88 | $1^-, 0$ | $p^5[41]$ $L_1=1$ $S_1=\frac{1}{2}$ $T_1=\frac{1}{2}$ $J_1=\frac{3}{2}$, 2s: $J=1$ $T=0$ | $Be^9+p$ | 0 | 0.8 | 0.15 (0.5) | |
| | | | | $Be^8+d$ | 1 | 0.1 | 0.12 (0.4) | |
| | | | | $Li^6+\alpha$ | 1 | 0.01 | 0.013 (0.05) | |
| | 8.89 | $2^+, 1$ | $p^5[42]$ $D_I$ $S=0$ $T=1$ | $Li^{6*}_{3.58}+\alpha$ | 2 | 0.3 | 0.33 | |
| | | | | $Be^9+p$ | 1 | 0.05 | 0.0016 | |
| $B^{11}$ | 11.68 | $(\frac{5}{2}^+), \frac{1}{2}$ | $p^5[42]$ $D_{II}$ $S_1=1$ $T_1=0$ $J_1=3$, 2s: $J=\frac{5}{2}$ $T=\frac{1}{2}$ | $Li^7+\alpha$ | 1(3) | $\Gamma_{\Lambda=1}=215$ keV<br>$\Gamma_{\Lambda=3}=20$ keV | $\Gamma \approx 300$ keV | 4.9 |
| $C^{12}$ | 7.65 | $0^+, 0$ | $\sqrt{\frac{3}{13}}\lvert s^3 2s,\ p^5[44]{:}00\rangle$ $+\sqrt{\frac{10}{13}}\lvert s^4,\ p^7\ 2p[44]{:}\ 00\rangle$ | $Be^8+\alpha$ | 0 | 0.9 | 0.1, $\approx 1.0$ | |

width to about 0.01 Wigner unit. It is assumed that this level results from the motion of the deuteron about the triton, i.e., its wave function is $|s^3p^2\, L = 0\ S = 1\, T = 0 : J = \frac{3}{2}^+\rangle$. The calculation gives good agreement with experiment for this configuration.

### 3.2. THE NUCLEUS $Li^7$ ($Be^7$)

The level at 7.2—7.5 MeV is often regarded as the second component of the doublet $^{22}F_{\frac{5}{2},\frac{7}{2}}$, but there are indications that it rather has the characteristic $^{24}P_{\frac{3}{2}}$, and that the level $^{22}F_{\frac{5}{2}}$ lies lower, at approximately 5—6 MeV[18,19]). According to our calculation the reduced width of a triton for the state $^{24}P_{\frac{3}{2}}$ is equal to zero. If we take into account small admixtures of other states we obtain a small triton width in agreement with the experimental value. For the state $^{22}F_{\frac{5}{2}}$ the calculated width is equal to 0.8 in contradiction to experiment. Thus it follows from our results that the characteristic $^{24}P_{\frac{3}{2}}$ corresponds better to the 7.2—7.5 MeV level, if the experimental values $\theta_t^2$ are determined accurately. The same conclusion is warranted by the data on the nucleon width [20]).

### 3.3. THE NUCLEUS $B^{10}$

For the level $J = 1^-$, $T = 0$ of energy 6.88 MeV Wilkinson [21]) considered the wave function $|p^5[41], 2s\rangle$. The calculated radiative width proved to be in good agreement with experiments on $Be^9$ (p, $\gamma$)$B^{10}$. As has been pointed out in this paper, data on the elastic scattering of protons on $Be^9$ show this level to result from the motion of a 2s nucleon over the ground state of $Be^9$, as expressed by the selected wave function. Calculated with the wave function of $LS$ coupling the reduced deuteron and $\alpha$ widths are in good agreement with experiment. For $jj$ coupling the calculated quantities are considerably lower than the experimental ones. It should be noted that in the wave function of this level there may be expected an admixture $T = 1$ of the order of 20 to 50 % in intensity [20]). Nevertheless, even with this admixture the agreement between calculated and experimental widths is preserved in order of magnitude. The level $J = 2^+$, $T = 1$ of energy 8.89 MeV decays with high probality into an $\alpha$-particle and a second excited state of $Li^6$. For this level we assumed the configuration $s^4p^6[42]$. The latter corresponds to two different states of momentum 2, viz. $^{31}D_I$ and $^{31}D_{II}$. The calculation of Kurath [22]) for intermediate coupling shows that the level in which the state $D_I$ has an essential share will lie in this energy region for $\xi/K \approx 5$, $L/K = 6.8$. The value $\xi/K$ taken here does not essentially differ from the value 4.75 used by Kurath for comparing theory and experiment and is not improbable. The state in which $D_{II}$ predominates lies lower by 3 or 4 MeV (Wilkinson compared the state $D_{II}$ with a level at 5.16 MeV). The wave function $^{31}D_I$ gives the nucleon and $\alpha$ particle reduced widths in good agreement with experimental data for the 8.89 level. (For $^{31}D_{II}$, one finds $\theta_p^2 \approx 1$, $\theta_\alpha^2 \approx 0.05$.)

### 3.4. THE NUCLEUS $B^{11}$

In the reactions $B^{10}(n, \alpha)\,Li^7$, $B^{10}(n, \alpha)\,Li^{7*}$ with neutrons of very low energies (0—250 keV), as well as in the scattering $Li^7(\alpha, \alpha)Li^7$ and $Li^7(\alpha, \alpha')Li^{7*}$, at least two levels of $B^{11}$ are manifested with excitations $\approx 11.46$ MeV and 11.68 MeV. For the latter level the hypothetical momentum and parity are $\frac{7}{2}^+$, $\frac{5}{2}^+$. Because of the smallness of the neutron energy we assume that these levels arise as a result of the motion of 2S nucleon over the ground state of $B^{10}$. In the case of *LS*-coupling for the level with spin $\frac{5}{2}^+$ the $\alpha$ width, as is clear from the table, is equal to about 250 keV. In the case of *jj*-coupling $\Gamma_\alpha$ proves to be $\leqq 1$ keV. For the level $\frac{7}{2}^+$ it is very small. The states of this configuration decay mainly into the ground state of $Li^7$. It can be assumed that the results of this calculation for $J = \frac{5}{2}^+$ are in agreement with the experimental data of Bergman *et al.* [23]) who pointed to the possibility of the existence of the level $\frac{5}{2}^+$ for a neutron energy of 250 keV with $\Gamma_\alpha \approx 400$ keV.

The scattering of $\alpha$ particles on $Li^7$ shows that for the level at 11.46 MeV, one has $\Gamma_\alpha = 70$ keV $\gg \Gamma_n$. and that the decay of this level in 94 % of the cases leads to an excited of $Li^7$. The configurations $s^4p^6$ 2s yield no explanation of a decay largely into an excited state of $Li^7$. It can be suposed that here we have the configuration $|s^3, p^8[44]\, L = 4\, J = \frac{7}{2}\, T = \frac{1}{2}\rangle$, which yields, for the transition into an excited state of $Li^7$, a width three or four times as large as for the transition into the ground state. Besides, there appears a small nucleon width. The reason why such a state should lie very low is not clear.

### 3.5. THE NUCLEUS $C^{12}$

At present there are many papers concerned with the structure of the $0^+$ level of energy 7.65 MeV. The probability of the transiton into the ground state with emission of an electron pair can be accounted for sufficiently well by the assumption of a single particle excitation in this state of the type [23])

$$s^3 2s,\ p^8, \qquad s^4 p^7 2p. \tag{23}$$

The assumption that the level in question corresponds to small monopole oscillations of the nucleus, made by Ferell and Visscher [24]), leads to the following wave function:

$$\psi = \sqrt{\tfrac{3}{13}}\,|s^3 2s,\ p^8[44]\,00\rangle + \sqrt{\tfrac{10}{13}}\,|s^4,\ p^7 2p[44]\,00\rangle.$$

For this function $\theta_\alpha^2$ proves to be equal to 0.9 of the Wigner limit. The experimental data on the width of this level are not yet sufficiently known ($\theta^2 \approx 0.1$ is given in ref. [25]), $\theta^2 \approx 1$ in ref. [26])). Perhaps a better measurement of the width will make it possible to draw more definite conclusions on the structure of this level.

The results of the calculations performed in this investigation show that the method proposed in ref. [2]) for calculating the reduced widths for nucleon

clusters give good agreement with experiment for a number of the levels of light nuclei. This fact holds out the hope that the present method can be effectively used for investigating the structure of the wave functions of nuclear states with the aid of experimentally measured widths for nucleon clusters. Since the d, t, $\alpha$ widths can yield valuable information on the properties of the levels of nuclei it is desirable to make experiments on light nuclei to measure these quantities.

Of considerable interest are the direct reactions with emission of complex particles which would make it possible to determine the widths for nucleon clusters in bound states. The method set down above for the analysis of nucleon clusters in light nuclei on the basis of the shell model can also be applied to the investigation of direct processes and photo-nuclear reactions with emission of complex particles.

In conclusion the authors express gratitude to docent Yu. M. Shirokov, V. G. Neudachin, M. Sc. (Phys.-Math.) and V. V. Balashov, M. Sc. (Phys.-Math.) for valuable discussions, useful advice and assistance.

## References

1) I. K. Perring and T. H. R. Skyrme, Proc. Phys. Soc. A **69** (1956) 600;
K. Wildermuth and Th. Kannelopoulos, Nuclear Physics **7** (1958) 150;
V. G. Neudachin, Yu. F. Smirnov and N. P. Yudin, JETP **37** (1959) 1781
2) V. V. Balashov *et al.*, JETP **37** (1959) 1385
3) T. Teichman and E. P. Wigner, Phys. Rev. **87** (1952) 123
4) A. M. Lane, Proc. Phys. Soc. A **66** (1953) 177
5) Handbuch der Physik, ed. by Flügge (Springer Verlag, Berlin, 1957) Vol. **39**
6) A. M. Lane, and D. H. Wilkinson, Phys. Rev. **97** (1955) 1199
7) H. A. Jahn and H. Van-Wieringen, Proc. Roy. Soc. A **209** (1951) 502
8) H. A. Jahn, Proc. Roy. Soc. A **205** (1951) 192;
A. R. Edmonds and B. H. Flowers, Proc. Roy. Soc. A **214** (1952) 515
9) H. A. Jahn, Phys. Rev. **96** (1954) 989
10) J. P. Elliot, J. Hope and H. A. Jahn, Phil. Trans. Roy. Soc. A **246** (1953) 241
11) T. Talmi, Helv. Phys. Acta **25** (1952) 185;
M. Moshinsky, Nuclear Physics **13** (1959) 104
12) Yu. F. Smirnov, Nuclear Physics, in the press
13) J. P. Elliot and T. H. R. Skyrme, Proc. Roy. Soc. A **232** (1955) 561
14) A. Edmonds, Angular Moments in Quantum Mechanics (Princeton, 1957)
15) H. Matsunobu and I. Takebe, Progr. Theor. Phys. **14** (1955) 589
16) G. E. Fischer and V. K. Fischer, Phys. Rev. **114** (1959) 533
17) I. G. Likely and F. P. Brady, Phys. Rev. **104** (1956) 118
18) F. Ajzenberg-Selove and T. Lauritsen, Nuclear Physics **11** (1959) 1
19) C. E. Meskov and S. Ufford, Phys. Rev. **101** (1956) 734
20) E. W. Hamburger and J. R. Cameron, Phys. Rev. **117** (1960) 781
21) D. H. Wilkinson and A. Clegg, Phil. Mag. **1** (1956) 291
22) D. Kurath, Phys. Rev. **101** (1956) 216
23) A. A. Bergman *et al.*, JETP **33** (1956) 9
24) P. J. Redmond, Phys. Rev. **101** (1956) 751;
R. A. Ferell and W. M. Visscher, Phys. Rev. **104** (1956) 475
25) Cook *et al.*, Phys. Rev. **107** (1957) 516
26) D. E. Alburger, Phys. Rev. Letters **3** (1959) 280

2.I

*Nuclear Physics* **26** (1961) 321—323; © *North-Holland Publishing Co., Amsterdam*

Not to be reproduced by photoprint or microfilm without written permission from the publisher

# THE $(\gamma, 3n)$ REACTION IN $Pr^{141}$

G. MOSCATI †

*Departamento de Física, Faculdade de Filosofia, Ciências e Letras da Universidade de São Paulo, São Paulo, Brasil*

Received 30 January 1961

**Abstract:** The isotope $Pr^{141}$ was irradiated with a bremsstrahlung beam of 33 MeV maximum energy in the Saclay Linac. Activity due to $Pr^{138}$ was detected and a lower limit of the integrated cross section from threshold to 33 MeV was obtained as being 1 MeV · mb. Some features of the accepted decay scheme are confirmed.

## 1. Introduction

The isotope $Pr^{141}$ is one of the few in which $(\gamma, n)$, $(\gamma, 2n)$ and $(\gamma, 3n)$ reactions can be studied by residual activity methods. The interest in the $(\gamma, 3n)$ reaction arises from the fact that the $(\gamma, n)$ and $(\gamma, 2n)$ reactions are rather well known [1, 2]) and a complete knowledge of the photon absorption cross section, above the giant resonance, depends on the behaviour of the $(\gamma, 3n)$ process.

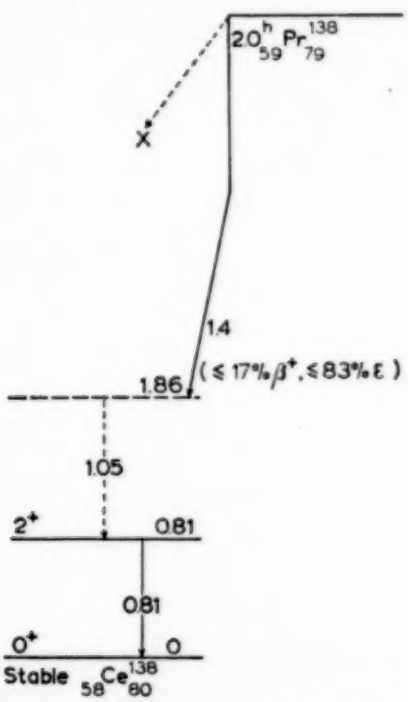


Fig. 1. Decay scheme of $Pr^{138}$ (ref. [5])).

† Work performed at the S.P.N.M.E. Saclay, C.E.A., France and supported in part by the "Conselho Nacional de Pesquisas" of Brazil.

Difficulties arise from the fact that the ($\gamma$, 2n) reaction is present with an abundant $\beta^+$ and $\gamma$ activity of 4.5 h half-life while the ($\gamma$, 3n) reaction end product is a $\beta^+$ and $\gamma$ emitter of 2 h half-life of much lower activity. One can separate these activities by detecting coincidences between either of the two $\gamma$'s and the $\beta^+$ annihilation radiation [3–6]) (see fig. 1).

## 2. Experimental Procedure

Two irradiations were performed at the Saclay Linac at energies of 30.5 and 33 MeV. The 0.3 $\mu$A electron beam, magnetically analysed to 1 % resolution, produced thick target bremsstrahlung radiation in a 0.4 mm. Pt radiator.

The Pr target was in the form of $Pr_6O_{11}$ powder (97 % pure) in a plastic container. The samples were of about 3 g.

The activity was measured by a system of two 3.7 cm in diameter by 2.5 cm height NaI crystals that viewed the source at 90° to each other. The source was contained in a copper tube to stop the $\beta^+$. The signals were connected to a fast-slow coincidence circuit which gave the spectra in a 100 channel analyser in coincidence with a one-channel analyzer set at the 0.5 MeV $\gamma$ annihilation radiation. Spectra without coincidences were also obtained.

## 3. Results and Conclusions

The analysis of the spectra obtained at 33 MeV shows that the 0.81 and 1.05 MeV $\gamma$'s are emitted in coincidence with the 0.5 MeV annihilation radiation and with a 2 h half-life. The intensities of the lines are consistent with a one to one ratio which is expected if the $\gamma$-lines are emitted in cascade as shown in fig. 1. The 30.5 MeV irradiation gave a much lower activity which indicates that the 2 h half-life is not due to contributions of ($\gamma$, n) or ($\gamma$, 2n) reactions in impurities present in the sample, which would give activities approximately energy independent in this region.

The known electron current and geometrical factors as well as detection efficencies allowed us to evaluate the integrated cross section, from threshold to 33 MeV for the ($\gamma$, 2n) and ($\gamma$, 3n) reactions. For the ($\gamma$, 2n) reaction the value obtained is consistent with the published values [1, 2]). The ($\gamma$, 3n) reaction, for which the calculated [7]) threshold is $26.6 \pm 0.6$ MeV, gave an integrated cross section of 1 MeV · mb under the assumption that it starts at 27 MeV and grows linearly until 33 MeV.

This value is much lower than that obtained in Ta, even taking into account threshold and mass differences [8]). Experimental uncertainties allow a factor of two in the value obtained. This must be regarded as a lower limit to the integrated cross section since the uncertainty in the $\beta^+$ ratio ($\leqq$ 17 %) would increase this value.

One can conclude that there are indications that the ($\gamma$, 3n) process is not important under 33 MeV.

The author wishes to acknowledge Mr. C. Tzara and his group for the kind hospitality offered him at the S.P.N.M.E. at the Saclay Centre and Mme. Papineau and her group for the electronic circuits used in this work. Discussions with Professor J. Goldemberg, Mr. C. Tzara and Professor L. Marquez were appreciated. We are indebted to the accelerator crew for the irradiations. The Pr source was kindly supplied by Dr. Krumholtz from Industrias Quimicas Orquima, Brasil.

## References

1) F. Ferrero, R. Malvano, E. Silva, J. Goldemberg and G. Moscati, Nuclear Physics **10** (1959) 234
2) J. H. Carver and W. Turchinetz, Proc. Phys. Soc. **73** (1959) 110
3) B. J. Stover, Phys. Rev. **81** (1951) 8
4) T. H. Handley and E. L. Olson, Phys. Rev. **96** (1954) 1003
5) National Research Council, Nuclear Data Sheets (1958)
6) D. Strominger, J. M. Hollander and G. T. Seaborg, Revs. Mod. Phys., **30** (1958) 585
7) W. H. Johnson, Jr. and A. O. Nier, Phys. Rev. **105** (1957) 1014
8) J. H. Carver and W. Turchinetz, Proc. Phys. Soc. **71** (1958) 613

8.B

*Nuclear Physics* **26** (1961) 324—337; © *North-Holland Publishing Co., Amsterdam*

Not to be reproduced by photoprint or microfilm without written permission from the publisher

# THE STRUCTURE OF MOMENTUM SPACE, THE NEUTRINO AND THE PAULI PRINCIPLE

H. FRÖHLICH,

*Department of Theoretical Physics, University of Liverpool*

Received 20 February 1961

**Abstract:** Although right and left-handedness cannot be defined geometrically, the distinction between the two concepts can be so defined. From this observation it is concluded that the quantity in terms of which this distinction is made should be introduced as an explicit feature in the mathematical treatment of space. Application of this idea to null vectors in momentum space leads to an equation which formally is identical with the wave equation of the two-component neutrino field theory together with the reflected equation. Moreover, from the requirement of invariance of covariant quadratic expressions under phase transformation, it follows with necessity not only that the field must be quantizied but also that this must be done according to the Pauli principle. A complete geometrical interpretation of the neutrino is thus obtained. The neutrino charge in particular is found to be given in terms of the newly introduced coordinate which describes the distinction between right- and left-handedness.

## 1. Introduction

Reasons have recently been forwarded [1, 2]) for considering the usual treatment of reflexions as unsatisfactory. In pursuance of these considerations it has been found necessary to investigate critically the definition of momentum space. The present paper refers mainly to the subspace formed by null vectors, for which the square of the length of the space components $\sum p_k^2$ is equal to the square of the time component $p_0^2$.

The following investigations are principally based on the observation that although right-handedness and left-handedness cannot be defined geometrically, the distinction between the two concepts can be so defined. It seems desirable, therefore, to introduce the quantity in terms of which this distinction is made as an explicit feature. This has two consequences. The first is that the usual definition of momentum space in terms of the invariance of $p_0^2 - \sum p_k^2$ under appropriate transformations is insufficient because this expression does not permit to distinguish $p_k$-frames of opposite handednesses. The possibility of this distinction requires linearisation of the above quadratic expression. The second consequence refers to the coordinate system in configuration space $x_k$, on which the $p_k$ space is based. Here both a right-handed and a left-handed system will be used simultaneously to describe the same situation in momentum space.

The development of these ideas leads to the replacement of the above quadratic expression by a linear one which has the form of a wave equation which is formally identical with the two-component neutrino wave equation together with the reflected equation. The symmetrization required by the second observation leads to the formulation of a phase invariance of the field quantities. From this it follows with necessity that the field quantities do not commute, i.e. must be quantized, and further more that this quantization must be carried out in accordance with the Pauli principle. The distinguishing feature between right-handedness and left-handedness then must be interpreted as neutrino charge.

## 2. Momentum Space

### 2.1. DEFINITIONS

In four-dimensional space-time in a certain Lorentz frame, the four components of the momentum operator are expressed by $-i\partial_k$, $i\partial_0$ in terms of the coordinates $x_k$, $x_0$ ($k = 1, 2, 3$). When applied to the transformation function $\exp i(p_k x_k - p_0 x_0)$, they lead to a four-vector field with components $(p_k, p_0)$ $\exp i(p_k x_k - p_0 x_0)$. The four numbers $(p_k, p_0)$ can be considered as the components of a radius vector in a fourmomentum space whose coordinate axes are parallel to those of the $(x_k, x_0)$ space.

This 4-momentum space consists of all radii vectores $(p_k, p_0)$. Its properties shall for the present be expressed through the definition of an invariant $L$ by

$$L = p_0^2 - \sum p_k^2, \tag{2.1}$$

together with the postulate that this definition be in variant under continuous Lorentz transformations. If $L = m^2 \geqq 0$, then the action of the whole group of these transformations on two specific radii vectores $(p_k, p_0)$ and $(p_k, -p_0)$ both satisfying $p_0^2 - p_k^2 = m^2 \geqq 0$ leads in a continuous way to all possible numbers $p'_k$, $p'_0$ satisfying (2.1) with $L = m^2$. These transformations may thus be considered as generating two three-dimensional subspaces (one with $p_0 > 0$ the other with $p_0 < 0$), and simultaneously demonstrating the continuity of each of them.

A Lorentz transformation in 4-momentum space may be interpreted in two ways: either the coordinate axes are considered fixed and the radius vector has been changed, or vice versa. The latter interpretation determines the possible coordinate frames in 4-momentum space in terms of the frame originally used in $(x_k, x_0)$ space. In the usual treatment, this frame has certain features that can be chosen arbitrarily; its space axes may for instance form a right-handed system. Momentum space then from its present definition must use right-handed frames only for its $p_k$-subspaces.

Spatial reflexions in $x_k$ -space can be interpreted as replacing the operators $\partial_k$ by $-\partial_k$, and hence each spatial momentum component $p_k$ by $-p_k$ without

changing the $x_k$-frame. In terms of the second interpretation of transformations they transform a right-handed frame in $p_k$-subspace (assuming that the $x_k$-frame was right-handed) into a left-handed one. Use of these frames was not included in the above definition of momentum space. Thus extension of the definition of momentum space to include space reflexions in addition to continuous Lorentz transformations requires — for a given $x_k$-frame — a doubling of momentum space, one permitting right-handed and the other left-handed $p_k$-frames.

It is obvious that the definition (2.1) from which the properties of momentum space were originally defined does not permit distinction between right-handed and left-handed systems because it does not depend on $p_k$ but only on $p_k^2$. It is for this reason that one must demand that (2.1) be replaced by another definition which depends linearly on the components $p_k$. This linearisation will show in a different way the need for doubling of momentum space (see below).

Similar arguments hold for reflexion of $p_0$, and of $(p_k, p_0)$. It will be shown later that the last two cases need not be considered in addition to $p_k$ reflexions if $L = 0$, i.e. in the case of null vectors. In the present paper null vectors only are investigated.

### 2.2. DOUBLING OF MOMENTUM SPACE

In order to give an independent and more explicit argument for the doubling of momentum space, let us now return to equation (2.1) which defined momentum space in terms of continuous Lorentz transformations, i.e. prior to the argument concerning reflexions. For a null vector,

$$p_0^2 = \sum p_k^2 \tag{2.2}$$

so that

$$p^2 = \sum p_k^2 \tag{2.3}$$

$$p_0 = \pm p, \qquad p \geqq 0. \tag{2.4}$$

Here $(p_k, p_0)$ are the momentum components in the 4-momentum space whose coordinate axes coincide with those of $(x_k, x_0)$ space.

It has been argued that consideration of reflexions requires linearisation of (2.1), i.e. of (2.2) in the case of null vectors, so as to permit distinction between the vector $(p_k, p_0)$ and the reflected vector $(-p_k, p_0)$. This linearisation, as is well known, requires in its simplest form the introduction of Pauli matrices $\sigma_k$ acting on a spinor, say $\xi$, for $(\sigma_k p_k)^2 = \sum p_k^2$ (we use notations $\boldsymbol{\sigma} \cdot \mathbf{p} = \sigma_k p_k = \sum \sigma_k p_k$). The formal process of linearising $\sum p_k^2$ has, however, two non-equivalent solutions, namely $+\sigma_k p_k$ and $-\sigma_k p_k$. Thus the result of linearisation of (2.3) can be written as

$$(g\,\boldsymbol{\sigma} \cdot \mathbf{p} + p)\xi = 0, \qquad g = \pm 1, \tag{2.5}$$

where $g$ is a new parameter capable of the two values $+1$ and $-1$. As a result,

therefore, while a momentum vector still has the four components $(p_k, p_0)$ with respect to $(x_k, x_0)$ space coordinate axes, its full description requires decision on whether $g = 1$ or $g = -1$. Clearly this is equivalent with a doubling of momentum space, one referring to $g = 1$, the other to $g = -1$. The quantity $g$ decides whether the $p_k$-frame has equal or opposite handedness to that of the $x_k$-frame.

One might have been tempted to write the operator acting on $\xi$ as a result of the linearisation as $g\boldsymbol{\sigma} \cdot \mathbf{p} + hp$, with $h = \pm 1$, $hp = p_0$. This, however, would simply repeat the two equations obtained from (2.5) by using there $g = 1$ and $g = -1$, which seems superfluous. It must be emphasised that this procedure is only possible in the case of null vectors. In this present case, therefore, equation (2.5) will be considered as equivalent to

$$(\boldsymbol{\sigma} \cdot \mathbf{p} + p_0)\xi(p_k, g) = 0, \tag{2.6}$$

where $p_0 = gp$. For a null vector, therefore, the two three-dimensional subspaces arising from the two possible signs of $p_0$ and the two signs of $(\boldsymbol{\sigma} \cdot \mathbf{p})$ are treated as identical.

The detailed treatment of these two subspaces follows from the condition that $\xi$ be a continuous function in momentum space. From equations (2.5) or (2.6) it can be seen that $\xi$ must have the form

$$\xi(p_k, g) = a(p_0, g)s(p_k/p, g) \tag{2.7}$$

where $a(p_k, g)$ is a one-component function while $s$ is a spinor which depends on $g$ and $p_k/p$ only. Now $p_k/p$ can be described in terms of coordinates on a spherical surface, so that $s$ depends on the coordinates of two spherical surfaces since $g = \pm 1$. It may be remembered now that the two-valued quantity $g$ arose from formally taking the square root of $\sum p_k^2$. The corresponding case of the square root of a function of a complex variable may be recalled, which also leads to a doubling of space in terms of Riemannian surfaces, which in this case consist of two interconnected sheets such that the azimuth $\varphi$ in terms of which the complex plane is described, has a range of $4\pi$, instead of $2\pi$ for a single plane. For our case, introduce a polar angle $\vartheta$ and an azimuth $\varphi$ on two spheres distinguish by $g = 1$ and $g = -1$, such that

$$gp_1/p = \sin\vartheta\cos\varphi, \qquad gp_2/p = \sin\vartheta\sin\varphi, \qquad gp_3/p = \cos\vartheta, \tag{2.8}$$

with the range

$$0 \leqq \vartheta \leqq \pi, \qquad -2\pi \leqq \varphi \leqq 0^- \text{ if } g = -1, \qquad 0^+ \leqq \varphi \leqq 2\pi \text{ if } g = 1; \tag{2.9}$$

this links the two values of $g$ to two different ranges of $\varphi$.

The necessity for this arrangement also arises from the detailed form of $s$ which on a single sphere would be discontinuous. For from (2.11), $s$ is seen to depend on $\exp(\pm\frac{1}{2}i\varphi)$, i.e., using (2.8), on $(gp_1 \pm igp_2)^{\frac{1}{2}}$. There are two $\varphi$ values within the range (2.9), differing by $2\pi$, which correspond to a given $gp_1$, $gp_2$.

One of them leads to the positive, the other to the negative root of $(gp_1 \pm igp_2)$, similarly to the case of the complex planes.

A definite model, inspired by Riemannian surfaces, consists of a spherical surface in which the outside corresponds to $g = +1 (\varphi > 0)$ and the inside to $g = -1$ $(\varphi < 0)$ such that $\varphi(\text{outside}) = \varphi(\text{inside}) + 2\pi$ along any ray penetrating through the surface. To prevent discontinuities of $s$, this surface must be cut, say between $\varphi = 0^+$ and $2\pi$ outside, corresponding to $\varphi = -2\pi$ and $0^-$ inside. Then $0^+$ is connected to $0^-$, and $2\pi$ to $-2\pi$, giving $\varphi$ a continuous range from $-2\pi$ to $2\pi$. The components of $s$ and hence for appropriate $a$ also those of $\xi$ will then be continuous functions over the whole range, for in the representation

$$\sigma_1 = \begin{pmatrix} 0 & 1 \\ 1 & 0 \end{pmatrix}, \qquad \sigma_2 = \begin{pmatrix} 0 & -i \\ i & 0 \end{pmatrix}, \qquad \sigma_3 = \begin{pmatrix} 1 & 0 \\ 0 & -1 \end{pmatrix}, \tag{2.10}$$

one finds

$$s(p_k/p, g) = \begin{pmatrix} -\sin \tfrac{1}{2}\vartheta \, e^{-\frac{1}{2}i\varphi} \\ \cos \tfrac{1}{2}\vartheta \, e^{\frac{1}{2}i\varphi} \end{pmatrix}. \tag{2.11}$$

Other possibilities exist for the joining of the $g = 1$ and $g = -1$ surfaces. Thus, in particular, the prescription (2.9) may be used for $\varphi$, but the $\vartheta$-range $0 \leqq \vartheta \leqq \pi$ will hold for $g = 1$ only, while $-\pi \leqq \vartheta \leqq 0$ if $g = -1$, so that in penetrating through the sphere one is led from $\vartheta, \varphi$ at $g = 1$ to $\vartheta - \pi$, $\varphi - 2\pi$ at $g = -1$.

### 2.3. GENERALIZATION

The previous considerations were based on a coordinate system of a definite handedness (left or right) in $x_k$-space. From this the two $p_k$-spaces were derived, of which the one with $g = 1$ has equal, that with $g = -1$ opposite handedness to the $x_k$-system. Clearly the use of a $x_k$-system with definite handedness introduces an asymmetry; since $p_k = -i\partial_k$ holds for either system, a vector $(p_k, g)$ in terms of the original $x_k$-system is described by $(-p_k, g)$ in the $x_k$-system with opposite handedness. Equations (2.5) or (2.6) should thus be supplemented by

$$(-g\boldsymbol{\sigma} \cdot \mathbf{p} + p)\xi^{\mathrm{r}} = 0, \quad \text{or} \quad (-\boldsymbol{\sigma} \cdot \mathbf{p}_0 + p_0)\xi^{\mathrm{r}} = 0, \qquad p_0 = gp. \tag{2.12}$$

Here $\xi^{\mathrm{r}}$ is not independent of $\xi$, as both describe the same vector in momentum space. The correlation of $\xi^{\mathrm{r}}$ to $\xi$ is obtained by the transformation

$$\xi^{\mathrm{r}} = -i\sigma_{\mathrm{c}}\xi^*. \tag{2.13}$$

For taking the complex conjugate (indicated by a star) to (2.5) a matrix $\sigma_{\mathrm{c}}$ always exists such that $\sigma_{\mathrm{c}}^{-1}\sigma_k\sigma_{\mathrm{c}} = -\sigma_k{}^*$; in representation (2.10),

$$\sigma_{\mathrm{c}} = \sigma_2, \tag{2.14}$$

thus leading to (2.12).

Eq. (2.12) can be joined to (2.5) or (2.6) in the form

$$(\rho_3\sigma_k p_k + p_0)\eta = 0, \qquad p_0 = gp, \tag{2.15}$$

where three new Pauli matrices $\rho_k$ have been introduced, given in representation (2.10). The operator $\rho_3\sigma_k$ is a direct product, and

$$\eta = \frac{1}{\sqrt{2}}\begin{pmatrix}\xi\\ \xi^{\mathrm{r}}\end{pmatrix} = (\tfrac{1}{2}a(1+\rho_3)+\tfrac{1}{2}a^+(1-\rho_3))X, \tag{2.16}$$

with

$$X = \frac{1}{\sqrt{2}}\begin{pmatrix}s\\ s^{\mathrm{r}}\end{pmatrix} = \frac{1}{\sqrt{2}}\begin{pmatrix}-\sin\frac{1}{2}\vartheta\ \mathrm{e}^{-\mathrm{i}i\varphi}\\ \cos\frac{1}{2}\vartheta\ \mathrm{e}^{\ \mathrm{i}i\varphi}\\ -\cos\frac{1}{2}\vartheta\ \mathrm{e}^{-\mathrm{i}i\varphi}\\ -\sin\frac{1}{2}\vartheta\ \mathrm{e}^{\ \mathrm{i}i\varphi}\end{pmatrix}, \quad \text{i.e.} \quad X^+X = 1. \tag{2.17}$$

Thus we have

$$\rho_3\begin{pmatrix}\xi\\ \xi^{\mathrm{r}}\end{pmatrix} = \begin{pmatrix}\xi\\ -\xi^{\mathrm{r}}\end{pmatrix},$$

etc. The particular form of $\eta$ required by (2.16) can be expressed as

$$\eta = -\rho_2\sigma_2\eta^*. \tag{2.18}$$

Representation (2.10) has been used, and will be used in the following.

### 2.4. PRELIMINARIES ON THE PAULI PRINCIPLE.

The previous developments have led to a replacement of (2.2) by (2.15) and (2.18) as a definition of momentum space, together with the requirement that this be invariant under continuous Lorentz transformations, and under reflexions. This required the introduction of operators, and it is desirable to regain relations between these operators and the original coordinates, in momentum space, $(p_k, g)$, which are numbers. From equation (2.5) for instance, one has $\xi^\dagger\sigma_k\xi = -p_k/gp$ provided $\xi$ is normalized in such a way that $\xi^\dagger\xi = 1$ (a cross indicates the hermitian conjugate). This relation is independent of a phase transformation $\xi \to e^{i\alpha}\xi$. Equation (2.15), which has to be used rather than (2.5), permits the formation of corresponding quadratic expressions. They have the form $\eta^+Q\eta$ where $Q$ is an operator formed from the $\rho_k$ and $\sigma_k$. The corresponding phase transformation takes the form

$$\eta \to \mathrm{e}^{i\alpha\rho_3}\eta. \tag{2.19}$$

It is easily seen that both (2.15) and (2.18) are invariant under this replacement The requirement that $\eta^\dagger Q\eta$ be also invariant under (2.19) then leads to the condition

$$\eta^\dagger \mathrm{e}^{-i\alpha\rho_3}Q\mathrm{e}^{i\alpha\rho_3}\eta = \eta^\dagger Q\eta. \tag{2.20}$$

Amongst the sixteen $Q$, eight obviously do not satisfy this condition identically

because they contain $\rho_1$ or $\rho_2$. For two of them, $\rho_1 \cdot 1$ and $\rho_2 \cdot 1$, the expression $\eta^\dagger Q \eta$ vanishes however. For the remaining six, $\rho_l \sigma_k$, $l = 1,2$, condition (2.20) can only satisfied if

$$\eta^\dagger \rho_l \sigma_k \eta = 0, \qquad l = 1, 2. \tag{2.21}$$

Use of (2.16), (2.17) shows that (2.21) requires

$$a^2 = 0, \qquad a^{\dagger 2} = 0 \qquad \text{for all} \quad p_k, g. \tag{2.22}$$

One has to conclude, therefore, that either do all $a$, $a^\dagger$ vanish and momentum space does not exist, or otherwise $a$ and $a^\dagger$ are operators. Choosing the latter alternative, the quadratic expressions $\eta^\dagger Q \eta$ are not numbers but remain operators. They must then act on a further operator, say $\Psi$, denoted as state vector, such that expressions of the form $\Psi^\dagger \eta^\dagger Q \eta \Psi$ are numbers.

Equations (2.22) are well known to express part of the Pauli principle. They do not completely determine the form of $a$ and $a^\dagger$, even if a single $p_k, g$ only is considered, for this requires in addition a relation between $a$ and $a^\dagger$. In the eight non-vanishing $\eta^\dagger Q \eta$, the combinations which occur are $a^\dagger a \pm a a^\dagger$. One of these must be given in terms of a real number so as to complete for given $(p_k, g)$ the definition of $a$ and $a^\dagger$. Without lack of generality the magnitude of this number may be chosen as unity. It will now be shown that of these two possibilities,

$$a^\dagger a - a a^\dagger = \pm 1, \tag{2.23$^-$}$$

$$a^\dagger a + a a^\dagger = 1, \tag{2.23$^+$}$$

the first one contradicts (2.22). For squaring (2.23$^-$) and use of (2.22) leads to $a^\dagger a a^\dagger a + a a^\dagger a a^\dagger = 1$. Using (2.23$^-$) again one can derive by further application of (2.22) that $a^\dagger a + a a^\dagger = 1$ and $a^\dagger a + a a^\dagger = -1$, clearly a contradiction. Eq. (2.23$^+$) on the other hand is compatible with (2.22).

## 3. The Pauli Principle

### 3.1. DERIVATION

Return from momentum space $(p_k, p_0)$ to ordinary space $(x_k, x_0)$ permits a fuller view of the situation that has been reached. Thus if $V$ is a volume in $x_k$-space, define a wave function $\psi$ by

$$\psi = \frac{1}{\sqrt{V}} \sum_g \sum_{p_k} e^{i\rho_3 (p_k x_k - p_0 x_0)} \eta(p_k, g), \qquad p_0 = gp. \tag{3.1}$$

According to (2.15) it satisfies the wave equation

$$(\rho_3 \sigma_k \partial_k - \partial_0)\psi = 0 \tag{3.2}$$

together with the condition (cf. (2.18); use representation (2.10))

$$\psi = -\rho_2 \sigma_2 \psi^*. \tag{3.3}$$

Frequently it is useful to multiply (3.2) by $-i\rho_2$, to use Dirac matrices $\gamma_k = \rho_1\sigma_k$, $\gamma_4 = -\rho_2$, $\gamma_5 = \rho_3$, and to employ the notation $x_4 = ix_0$, $p_4 = ip_0$ etc., so that with $\mu = 1, 2, 3, 4$ and representation (2.10),

$$\gamma_\mu \partial_\mu \psi = 0, \qquad \partial_\mu \bar{\psi}\gamma_\mu = 0, \qquad \bar{\psi} = \psi^\dagger \gamma_4, \qquad \psi = i\gamma_5\gamma_2\psi^*. \tag{3.4}$$

A number of relations between covariant expressions can be derived from (3.4). They concern four 4-vectors,

$$\partial_\mu J_\mu = 0, \qquad \partial_\mu D_\mu = 0, \qquad \partial_\mu j_\mu = 0, \qquad \partial_\mu j_{5\mu} = 0 \tag{3.5}$$

one antisymmetric tensor $f_{\mu\nu}$ (and its dual $f_{5\mu\nu}$) satisfying

$$\partial_\mu f_{\nu\mu} = j_\nu, \qquad \partial_\mu f_{5\nu\mu} = j_{5\nu}; \tag{3.6}$$

and two tensors $T_{\mu\nu}$ and $T_{5\mu\nu}$ satisfying

$$\partial_\mu T_{\mu\nu} = 0, \qquad \partial_\nu T_{\mu\nu} = 0, \qquad \partial_\mu T_{5\mu\nu} = 0, \qquad \partial_\nu T_{5\mu\nu} = 0, \tag{3.7}$$

so that the symmetric tensors $(T_{\mu\nu}+T_{\nu\mu})$, $(T_{5\mu\nu}+T_{5\nu\mu})$ satisfy the corresponding relations. Further relations of the nature $\partial_1 J_2 - \partial_2 J_1 = 2i(T_{34}-T_{43})$ exist.

Here we have

$$J_\mu = -i\bar{\psi}\gamma_5\gamma_\mu\psi, \qquad D_\mu = -i\bar{\psi}\gamma_\mu\psi, \qquad f_{\nu\mu} = \tfrac{1}{4}\bar{\psi}(\gamma_\nu\gamma_\mu - \gamma_\mu\gamma_\nu)\psi, \tag{3.8}$$

$$j_\mu = \tfrac{1}{2}(\bar{\psi}\partial_\mu\psi - (\partial_\mu\bar{\psi})\psi), \qquad T_{\mu\nu} = \tfrac{1}{2}(\bar{\psi}\gamma_\mu\partial_\nu\psi - (\partial_\nu\bar{\psi})\gamma_\mu\psi). \tag{3.9}$$

The quantities $f_{5\nu\mu}$, $T_{5\mu\nu}$ and $j_{5\mu}$ are obtained by the replacement of $\bar{\psi}$ by $\bar{\psi}\gamma_5$ in $f_{\nu\mu}$, $T_{\mu\nu}$ and $j_\mu$ respectively.

Corresponding to (2.19) the phase transformation

$$\psi \to e^{i\alpha\gamma_5}\psi, \qquad \text{i.e. } \bar{\psi} \to \psi^\dagger e^{-i\alpha\gamma_5}\gamma_4 = \bar{\psi}e^{i\alpha\gamma_5} \tag{3.10}$$

leaves eqs. (3.2)—(3.4) invariant. In order to give a simple meaning to the relations (3.5)—(3.7) it is required that they also be invariant under phase transformation (3.10). Amongst the quantities defined in (3.8) and (3.9), $f_{\mu\nu}$ (and hence $f_{5\mu\nu}$), $j_\mu$ and $j_{5\mu}$ are not invariant. From (3.6) it must be concluded, therefore, that $f_{\mu\nu} = 0$. The dual tensor $f_{5\mu\nu}$ then vanishes automatically; hence $j_\mu$ and $j_{5\mu}$ also vanish in view of (3.6). From $f_{\mu\nu} = 0$, using (3.8) and representation (2.10), one finds

$$\psi^\dagger\rho_l\sigma_k\psi = 0, \qquad l = 1, 2;\ k = 1, 2, 3, \tag{3.11}$$

in close correlation to (2.21).

To put these six conditions into more explicit form, use

$$\psi = \begin{pmatrix}\varphi\\ \varphi^r\end{pmatrix}, \qquad \varphi = \begin{pmatrix}\varphi_1\\ \varphi_2\end{pmatrix}, \qquad \varphi^r = -i\sigma_2\varphi^* = \begin{pmatrix}-\varphi_2^*\\ \varphi_1^*\end{pmatrix}, \tag{3.12}$$

so that

$$\varphi = \frac{1}{(2V)^{\frac{1}{2}}} \sum_{p_k} \sum_{g} a(p_k, g) s\left(\frac{p_k}{p}, g\right) e^{ip_\mu x_\mu}. \tag{3.13}$$

With the notation $[A, B] = AB + BA$ and with $x$ representing the four components $x_\mu$, the six conditions (3.11) can now be expressed as

$$[\varphi_l(x), \varphi_t(x)] = 0, \qquad [\varphi_l^\dagger(x), \varphi_t^\dagger(x)] = 0, \qquad t, l = 1, 2. \tag{3.14}$$

Inserting (3.13) with (2.11) into (3.14) yields a generalisation of (2.22) namely

$$[a(p_k, g), a(p'_k, g')] = 0, \qquad [a^\dagger(p_k, g), a^\dagger(p'_k, g')] = 0. \tag{3.15}$$

This in turn leads to a generalization of (3.14) referring to different space time points $x$, $x'$,

$$[\varphi_l(x'), \varphi_t(x)] = 0, \qquad [\varphi_l^\dagger(x'), \varphi_t^\dagger(x)] = 0. \tag{3.16}$$

These relations (3.15), (3.16) form a part of the well known rules for the quantization of fields according to the Pauli principle. They do not completely determine the $a$, $a^\dagger$, i.e. the form of the $\varphi_l$, $\varphi_l^\dagger$, and must be completed by relations between the $\varphi_l^\dagger(x')$ and $\varphi_t(x)$. The required argument for obtaining these relations can proceeed in exact parallel to the one selecting (2.23+), and showing that (2.23−) leads to a contradiction. For this purpose define first a generalization of the covariant quantities (3.8), (3.9) to refer to two space time points $x$, $x'$ by

$$J_\mu(x', x) = \tfrac{1}{2} i(\bar\psi(x')\gamma_5\gamma_\mu\psi(x) + \bar\psi(x)\gamma_5\gamma_\mu\psi(x')),$$
$$D_\mu(x', x) = \tfrac{1}{2} i(\bar\psi(x')\gamma_\mu\psi(x) + \bar\psi(x)\gamma_\mu\psi(x')), \tag{3.17}$$

etc. With (3.12) it is found that $J_\mu(x', x)$ and $T_{\mu\nu}(x', x)$ are expressible as sums of commutators, while $D_\mu(x', x)$ and $T_{5\mu\nu}(x', x)$ have the form of sums of anti-commutators. Thus e.g. ($\bar\varphi = \varphi^{\dagger *}$)

$$D_4(x', x) = iD_0(x', x)$$
$$= -\tfrac{1}{2} i((\varphi^\dagger(x')\varphi(x) + \bar\varphi(x)\varphi^*(x')) + (\varphi^\dagger(x)\varphi(x') + \bar\varphi(x')\varphi^*(x)), \tag{3.18}$$

and

$$J_4(x', x) = iJ_0(x', x)$$
$$= \tfrac{1}{2} i((\varphi^\dagger(x')\varphi(x) - \bar\varphi(x)\varphi^*(x')) + (\varphi^\dagger(x)\varphi(x') - \bar\varphi(x')\,\varphi^*(x)). \tag{3.19}$$

The required relation between the $\varphi^\dagger$ and $\varphi$ must express either the $J_\mu(x', x)$ or the $D_\mu(x', x)$ in terms of universal $c$-number functions — corresponding to the real number used in (2.23). The only permissible existing quantities of this nature are the Pauli invariant $D(x-x')$ function (for zero mass) or its derivatives $\partial_\mu D$, $\partial_\mu\partial_\nu D$ forming a scalar, 4-vector, symmetric tensor respectively.

For reasons of covariance, then, either $J_\mu(x', x)$ or $D_\mu(x', x)$ must be equated to $\partial_\mu D(x'-x)$. The use of $J_\mu(x', x)$ leads to a contradiction in a similar way as

(2.23⁻) did. To show this in a simple manner use the special case $x_0 = x'_0$ so that $\partial_k D = 0$ and $-\partial_4 D = i\delta^3(\mathbf{x}-\mathbf{x}')$. From $J_\mu = \partial_\mu D$ for $\mu = 3,4$ one can then derive e.g.

$$\varphi_1^*(x')\varphi_1(x)-\varphi_1(x)\varphi_1^*(x') = \delta^3(\mathbf{x}-\mathbf{x}'), \tag{3.20}$$

where $x = (\mathbf{x}, x_0)$, $x' = (\mathbf{x}', x_0)$. Squaring this expression and using (3.16) yields

$$\varphi_1^*(x')\varphi_1(x)\varphi_1^*(x')\varphi_1(x)+\varphi_1(x)\varphi_1^*(x')\varphi_1(x)\varphi_1^*(x') = (\delta^3(\mathbf{x}-\mathbf{x}'))^2.$$

Re-application of (3.20) and further use of (3.16) then results in $[\varphi_1^*(x'), \varphi_1(x)]$ being equal to either $+\delta^3(\mathbf{x}-\mathbf{x}')$ or $-\delta^3(\mathbf{x}-\mathbf{x}')$, clearly a contradictory result.

The alternative,

$$D_\mu(x', x) = \partial_\mu D(x-x'), \tag{3.21}$$

on the other hand is found compatible with (3.16) and must, therefore, be used. Inserting for $\psi$ from (3.12), (3.13) leads immediately to

$$[a^\dagger(p_k, g), a(p'_k, g')] = \delta^3_{p_k p'_k}\delta_{g,g'}, \tag{3.22}$$

which together with (3.15) establishes the Pauli principle — as does the alternative form (3.21) with (3.16). It is of interest to note that as a consequence one finds

$$T_{5\mu\nu}(x', x) = \partial_\mu\partial_\nu D(x-x'), \tag{3.23}$$

whereas $T_{\mu\nu}(x', x)$ like $J_\mu(x', x)$ is expressible in terms of commutators.

Thus the first part of the Pauli principle, (3.15) or (3.16), has been derived from the condition of invariance under phase transformations. The second part, (3.22) or (3.21), then follows as the only available compatible condition for supplementation.

### 3.2. VOLUME INTEGRALS OF $J_\mu$ AND $T_{4\mu}$

It will be useful to integrate $J_\mu$ and $T_{4\mu}$ over the volume $V$ in $x_k$-space. One finds †

$$\int J_0 \mathrm{d}^3k = \sum \tfrac{1}{2}(a^\dagger a-aa^\dagger), \qquad \int J_k \mathrm{d}^3k = \sum \tfrac{1}{2} g \frac{p_k}{p}(a^\dagger a-aa^\dagger), \tag{3.24}$$

$$P_\mu = -i\int T_{4\mu}\mathrm{d}^3x = \sum \tfrac{1}{2} p_\mu (a^\dagger a-aa^\dagger). \tag{3.25}$$

Here $a^\dagger a$ stands for $a^\dagger(p_k, g)a(p_k, g)$ and all sums extend over $p_k$ and $g$.

By making use of identities like

$$0 = \sum g = \sum g(a^\dagger a+aa^\dagger), \qquad 0 = \sum p_k g = \sum p_k g(a^\dagger a+aa^\dagger), \tag{3.26}$$

† In $\int J_k \mathrm{d}^3x$, $x_0$-dependent terms (Zitterbewegung) have been omitted.

the above expressions can be written as

$$\int J_0 \mathrm{d}^3x = \sum g n(p_k, g), \qquad \int J_k \mathrm{d}^3x = \sum g v_k n(p_k, g), \tag{3.27}$$

$$P_0 = -iP_4 = -N + \sum p n(p_k, g), \qquad P_k = \sum p v_k n(p_k, g). \tag{3.28}$$

Here $n(p_k, g)$ and $v_k$ are defined by

$$n(p_k, g) = \tfrac{1}{2}(1+g)a^\dagger a + \tfrac{1}{2}(1-g)aa^\dagger, \qquad v_k = (p_k/p)g \tag{3.29}$$

whereas

$$N = \sum p(a^\dagger a + aa^\dagger) = \sum p \tag{3.30}$$

is an infinite number.

Alternatively if one defines

$$\bar{n}(p_k, g) = \tfrac{1}{2}(1-g)a^\dagger a + \tfrac{1}{2}(1+g)aa^\dagger, \tag{3.31}$$

then

$$\int J_0 \mathrm{d}^3x = \sum(-g)\bar{n}(p_k, g), \qquad \int J_k \mathrm{d}^3x = -\sum g v_k \bar{n}(p_k, g) \tag{3.32}$$

and

$$-P_0 = -N + \sum p\bar{n}(p_k, g), \qquad -P_k = \sum p v_k \bar{n}(p_k, g). \tag{3.33}$$

## 4. Interpretation and Discussion

### 4.1. GENERAL

The present paper is largely based on the observation that the concepts of right and left handedness can be distinguished geometrically although individually they cannot be defined in purely geometrical terms. Definition of momentum space was then obtained from a modification of the usual definition in terms of an expression (2.1) which must be invariant under Lorentz transformations. This modification makes use of a linearisation of (2.1) and leads to the introduction of a new coordinate $g$ — capable of the values $\pm 1$ only — in terms of which right and left handedness are distinguished. The case of a null vector only is treated in detail; this case permits a simplification such that the two possible values of $g$ can be identified with the two possible signs of the time component $p_0$. This identification is restricted to null vectors.

Application of this basic observation to $x_k$-space required similtaneous use of right-handed and left-handed systems. This together with the linearisation has led to the introduction of a number of operators and finally to the replacement of (2.1) by eqs. (2.15) and (2.18), or after transformation from momentum space to ordinary $(x_k, x_0)$ space to eqs. (3.4). It should be mentioned that it is possible to start from the postulation of (3.4) and from there arrive at a definition of momentum space by retracing the steps taken in sect. 2. Continuity of $\eta$ in momentum space is then an essential part of the argument that leads to the interpretation of $g$.

Interpretation of the basic eqs. (3.4) or (2.15) requires the formation of quadratic expressions in terms of which it was expected to regain the numbers $(p_k, g)$ from the operators $\gamma_\mu$, $\psi$. These quadratic expressions satisfy a number of covariant relations. The possibility of a simple interpretation of these relations (3.5) — (3.7) required their invariance under the phase transformation (3.10). To satisfy this requirement it had to be concluded that the four components of $\psi$ do not commute, i.e. that they are operators; in other words it led to the need for quantization of the fields $\psi$. Moreover it followed that quantization according to the Pauli exclusion principle is the only possible form which this quantization can take.

Quantization of fields then, necessitates the introduction of state vectors $\Psi$ so as to obtain an interpretation of the quadratic expressions $\psi^\dagger Q\psi$. The formalism of abstract field theory can then be followed, including definition of creation and annihilation operators. A statement like "let us consider a momentum space vector $(p_k, g)$" can then be formulated in terms of a particular state vector. The Pauli principle then expresses the impossibility of replacing the above statement by "let us consider 2, 3, . . . momentum state vectors, all with equal $(p_k, g)$". Clearly such a result must be expected from a systematic theory.

### 4.2. NEUTRINOS

Eqs. (3.4) are formally identical with the equations of the two-component neutrino theory in terms of a field $\varphi$, together with the reflected field, $\varphi^r$. This formal identity permits interpretation of all properties of (free) neutrinos in terms of purely geometrical quantities. Thus, as usual, number operators $n(g)$ can be introduced by (3.29); $v_k$ represents the velocity, and the new coordinate $g$ then plays the role of neutrino charge so that $\int J_0 \mathrm{d}^3x$ (cf. eq. (3.27)), becomes the total neutrino charge. The covariant quantities $J_\mu$, $T_{\mu\nu}$ have automatically the form required by hole theory.

A statement "let us consider a neutrino (anti neutrino)" is then tautological with a statement "let us consider a vector in momentum space with $g = 1$ $(g = -1)$". To be conclusive this implies of course the possibility of interpreting other particles, and interactions, in geometrical terms.

It will also be noticed that an ambiguity exists with regard to the definition of number operators, as is seen from the two possibilities (3.29) or (3.31). In definition (3.29) $a(p_k, g)$ is an annihilation operator if $g = 1$, and a creation operator if $g = -1$; in (3.31) the opposite choice is made. Accordingly in comparing (3.27) with (3.32), the neutrino charge is $+g$ and $-g$ in the two cases. Also the energy must be defined as $N+P_0$ in the first, and $N-p_0$ in the second case, with $+P_k$ or $-P_k$ as momentum. The choice between the two possibilities rests with the definition of the properties of the state vector for the vacuum.

*Note added in proof:* The infinite quantity $N$ can be eliminated from the energy by redefinition of the energy momentum tensor as $N_{\nu\mu}+T_{\nu\mu}$ or $N_{\nu\mu}-T_{\nu\mu}$ in the two cases. Here we put

$$N_{\nu\mu} = \tfrac{1}{2}(\bar{\psi}\gamma_\nu Q\partial_\mu\psi - (Q\partial_\mu\bar{\psi})\gamma_\nu\psi), \quad \text{with} \quad Q = \frac{1}{\pi}\int_{-\infty}^{\infty}\frac{\sin(zi\partial_0)}{z}\,\mathrm{d}z,$$

so that

$$\int N_{4\mu}\,\mathrm{d}^3x = -\delta_{4,\mu}N$$

and

$$-\int (N_{44}\pm T_{44})\,\mathrm{d}^3x = \sum p(\tfrac{1}{2}(1\pm g)a^\dagger a + \tfrac{1}{2}(1\mp g)aa^\dagger).$$

### 4.3. TRANSFORMATIONS

Invariance of the wave equations (3.4) under continuous Lorentz transformations is well known. In the present case invariance of condition (3.3) must also be proved, but this can easily be verified. Reflexions, however, are to be considered in a different spirit because the wave function $\psi$ contains with $\varphi$ already its space reflected $\varphi^r$. It should first be mentioned that replacement of $(x_k, x_0)$ by $(-x_k, x_0)$ leaves the wave equations (3.4) obviously invariant. In the wave functions, however, using (3.12), (3.13) (2.11) and (2.8) this replacement leads to invariance (apart from a phase transformation) only through the further replacements

$$a(p_k, g) \to a(-p_k, -g), \qquad a^\dagger(p_k, g) \to a^\dagger(-p_k, -g). \tag{4.1}$$

Again, all four $J_\mu$ are invariant under $x_\mu \to -x_\mu$ as well as under (4.1). All $P_\mu$ on the other hand change sign under $x_\mu \to -x_\mu$ but clearly remain invariant if (4.1) is included because $\psi$ is then invariant. Replacement (4.1) implies a change of the interpretation of the number operator from (3.29) to (3.31). This has to be effected by an appropriate transformation of the state vectors.

Space reflexion, $x_k \to -x_k$, simply means that the two $x_k$-systems (referring to $\varphi$ and to $\varphi^r$) have been interchanged, which implies replacement of $\rho_3$ by $-\rho_3$. This can be done by canonical transformation by $i\rho_2$ (or by $\rho_1$). This transformation, i.e. $x_k \to -x_k$ together with $i\rho_2$ leads to the replacements

$$J_0 \to -J_0, \qquad J_k \to J_k, \qquad P_0 \to P_0, \qquad P_k \to -P_k. \tag{4.2}$$

In terms of the interpretation (3.27)—(3.29) this is equivalent with the replacements

$$g \to -g, \qquad v_k \to -v_k, \tag{4.3}$$

i.e. with reversal of both velocity and neutrino charge. Thus the geometrical interpretation of neutrino charge leads under space reflexion automatically to its conjugation in conjunction with a reversal of the velocity.

4.4. CONCLUDING REMARKS

Eq. (3.4) is identical with the neutrino wave equation mentioned in Note 1 (added in proof) of a previous paper [2]). This equation occurs together with wave equations for electrons. The principle of phase invariance which in sect. 3 has led to the establishment of the Pauli principle can clearly be applied in this case as well. It might also be expected that the same principle applied to boson wave equations would lead to a derivation rather than a postulation of the reality conditions (5.10) of this paper [2]), for $k \neq l$, and hence exclude quantization according to the Pauli principle.

## References

1) H. Fröhlich, Proc. Roy. Soc. A. **257** (1960) 147, 283
2) H. Fröhlich, Helv. Phys. Acta **33** (1960) 803

4.C

*Nuclear Physics* **26** (1961) 338—350; © *North-Holland Publishing Co., Amsterdam*

Not to be reproduced by photoprint or microfilm without written permission from the publisher

# INDUCED PSEUDOSCALAR INTERACTION IN $0^- \rightarrow 0^+$ BETA TRANSITIONS

D. TADIĆ

*Institute "Rudjer Bošković", Zagreb*

Received 27 February 1961

**Abstract:** The induced pseudoscalar term is of the form $\beta\gamma_5\{\psi_e^\dagger \beta\gamma_5 \psi_\nu + (\alpha Z/r_0)\psi_e^\dagger \gamma_5 \psi_\nu\}$. In the case of nuclei with high $Z$, the second part of this expression is about 20 times larger than the first, which corresponds to the phenomenologically introduced pseudoscalar coupling. The correction factors for the spectrum and longitudinal polarization in $0^- \rightarrow 0^+$ transitions and the cross terms with the induced pseudoscalar in the allowed transitions are calculated. Numerical analyses are undertaken for the $Pr^{144} \rightarrow Nd^{144}$ transition. A limitation on the ratio $b_P/g_A$ of the induced pseudoscalar form factor $b_P$ and the axial vector coupling constant $g_A$ is found ($|b_P/g_A| \leqq 2.7$, $|f| \leqq 50$). All available experimental results can also be explained with $b_P \approx 0$.

## 1. Introduction

It is easy to prove that in nuclear $\beta$ decay the induced pseudoscalar term in the $\beta$ decay interaction Hamiltonian is entirely different from the phenomenologically introduced pseudoscalar term, which has mostly been investigated so far.

It is well known that starting with the axial vector interaction as a primary interaction, a pseudoscalar term is induced [1, 2]. The most general $\beta$ decay interaction Hamiltonian, when nucleons are treated in configuration space, is [1]

$$H_{\text{int}} = \sum_K \left\{ g_{AK}(i\gamma_\mu\gamma_5)_K(\bar{\psi}_e i\gamma_\mu\gamma_5\eta\psi_\nu)_K + b_{PK}(\gamma_4\gamma_5)_K \frac{\partial}{\partial x_\mu}(\bar{\psi}_e\gamma_\mu\gamma_5\,\eta\psi_\nu)_K \right\}, \quad (1)$$

where $\eta = (1+\gamma_5)/\sqrt{2}$. The summation goes over all available nucleons. The quantities $\psi_e$ and $\psi_\nu$ are the electron and neutrino fields. The $\gamma$ matrices are defined as in ref. [3]). Other notations have the usual meaning. This Hamiltonian is derived on the basis of the most general invariance properties of strong interactions [1, 2]). The $G$ non-conserving terms [2]) are omitted. Kuchowicz [4]) tried to establish the existence of such terms in the case of the allowed $\beta$ decay †. The second term in the Hamiltonian (1) is the so-called induced pseudoscalar coupling resulting from the influence of strong interactions.

† Kuchowicz actually claimed to have found an indication for the existence of such terms. His calculations are based on theoretical expressions for the correction factors derived by Alaga, Šips and Tadić [5, 6]). He omitted some terms which are of the same order of magnitude as those taken account into in his analysis.

The probability of $\beta$ decay is influenced by the electromagnetic field of atomic nuclei, which in the first approximation (usually taken in the $\beta$ decay theory) is described by the static potential $V$. With the help of the Dirac equations for leptons

$$\frac{\partial}{\partial x_\mu}\gamma_\mu\psi_\nu = 0 \quad \frac{\partial}{\partial x_\mu}\bar{\psi}_e\gamma_\mu = m_e\bar{\psi}_e + V\bar{\psi}_e\gamma_4, \tag{2}$$

it is possible to reduce the second term of eq. (1) to the form

$$b_P\beta\gamma_5[m_e\psi_e^\dagger\beta\gamma_5\eta\psi_\nu - V\psi_e^\dagger\gamma_5\eta\psi_\nu]. \tag{3}$$

The summation over individual nucleons is understood. The interaction Hamiltonian can then be written in the form

$$H_{int} = g_A\boldsymbol{\sigma}\cdot\mathbf{L}_A - g_A\gamma_5 L_A + b_P\beta\gamma_5[m_e L_P - V L_A], \tag{4}$$

$$\mathbf{L}_A = \psi_e^\dagger\boldsymbol{\sigma}\eta\psi_\nu, \tag{5}$$

$$L_A = \psi_e^\dagger\gamma_5\eta\psi_\nu, \tag{6}$$

$$L_P = \psi_e^\dagger\beta\gamma_5\eta\psi_\nu. \tag{7}$$

The first part of the induced pseudoscalar coupling corresponds to the phenomenological one. In conventional units, with $m_e = 1$, the potential is $V \approx -2$ even for the decay of a free neutron, so that the second part cannot be neglected in any case †. In the decay of nuclei with high atomic number, the second part is the most important one. For example, $V \approx -20$ in the case of $Pr^{144}$. This is the reason why the analysis [7–10]) of the decay of $Pr^{144}$ in which the pseudoscalar coupling is treated as phenomenological does not give any information about the possible existence of the induced pseudoscalar term.

Present theories of strong interactions indicate that $b_P$ is small [1]) in the nuclear $\beta$ decay. It seems worthwhile to try to find some limitations on $b_P$ from experiments. The analysis will be based on the supposition that pure V-A coupling is the only interaction present in the nuclear $\beta$ decay. The only assumption made about $b_P$ is that it can be treated as a constant parameter.

The $0^- \to 0^+$ transitions, especially those with a relatively low $ft$ value, are suitable cases for analysis. It will be further worthwhile to search for some positon $0^- \to 0^+$ decays ††. Some rough calculations are made in the next section for the decay of $Pr^{144}$, where the best measurements exist. Some brief remarks about the contribution of the induced pseudoscalar coupling to the allowed transitions are given in Appendix 2.

† The second part of the induced pseudoscalar coupling is neglected in the theories of $\mu$-meson capture [1]). Since the mass of a $\mu$-meson is much larger than the electron mass, this is allowed for nuclei with low atomic number $Z$. But in the treatment of nuclei with higher $Z$, this term is important.

†† Only one decay, $Eu^{152}$, is known to the author, but it has very low intensity [13]).

## 2. Correction Factors for $0^- \to 0^+$ Transitions

In ref. [10]) some problems about treating the pseudoscalar interaction are discussed. Here it is only necessary to apply the results of ref. [10]) to the induced pseudoscalar coupling. The most general correction factor for the spectrum in the case of $0^- \to 0^+$ transitions is

$$
\begin{aligned}
C_\beta = g_A{}^2 \Big\{ & |\langle \boldsymbol{\sigma}\cdot\mathbf{r} f_1\rangle|^2 C_1 + 2\langle \boldsymbol{\sigma}\cdot\mathbf{r} f_1\rangle \left\langle \frac{i\boldsymbol{\sigma}\cdot\mathbf{p}}{M} + f_2 \right\rangle^* C_2 \\
& + \langle \boldsymbol{\sigma}\cdot\mathbf{r} f_1\rangle \langle \boldsymbol{\sigma}\cdot\mathbf{r} f_3\rangle^* \frac{C_3}{M} + \left| \left\langle \frac{i\boldsymbol{\sigma}\cdot\mathbf{p}}{M} + f_2 \right\rangle \right|^2 C_4 \\
& + \left\langle \frac{i\boldsymbol{\sigma}\cdot\mathbf{p}}{M} + f_2 \right\rangle \langle \boldsymbol{\sigma}\cdot\mathbf{r} f_3\rangle^* \frac{C_5}{M} + \langle \boldsymbol{\sigma}\cdot\mathbf{r} r^2 f_1\rangle \langle \boldsymbol{\sigma}\cdot\mathbf{r} f_1\rangle^* \bar{C}_1 \\
& + 2\langle \boldsymbol{\sigma}\cdot\mathbf{r} r^2 f_1\rangle \left\langle \frac{i\boldsymbol{\sigma}\cdot\mathbf{p}}{M} + f_2 \right\rangle^* \bar{C}_2 + \left\langle r^2 \left( \frac{i\boldsymbol{\sigma}\cdot\mathbf{p}}{M} + f_2 \right) \right\rangle \left\langle \frac{i\boldsymbol{\sigma}\cdot\mathbf{p}}{M} + f_2 \right\rangle^* \bar{C}_4 \\
& + g_A b_P \Big\{ \langle \boldsymbol{\sigma}\cdot\mathbf{r} f_1\rangle \langle \boldsymbol{\sigma}\cdot\mathbf{r} f_4\rangle^* \frac{C_{11}}{M} + \left\langle \frac{i\boldsymbol{\sigma}\cdot\mathbf{p}}{M} + f_2 \right\rangle \langle \boldsymbol{\sigma}\cdot\mathbf{r} f_4\rangle^* \frac{C_{12}}{M} \\
& + 2\langle \boldsymbol{\sigma}\cdot\mathbf{r} f_1\rangle \langle \boldsymbol{\sigma}\cdot\mathbf{r} f_5\rangle^* C_{13} + 2\left\langle \frac{i\boldsymbol{\sigma}\cdot\mathbf{p}}{M} + f_2 \right\rangle \langle \boldsymbol{\sigma}\cdot\mathbf{r} f_5\rangle^* C_{14} \Big\} \\
& + b_P{}^2 \Big\{ |\langle \boldsymbol{\sigma}\cdot\mathbf{r} f_4\rangle|^2 \frac{C_{16}}{4M^2} + |\langle \boldsymbol{\sigma}\cdot\mathbf{r} f_5\rangle|^2 C_{15} + \langle \boldsymbol{\sigma}\cdot\mathbf{r} f_4\rangle \langle \boldsymbol{\sigma}\cdot\mathbf{r} f_5\rangle^* \frac{C_{17}}{M} \Big\} .
\end{aligned}
\tag{8}
$$

All notations are the same as in ref. [10]), where almost all $C_i$ are listed. The $f_i$ are some unknown combinations of nuclear potentials and operators. The simplest assumption about them is $f_1 = f_3 = f_4 = 1$, $f_2 = 0$, $f_5 = G(r)$, where $G(r)$ is an unknown function. Longitudinal polarization is defined as

$$
\mathbf{P} = \mp \frac{\mathbf{p}_e}{W} \frac{P_\beta}{C_\beta} ; \tag{9}
$$

$P_\beta$ is easily obtained from (8) if all $C_i$ are replaced by the corresponding $P_i$. A complete list of all $P_i$ and $C_i$ is given in Appendix 1 †. The upper and lower sign in (9) refer to the negaton and positon emission respectively. For the emission of positons it is necessary to replace all the electron wave functions in the expressions for $P_i$ and $C_i$ by the wave functions for positons, and to put $V \to -V$.

Some calculations were made for two extreme cases: when the pseudoscalar coupling involves or does not involve derivatives. Those calculations served only as an orientation. Finite size corrections and screening were not taken

† In ref. [10]) there is a number of misprints.

into account. The combinations $A_V$, $B_V$, $C_V$ and $D_V$ were obtained by interpolating numerical tables for the spectra [13]).

The physical assumptions are the same as in ref. [10]) for Case I, when the pseudoscalar coupling involves derivatives, and for Case II, when it does not.

### 2.1. CASE I. PSEUDOSCALAR WITH DERIVATIVES

The correction factor is given by

$$C_\beta = |\langle \boldsymbol{\sigma} \cdot \mathbf{r} \rangle|^2 g_A{}^2 \left\{ C_1 + 2fC_2 + \frac{C_3}{M} + f^2 C_4 + f\frac{C_5}{M} + s\bar{C}_1 + 2sf\bar{C}_2 + tf^2\bar{C}_4 + \varepsilon\frac{C_{11}}{M} + \varepsilon f\frac{C_{12}}{M} + \varepsilon^2\frac{C_{16}}{4M^2} \right\}, \tag{10}$$

where

$$f = \frac{\left\langle \frac{i\boldsymbol{\sigma} \cdot \mathbf{p}}{M} \right\rangle}{\langle \boldsymbol{\sigma} \cdot \mathbf{r} \rangle}, \qquad \varepsilon = \frac{b_P}{g_A}, \tag{11}$$

$$s \approx t \approx r_0{}^2. \tag{12}$$

The polarization $P_\beta$ is obtained from (11) by the replacement $C_i \to P_i$. The term with $\varepsilon^2$ is included because for $|\varepsilon| > 1$ it becomes more and more important. For $|\varepsilon| < 1$ the contribution of this term is practically negligible, except in the region of destructive interference, where $C_\beta$ is small.

Detailed numerical analyses for $Pr^{144}$, apart from those of refs. [7–10]), were also undertaken by Bhalla and Rose [11]) for the axial vector interaction with a phenomenological pseudoscalar coupling. They used the wave functions for electrons with finite size corrections [14]) but neglected the terms $C_3$, $C_5$, $\bar{C}_1$, $\bar{C}_2$ and $\bar{C}_4$. They fitted the experimental shape factor of Porter and Day [15]) by a polynomial in the electron momentum $p$, and then searched for all theoretical factors which led to deviations by less than 4 % from this polynomial. Fig. 1 represents the region of parameters $f$ and $\varepsilon$ satisfying this condition (ref. [11]), eq. (16)). The calculations were made for the electron momenta $p = 1$, 2 and 5. The point $p = 2$ was normalized to the polynomial which fitted the experimental shape factor. In points $p = 1$ and $p = 5$ the permissible deviations were less than 3 %. The agreement with the results of Bhalla and Rose [11]) is quite satisfactory for the case $b_P = 0$.

The conclusion is that with an admixture of induced pseudoscalar coupling it is possible to obtain an agreement with experiments for $f \leqq 5$ and also for $f \geqq 40$. For $0 \leqq f \leqq 30$ there is a region of destructive interference of the two parts of the axial vector interaction. Even with the admixture of induced pseudoscalar coupling, the value of the correction factor is rather small in this region. This seems to be in disagreement with the relatively low $ft$ value

in the decay of $Pr^{144}$. One might perhaps extend the region of destructive interference even further than is represented in fig. 1, but the results of numerical calculations are not accurate enough to draw any definite conclusions.

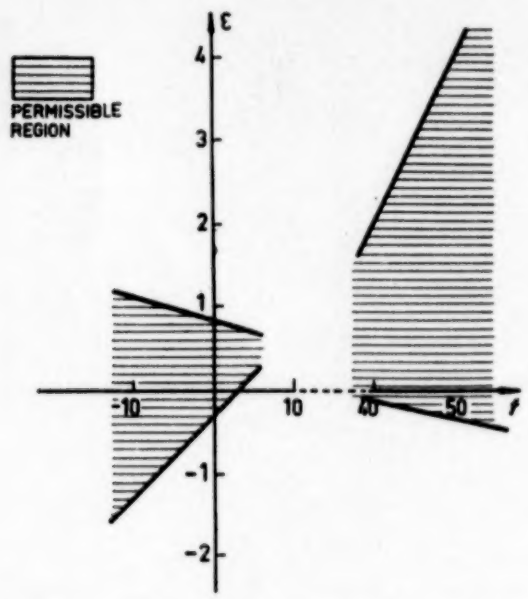


Fig. 1. Permissible region of parameters $f$ and $\varepsilon$ defined by eq. (11) for the shape factor data of refs. [15, 11]).

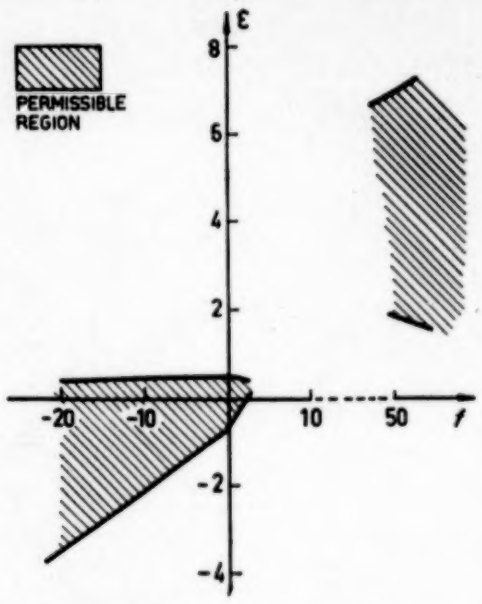


Fig. 2. Permissible region of parameters $f$ and $\varepsilon$ defined by eq. (11) if the mean deviation of the theoretical shape factor from the straight line is less than 3.5 %.

In ref. [10]) the condition for the calculated shape factor was that its mean deviation from a straight line had to be less than 3.5 %. That condition leads

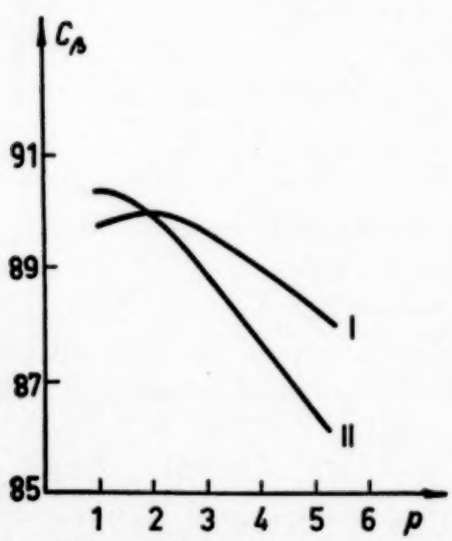


Fig. 3. Theoretical shape factor $C_\beta$ defined by eq. (10) plotted in arbitrary units as a function of the electron momentum. Curve I corresponds to $f = -5$, $\varepsilon = 0$, Curve II corresponds to $f = -5$, $\varepsilon = 0.7$.

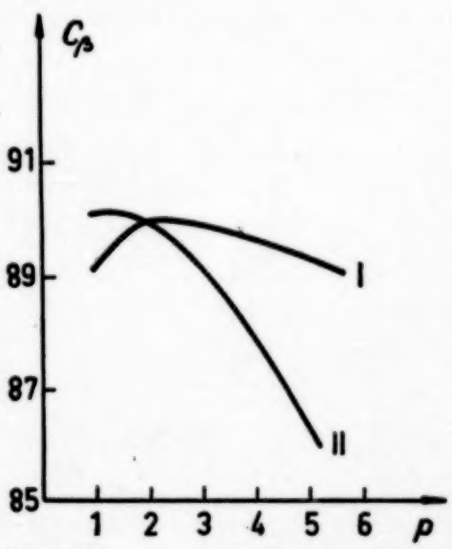


Fig. 4. The same as in fig. 3, except that here Curve I corresponds to $f = 2$, $\varepsilon = 0$, and Curve II corresponds to $f = 2$, $\varepsilon = 0.7$.

to somewhat different conclusion from the conditions applied in obtaining fig. 1. For such a case the permissible region for $f$ and $\varepsilon$ is shown in fig. 2. Under such conditions the region $5 \leqq f \leqq 200$ is not permissible for $\varepsilon = 0$.

As an illustration of the possible influence of the induced pseudoscalar coupling the correction factors $C_\beta$ for various values of $f$, and for $\varepsilon = 0$ and $\varepsilon = 0.7$ are plotted in figs. 3, 4 and 5. In all the figures the correction factors are normalized to the same point, in order to facilitate comparison. The correction factors for longitudinal polarization are not very sensitive to the admixture of induced pseudoscalar coupling. In table 1 the $P_\beta/C_\beta$ ratios for some values of the parameters are given.

TABLE 1

$P_\beta/C_\beta$ ratio

| $p$ \ $f$, $\varepsilon$ | −5, 0 | 5, 0.7 | 2, 0 | 2, 07 | 50, 0 | 50, 0.7 |
|---|---|---|---|---|---|---|
| 1.0 | 1.025 | 1.023 | 1.036 | 1.036 | 0.989 | 0.991 |
| 2.0 | 1.017 | 1.017 | 1.026 | 1.027 | 0.995 | 0.996 |
| 5.0 | 1.006 | 1.005 | 1.009 | 1.008 | 0.997 | 0.998 |

Under the most favourable circumstances the method for the experimental determination of $\varepsilon$ can be as follows: from longitudinal polarization, measured as a function of energy, it is possible to determine a value of $f$, and then it is necessary to adjust $\varepsilon$ to fit the measured spectrum shape $C_\beta$. This consideration is based on the supposition that the treatment of the induced pseudoscalar coupling in Case I is correct, and that $|\varepsilon|$ is smaller than 1.

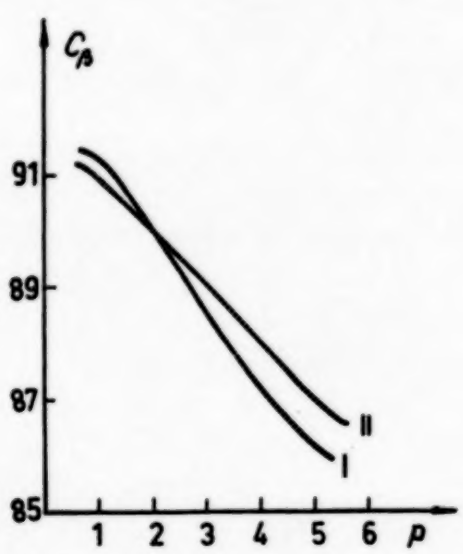


Fig. 5. The same as in fig. 3, except that here Curve I corresponds to $f = 50$, $\varepsilon = 0$, and Curve II corresponds to $f = 50$, $\varepsilon = 0.7$.

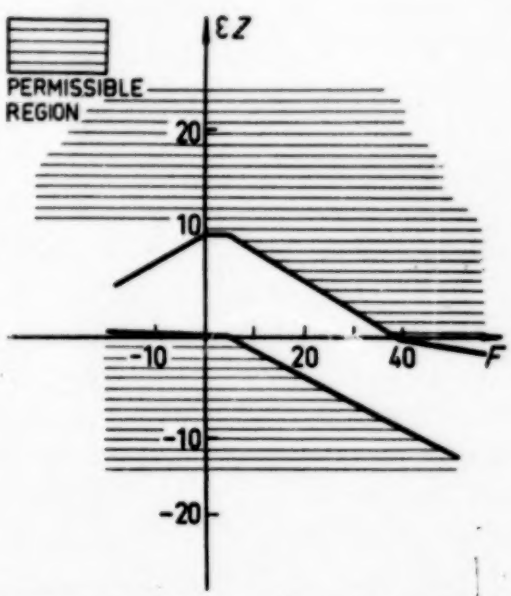


Fig. 6. Permissible region of parameters $F$ and $\varepsilon Z$ defined by eqs. (14) and (15) respectively for the shape factor data of refs. [15, 11]).

### 2.2. CASE II. PSEUDOSCALAR WITHOUT DERIVATIVES

In our present state of knowledge about atomic nuclei it is impossible to reach any definite conclusion about the presence or absence of derivatives in the pseudoscalar coupling †. The terms with derivatives and the cross-terms between the terms with and without derivatives are here neglected for simplicity.

The correction factor is then given by

$$C_\beta = |\langle \boldsymbol{\sigma}\cdot\mathbf{r}\rangle|^2 g_A{}^2 \Big\{ C_1 + 2FC_2 + \frac{C_3}{M} + F^2 C_4 + F\frac{C_5}{M} + s\bar{C}_1 + 2sF\bar{C}_2 + tF^2\bar{C}_4 + 2\varepsilon Z C_{13} + 2\varepsilon Z F C_{14} + (\varepsilon Z)^2 C_{15} \Big\}, \tag{13}$$

$$F = \frac{\left\langle i\dfrac{\boldsymbol{\sigma}\cdot\mathbf{p}}{M} - 2\boldsymbol{\sigma}\cdot\mathbf{r}G(r)\right\rangle}{\langle \boldsymbol{\sigma}\cdot\mathbf{r}\rangle} \quad \text{or} \quad F = -\frac{\langle i\gamma_5\rangle}{\langle \boldsymbol{\sigma}\cdot\mathbf{r}\rangle}, \tag{14}$$

$$Z = \frac{\langle \boldsymbol{\sigma}\cdot\mathbf{r}G(r)\rangle}{\langle \boldsymbol{\sigma}\cdot\mathbf{r}\rangle} \quad \text{or} \quad Z = \frac{\langle i\beta\gamma_5\rangle}{\langle \boldsymbol{\sigma}\cdot\mathbf{r}\rangle}, \tag{15}$$

$$s \approx t \approx r_0{}^2. \tag{16}$$

For details about $F$ and $Z$ see ref. [10]). The polarization $P_\beta$ is easily obtained from (13) by the replacement $C_i \to P_i$. In fig. 6 the permissible region for the parameters $F$ and $\varepsilon Z$ is derived under the same conditions as those used in deriving fig. 1. In the region of destructive interference, for a high value of $\varepsilon Z$, the correction factor is large enough to be in agreement with the $ft$ value for the decay of $Pr^{144}$. But such high values of $\varepsilon Z$ are not very reliable.

## 3. Conclusion

The present paper and refs. [16, 10, 11]) cover some interesting features of the phenomenological pseudoscalar interaction and the induced pseudoscalar interaction. The best way of analysing the experimental results is to try all possibilities. On the basis of our present knowledge the simultaneous appearance of the induced and phenomenological pseudoscalar couplings is possible. It is easy to combine the expressions of ref. [10]) and of this paper for such a case, since the notation and normalization are the same. All $P_i$ and $C_i$ with the same index, here and in ref. [10]), are identical.

The correction factors resulting from the induced pseudoscalar term are multiplied by the Coulomb potential $V$ and are therefore rather large in the

† In the case of the allowed transitions the difference between the two treatments is not so great as in the case of $0^- \to 0^+$ transitions. See Appendix 2.

case of nuclei with high $Z$. Their contribution to the spectrum shape factor and to longitudinal polarization depends on the ratio between the form factor $b_P$ and the axial vector coupling constant $g_A$. Even for $b_P/g_A \approx 0.1$ this contribution is not negligible in some cases.

The most general treatment of the induced pseudoscalar coupling, given by eq. (8), can explain all known experimental results. A great variety of parameter values is possible. It is necessary to point out that all available measurements could be explained without any pseudoscalar interaction at all, if the matrix element ratio $f(F)$ is treated as an adjustable parameter. Theoretical results [19–22]) for $f$ were evaluated on the basis of some simple nuclear models. The results cover the region $2.5 \leqq f \leqq 37$. The experimental results for these values of $f$ can be reproduced only with an admixture of some kind of pseudoscalar interaction †. The $\pi \to \mu+\nu$ to $\pi \to e+\nu$ decay ratio [23, 24]) indicates that the phenomenological pseudoscalar coupling is absent in weak interactions. The theoretical calculations of the nuclear matrix elements and the ratio mentioned above are an indication (although a weak one) that the $b_P/g_A$ ratio is not very small. For more definite conclusions it will be useful to combine the results for different atomic nuclei, and if possible, for some positon emitters.

## Appendix 1. Complete List of all $P_i$ and $C_i$

We give firstly the following list of all $C_i$:

$$C_1 = M_0 - \tfrac{2}{3}qN_0 + \tfrac{1}{9}q^2 L_0, \tag{A.1}$$

$$C_2 = N_0 - \tfrac{1}{3}qL_0, \tag{A.2}$$

$$C_3 = \tfrac{1}{9}q^2(W-V+q)L_0 + (W-V-\tfrac{1}{3}q)M_0 - \tfrac{2}{3}q(W-V+\tfrac{1}{3}q)N_0 - \tfrac{1}{9}q^2 P_0 - Q_0, \tag{A.3}$$

$$C_4 = C_{10} = L_0, \tag{A.4}$$

$$C_5 = (W-V-\tfrac{1}{3}q)N_0 + R_0 - \tfrac{1}{3}q(W-V+q)L_0 + \tfrac{1}{3}qP_0, \tag{A.5}$$

$$C_6 = M_0 - UQ_0 - \tfrac{2}{3}q(2Q_0+N_0) + \tfrac{1}{9}q^2(L_0 - UP_0 - 4R_0) \tag{A.6}$$

$$C_7 = UR_0 + N_0 + \tfrac{1}{3}q(UP_0 - L_0 + 4R_0), \tag{A.7}$$

$$C_8 = \tfrac{1}{3}qP_0 - R_0, \tag{A.8}$$

$$C_9 = -P_0, \tag{A.9}$$

$$\bar{C}_1 = \tfrac{8}{45}q^3 N_0 - \tfrac{1}{45}q^4 L_0 - \tfrac{1}{3}q^2 M_0, \tag{A.10}$$

$$\bar{C}_2 = \tfrac{4}{45}q^3 L_0 + \tfrac{1}{3}qM_0 - \tfrac{4}{9}q^2 N_0, \tag{A.11}$$

$$\bar{C}_4 = \tfrac{2}{3}qN_0 - \tfrac{1}{3}q^2 L_0, \tag{A.12}$$

† Of course, if the tensor interaction is excluded.

$$C_{11} = C_6 + VC_3, \tag{A.13}$$

$$C_{12} = C_7 + VC_5, \tag{A.14}$$

$$C_{13} = C_8 - VC_2, \tag{A.15}$$

$$C_{14} = C_9 - VC_4, \tag{A.16}$$

$$C_{15} = (1+V^2)C_4 - 2VC_9, \tag{A.17}$$

$$C_{16} = \alpha_1 + V^2\alpha_2 - 2V\alpha_3, \tag{A.18}$$

$$\begin{aligned} C_{17} = {} & -V^2C_5 - VC_7 + \tfrac{1}{3}qP_0 - (W-V+\tfrac{1}{3}q)N_0 - R_0 - \tfrac{1}{3}qUL_0 \\ & + V[\tfrac{1}{3}q(W-V+q)P_0 - N_0 - (W-V-\tfrac{1}{3}q)R_0 - \tfrac{1}{3}qL_0], \end{aligned} \tag{A.19}$$

In these formulae, we used

$$\begin{aligned} \binom{\alpha_1}{\alpha_2} = {} & [(W-V)^2+1]M_0 - 2(W-V)Q_0 + \tfrac{1}{9}q^2\{M_0 - 4(W-V)N_0 - 8R_0 \\ & - 2(W-V)P_0 + [(W-V)^2+1]L_0 + 8L_1\} \pm \tfrac{2}{3}q\{(W-V)M_0 - Q_0 \\ & + [(W-V)^2-1]N_0\} \mp \tfrac{2}{9}q^3[(W-V)L_0 - P_0 + N_0] + \tfrac{1}{9}q^4L_0, \end{aligned} \tag{A.20}$$

$$\begin{aligned} \alpha_3 = {} & [(W-V)^2+1]Q_0 - 2(W-V)M_0 + \tfrac{1}{9}q^2\{8(W-V)R_0 + 4N_0 - Q_0 \\ & + [(W-V)^2+1]P_0 - 2(W-V)L_0 - 8P_1\} - \tfrac{1}{9}q^4P_0, \end{aligned} \tag{A.21}$$

$$U = W - V - q, \tag{A.22}$$

$$V = -\frac{\alpha Z}{r_0}. \tag{A.23}$$

All other notations have the usual meaning. The parameter $\alpha_1$ corresponds to the quadratic term of the phenomenological pseudoscalar coupling, and it was calculated by Rose and Osborn [16]).

Now we give the following list of all $P_i$:

$$P_1 = (\tfrac{1}{9}q^2A_0 - \tfrac{2}{3}qC_0 - B_0)n, \tag{A.24}$$

$$P_2 = (C_0 - \tfrac{1}{3}qA_0)n, \tag{A.25}$$

$$P_3 = [\tfrac{1}{9}q^2(W-V+q)A_0 - (W-V-\tfrac{1}{3}q)B_0 - \tfrac{2}{3}q(W-V+\tfrac{1}{3}q)C_0 - \tfrac{2}{3}qD_0]n, \tag{A.26}$$

$$P_4 = A_0n, \tag{A.27}$$

$$P_5 = -[\tfrac{1}{3}q(W-V+q)A_0 - (W-V-\tfrac{1}{3}q)C_0 - D_0]n, \tag{A.28}$$

$$P_6 = [\tfrac{1}{9}q^2A_0 - B_0 - \tfrac{2}{3}qC_0 - \tfrac{2}{3}q(W-V-\tfrac{1}{3}q)D_0]n, \tag{A.29}$$

$$P_7 = [(W-V+\tfrac{1}{3}q)D_0 - \tfrac{1}{3}qA_0 + C_0]n, \tag{A.30}$$

$$P_8 = D_0n, \tag{A.31}$$

$$P_9 = 0, \tag{A.32}$$

$$P_{10} = -A_0 n, \tag{A.33}$$

$$\bar{P}_1 = (\tfrac{8}{45}q^3 C_0 + \tfrac{1}{3}q^2 B_0 - \tfrac{1}{45}q^4 A_0)n, \tag{A.34}$$

$$\bar{P}_2 = (\tfrac{4}{45}q^3 A_0 - \tfrac{1}{3}qB_0 - \tfrac{4}{9}q^2 C_0)n, \tag{A.35}$$

$$\bar{P}_4 = (\tfrac{2}{3}qC_0 - \tfrac{1}{3}q^2 A_0)n, \tag{A.36}$$

$$P_{11} = P_6 + VP_3, \tag{A.37}$$

$$P_{12} = P_7 + VP_5, \tag{A.38}$$

$$P_{13} = P_8 - VP_2, \tag{A.39}$$

$$P_{14} = -VP_4, \tag{A.40}$$

$$P_{15} = (V^2-1)P_4, \tag{A.41}$$

$$P_{16} = (\beta_1 + V^2\beta_2 - 2V\beta_3)n, \tag{A.42}$$

$$\begin{aligned} P_{17} = {} & -V^2P_5 - VP_7 + [(W-V+\tfrac{1}{3}q)C_0 + D_0 + \tfrac{1}{3}qUA_0]n \\ & + V[\tfrac{1}{3}qA_0 + (W-V-\tfrac{1}{3}q)D_0 + C_0]n. \end{aligned} \tag{A.43}$$

In eq. (A.42) we have used the following notation:

$$\begin{aligned} \begin{pmatrix}\beta_1\\ \beta_2\end{pmatrix} = {} & \pm[(W-V)^2-1]B_0 + \tfrac{1}{3}q\{2(W-V)B_0 - 2[(W-V)^2+1]C_0 \\ & -4(W-V)D_0\} + \tfrac{2}{9}q^3[C_0 + (W-V)A_0] \pm \tfrac{1}{9}q^2\{4D_0 + 4(W-V)C_0 \\ & -[(W-V)^2-1]A_0 + B_0 - 8A_1\} \mp \tfrac{1}{9}q^4 A_0, \end{aligned} \tag{A.44}$$

$$\beta_3 = \tfrac{1}{3}q\{2[(W-V)^2+1]D_0 - 2B_0 + 4(W-V)C_0\} + \tfrac{2}{9}q^3(D_0 - A_0). \tag{A.45}$$

The term $\beta_1 n$ corresponds to the quadratic term of the phenomenological pseudoscalar coupling. It was calculated by Bhalla and Rose [11]). The coefficients $A_r, B_r, C_r, D_r$ and $n$ are defined in ref.[10]). The correspondence with the notations of Bhalla and Rose is

$$-\frac{\not{p}}{W}A_r n = A_r, \tag{A.46}$$

$$-\frac{\not{p}}{W}B_r n = B_r, \tag{A.47}$$

$$-\frac{\not{p}}{W}C_r n = \tfrac{1}{2}D_r, \tag{A.48}$$

$$-\frac{\not{p}}{W}D_r n = \tfrac{1}{2}C_r, \tag{A.49}$$

where the symbols on the right-hand side are those used in ref. [11]).

## Appendix 2. Contribution to the Allowed Transitions of the Induced Pseudoscalar

In the case of the allowed Gamow-Teller transitions the difference between the terms with and without derivatives of the pseudoscalar coupling is not so great as in the case of $0^- \to 0^+$ transitions.

CASE I. PSEUDOSCALAR WITH DERIVATIVES

The results for the cross-terms between the axial vector and the induced pseudoscalar couplings are

$$g_A b_P \frac{4\pi|\langle||T_{10}||\rangle|^2}{M} \tfrac{1}{3}\{[L_0 - UP_0 + V([U+2q]L_0 - P_0)] + K([W-V]P_0 - L_0 + 3R_0) + V(P_0 - 3N_0 - [W-V]L_0)]\}, \tag{A.50}$$

where

$$K = \frac{\sqrt{2}\langle||T_{12}||\rangle}{\langle||T_{10}||\rangle}.$$

This expression can be used with the correction factors calculated by Alaga, Šips and Tadić [5, 6]), where the tensor operators $T_{JA}$ are defined. The corresponding term in $P_\beta$ is

$$g_A b_P \frac{4\pi|\langle||T_{10}||\rangle|^2}{M} \tfrac{1}{3}\{[A_0 + V(W-V+q)A_0] + K[3D_0 - A_0 - V(3C_0 + [W-V]A_0)]\}n. \tag{A.51}$$

CASE II. PSEUDOSCALAR WITHOUT DERIVATIVES

In this case the result is

$$g_A b_P 2\langle\boldsymbol{\sigma}\rangle\langle i\beta\gamma_5 \mathbf{r}\rangle^* \left\{V\left(N_0 - \frac{q}{3}L_0\right) - \tfrac{1}{3}qP_0 - R_0\right\}. \tag{A.52}$$

This term can be used with the correction factor calculated by Morita [17, 18]). For $P_\beta$ the following result is obtained:

$$g_A b_P 2\langle\boldsymbol{\sigma}\rangle\langle i\beta\gamma_5 \mathbf{r}\rangle^* \{V(C_0 - \tfrac{1}{3}qA_0) - D_0\}n. \tag{A.53}$$

It is interesting to make a comparison of the expressions (A.50) and (A.52) in the low-$Z$ limit. For the nuclear matrix elements the following relations were used:

$$4\pi|\langle||T_{10}||\rangle|^2 = |\langle\boldsymbol{\sigma}\rangle|^2, \tag{A.54}$$

$$\langle i\beta\gamma_5 \mathbf{r}\rangle \approx -\frac{\langle\boldsymbol{\sigma}\rangle}{2M}. \tag{A.55}$$

The relation (A.55) is based on eq. (A.1) of ref. [17]). The results are

$$g_A b_P \frac{|\langle\sigma\rangle|^2}{M} \frac{1}{3}\left\{\left[\frac{E_0}{W} - 4\xi^2 - 2E_0\xi - 1\right] + K\left[-\frac{\xi}{W} - 2\xi^2\right]\right\}, \qquad \text{(A.50a)}$$

$$g_A b_P \frac{|\langle\sigma\rangle|^2}{M} \frac{1}{3}\left\{\frac{E_0 - \xi}{W} - 6\xi^2 - 2E_0\xi - 1\right\}, \qquad \text{(A.52a)}$$

$$\xi = \frac{\alpha Z}{2r_0}. \qquad \text{(A.56)}$$

Here, $E_0$ is the maximum kinetic energy of the emitted particle. Eqs. (A.50a) and (A.52a) are identical for $K = 1$. But of course, $K$ varies from nucleus to nucleus, its sign being either positive or negative. This comparison may be an illustration of the difference between Morita's treatment [17, 18]) and the treatment applied in ref. [5]) †.

Some estimations for the case of the $B^{12} \to C^{12}$ transition show that the influence of the pseudoscalar term for $b_P/g_A = 0.7$ is practically unobservable. The variation in energy is lower than 0.3 % over the whole spectrum region. Some larger effects are expected for nuclei with higher atomic number.

A more detailed account for the allowed transitions is to be published elsewhere [25]).

*Note added in proof:* Case I (subsect. 2.1) was recalculated using more accurate tables for electron wave functions of C. P. Bhalla and M. E. Rose, ORNL-2954. The calculations were made under the same conditions as those for fig. 1, except that the point $p = 1$ was normalized to the polynomial which fitted the experimental shape factor.

The results can be presented in the following table:

| | |
|---|---|
| $f = -50$ | $-2.7 \leqq \varepsilon \leqq 2.5$ |
| $-10$ | $-0.7 \leqq \varepsilon \leqq 1.2$ |
| 0 | $-0.1 \leqq \varepsilon \leqq 0.9$ |
| 5 | $0.2 \leqq \varepsilon \leqq 0.7$ |
| 10 | no conclusion is possible |
| 20 | $0.2 \leqq \varepsilon \leqq 0.8$ |
| 30 | $-0.1 \leqq \varepsilon \leqq 1.4$ |
| 50 | $-0.8 \leqq \varepsilon \leqq 2.5$ |

A new limitation on the $b_P/g_A$ ratio is

$$|b_P/g_A| \leqq 2.7 \quad \text{for} \quad |f| \leqq 50.$$

† Similar conclusions can be made for the term induced by weak magnetism.

Instead of table 1, we now obtain table 1a.

TABLE 1a

$P_\beta/C_\beta$ ratio

| $p$ \ $f, \varepsilon$ | −5, 0 | −5, 0.7 | 2, 0 | 2, 0.7 | 50, 0 | 50, 07 |
|---|---|---|---|---|---|---|
| 1.0 | 1.026 | 1.024 | 1.040 | 1.040 | 0.990 | 0.993 |
| 2.0 | 1.017 | 1.015 | 1.025 | 1.024 | 0.994 | 0 995 |
| 5 0 | 1.006 | 1.006 | 1.009 | 1.010 | 0.997 | 0.998 |

I wish to express my thanks to Professor M. E. Rose and Dr. C. P. Bhalla for sending me the preprint of their tables for electron wave functions and for some discussions.

## References

1) M. L. Goldberger and S. B. Treiman, Phys. Rev. **111** (1958) 354
2) S. Weinberg, Phys. Rev. **112** (1958) 1375
3) R. H. Good, Jr., Rev. Mod. Phys. **27** (1955) 187
4) Br. Kuchowicz, Dubna Report (1960) E 611; Acta Phys. Polon **20** (1961) 342
5) G. Alaga, L. Šips and D. Tadić, Nuclear Physics **6** (1958) 305
6) G. Alaga, L. Šips and D. Tadić, Nuclear Physics **26** (1961) 351
7) R. L. Graham, J. S. Geiger and T. A. Eastwood, Can. J. Phys. **36** (1958) 1084
8) W. Bühring, Z.f. Phys. **155** (1959) 566
9) S. G. Cohen and R. Wiener, Nuclear Physics **15** (1960) 79
10) D. Tadić, Nuclear Physics **18** (1960) 138
11) C. P. Bhalla and M. E. Rose, Phys. Rev. **120** (1960)
12) Nuclear Data Sheets, NRC 59−4−78
13) M. E. Rose, C. L. Perry and N. M. Dismuke, ORNL−1459
14) C. P. Bhalla and M. E. Rose, ORNL−2954
15) F. T. Porter and P. P. Day, Phys. Rev. **114** (1959) 1286
16) M. E. Rose and R. K. Osborn, Phys. Rev. **93** (1954) 1315
17) M. Morita, Phys. Rev. **113** (1959) 1584
18) M. Morita, Nuclear Physics **14** (1959) 106
19) D. L. Pursey, Phil. Mag. **42** (1951) 1193
20) T. Ahrens and E. Feenberg, Phys. Rev. **86** (1952) 64
21) M. E. Rose and R. K. Osborn, Phys. Rev. **93** (1954) 1326
22) J. M. Pearson, Can. J. Phys. **38** (1960) 148 and private communication
23) E. J. Konopinski, Annual Review of Nuclear Science **9** (1959)
24) J. J. Sakurai, Lectures in Theoretical Physics (Interscience Publishers, New York, 1960)
25) B. Eman and D. Tadić, Glasnik mat.-fiz. i astr., in the press

10.E *Nuclear Physics* **26** (1961) 351—352; © *North-Holland Publishing Co., Amsterdam*

# ERRATUM AND ADDENDUM

G. Alaga, L. Šips and D. Tadić, Calculation of some relativistic corrections to the allowed and *l*-forbidden beta transitions, Nuclear Physics **6** (1958) 305.

Some of the positon signs in the formulas (3), (4), (8), (9), (10) and (9a) are incorrect. The correct signs for positons are obtained from those of negatons by the substitution $g_1 \to -g_1$, $g_2 \to g_2$, $g_3 \to g_3$, $g_4 \to -g_4$ and $g_5 \to -g_5$. For the Coulomb field the substitution $Z \to -Z$ also has to be made. The correct formulas are:

$$A_F = g_1^2+g_2^2 \pm g_1 g_2 \frac{1}{W} + \frac{1}{M}\left[g_2(\pm g_1+g_3)\frac{q}{W} - (\pm g_1 g_3 - g_2^2)\frac{p^2}{W} + (\pm g_1 g_3 + g_2^2) q\right]$$
$$+ \left\{\frac{g_2^2-g_1^2}{W} + \frac{1}{M}\left[\frac{g_2(\pm g_1+g_3)-(\pm g_1 g_3 - g_2^2)q}{W} + (\pm g_1 g_3 + g_2^2)\right]\right\} p \cos\theta, \qquad (3)$$

$$C_F = (g_1^2+g_2^2)L_0 \pm g_1 g_2 2P_0$$
$$+ \frac{1}{M}\{(UP_0-L_0)g_2(\pm g_1 - g_3) - (UL_0-P_0)(\pm g_1 g_3 - g_2^2) + 2q(L_0 g_2 \pm P_0 g_1) g_2\}, \qquad (4)$$

$$A_{GT} = g_3^2+g_4^2 \pm g_3 g_4 \frac{2}{W} + \frac{1}{3M}\left[\pm(g_3 g_5 + 2g_2 g_4)\left(q - \frac{p^2}{W}\right)\right.$$
$$+ (g_4^2+2g_3^2)\left(q+\frac{p^2}{W}\right) + (\pm 3 g_3 g_4 + g_4 g_5 + 2 g_2 g_3)\left.\frac{q}{W}\right]$$
$$+ \tfrac{1}{3}\left\{(g_3^2-g_4^2)\frac{p}{W} + \frac{1}{M}\left[\pm(g_3 g_5 + 2 g_2 g_4)\left(1-\frac{q}{W}\right)p\right.\right. \qquad (8)$$
$$\left.\left. + (g_4^2+2g_3^2)\left(1+\frac{q}{W}\right)p + (\pm 3 g_3 g_4 + g_4 g_5 + g_2 g_3)\frac{p}{W}\right]\right\}\cos\theta,$$

$$C_{GT} = (g_3^2+g_4^2)L_0 \pm 2 g_3 g_4 P_0 + \frac{1}{3M}[(2g_3^2 \mp g_2 g_3 \mp g_3 g_5 + g_4^2)(UL_0 - P_0) \qquad (9)$$
$$+ (\pm g_3 g_4 - 2 g_2 g_3 - g_4 g_5)(UP_0 - L_0) + (2g_3^2+g_4^2)2qL_0 \pm 6 g_3 g_4 q P_0],$$

$$C_{TG_1} = \frac{1}{(2M)^2}\frac{2}{g}|\langle\|r^2 T_{12}(\mathbf{r},\boldsymbol{\sigma})\|\rangle_\beta|^2 \frac{1}{r_0^4}\left\{[g_2^2+g_3^2+g_4^2+g_5^2\right.$$
$$\mp 2(g_2 g_4 + g_3 g_5)]\{[(W-V_c)^2+1]L_0 + (6N_0 - 2P_0)(W-V_c) - 6R_0 + 9M_0\}$$
$$+ 2[\pm(g_2 g_5 + g_3 g_4) - (g_2 g_3 + g_4 g_5)]\{[(W-V_c)^2+1]P_0 \qquad (10)$$
$$\left. + (6R_0 - 2L_0)(W-V_c) - 6N_0 - 9Q_0\}\right\},$$

$$\frac{2\pi\sqrt{2}}{3M}\,[\langle||T_{10}||\rangle\langle||r^2T_{12}||\rangle^*+\text{c.c.}]\,\frac{1}{r_0^{\,2}}\,\{(\pm 2g_3g_4-g_4g_5-g_3g_2)\qquad(9a)$$
$$\times[(W-V_c)P_0-L_0+3R_0]+(g_4^{\,2}+g_3^{\,2}\mp g_2g_4\mp g_3g_5)[(W-V_c)L_0-P_0+3N_0]\}.$$

From the positon spectrum the electron capture probability can be obtained by making the substitutions $P_k \to -P'_k$, $Q_k \to -Q'_k$, $N_k \to -N'_k$, $W \to -W$, $V_c = +\alpha Z/r_0$, where $P'_k$, $Q'_k$ etc. are defined in the same way as in H. Brysk and M. E. Rose, Rev. Mod. Phys. **30** (1958) 1169. For the radial functions bound solutions for electrons, with $W < 1$, have to be taken. Summation over the electron shells has to be performed.

# NORTH-HOLLAND BOOKS

**Announcing the new series**

# PROGRESS IN OPTICS

**A new international series of review articles devoted to advances in theoretical and applied optics and to related fields**

**Edited by**

**EMIL WOLF**

**Institute of Optics**
**University of Rochester**
**Rochester, N.Y., U.S.A.**

**EDITORIAL ADVISORY BOARD**

M. Françon *(Paris)*
A. C. S. van Heel *(Delft)*
E. Ingelstam *(Stockholm)*
K. S. Krishnan *(New Delhi)*
H. Kubota *(Tokyo)*
E. L. O'Neill *(Boston)*
J. Picht *(Potsdam)*
A. Rubinowicz *(Warszawa)*
W. H. Steel *(Sydney)*
G. Toraldo di Francia *(Firenze)*
W. T. Welford *(London)*
H. Wolter *(Marburg)*

**NORTH-HOLLAND PUBLISHING COMPANY**

**P.O. BOX 103 — AMSTERDAM**

**Please turn over**

# NORTH-HOLLAND BOOKS

# PROGRESS IN OPTICS

Edited by

**EMIL WOLF**

**University of Rochester N.Y.**

just out
**VOLUME I**

**CONTENTS**

R. J. PEGIS *(Rochester, N.Y., U.S.A.)*
The Modern Development of Hamiltonian Optics

K. MIYAMOTO *(Tokyo, Japan)*
Wave Optics and Geometrical Optics in Optical Design

R. BARAKAT *(Boston, Mass., U.S.A.)*
Intensity Distribution and Total Illumination of Aberration-free Diffraction Images

D. GABOR *(London, England)*
Light and Information

H. WOLTER *(Marburg, Germany)*
On Basic Analogies and Principal Differences between Optical and Electronic Information

H. KUBOTA *(Tokyo, Japan)*
Interference Color

A. FIORENTINI *(Arcetri-Firenze, Italy)*
Dynamic Characteristics of Visual Processes

A. C. S. VAN HEEL *(Delft, Netherlands)*
Modern Alignment Devices

**6 x 9" XII + 342 pp. 157 ill. Gld. 35.00 (70s.)**

*Ask your bookseller or*

**NORTH-HOLLAND PUBLISHING COMPANY**

**P.O. BOX 103 — AMSTERDAM**

*Distributor for U.S.A.: Interscience Publishers, Inc. — New York*